THE UNIVERSITY OF CHICAGO

THE “GOLDEN APPLE”: GOLD CATALYSIS IN THE SYNTHESIS OF CAGED INDOLE ALKALOIDS, STRICTAMINE AND ARBORISIDINE, AND HARZIANE DITERPENES

A DISSERTATION SUBMITTED TO

THE FACULTY OF THE DIVISION OF THE PHYSICAL SCIENCES

IN CANDIDACY FOR THE DEGREE OF

DOCTOR OF PHILOSOPHY

DEPARTMENT OF CHEMISTRY

BY

ZHIYAO ZHOU

CHICAGO, ILLINOIS

JUNE 2020

Table of Contents

List of Schemes

List of Figures

List of Tables

List of Abbreviations

Ac	Acetyl
Alloc	Allyloxycarbonyl
Ar	Aryl
BARF	Tetrakis[3,5-bis(trifluoromethyl)phenyl]borate
9-BBN	9-Borabicyclo[3.3.1]nonane
BHT	2,6-di-*tert*-butyl-4-methylphenol
BINAP	2,2'-bis(diphenylphosphino)-1,1'-binaphthyl
Bn	Benzyl
Boc	tert-Butyloxycarbonyl
BPin	pinacolboryl
bpy	2,2’-Bipyridine
Bz	Benzoyl
CBS	Corey-Bakshi-Shibata reduction
^{c}Hex	Cyclohexyl
COD	1,5-Cyclooctadiene
COSY	Correlated spectroscopy
coll	Collidine; 2,4,6-trimethylpyridine
Cp	Cyclopentadienyl
CSA	Camphor-10-sulfonic acid
dr	Diastereomeric ratio
dba	Dibenzylideneacetone
DBU	1,8-Diazabicyclo(5.4.0)undec-7-ene
DCE	1,2-Dichloroethene
DIBAL-H	Diisobutylaluminium hydride

DIPEA	N,N-Diisopropylethylamine
DMAP	4-Dimethylaminopyridine
DMEDA	N,N'-Dimethyl ethanediamine
DMF	Dimethylformamide
DMP	Dess–Martin periodinane
DMSO	Dimethyl sulfoxide
dpm	2,2,6,6-tetramethyl-3,5-heptanedionate
dppbz	1,2-Bis(diphenylphosphino)benzene
dppf	1,1′-Ferrocenediyl-bis(diphenylphosphine)
ee	Enantiomeric excess
Et	Ethyl
FePc	Iron (II) phthalocyanine
FGA	Functional group addition
HFIP	1,1,1,3,3,3-Hexafluoro-2-propanol
HG-II	Hoveyda-Grubbs Catalyst™ 2nd Generation
HMPA	Hexamethylphosphoramide
^{i}Pr	Isopropyl
IPr	1,3-Bis(2,6-diisopropylphenyl-imidazol-2-ylidene)
$[Ir(dtbbpy)(ppys)_2]PF_6$	[4,4′-Bis(1,1-dimethylethyl)-2,2′-bipyridine-*N*1,*N*1′]bis[2-(2-pyridinyl-*N*)phenyl-C]iridium(III) hexafluorophosphate
JohnPhos	(2-Biphenyl)di-tert-butylphosphine
KHMDS	Potassium bis(trimethylsilyl)amide
LDA	Lithium diisopropylamide
LiHMDS	Lithium bis(trimethylsilyl)amide
*m*CPBA	3-Chloroperoxybenzoic acid

Me	Methyl
Mes	Mesityl
Ms	Mesylate
MS	Molecular sieves
NBS	N-Bromosuccinimide
^{n}Bu	n-Butyl
NHC	N-heterocyclic Carbenes
NOESY	Nuclear Overhauser effect spectroscopy
Ns	2-Nitrobenzenesulfonyl
o-DCB	*o*-Dichlorobenzene
p-ABSA	4-Acetamidobenzenesulfonyl azide
Ph	Phenyl
PIDA	(Diacetoxyiodo)benzene
Piv	Pivaloyl, 2,2-Dimethylpropionyl
PMHS	Polymethylhydrosiloxane
PP	Pyrophosphoryl
*p*TsOH	*p*-Toluenesulfonic acid monohydrate
Rf	Retardation factor
Rh_2(S-DOSP)$_4$	Tetrakis[(S)-(+)-N-(*p*-dodecylphenylsulfonyl)prolinato]dirhodium(II)
SPhos	2-Dicyclohexylphosphino-2′,6′-dimethoxybiphenyl
TBAF	Tetrabutylammonium fluoride
TBAT	Tetrabutylammonium difluorotriphenylsilicate
TBHP	tert-Butyl hydroperoxide
TBDPS	tert-Butyldiphenylsilyl
TBME	tert-Butyl methyl ether

TBS	tert-Butyldimethylsilyl
^{t}Bu	tert-Butyl
^{t}BuXPhos	2-Di-tert-butylphosphino-2′,4′,6′-triisopropylbiphenyl
TES	Triethylsilyl
Tf	Trifluoromethanesulfonyl
TFA	Trifluoroacetic acid or trifluoroacetyl
TFAA	Trifluoroacetic anhydride
TFE	2,2,2-Trifluoroethanol or 2,2,2-trifluoroethyl
THF	Tetrahydrofuran
TIPS	Triisopropylsilyl
TLC	Thin-layer chromatography
TMS	Trimethylsilyl
Trp	Trptophan
Ts	Tosyl
TTMSS	Tris(trimethylsilyl)silane
Xantphos	4,5-Bis(diphenylphosphino)-9,9-dimethylxanthene
XPhos	2-Dicyclohexylphosphino-2′,4′,6′-triisopropylbiphenyl

Acknowledgement

During the five and half year of my Ph. D., I would have not been proceeding in my research odyssey against frustrations, challenges and downhills in the absence of the enormous support and love from my surroundings. I would like to thank:

Prof. Scott A. Snyder, for being fully supportive and considerate during my Ph. D., especially in my hard times of projects being scooped and deadends in research, and giving me the opportunity to explore new fields of chemistry. Thank you also for your training on my research and presentation skills.

The Snyder Group, for your support in chemistry and your efforts in maintaining an ameable environment so I can pursue on my science path. It is really a pleasure working with every one of you and I wish you all the best.

Dr. Myles Smith, for your mentorship, ideas and knowledgable suggestions in the collaboration of strictamine project, my first project in Ph. D.

Dr. Alison Gao, for your tremendous help in chemistry and experimental skills in the collaboration of both strictamine and arborisidine projects, and for being a wonderful friend.

Phil Gemmel, for your dedications and helpful discussions in the collaboration of my last thesis project, and wish us good luck in finishing it. Thank you also for your help in the proofreading of my thesis.

Cheng Peng, **Piyush Arya**, **Charles Cole**, **Kevin Zong** and **Dr. Takuya Shimbayashi**, for your help and support in our collaborations. **Charles** is also thanked for the help in the proofreading of my thesis.

Dr. Yu-An Zhang and **Dr. Minxing Shen**, for being great friends during these years, from Jupiter to Chicago, and for your help in chemistry and otherwise. I wish you success in your next adventures in chemistry.

Cooper Taylor and **Tessa Lynch-Colameta**, for your help in the proofreading of my thesis.

Prof. Guangbin Dong and **Prof. Viresh Rawal**, for serving as my dissertation committee members and your helpful discussions in chemistry.

Dr. Xiangming Kong (The Scripps Research Institute), **Dr. Antoni Jurkiewicz** (The University of Chicago), **Dr. Josh Kurutz** (The University of Chicago), **Dr. C. Jin Qin** (The University of Chicago) for immense support in providing expertise in spectroscopic analysis.

Dr. Alexander Filatov and **Mr. Andrew Mcneece** for your support and expertise in X-ray analysis.

Cheryl Marra, **Jennifer Kabis**, **Dr. Vera Dragisich** and **Melinda Moore**, for your assistance of my student life over these years.

Prof. Zhen Yang, **Prof. Jiahua Chen** and **Prof. Tuoping Luo**, for your support and mentorship during my undergraduate studies at Peking University, and leading me to the fascinating field of organic chemistry.

Department of Chemistry at The University of Chicago, for financial support from The Edith Barnard Memorial Fellowship.

My family, for your continuing support, tolerance and love. I cannot imagine what I could do without your encouragement and understanding. It's a pity that you are not able to attend my defense during this special and stressful time, and I wish you good health and safety.

My girlfriend, Shilan Wu, for your support and understanding during these busy and stressful years, and for your love and care that give me strenghth and courage.

My stuffed animals, for the joy that you bring to me.

Abstract

The “Golden Apple”: Gold Catalysis in the Synthesis of Caged Indole Alkaloids, Strictamine and Arborisidine, and Harziane Diterpenes

Chapter 1 Gold Catalysis: Strategic Advantages in the Total Syntheses of Complex Natural Products

Since its early use in the late 1980 and 1990, homogeneous gold catalysis has emerged as a powerful tool in the field of natural product synthesis. Herein, we illustrated with recent examples that the incorporation of gold catalysis in total synthesis has benefited tremendously in the rapid construction of challenging all-carbon quaternary centers and medium-sized ring.

Chapter 2 Formal Synthesis of (+)-Strictamine

Strictamine is a pentacyclic Akuammiline alkaloid isolated in 1966 bearing a unique methanoquinolizidine core and its total synthesis puzzle has not been solved for 50 years. While a number of total and formal syntheses of strictamine were discloses by other labs in recent years, all of them required no less than 14 steps of chemical transformations. We developed a gold-catalyzed *6-endo*-dig cyclization with “protonation as traceless protection” strategy to access the key intermediate towards strictamine and accomplished a concise formal synthesis of strictamine (6 step racemic, 7 step asymmetric). The application of an enantioselective propargylation developed

during the course of our research was also demonstrated in the catalytic asymmetric synthesis of other indole alkaloids.

Chapter 3 Total Synthesis of (+)-Arborisidine

Arborisidine is a pentacyclic indole alkaloid isolated in 2016 containing a rare fully substituted cyclohexanone moiety, with promising *in vitro* inhibition activity of gastric cancer in combination of pimelautide. The presence of *aza*-quaternary center and dense substitutions raised significant synthetic challenges. Herein, we discussed our elaborations of *6-endo*-dig cyclization reactions and detours to access the intriguing core of arborisidine, and additional efforts in the regioselective functionalization of dienes as well as late-stage one-pot redox manipulations, which ultimately led to the first total synthesis of arborisidine (7 steps racemic, 9 steps asymmetric). The development of chemoselective decyanation reaction also provided alternative entry to the enantioenriched 1-acyl tetrahydro-β-carboline building blocks.

Chapter 4 Studies toward Total Synthesis of Harziane Diterpenes

Harziane diterpenes, mostly isolated from *Trichoderma* fungi species, constitute of a considerable number of members sharing a complicated tetracyclic scaffold with four-, five-, six- and seven membered rings, at least five stereocenters and three all-carbon quaternary centers, in which two are vicinal. We designed a unified approach taking advantage of the gold-catalyzed [2+2] cycloaddition reaction to access the unique 7-4 fused bicyclic system with different types of ring tethers. A ring

reorganization strategy was also devised, complementary to the innate selectivity of Favorskii-type ring contraction. These establishments allowed access to a key ketoaldehyde intermediate in 10 steps that contains the major stereocenters in the right half of harziane diterpenes. With the aid of versatile diene functionalizations, we would hopefully complete the collective total synthesis of harziane diterpene natural products in the near future.

Chapter 1 Gold Catalysis: Strategic Advantages in the Total Syntheses of Complex Natural Products

1.1 Introductions

Gold (Au, a.u. = 196.97, electron configuration $[Xe]4f^{14}5d^{10}6s^{1}$) is the 79th element in the periodic table, belonging to Group VIII. It was also the first elemental metal utilized in human society and played an essential role in the ancient times, mainly used in currency, upper class decorations and as the symbol of intrinsic worth and perfection, owing to its bright, shining color as well as eternal stability. The unique color of gold among most other metals, however, is now explained via the relativistic effect[1] of heavy atoms contracting its 6s orbital and expanding its 5d orbitals. This same effect also armors cationic gold complexes with extraordinary π-acidity and good capacity to stabilize the neighboring carbocation through backbonding, making the "stable" gold species a powerful catalyst in organic synthesis.

Gold was first used in homogeneous catalysis in 1986 in an enantioselective [3+2] cycloaddition reaction between aldehydes (**1**) and isocyanoacetates (**2**) to generate oxazoline (**3**)[2]; the first example of alkyne activation emerged in 1998[3] (Scheme 1.1). The field has been quickly expanding since early 2000 and the mode of gold catalysis has been broadened to a significant level, including classical activating alkyne[4] and other unsaturated functionalities, asymmetric catalysis[5], carbenoid reactions[6], cross coupling[7], photocatalysis[8] and other reactions[9].

Scheme 1.1 Early examples of homogeneous gold catalyzed organic reactions

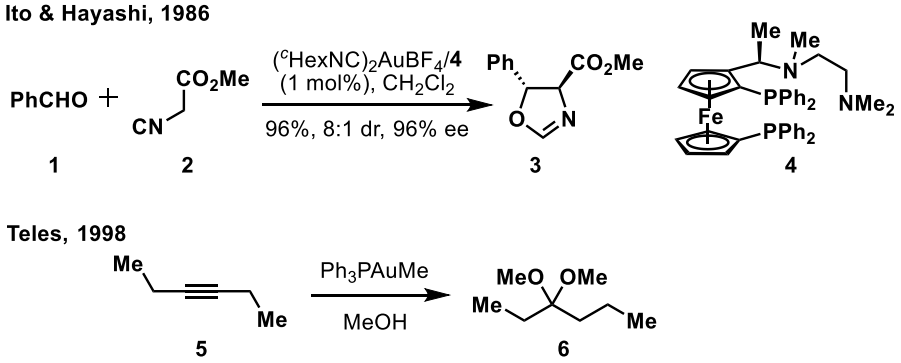

The continuous elucidations of various mechanisms[10] in gold catalysis has also driven the discoveries of new reactions that were ultimately reflected in the efficient syntheses of natural products[11] and other complex molecules. In this chapter, we would like to demonstrate such strategic advantages of gold catalysis in the total syntheses of complex natural products with selected recent examples from numerous impressive works in the past two decades. Through meticulous design and orchestration, the gold-catalyzed alkyne activation has tremendously accelerated the key C-C bond formation events toward building all-carbon quaternary stereocenters and medium-sized carbo-/heterocycles within natural product targets.

1.2 Gold Catalysis Enables Rapid Construction of All-Carbon Quaternary Stereocenters

One of the most widely used reactions in total syntheses employing gold catalysis is the cycloisomerization of 1,n-enyne substrates[10a] (including Conia-ene[12] reactions). The highly active gold(I) species allows for the effective and stereoselective formation of all-carbon quaternary stereocenters, which often present significant challenges[13] throughout the synthesis. In 2017, Barriault and coworkers disclosed an

elegant synthesis of magellanine (**9**)[14] in which the key step involved a formal [4+2] cycloaddition reaction of **7**. This event was triggered by the cyclization of the silyl enol ether, followed by ring opening of the three-membered ring of **10** with subsequent elimination. Such design has enabled an 11-step synthesis of (±)-**9**.

Scheme 1.2 Barriault's total synthesis of magellanine (**9**)

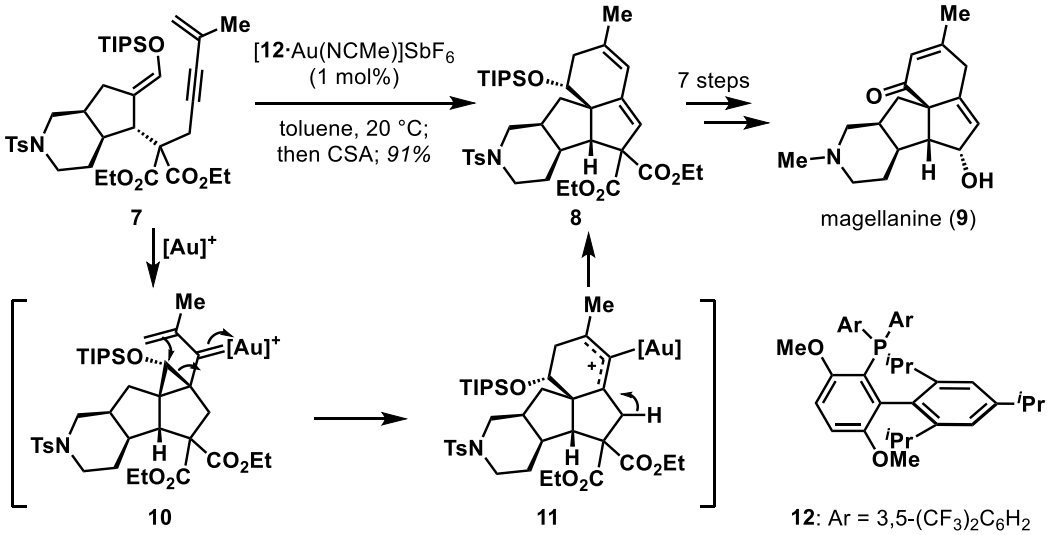

Another way to implement gold-catalyzed cycloisomerization includes the combination of semi-pinacol rearrangement to terminate the carbocation and generate quaternary centers stereoselectively. In 2010, Overman and coworkers completed the first total synthesis of (+)-sieboldine A (**15**, Scheme 1.3) using such a strategy[15].

Scheme 1.3 Overman's total synthesis of (+)-sieboldine A (**15**)

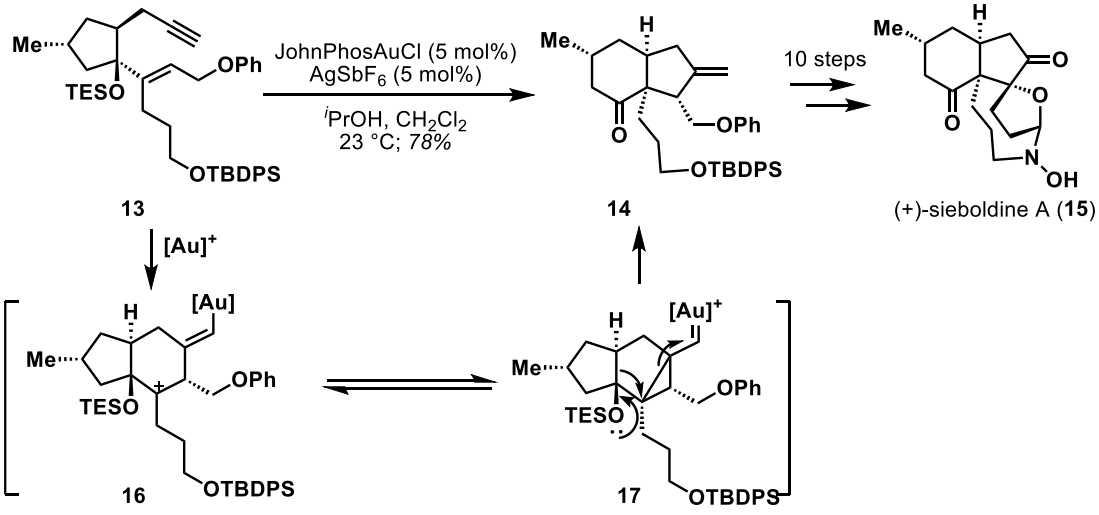

Carreira and coworkers took advantage of gold catalyst to promote the Claisen rearrangement of propargyl ether[16] (also known as Saucy-Marbet rearrangement), generating the desired quaternary stereocenter in intermediate **19** towards their first total synthesis of indoxamycin B[17](**21**, Scheme 1.4) in 2012. The employment of gold catalysis allowed for complete stereocontrol and high yield, while simple thermal conditions failed to give the desired product. The resultant allenyl group in **19** also participated in the subsequent hydroalkoxylation with a different gold catalyst to form the tetrahydrofuran moiety in **20**.

Scheme 1.4 Carreira's total synthesis of indoxamycin B (**21**)

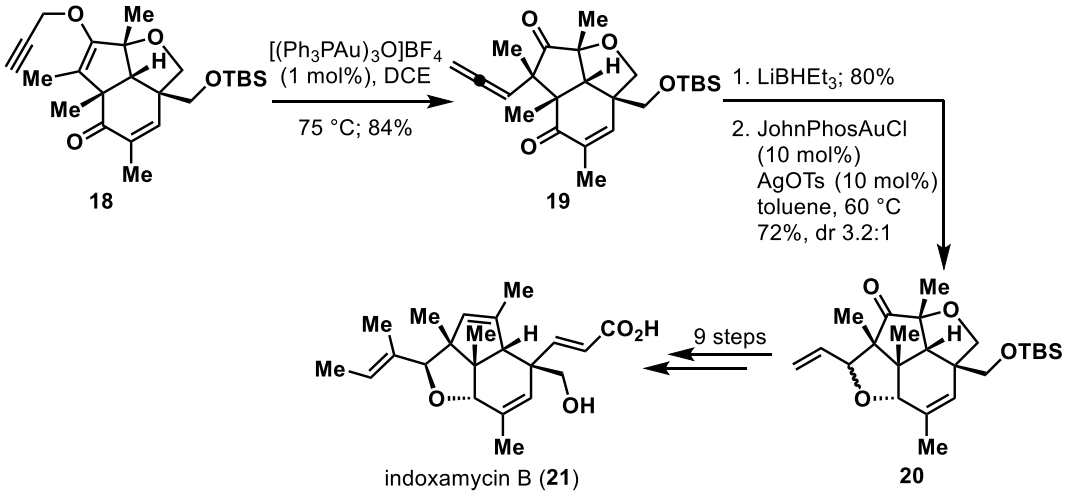

1.3 Gold Catalysis Allows Facile Medium-Size Ring Synthesis

Gold catalysis also exhibits great potential in the efficient synthesis of medium-sized rings (typically 7- and 8-memebered rings). An impressive cascade cyclization developed by Echavarren and coworkers has enabled a concise entry into various diterpene scaffolds[18], which was applied by both the Echavarren lab [19a] and Ma lab [19b] in their asymmetric total syntheses of (−)-englerin A (**24**) in 2010 (Scheme 1.5).

Scheme 1.5 Echavarren's and Ma's total syntheses of (-)-englerin A (**24**)

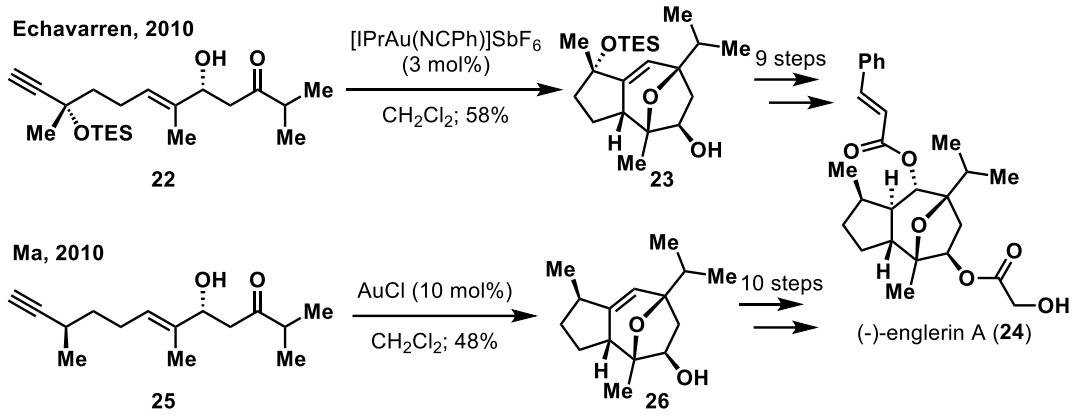

Mechanistically, this cascade reaction (Scheme 1.6) was postulated through an enyne cyclization followed by an intramolecular nucleophilic attack of carbonyl group onto the cyclopropane of **27** and a sebsequent Prins-type cyclization of **28** to form the bridged bicyclic moiety.

Scheme 1.6 Proposed mechanism of cascade cyclization in the total synthesis of (-)-englerin A **24**

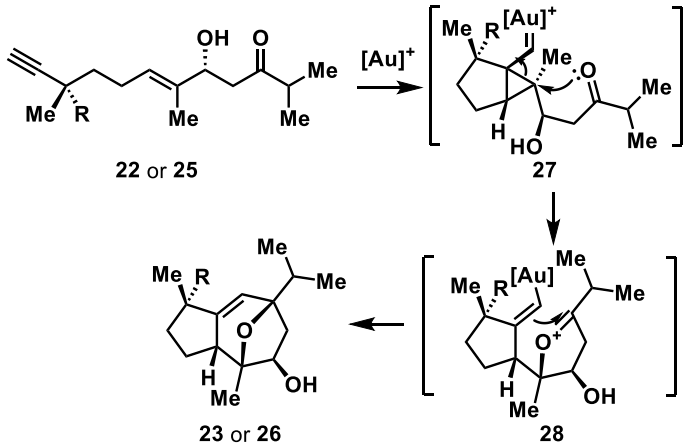

More recently (2016 and 2018), the Echavarren lab has published their systematic studies on the asymmetric total syntheses of pyrroloazocine indole alkaloids, including lundurine A-C (**33**-**35**)[20], lapidilectine A-B (**38**, **36**) [21], isolapidilectine (**41**) [21], lapidilectam (**39**) [21] and grandilodine A-C (**40**, **42**, **37**)[21] (Scheme 1.7). The unified synthetic routes relied heavily on the gold-catalyzed *8-endo*-dig cyclization of intermediates **29** and **31** to build the key 8-membered ring fusion.

Scheme 1.7 Echavarren's total synthesis of pyrroloazocine alkaloids

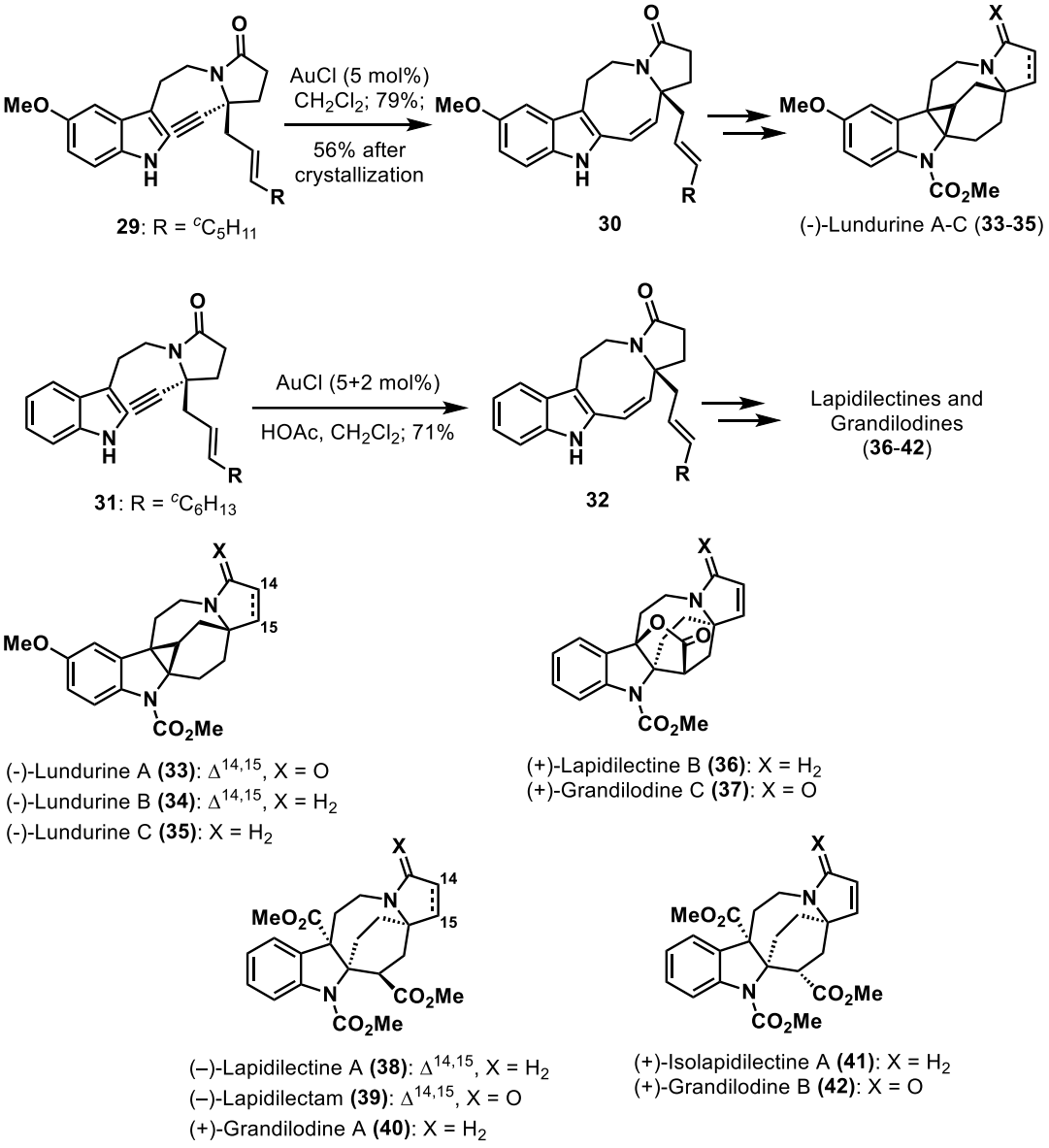

In 2020, Yang, Chen and coworkers accomplished the asymmetric total synthesis of pre-schisanartanin C (**47**)[22], a *schisandra* nortriterpenoid natural product. After tremendous efforts to build up the polycyclic skeleton, a gold-catalyzed propargylic ester rearrangement with subsequent intramolecular cyclopropanation of the thus-formed gold carbenoid **45** was successfully incorporated to establish the 8-member ring junction. The protecting group choice of 4-fluorobenzyl ($^{p\mathrm{F}}$Bn) in place of benzyl in **43** effectively prevented the complexation caused by hydride shift of

benzylic protons onto the vinyl gold carbenoid in **45**. The successful execution of this transformation in such a highly complicated system also demonstrated the mildness and versatility of gold catalysis in complex natural product synthesis.

Scheme 1.8 Yang and Chen's total synthesis of pre-schisanartanin C (**47**)

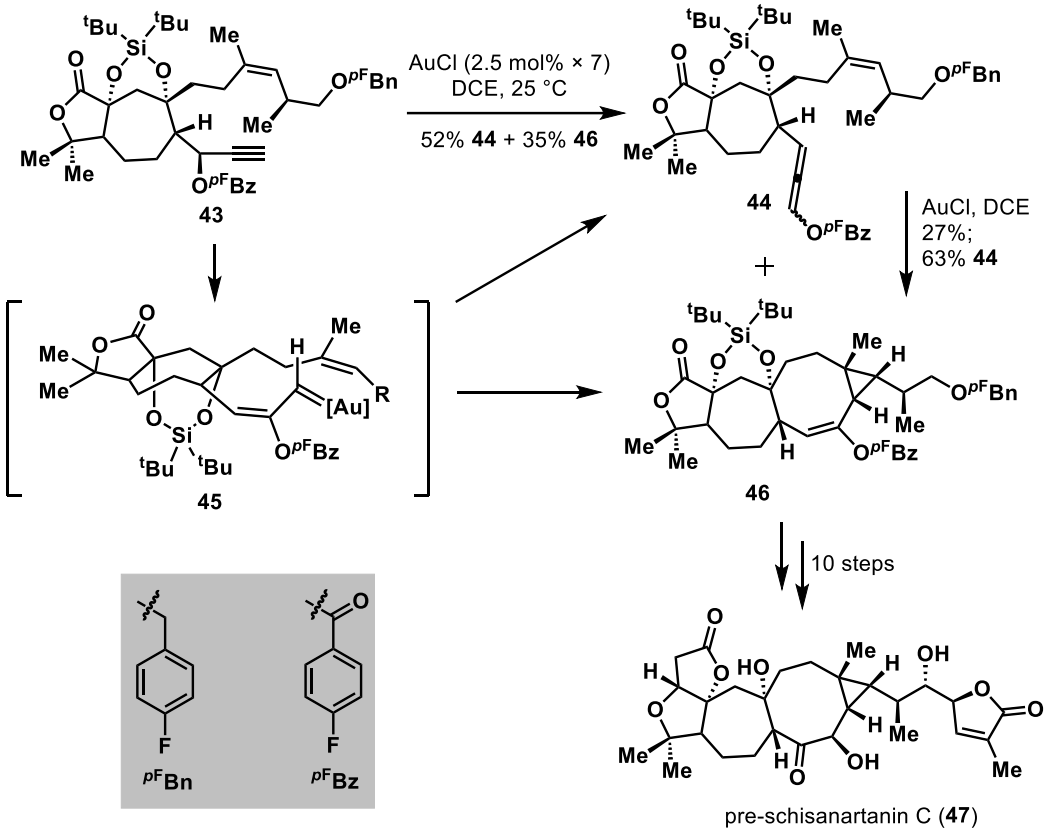

1.4 References

[1] Gorin, D. J.; Toste, F. D. *Nature*, **2007**, *446*, 395.
[2] Ito, Y.; Sawamura, M.; Hayashi, T. *J. Am. Chem. Soc.* **1986**, *108*, 6405
[3] Teles, J. H.; Brode, S.; Chabanas, M. *Angew. Chem., Int. Ed.* **1998**, *37*, 1315
[4] Dorel, R.; Echavarren, A. M. *Chem. Rev.* **2015**, *115*, 9028.
[5] Zi, W.; Toste, F. D. *Chem. Soc. Rev.* **2016**, *45*, 4567.
[6] (a) *Gold Carbenes*: L. Zhang, in *Contemporary Carbene Chemistry* (Eds. R. A. Moss, M. P. Doyle), Wiley, Hoboken, **2013**, 526; (b) Mato, M.; García-Morales, C.; Echavarren, A. M. *ChemCatChem* **2019**, *11*, 53.
[7] Hopkinson, M. N.; Tlahuext-Aca, A.; Glorius, F. *Acc. Chem. Res.* **2016**, *49*, 2261.
[8] (a) Hopkinson, M.N.; Gee, A.D.; Gouverneur, V. *Chem.–Eur. J.* **2011**, *17*, 8248; (b) Nijamudheen, A.; Datta, A. *Chem.–Eur. J.* **2020**, *26*, 1442.
[9] Hashmi, A. S. K.; Toste, F. D. *Modern Gold Catalyzed Synthesis*; Wiley-VCH: Weinheim, **2012**.
[10] (a) Jiménez-Núñez, E.; Echavarren, A. M. *Chem. Rev.* **2008,** *108,* 3326; Lu, Z.; Hammond, G. B.; Xu, B. *Acc. Chem. Res.* **2019**, *52*, 1275.
[11] Zhang, Y.; Luo, T.; Yang, Z. *Nat. Prod. Rep.* **2014**, *31*, 489; (b) Pflasterer, D.; Hashmi, A. S. *Chem. Soc. Rev.* **2016**, *45*, 1331.
[12] (a) Kennedy-Smith, J. J.; Staben, S. T.; Toste, F. D. *J. Am. Chem. Soc.* **2004**, *126*, 4526; for a review, see: (b) Hack, D.; Blümel, M.; Chauhan, P.; Philipps, A. R.; Enders, D. *Chem. Soc. Rev.* **2015**, *44*, 6059.
[13] Quasdorf, K. W.; Overman, L. E. *Nature* **2014**, *516*, 181.
[14] McGee, P.; Betournay, G.; Barabe, F.; Barriault, L. *Angew. Chem., Int. Ed.* **2017**, *56*, 6280
[15] Canham, S. M.; France, D. J.; Overman, L. E. *J. Am. Chem. Soc.* **2010**, *132*, 7876.
[16] Sherry, B. D.; Toste, F. D. *J. Am. Chem. Soc.* 2004, **126**, 15978.
[17] Jeker, O. F.; Carreira, E. M. *Angew. Chem., Int. Ed.* **2012**, *51*, 3474.
[18] (a) Jiménez-Núñez, E.; Raducan, M.; Lauterbach, T.; Molawi, K.; Solorio, C. R.; Echavarren, A. M. *Angew. Chem., Int. Ed.* **2009**, *48*, 6152; (b) Jiménez-Núñez, E.; Molawi, K.; Echavarren, A. M. *Chem. Commun.* **2009**, 7327.
[19] (a) Molawi, K.; Delpont, N.; Echavarren, A. M. *Angew. Chem., Int. Ed.* **2010**, *49*, 3517; (b) Zhou, Q.; Chen, X.; Ma, D. *Angew. Chem., Int. Ed.* **2010**, *49*, 3513.
[20] Kirillova, M. S.; Muratore, M. E.; Dorel, R.; Echavarren, A. M. *J. Am. Chem. Soc.* **2016**, *138*, 3671.
[21] Miloserdov, F. M.; Kirillova, M. S.; Muratore, M. E.; Echavarren, A. M. *J. Am. Chem. Soc.* **2018**, *140*, 5393.
[22] Jiang, Y.-L.; Yu, H.-X.; Li, Y.; Qu, P.; Han, Y.-X.; Chen, J.-H.; Yang, Z. *J. Am. Chem. Soc.* **2020**, *142*, 573.

Chapter 2 Formal Synthesis of (+)-Strictamine

2.1 Isolation, Structure Feature and Bioactivity of Strictamine

Strictamine (**1**) is an akuammiline alkaloid isolated in 1966 from *Rhazya stricta* decaisne[1]. In 1977, the X-ray crystallographic analysis of its monohydrate revealed [2] the structure of **1** as a caged pentacyclic molecule bearing a rare, constrained methanoquinolizidine moiety (**2**), in which both piperidine rings reside in boat-like conformation (highlighted in red, Figure 2.1). This unusual scaffold contributes to the most of ring strain in **1**.

Figure 2.1 Structure of strictamine (**1**) and methanoquinolizidine (**2**) moiety

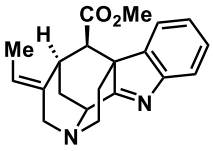

strictamine (**1**)

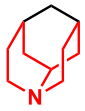

methanoquinolizidine (**2**)

Later investigations of **1** have revealed various biological activities[3], including monoamine oxidase antagonist activity[3a], antiviral activity against herpes simplex virus (HVP) and adenovirus (Adv)[3b] and inhibition activity of neuron factor κB (NF-κB)[3c], a protein complex that plays an essential role in the transcription of DNA and immune response to infection.

2.2 Efforts on Total and Formal Syntheses of Strictamine in recent years

The unique pentacyclic structure as well as potential biological activities of strictamine (**1**) have made it a hot target in the synthetic community. However, the intriguing and highly strained ring system with the presence of two basic nitrogen atoms rendered considerable challenges itself and there had been no total syntheses reported before we launched our project. Nevertheless, the first total synthesis of (+)-strictamine

(**1**) was completed in early 2016, by Garg and coworkers[4] (Scheme 2.1). Starting from asymmetric material **3**, a gold-catalyzed *6-exo*-dig Conia-ene reaction was employed, delivering the desired bicyclic intermediate **4** as the major regioisomer, which could be converted into the corresponding β-hydroxyl enal **5** in a modest overall yield. Through another 7-step sequence, tricyclic intermediate **6** could be obtained which was used in the following Fisher indole synthesis and subsequent reduction of the imine in the same pot to form indoline **7**. Although **7** contains almost all the carbon skeleton and oxidation states, another 9-step chemical transformations were required to achieve the final target, (+)-**1** (Scheme 4.1), with a total step count of 24 steps.

Scheme 2.1 Garg's enantioselective total synthesis of (+)-strictamine (**1**)

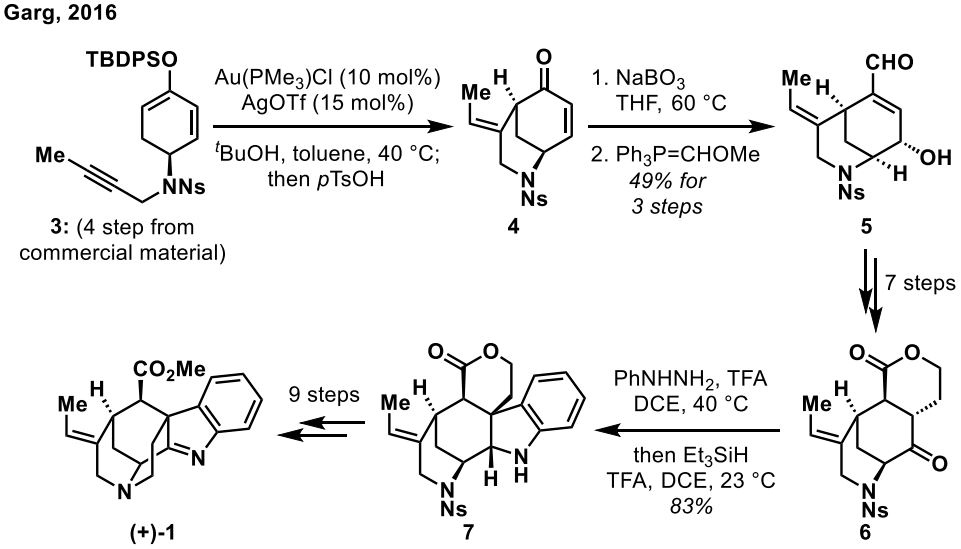

Almost at the same time, Zhu and coworkers also published their own effort in the total synthesis of (±)-strictamine[5] (Scheme 2.2). It is also the shortest total synthesis to date. Using known intermediate **8**[6], an α-bromination was conducted followed by an intramolecular S_{N2} substitution and demethylation of **9** to generate the bicyclic compound **10**, which could be further transformed into **11** in three steps. The installation of the vinyl iodide side chain (**12**) and subsequent Ni-catalyzed reductive

cyclization would deliver (±)-**1** albeit low yield in the last step. This work also revealed a common intermediate, **11**, the same intermediate we were pursuing at the time[7], and all the subsequent formal syntheses were based upon **11** and **13**.

Scheme 2.2 Zhu's total synthesis of (±)-strictamine (**1**)

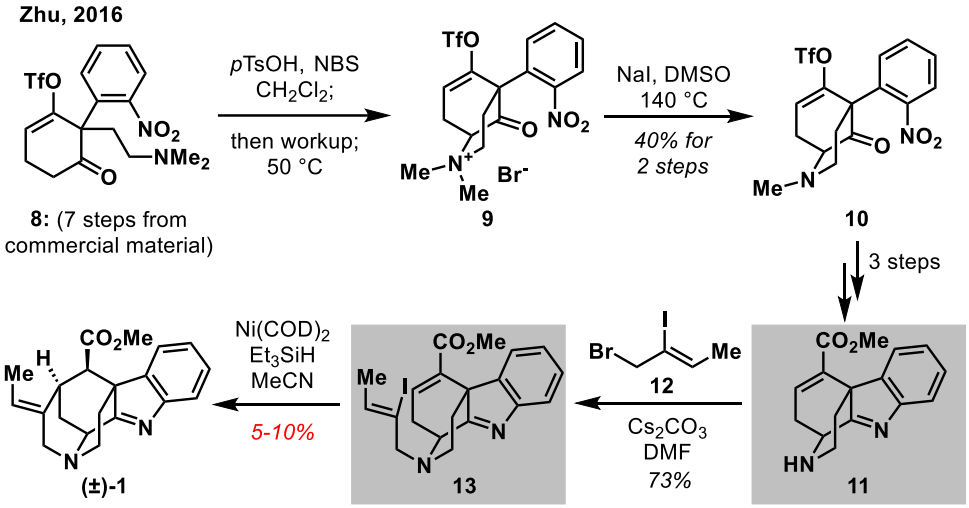

In 2017, Zu and coworkers reported a unified strategy in the syntheses of (±)-strictamine (**1**) and other members of the akuammiline alkaloids[8] (Scheme 2.3). Starting from the advanced tetracyclic intermediate **14** developed by the same lab[9], they were able to prepare the corresponding alkene substrate **15** that underwent a Ni(0)-catalyzed Heck-type carbonylation reaction to generate **16**. With two more steps involving oxidation state adjustment, the common intermediate **17** was obtained and subjected to excess samarium (II) diiodide which facilitated a reductive rearrangement, generating **18**. Finally, additional oxidation state manipulations led to (±)-**1**.

Scheme 2.3 Zu's total synthesis of (±)-strictamine (**1**)

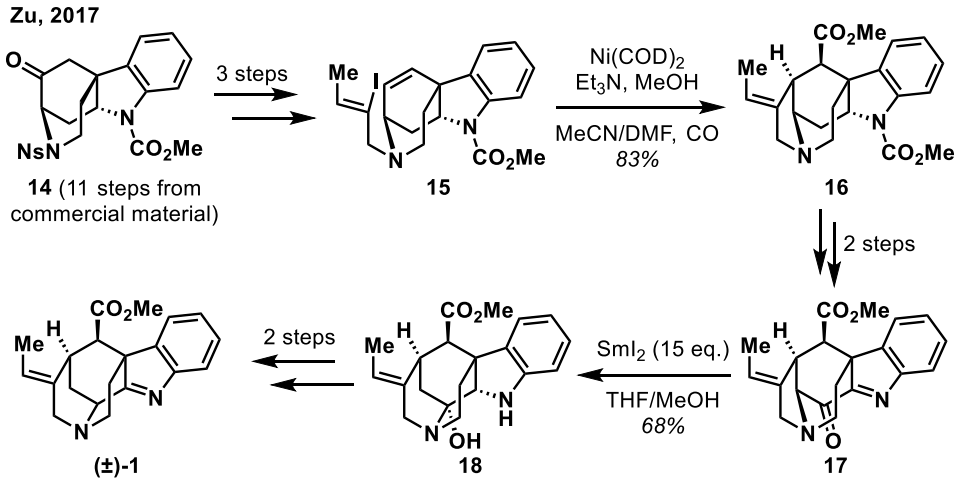

In 2018, Tang, Qin and coworkers reported an enantioselective total synthesis of (+)-strictamine[10a] (Scheme 2.4), based on their intermediate **19**[10b]. The key transformation included a Johnson-Claisen rearrangement between **20** and orthoester **21** to circumvent the low-yielding problem in the final ring-closure step in Zhu's synthesis (Scheme 2.2). However, this reaction suffered from poor diastereoselectivity with desired **23** being only 30% (and 60% the other diastereomer). With **23** in hand, the subsequent reactions went smoothly to give (+)-**1** in 10 steps.

Scheme 2.4 Tang & Qin's asymmetric total synthesis of (+)-strictamine (**1**)

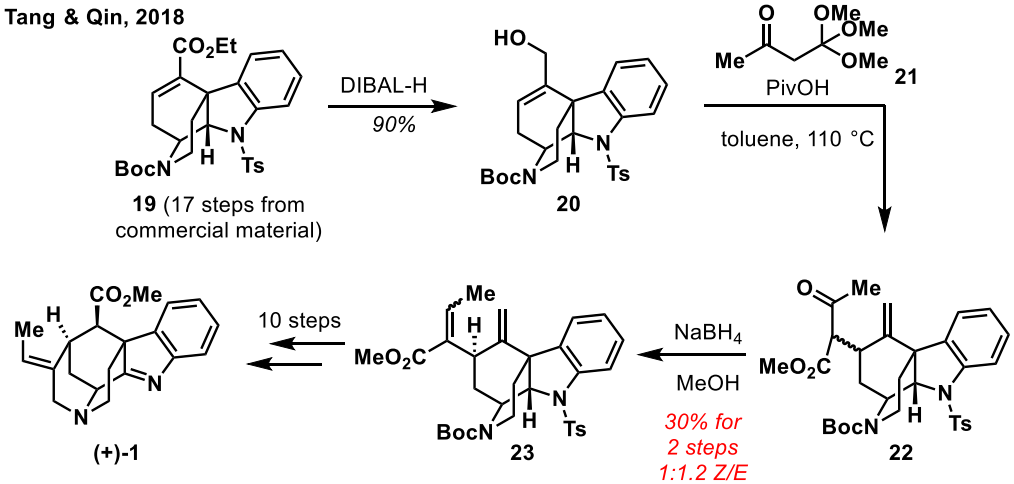

Qin and coworkers have further devised a second-generation synthesis of (–)-strictamine in 2019[11] (Scheme 2.5). From enantiopure material **24**[12], an efficient

photoredox cascade cyclization/conjugate addition reaction was employed with good diastereoselectivity, followed by a one-pot Grignard addition and *p*-tosyl deprotection, to generate the tricyclic compound **25**. With two more steps, the resultant allylic carbonate **26** underwent a dearomative allylation to produce **27** containing the core of strictamine. Given previous challenges with the final ring closure in the presence of the bridged lactam moiety in **27**, they decided to open up the lactam to facilitate the late-stage Ni-catalyzed Heck-type coupling (**28** to **29**), which required an additional 15 steps to reach the final target, (–)-**1**.

Scheme 2.5 Qin's 2nd-generation total synthesis of (–)-strictamine (**1**)

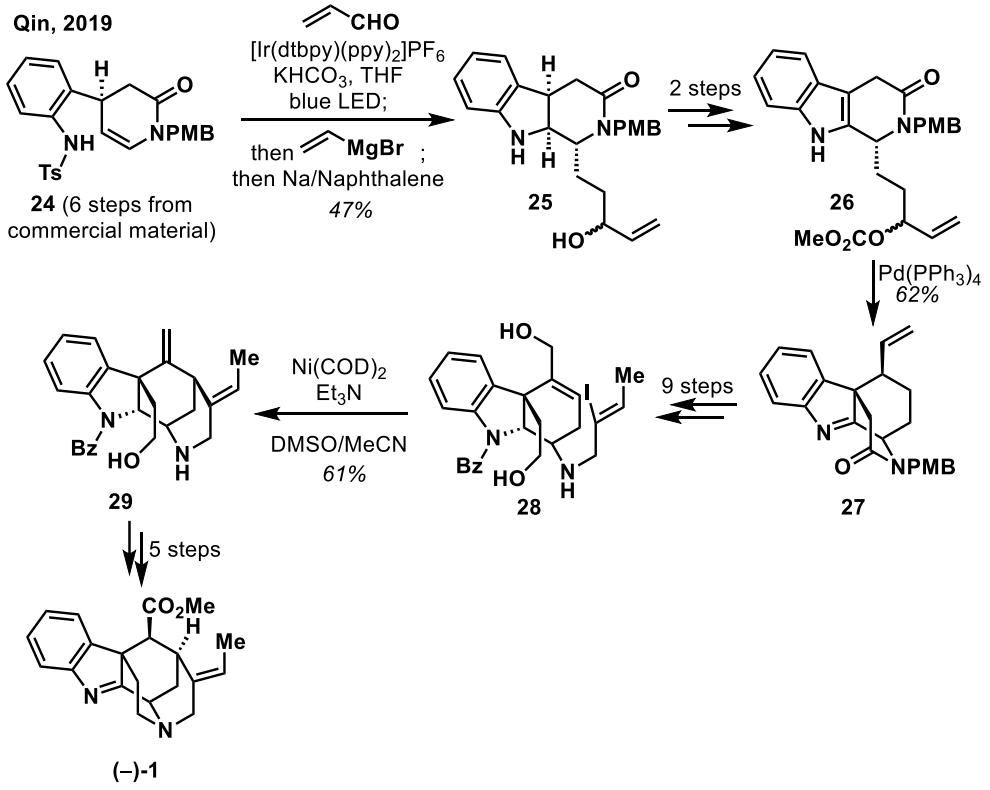

Besides these elegant works on the total synthesis, there were also other reports, besides ours, on the formal synthesis of strictamine[10b,13] through the synthesis of intermediate **13**, which are summarized in Scheme 2.6. Among these, Fuji, Ohno and

coworker published the first formal synthesis[13a] in which a similar gold-catalyzed *6-endo*-dig cyclization of **30** was incorporated.

Scheme 2.6 Other formal syntheses of strictamine targeting **13**

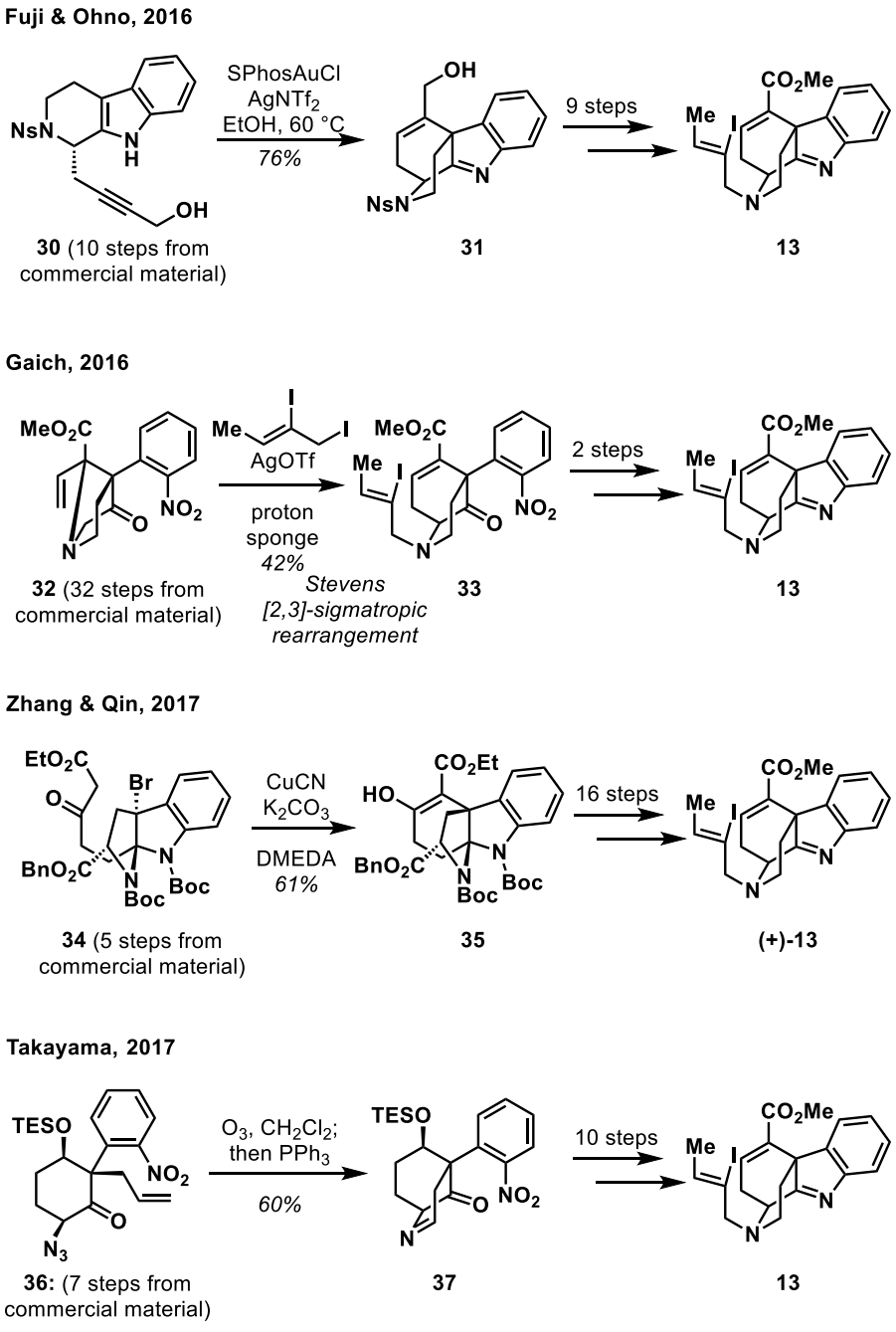

2.3 Our Initial Approach of *6-Endo*-Dig Cyclization

In collaboration with Dr. Myles Smith and Dr. Alison Gao, our goal was to pursue a concise and asymmetric synthesis of strictamine (**1**) via a *6-endo*-dig

cyclization of alkyne **38** (Table 2.1). Initially, we found that stoichiometric $AgBF_4$ could serve as an effective promoter[7] for the electron-neutral alkyne substrates (**38a**), but gave low yield with electron-deficient ynoate substrates (**38b** or **38c**) which are structurally more similar to **1** or **11**. Switching the protecting group to Alloc (**38d**) could partially solve this problem, but at the price of overall efficiency, as extra protection and deprotection steps were required to prepare **38d**. A better solution that could restore the reactivity as well as maintain the conciseness of the route was thus demanded.

Table 2.1 Initial condition for *6-endo*-dig cyclization

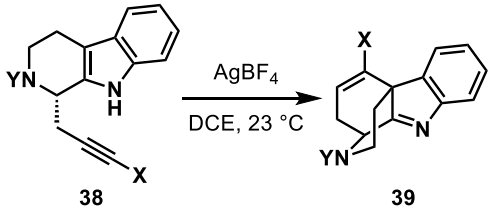

substrate 38	yield of 39
38a: X = H, CH_2OH	*50-66%*
38b: X = CO_2Me, Y = CO_2Me	*15%*
38c: X = CO_2Me, Y = Ns	*37%*
38d: X = CO_2Me, Y = Alloc	*62%*

2.4 Protonation as Traceless Protection and Formal Synthesis of (±)-Strictamine

During the progress of seeking appropriate protecting groups, we proposed the use of a protonated ammonium salt as a traceless and "transient" protecting group (Scheme 2.7), since it would also shield the nucleophilic secondary amine in substrates like **38e** against potential deactivation of cationic metal Lewis acids. However, the isolation of free amine **42** had failed (Scheme 2.7), possibly due to the intermolecular *aza*-Michael addition/ oligomerization between the free amine and electrophilic ynoate moiety. Thus, we decided to use its TFA salt **41** for further screening of the *6-endo*-dig cyclization.

Scheme 2.7 General design of “protonation as traceless protection” strategy

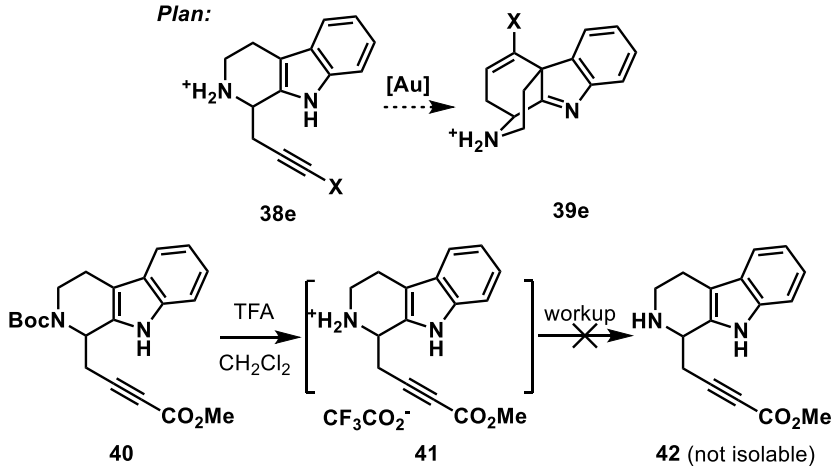

The desired reaction did not occur with 1 equivalent of $AgBF_4$ (Table 2.2, entry 1), but showed trace product in the presence of 5 mol% $Ph_3PAuNTf_2$ and 2 equivalents of methanesulfonic acid (MsOH, Table 2.2, entry 2); other Brønsted acid (CSA, HBF_4, HOTf, etc.) did not provide even trace product **11**. Interestingly, stoichiometric amount of $AgBF_4$ and catalytic Ph_3PAuCl (Table 2.2, entry 3) turned out to give a significant amount of desired product **11**, while control experiment indicated that either merely $AgBF_4$ (Table 2.2, entry 4) or both catalytic Ph_3PAuCl and $AgBF_4$ (Table 2.2, entry 5) resulted in trace product formation. Replacing $AgBF_4$ to $AgSbF_6$ (Table 2.2, entry 7) further improved the yield to 58%. The role of excess silver salt was not completely clear, but it might serve as a sacrificial agent to prevent coordinative deactivation of the active gold(I) catalyst from the potential nucleophilic species, such as the free amine, imine, and/or trifluoacetate anion in the reaction mixture.

Table 2.2 Screening of reaction conditions of *6-endo*-dig cyclization with ammonium salt **11**

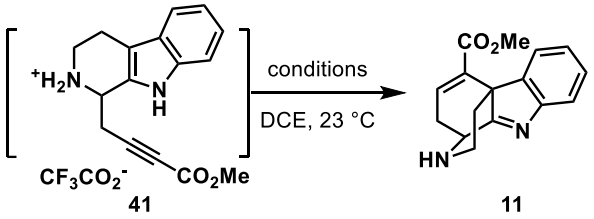

entry[a]	catalyst (%mol)	additive	results
1	$AgBF_4$ (100)	-	decomposition
2	$Ph_3PAuNTf_2$ (5)	MsOH (2)	trace product
3	Ph_3PAuCl (5), $AgBF_4$ (100)	MsOH (2)	37% **11**[b]
4	$AgBF_4$ (100)	MsOH (2)	decomposition
5	Ph_3PAuCl (5), $AgBF_4$ (5)	MsOH (2)	trace **11**
6	$Ph_3PAuNTf_2$ (5), $AgBF_4$ (100)	MsOH (2)	23% **11**[b]
7	Ph_3PAuCl (5), $AgSbF_6$ (100)	MsOH (2)	58% **11**[b]

a. Reaction run at 0.1-0.5 mmol scale in DCE (0.05 M); b. isolated yield from Boc-amide **40**.

Such protonation strategy could also be used in the *6-endo*-dig cyclization of the more electron-deficient trifluoroethyl (TFE) ynoate substrate **43**, although a harsher condition with 10 mol% Ph_3PAuCl and elevated temperature was required, and the yield of **44** was lower (Scheme 2.8).

Scheme 2.8 *6-endo*-dig cyclization with ammonium salt **43**

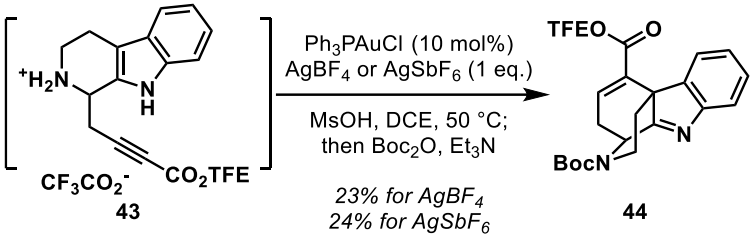

This method provided a rapid and scalable solution for the formal synthesis of (±)-strictamine (**1**), reaching intermediate **11**[5] in only 4 steps[14] (Scheme 2.9). Starting from inexpensive tryptamine (**45**), a one-pot Bischler–Napieralski reaction[15] could generate cyclic imine **46**, which then underwent a one-pot propargylation (with allenylBPin **47**) and Boc-protection to give **48**. Subsequent oxidative carboxylation[16] delivered the desired ynoate **40**; all the transformations up to this point were performed

on gram scale. After Boc deprotection, the *in situ* formed **41** was subjected to the *6-endo*-dig cyclization condition as discussed above to deliver the desired intermediate **11** on up to 450 mg scale (Scheme 2.9), which was only 2 more steps away from strictamine (**1**), as reported by Zhu and coworkers[5].

Scheme 2.9 Formal synthesis of (±)-strictamine (**1**) targeting **11**

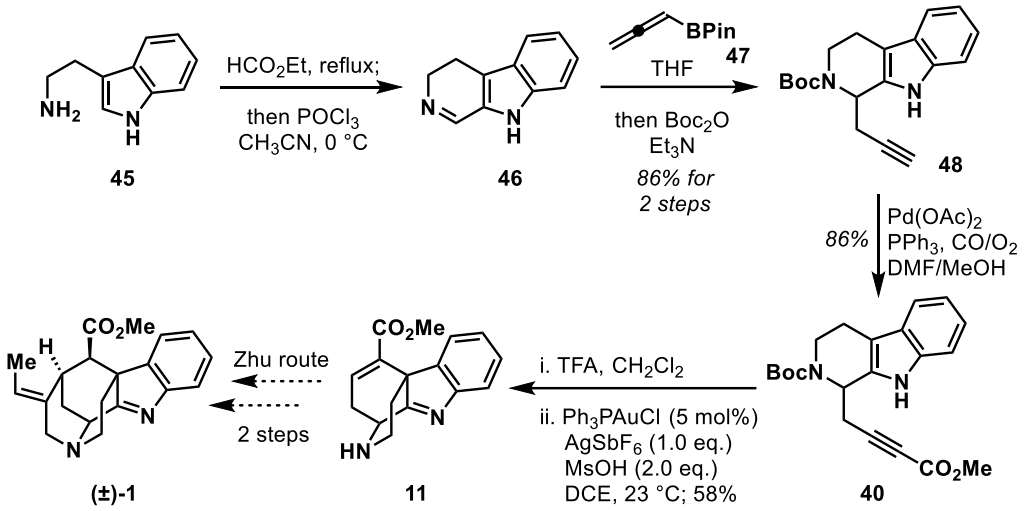

2.5 Enantioselective Propargylation and Its Application in the Total Synthesis of (+)-Strictamine and (–)-Decarbomethoxydihydrogambirtannine

After completing the formal synthesis of racemic strictamine (**1**), our next goal was to achieve an asymmetric formal synthesis, which would require the development of asymmetric propargylation of cyclic imine **46**, a method that remained blank at the time[17]. The most similar cases includes enantioselective propargylation between allenylBPin (**47**) and aldehydes, ketones or activated imines[18], in which either chiral phosphoric acid catalysis[18b,c] or transition metal catalysis, such as copper[18a,e] or silver[18d] complexes, were employed (Scheme 2.10).

Scheme 2.10 Previous examples on allenylBPin (**47**) mediated enantioselective propargylation reactions

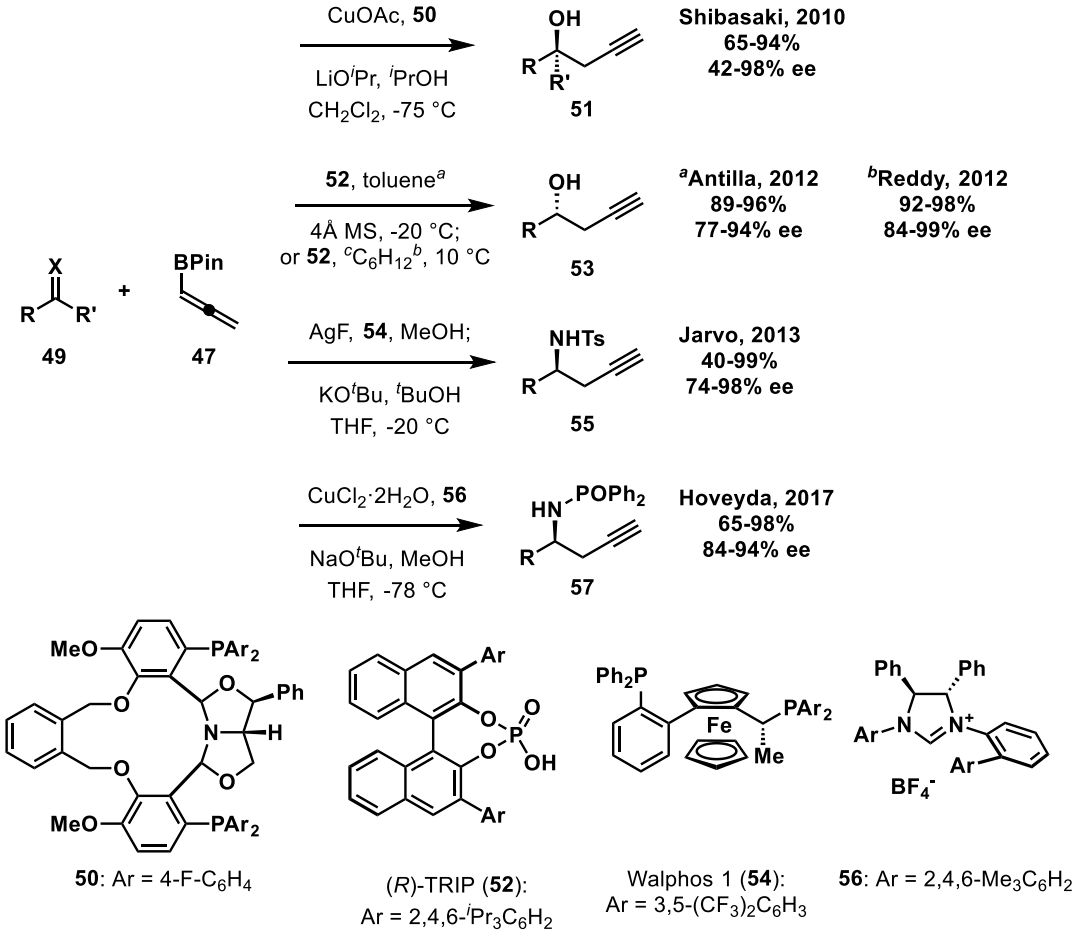

There were a few other examples of catalytic asymmetric propargylation and allylation of unactivated, cyclic imines[17,19]. Itoh and coworkers developed[19a] and optimized[19b] a copper-biphosphine catalyzed asymmetric allylation of cyclic imines **58** using allylsilane **59** with acceptable enantioselectivity (Scheme 2.11). During the time of our research, Fandrick and coworkers reported another copper-biphosphine catalyst system enabling the asymmetric propargylation of cyclic imines[17] (including **46**) with good yield and enantioselectivity, although in the case of **46**, a relatively high catalyst loading (20 mol%) was required (Scheme 2.11).

Scheme 2.11 Previous examples on enantioselective addition of cyclic imines

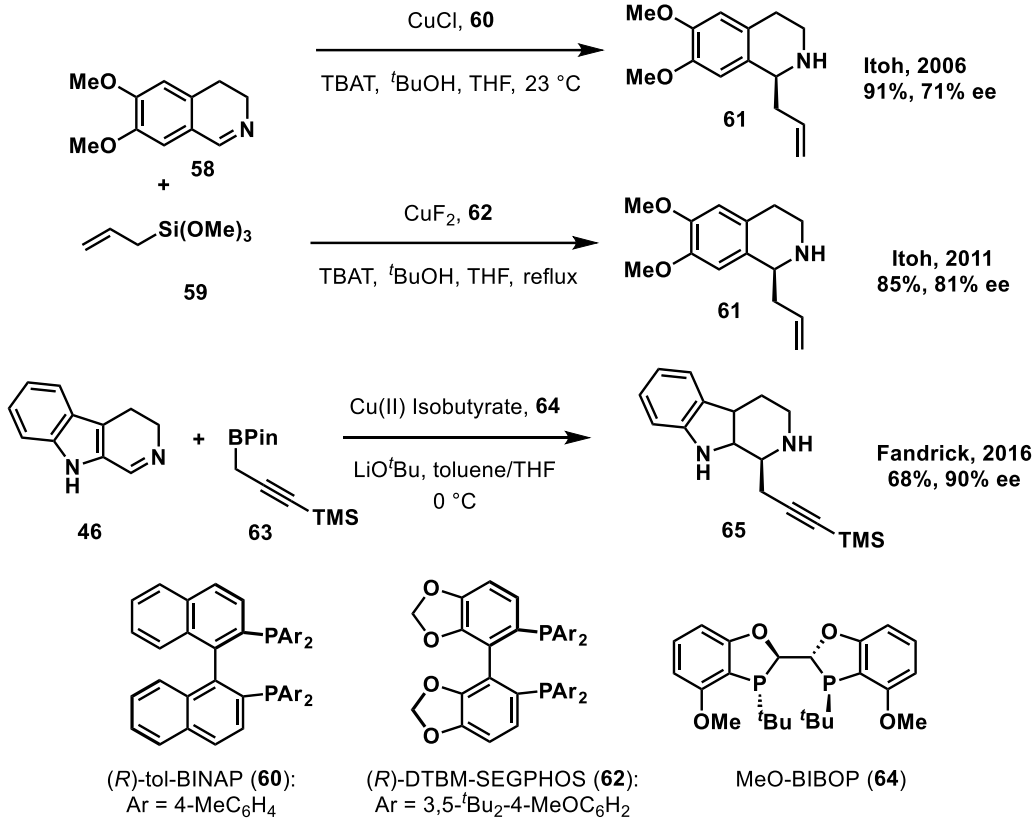

Based on known precedence, my coworker, Dr. Alison Gao, a senior grad student in our lab, started the reaction screening with TRIP catalyst (**52**) and various biphosphine ligands. She ultimately identified the optimal condition to be the combination of CuCl, NaO^{t}Bu and (*R*)-DTBM-SEGPHOS (**62**)[14]. With such condition in hand, a 63% yield and 86% ee value could be obtained on 136 mg scale to afford chiral Boc-amide **48**. The successful installment of such chiral center in **48** let us accomplish the asymmetric formal synthesis of (+)-strictamine [(+)-**1**], following the same route (Scheme 2.12).

Scheme 2.12 Enantioselective propargylation enabled formal synthesis of (+)-strictamine [(+)-**1**]

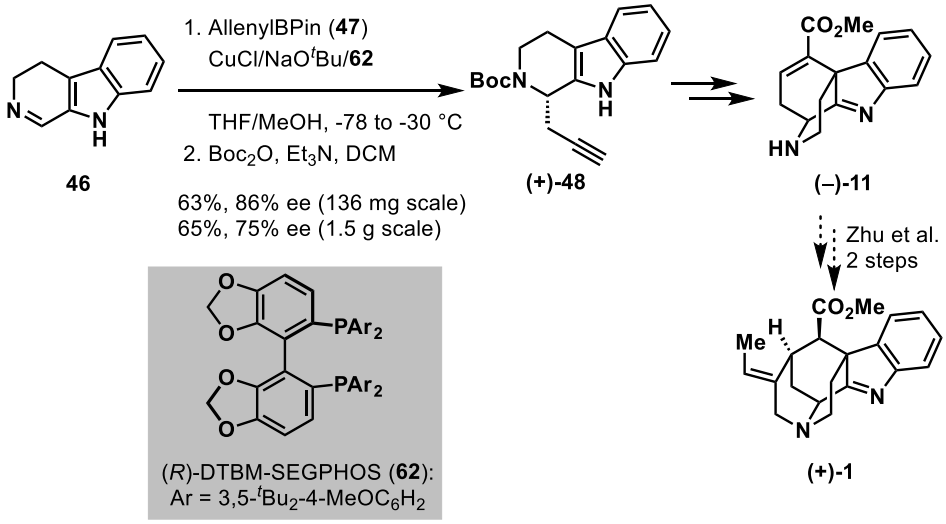

To further expand the utility of this catalytic enantioselective method, we also completed the total synthesis of (S)-(–)-decarbomethoxydihydrogambirtannine (**67**) through a rapid, three-step sequence starting from (+)-**48** (Scheme 2.13). The synthetic route of racemic **67** was previously scouted by my coworker, Dr. Takuya Shimbayashi, a visiting graduate student in our lab. Thus, a pyrone containing side chain **65**[20] was installed after Boc-removal of **48**, and an intramolecular thermal Diels-Alder/retro Diels-Alder reaction took place smoothly to give the target molecule **67**. Though this simple alkaloid has been prepared ten times[21], there is only one asymmetric synthesis of **67** through resolution[21b], and our approach provided the first catalytic enantioseletive solution. Furthermore, the versatility of the alkyne functional group would create great opportunities in the fast, asymmetric synthesis of other indole alkaloids (Scheme 2.13) such as dihydrogambirtannine (**68**)[22] and arborescidine C (**69**)[23]. The comparison of the optical rotation value of **67** also allowed us to determine the absolute configuration of starting material **48**.

Scheme 2.13 Enantioselective synthesis of **67** and other potential targets

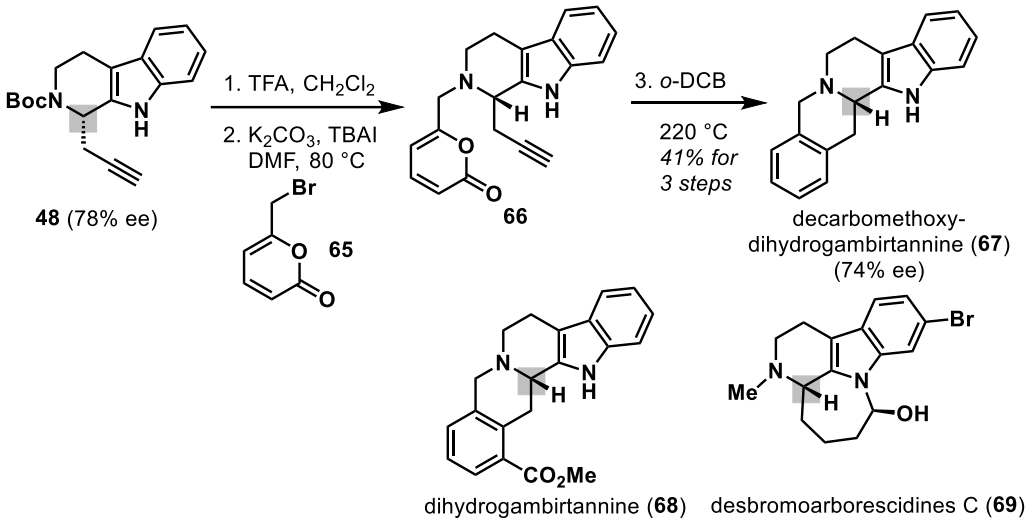

2.6 Conclusion

In this chapter, we have accomplished a concise formal synthesis of strictamine (6-step racemic and 7-step asymmetric). The highly efficient synthesis was realized through the minimization of protecting group usage and functional group manipulations, featuring a *6-endo*-dig cyclization of a rare protonated ammonium salt serving as a traceless protecting group. Such strategy exhibits tremendous potential in the rapid construction of the core skeleton in a wide range of Akuammiline alkaloids. The development of asymmetric propargylation reaction by my coworker, Dr. Alison Gao, also opened up additional avenues towards the enantioselective synthesis of various indole alkaloids.

2.7 Experimental Details

General Procedures. All reactions were carried out under an argon atmosphere with dry solvents under anhydrous conditions, unless otherwise noted. Dry

tetrahydrofuran (THF), toluene, acetonitrile, and dichloromethane (CH_2Cl_2) were obtained by passing commercially available pre-dried, oxygen-free formulations through activated alumina columns. Yields refer to chromatographically and spectroscopically (^1H and ^{13}C NMR) homogeneous materials, unless otherwise stated. Reagents were purchased at the highest commercial quality and used without further purification, unless otherwise stated. Reactions were magnetically stirred and monitored by thin-layer chromatography (TLC) carried out on 0.25 mm E. Merck silica gel plates (60F-254) using UV light as visualizing agent, and an ethanolic solution of phosphomolybdic acid and cerium sulfate, and heat as developing agents. Macherey-Nagel® silica gel (60, academic grade, particle size 0.040–0.063 mm) was used for flash column chromatography. The lactam formation reaction was performed using a Biotage microwave tube. Preparative thin-layer chromatography separations were carried out on 0.50 mm E. Merck silica gel plates (60F-254). NMR spectra were recorded on Bruker 500 MHz instruments and calibrated using residual undeuterated solvent as an internal reference. The following abbreviations were used to explain the multiplicities: s = singlet, d = doublet, t = triplet, br = broad, app = apparent. IR spectra were recorded on a Perkin-Elmer 1000 series FT-IR spectrometer. High-resolution mass spectra (HRMS) were recorded on a Waters Synapt G2-Si mass spectrometer using ESI (Electrospray Ionization) at the University of Chicago Mass Spectrometry Laboratory, and Agilent 6244 Tof-MS using ESI (Electrospray Ionization) at the University of Chicago Mass Spectroscopy Core Facility. High-pressure liquid chromatography

(HPLC) was performed on a Shimadzu Prominence UFLC System, using column ChiralPak® AD-H (0.46 cm × 25 cm).

3,4-dihydro-β-carboline (**46**). Prepared using a slightly modified procedure from that reported in the literature.[15] A 100 mL round-bottom flask was charged with tryptamine (**45**, 7.99 g, 49.9 mmol, 1.0 equiv) and ethyl formate (50 mL), and the resulting mixture was heated at reflux for 10 h under argon atmosphere. Upon completion, the reaction contents were cooled to 23 °C, the solvent was removed under reduced pressure, and the residue was then re-dissolved in MeCN (50 mL) and cooled to 0 °C. To this new solution was added a solution of $POCl_3$ (7.44 mL, 79.8 mmol, 1.6 equiv) in MeCN (10 mL) dropwise at 0 °C over 45 min. The resultant reaction mixture was then stirred at 0 °C for an additional 3 h. Upon completion, the reaction contents were poured into 1 M HCl (200 mL) and then transferred to a separatory funnel, washing with Et_2O (3 × 30 mL). The aqueous phase was then transferred into an Erlenmeyer flask and neutralized with saturated NaOH solution at 0 °C with vigorous stirring until a pH of 10 was reached. The resultant aqueous layer was then re-extracted with CH_2Cl_2 (3 × 200 mL). The combined organic layers were then dried ($MgSO_4$), filtered, and concentrated to give **9** (8.03 g, 95% yield) as an orange solid that was used in subsequent steps without any further purification. All spectroscopic data matched that reported in Ref. 15.

***t*-Butyl Carbamate 48**. To a solution of freshly-made 3,4-dihydro-β-carboline [**46**, 3.18 g, prepared from tryptamine (3.01 g, 18.8 mmol, 1.0 equiv)] in THF (180 mL) at 23 °C was slowly added allenylboronic acid pinacol ester (**47**, 3.55 mL, 19.7 mmol, 1.05 equiv). After stirring the reaction contents at 23 °C for 8 h, Et_3N (4 mL, 37.6 mmol, 2.0 equiv) and Boc_2O (6.15 g, 28.8 mmol, 1.5 equiv) were added sequentially and the mixture was stirred at 23 °C for an additional 1 h. Upon completion, the reaction contents were quenched by the addition of saturated aqueous $NaHCO_3$ (50 mL) and then were transferred to a separatory funnel, diluting with CH_2Cl_2 (100 mL). The layers were separated and the aqueous layer was extracted with CH_2Cl_2 (3 × 150 mL). The combined organic layers were then dried ($MgSO_4$), filtered, and concentrated. The resultant crude product was purified by flash chromatography (silica gel, EtOAc/hexanes, 1:10→1:3) to give *t*-butyl carbamate **48** (5.02 g, 86% yield over two steps from tryptamine) as a light yellow foam. **48**: R_f = 0.67 (silica gel, EtOAc/hexanes, 1/2); IR (film) ν_{max} 3307, 2975, 2927, 2852, 1671, 1415, 1367, 1253, 1233, 1166, 1114, 1103, 742 cm^{-1}; ^1H NMR (500 MHz, $CDCl_3$) δ 8.41–8.36 (m, 1 H), 7.50 (d, *J* = 7.7 Hz, 1 H), 7.35 (d, *J* = 8.0 Hz, 1 H), 7.18 (t, *J* = 7.5 Hz, 1 H), 7.11 (t, *J* = 7.4 Hz, 1 H), 5.43–5.27 (m, 1 H, two rotamers), 4.52–4.33 (m, 1 H, two rotamers), 3.15–3.07 (m, 1 H, two rotamers), 2.82–2.64 (m, 4 H), 2.26–2.25 (m, 1 H, two rotamers), 1.51 and 1.48 (s, 9 H, two rotamers); ^{13}C NMR (125 MHz, $CDCl_3$) 154.6 (154.2), 136.0, 133.1 (132.7), 126.3, 121.8, 119.3, 118.1, 111.0, 109.5 (108.8), 81.4, 80.3, 71.4, 50.3 (49.4), 39.3 (38.0), 28.4, 24.2 (23.9), 21.5 (21.2); HRMS (ESI) calcd for $C_{19}H_{23}N_2O_2^+$ [M + H^+] 311.1754, found 311.1743.

Ynoate Ester 40. Using a procedure modified from Kim and co-workers,[16] a solution of alkyne **48** (3.10 g, 10.0 mmol, 1.0 equiv 0.103 g, 0.382 mmol, 1.0 equiv) in MeOH (40 mL) was added to a stirred suspension of $Pd(OAc)_2$ (0.670 g, 3.00 mmol, 0.3 equiv) and Ph_3P (1.57 g, 6.00 mmol, 0.6 equiv) in DMF (80 mL) at 23 °C. The resultant mixture was then placed under an atmosphere of CO and O_2 (~1:1) and stirred at 23 °C for 16 h. Upon completion, the reaction contents were quenched by the addition of water (10 mL) and then transferred to a separatory funnel, diluting with Et_2O (200 mL) and water (50 mL). The layers were separated and the aqueous layer was extracted with Et_2O (3 × 150 mL). The combined organic layers were then washed with water (5 × 50 mL) and brine (50 mL), dried ($MgSO_4$), filtered, and concentrated. The resultant crude product was purified by flash chromatography (silica gel, EtOAc/hexanes, 1:10→1:5→1:3) to give ynoate ester **40** (3.15 g, 86% yield) as a light yellow gum. **40**: R_f = 0.54 (silica gel, EtOAc/hexanes, 1/2); IR (film) ν_{max} 3334, 2979, 2240, 1699, 1436, 1413, 1368, 1264, 1164, 1077, 738 cm^{-1}; ^1H NMR (500 MHz, $CDCl_3$) δ 8.38 and 8.27 (br s, 1 H), 7.50 (br s, 1 H), 7.36 (d, *J* = 8.1 Hz, 1 H), 7.20 (t, *J* = 7.5 Hz, 1 H), 7.12 (t, *J* = 7.3 Hz, 1 H), 5.51–5.34 (br s, 1 H), 4.54 (d, *J* = 10.2 Hz) and 4.35 (d, *J* = 9.1 Hz, 1 H, two rotamers), 3.84 and 3.81 (s, 3 H, two rotamers), 3.21–3.05 (m, 1 H), 2.95–2.74 (m, 4 H), 1.51 (s, 9 H); ^{13}C NMR (125 MHz, $CDCl_3$) δ 154.6 (154.0), 153.8, 136.2, 132.1 (131.7), 126.3, 122.3 (122.1), 119.7 (119.5), 118.4 (118.2), 111.1, 110.1, 109.4, 86.4, 80.8 (80.6), 75.3, 52.7, 50.0 (49.0), 39.3 (37.8), 28.4, 24.5 (24.2), 21.5 (21.2); HRMS (ESI) calcd for $C_{21}H_{24}N_2O_4Na^+$ [M + Na^+] 391.1628, found 391.1630.

Tetracyclic Amine 11. To a solution of compound **40** (0.450 g, 1.22 mmol, 1.0 equiv) in CH_2Cl_2 (54 mL) at 0 °C was added TFA (6 mL). The reaction contents were then warmed to 23 °C and after further stirring at 23 °C for 45 min, the reaction contents were evaporated directly under reduced pressure. The resultant residue of **41** was then re-dissolved in 1,2-dichloroethane (6 mL) and MsOH (0.160 mL, 2.44 mmol, 2.0 equiv) was added at 23 °C. Meanwhile, in a separate flask, to a solution of Ph_3PAuCl (30.2 mg, 0.061 mmol, 0.05 equiv) in 1,2-dichloroethane (6 mL) was added $AgSbF_6$ (0.420 g, 1.22 mmol, 1.0 equiv) and the resultant mixture was stirred at 23 °C for 15 min, at which point the solution of the deprotected substrate described above was added and the resultant mixture was stirred at 23 °C for 12 h. Upon completion, the reaction contents were quenched by the addition of a 50% aqueous solution of NH_4OH (50 mL) and the resulting slurry was stirred at 23 °C for 1 h. The reaction contents were then transferred to a separatory funnel, diluting with CH_2Cl_2 (100 mL). The layers were separated and the aqueous layer was extracted with CH_2Cl_2 (3 × 100 mL). The combined organic layers were then dried ($MgSO_4$), filtered, and concentrated. The resultant crude product was purified by flash chromatography (silica gel, MeOH/Et_3N/CH_2Cl_2, 2:1:100→5:1:100) to give amine **11** (0.189 g, 58% yield) as a brownish yellow foam. Of note, further scaling leads to a decrease in yield, as starting from **40** (0.985 g, 2.68 mmol), following the same procedure mentioned above, **11** could be obtained as a brownish yellow foam (0.166 g, 23% yield) after flash chromatography. **11**: R_f = 0.57 (silica gel, MeOH/CH_2Cl_2, 1/10); IR (film) ν_{max} 3298,

3052, 2951, 1715, 1632, 1598, 1437, 1349, 1282, 1199, 1124, 1074, 911, 831, 774, 748 cm^{-1}; ^{1}H NMR (500 MHz, $CDCl_3$) δ 7.91 (d, *J* = 7.2 Hz, 1 H), 7.63 (d, *J* = 7.7 Hz, 1 H), 7.36 (td, *J* = 7.6, 1.2 Hz, 1 H), 7.22 (td, *J* = 7.5, 1.0 Hz, 1 H), 7.07 (t, *J* = 3.6 Hz, 1 H), 4.20 (d, *J* = 6.2 Hz, 1 H), 3.75 (s, 3 H), 3.07–3.02 (m, 1 H), 2.92–2.85 (m, 4 H), 2.33 (br s, 1 H), 1.40–1.34 (m, 1 H); ^{13}C NMR (125 MHz, $CDCl_3$) δ 184.9, 165.7, 155.8, 141.5, 140.2, 128.3, 129.6, 126.2, 125.4, 120.7, 55.1, 51.6, 50.8, 41.9, 37.9, 36.7; HRMS (ESI) calcd for $C_{16}H_{17}N_2O_2^+$ [M + H^+] 269.1285, found 269.1280. All spectroscopic data matched that reported by Zhu and co-workers[5] as denoted below in Table 2.3 and 2.4.

Table 2.3 ^{1}H NMR data comparison of synthetic **11** with reported intermediate from Zhu

^{1}H NMR (in $CDCl_3$)	
Our intermediate 11 (500 MHz)	**Zhu's intermediate** (400 MHz)
7.91 (d, *J* = 7.2 Hz, 1 H)	7.93 (d, J = 7.5 Hz, 1 H)
7.63 (d, *J* = 7.7 Hz, 1 H)	7.66 (d, J = 7.7 Hz, 1 H)
7.36 (td, *J* = 7.6, 1.2 Hz, 1 H)	7.39–7.36 (m, 1 H)
7.22 (td, *J* = 7.5, 1.0 Hz, 1 H)	7.25–7.21 (m, 1 H)
7.07 (t, *J* = 3.6 Hz, 1 H)	7.09–7.07 (m, 1 H)
4.20 (d, *J* = 6.2 Hz, 1 H)	4.21 (d, J = 6.2 Hz, 1 H)
3.75 (s, 3 H)	3.76 (s, 3 H)
3.07–3.02 (m, 1 H)	3.09–3.02 (m, 1 H)
2.92–2.85 (m, 4 H)	2.98–2.80 (m, 4 H)
2.33 (br s, 1 H)	2.00 (br s, 1 H)
1.40–1.34 (m, 1 H)	1.41–1.34 (m, 1 H)

Table 2.4 ^{13}C NMR data comparison of synthetic **11** with reported intermediate from Zhu

^{13}C NMR (in $CDCl_3$)	
Our intermediate 11 (125 MHz)	**Zhu's intermediate** (101 MHz)
184.9	185.1
165.7	165.9
155.8	156.1
141.5	141.7
140.2	140.4
129.6	129.9
128.3	128.5
126.2	126.4
125.4	125.6
120.7	120.9
55.1	55.3
51.6	51.8
50.8	51.0
41.9	42.2
37.9	38.1
36.7	37.0
77.0 (t, $CDCl_3$)	77.2 (t, $CDCl_3$)

TFE Ynoate Ester 43. Performed as described above for compound **40** using **48** (0.500 g, 1.61 mmol, 1.0 equiv), $Pd(OAc)_2$ (0.108 g, 0.48 mmol, 0.3 equiv), Ph_3P (0.254 g, 0.97 mmol, 0.6 equiv) in a solvent mixture comprised of 2,2,2-trifluoroethanol (5 mL) and DMF (10 mL). Following initial work-up, the resultant crude product was purified by flash chromatography (silica gel, EtOAc/hexanes, 1:10→1:5) to give ynoate ester **43** (0.262 g, 37% yield) as a brownish yellow gum. **43**: R_f = 0.38 (silica gel, EtOAc/hexanes, 1/4); IR (film) ν_{max} 3324, 2978, 2931, 2242, 1732, 1692, 1670, 1452,

1413, 1368, 1294, 1233, 1168, 1086, 988, 966, 942, 852, 743 cm^{-1}; ^{1}H NMR (500 MHz, $CDCl_3$) δ 8.72 and 8.26 (br s, 1H, two rotamers), 7.50 (d, *J* = 7.5 Hz, 1 H), 7.33 (d, *J* = 7.5 Hz, 1 H), 7.21–7.18 (m, 1 H), 7.14–7.11 (m, 1 H), 5.65–5.42 (m, 1 H, two rotamers), 4.58–4.39 (m, 3 H), 3.27 (t, *J* = 10.7 Hz) and 3.11 (t, *J* = 10.6 Hz, 1 H, two rotamers), 2.98–2.75 (m, 4 H), 1.57 and 1.54 (s, 9 H, two rotamers); ^{13}C NMR (125 MHz, $CDCl_3$) δ 154.8 (154.0), 151.3, 136.2, 131.8 (131.4), 126.3, 122.5 (q, *J* = 277.3 Hz), 122.5 (122.2), 119.8 (119.6), 118.4 (118.2), 111.2, 110.3 (109.4), 89.2, 80.9 (80.8), 73.9 (73.7), 61.2 (q, *J* = 36.7 Hz) [61.0 (q, *J* = 36.7 Hz)], 49.8 (48.9), 39.2 (37.8), 28.4, 24.7 (24.4), 21.4 (21.1); HRMS (ESI) calcd for $C_{22}H_{24}F_3N_2O_4^+$ [M + H^+] 437.1683, found 437.1670.

Compound 44. To a solution of compound **43** (40.0 mg, 0.09 mmol, 1.0 equiv) in CH_2Cl_2 (4.5 mL) at 0 °C was added TFA (0.5 mL). The reaction contents were then warmed to 23 °C and after further stirring at that temperature for 45 min, the reaction contents were evaporated directly under reduced pressure. The resultant residue was then redissolved in 1,2-dichloroethane (1.5 mL) and methanesulfonic acid (12 μL, 0.18 mmol, 2.0 equiv) was added at 23 °C. Meanwhile, in a separate flask, to a solution of Ph_3PAuCl (4.6 mg, 0.009 mmol, 0.10 equiv) in 1,2-dichloroethane (1 mL) was added $AgBF_4$ (18.0 mg, 0.09 mmol, 1.0 equiv) or $AgSbF_6$ (31.6 mg, 0.09 mmol, 1.0 equiv) and the resultant mixture was stirred at 23 °C for 15 min, at which point the solution of the deprotected substrate described above was added and the resultant mixture was stirred at 50 °C for 3 h. The reaction mixture was then cooled to 23 °C and Et_3N (0.13

mL, 0.92 mmol, 10 equiv) and Boc_2O (40.0 mg, 0.18 mmol, 2.0 equiv) was added successively. The reaction mixture was then stirred at 23 °C for 1 h. Upon completion, the reaction mixture was quenched by the addition of saturated aqueous $NaHCO_3$ (5 mL) and then were transferred to a separatory funnel, diluting with CH_2Cl_2 (20 mL). The layers were separated and the aqueous layer was extracted with CH_2Cl_2 (3 × 20 mL). The combined organic layers were then dried ($MgSO_4$), filtered, and concentrated. The resultant crude product was purified by flash chromatography (silica gel, EtOAc/hexanes, 1:10→1:2) to give compound **44** (9.7 mg, 24% yield with $AgBF_4$; 9.1 mg, 23% yield with $AgSbF_6$) as a light yellow oil. **44**: R_f = 0.60 (silica gel, EtOAc/ hexanes, 1/2); IR (film) ν_{max} 2977, 2931, 1734, 1696, 1456, 1395, 1367, 1292, 1220, 1167, 1120, 1073, 982, 918, 773, 750, 734 cm^{-1}; ^1H NMR (500 MHz, $CDCl_3$) δ 7.89 (d, *J* = 7.5 Hz, 1 H), 7.67 (d, *J* = 7.5 Hz, 1 H), 7.41 (td, *J* = 7.6, 0.9 Hz, 1 H), 7.28–7.25 (m, 1 H), 7.22 (s, 1 H), 5.54–5.41 (m, 1H, two rotamers), 4.64– 4.60 (m, 1 H), 4.48 (br s, 1 H), 4.14–4.01 (m, 1 H, two rotamers), 3.21–3.16 (m, 1 H), 2.95–2.77 (m, 3 H), 1.48 (s, 9 H), 1.41–1.39 (m, 1 H); ^{13}C NMR (125 MHz, $CDCl_3$) δ 181.0, 163.0, 155.6, 154.1, 143.4, 142.8, 138.8, 128.9, 128.6, 126.2, 122.9 (q, *J* = 275.6 Hz), 121.2, 80.9, 60.6 (q, *J* = 36.7 Hz), 54.6, 50.3 (49.2), 37.1 (38.1), 34.4 (34.7), 28.3; HRMS (ESI) calcd for for $C_{22}H_{24}F_3N_2O_4^+$ [M + H^+] 437.1683, found 437.1681.

Alkaloid (–)-**67**. To a solution of chiral **48** (0.146 g, 0.47 mmol, 1.0 equiv, ee = 78%, obtained from Alison) in CH_2Cl_2 (5 mL) at 0 °C was added TFA (2.5 mL). The reaction contents were then warmed to 23 °C and after further stirring at 23 °C for

30 min, the reaction contents were evaporated directly under reduced pressure. The residue was dissolved in CH_2Cl_2 (50 mL) and washed with saturated aqueous $NaHCO_3$ (3 × 10 mL). The organic layer was then dried ($MgSO_4$), filtered, and concentrated. The residue was re-dissolved in DMF (5 mL) and 6-bromomethyl-2-pyrone (**65**, 0.098 g, 0.52 mmol, 1.1 equiv) [20], K_2CO_3 (0.130 g, 0.94 mmol, 2.0 equiv) and TBAI (34.7 mg, 0.09 mmol, 0.20 equiv) was added under argon. The reaction mixture was heated to 80 °C and stirred for 8 h. After cooling down to 23 °C, the reaction mixture was diluted with Et_2O (25 mL) and water (10 mL). The layers were separated and the aqueous layer was extracted with Et_2O (3 × 25 mL). The combined organic layers were then washed with water (5 × 15 mL) and brine (15 mL), dried ($MgSO_4$), filtered, and concentrated. The resultant crude **66** (0.150 g) was transferred to a microwave tube and *o*-DCB (6 mL) was added. The resulting solution was bubbled with argon for 1 h and then the vial was capped. The reaction mixture was then stirred at 220 °C for 2 h under microwave irradiation. Upon completion, the reaction mixture was loaded on column and purified by flash chromatography (silica gel, EtOAc/hexanes, 0:1→1:10→1:5) to give (–)-**67** (61.2 mg, 41% yield over three steps) as a light orange oil. (–)-**67**: R_f = 0.25 (silica gel, EtOAc/hexanes, 1/2); IR (film) ν_{max} 3408, 3052, 2905, 2801, 1494, 1451, 1346, 1321, 1272, 1161, 1106, 982, 743 cm^{-1}; ^1H NMR (500 MHz, $CDCl_3$) δ 7.89 (br. s, 1H), 7.53 (d, *J* = 7.6 Hz, 1H), 7.34 (d, *J* = 7.9 Hz, 1H), 7.20–7.10 (m, 6H), 4.12 (d, *J* = 14.9 Hz, 1H), 3.80 (d, *J* = 14.9 Hz, 1H), 3.72 (d, *J* = 11.4 Hz, 1H), 3.31 (dd, *J* = 11.1, 5.0 Hz, 1H), 3.21 (dd, *J* = 15.7, 3.7 Hz, 1H), 3.11–3.01 (m, 2H), 2.85–2.81 (m, 1H), 2.76 (td, *J* = 11.4, 4.0 Hz, 1H); ^{13}C NMR (125 MHz, $CDCl_3$) δ 136.33, 134.56, 134.39,

133.16, 128.63, 127.18, 126.43, 126.34, 126.11, 121.61, 119.53, 118.24, 110.80, 108.77, 57.78, 56.32, 52.38, 34.80, 21.49; HRMS (ESI) calcd for $C_{19}H_{19}N_2^+$ [M + H^+] 275.1543, found 275.1544; the enantiopurity was determined using chiral HPLC (AD-H column, 9:1 hexanes/*i*-PrOH, 1 mL/min) and found to be 74% ee; $[\alpha]_D^{23}$ = –132° (*c* = 0.1, $CHCl_3$).

2.8 References

[1] Schnoes, H. K.; Biemann, K.; Mokry, J.; Kompis, I.; Chatterjee, A.; Ganguli, G. *J. Org. Chem.* **1966**, *31*, 1641.

[2] Ahmad, Y.; Fatima, K.; Rahman, A.; Occolowitz, J. L.; Solheim, B. A.; Clardy, J.; Garnick, R. L.; Le Quesne, P. L. *J. Am. Chem. Soc.* **1977**, *99*, 1943.

[3] (a) S. K. Bhattacharya, R. Bose, S. C. Dutta, A. B. Ray, S. R. Guha. *Indian J. Exp. Biol.* **1979**, *17*, 598; (b) Zhang, L.; Zhang, C. J.; Zhang, D. B.; Wen, J.; Zhao, X. W.; Li, Y.; Gao, K. *Tetrahedron Lett.* **2014**, *55*, 1815; (c) Hou, Y.; Cao, X.; Wang, L.; Cheng, B.; Dong, L.; Luo, X.; Bai, G.; Gao, W. *J. Chromatogr. B* **2012**, *908*, 98.

[4] (a) Moreno, J.; Picazo, E.; Morrill, L. A.; Smith, J. M.; Garg, N. K. *J. Am. Chem. Soc.* **2016**, *138*, 1162; (b) Picazo, E.; Morrill, L. A.; Susick, R. B.; Moreno, J.; Smith, J. M.; Garg, N. K. *J. Am. Chem. Soc.* **2018**, *140*, 6483.

[5] Ren, W.; Wang, Q.; Zhu, J. *Angew. Chem., Int. Ed.* **2016**, *55*, 3500

[6] (a) Solé, D.; Bosch, J.; Bonjoch, J. *Tetrahedron* **1996**, *52*, 4013; (b) Ren, W.; Wang, Q.; Zhu, J. *Angew. Chem. Int. Ed.* **2014**, *53*, 1818.

[7] Smith, M. W. Ph.D. Dissertation, Columbia University, New York, NY, **2015**.

[8] Xie, X.; Wei, B.; Li, G.; Zu, L. *Org. Lett.* **2017**, *19*, 5430.

[9] Li, G.; Xie, X.; Zu, L. *Angew. Chem., Int. Ed.* **2016**, *55*, 10483.

[10] (a) Chen, Z.-T.; Xiao, T.; Tang, P.; Zhang, D.; Qin, Y. *Tetrahedron* **2018**, *74*, 1129; (b) Xiao, T.; Chen, Z.; Deng, L.; Zhang, D.; Liu, X.-Y.; Song, H.; Qin, Y. *Chem. Commun.* **2017**, *53*, 12665.

[11] Li, W.; Chen, Z.; Yu, D.; Peng, X.; Wen, G.; Wang, S.; Xue, F.; Liu, X.-Y.; Qin, Y. *Angew. Chem., Int. Ed.* **2019**, *58*, 6059.

[12] Wang, X.; Xia, D.; Qin, W.; Zhou, R.; Zhou, X.; Zhou, Q.; Liu, W.; Dai, X.; Wang, H.; Wang, S.; Tan, L.; Zhang, D.; Song, H.; Liu, X.-Y.; Qin, Y. *Chem* **2017**, *2*, 803.

[13] (a) Nishiyama, D.; Ohara, A.; Chiba, H.; Kumagai, H.; Oishi, S.; Fujii, N.; Ohno, H. *Org. Lett.* **2016**, 18, 1670; (b) Eckermann, R.; Breunig, M.; Gaich, T. *Chem. Commun.* **2016**, *52*, 11363; (c) Eckermann, R.; Breunig, M.; Gaich, T. *Chem. -Eur. J.* **2017**, *23*, 3938; (d) Sato, K.; Takanashi, N.; Kogure, N.; Kitajima, M.; Takayama, H. *Heterocycles* **2018**, *97*, 365.

[14] Smith, M. W.; Zhou, Z.; Gao, A. X.; Shimbayashi, T.; Snyder, S. A. *Org. Lett.* **2017**, *19*, 1004.

[15] Mirabal-Gallardo, Y.; Soriano, M. D. P. C.; Caballero, J.; Alzate-Morales, J.; Simirgiotis, M. J.; Santos, L. S. *Synthesis* **2012**, *44*, 144.

[16] Kim, G.; Sohn, T.; Kim, D.; Paton, R. S. *Angew. Chem. Int. Ed.* **2014**, *53*, 272

[17] Fandrick, D. R.; Hart, C. A.; Okafor, I. S.; Mercadante, M. A.; Sanyal, S.; Masters, J. T.; Sarvestani, M.; Fandrick, K. R.; Stockdill, J. L.; Grinberg, N.; Gonnella, N.; Lee, H.; Senanayake, C. H. *Org. Lett.* **2016**, *18*, 6192.

[18] (a) Shi, S.-L.; Xu, L.-W.; Oisaki, K.; Kanai, M.; Shibasaki, M. *J. Am. Chem. Soc.* **2010**, *132*, 6638; (b) Jain, P.; Wang, H.; Houk, K. N.; Antilla, J. C. *Angew. Chem., Int. Ed.* **2012**, *51*, 1391; (c) Reddy, L. R. *Org. Lett.* **2012**, *14*, 1142; (d) Kohn, B. L.; Ichiishi, N.; Jarvo, E. R. *Angew. Chem., Int. Ed.* **2013**, *52*, 4414; (e) Mszar, N. W.; Mikus, M. S.; Torker, S.; Haeffner, F.; Hoveyda, A. H. *Angew. Chem., Int. Ed.* **2017**, *56*, 8736.

[19] (a) Itoh, T.; Miyazaki, M.; Fukuoka, H.; Nagata, K.; Ohsawa, A. *Org. Lett.* **2006**, *8*, 1295; (b) Miyazaki, M.; Ando, N.; Sugai, K.; Seito, Y.; Fukuoka, H.; Kanemitsu, T.; Nagata, K.; Odanaka, Y.; Nakamura, K. T.; Itoh, T. *J. Org. Chem.* **2011**, *76*, 534.
[20] Wickel, S. M.; Citron, C. A.; Dickschat, J. S. *Eur. J. Org. Chem.* **2013**, 2906.
[21] (a) Liljegren, D. R.; Potts, K. T. *J. Org. Chem.* **1962**, *27*, 377; (b) Yamada, S.; Kunieda, T. *Chem. Pharm. Bull.* **1967**, *15*, 499; (c) Fry, E. M.; Beisler, J. A. *J. Org. Chem.* **1970**, *35*, 2809; (d) Ninomiya, I.; Naito, T.; Takasugi, H. *J. Chem. Soc., Perkin Trans. 1* **1976**, 1865; (e) Shono, T.; Yoshida, K.; Ando, K.; Usui, Y.; Hamaguchi, H. *Tetrahedron Lett.* **1978**, *19*, 4819; (f) Chatterjee, A.; Ghosh, S. *Synthesis* **1981**, *1981*, 818; (g) Frostell, E.; Jokela, R.; Lounasmaa, M. *Acta Chem. Scand.* **1981**, *35*, 671; (h) Cobas, A.; Guitian, E.; Castedo, L. *J. Org. Chem.* **1992**, *57*, 6765; (i) Knolker, H.-J.; Cammerer, S. *Tetrahedron Lett.* **2000**, *41*, 5035; (j) Pan, X.; Bannister, T. D. *Org. Lett.* **2014**, *16*, 6124;
[22] Merlini, L.; Mondelli, R.; Nasini, G.; Hesse, M. *Tetrahedron*, **1967**, *23*, 3129.
[23] Chbani, M.; Païs, M.; Delauneux, J.-M.; Debitus, C. *J. Nat. Prod.* **1993**, *56*, 99.

2.9 NMR Spectra of Selected Intermediates

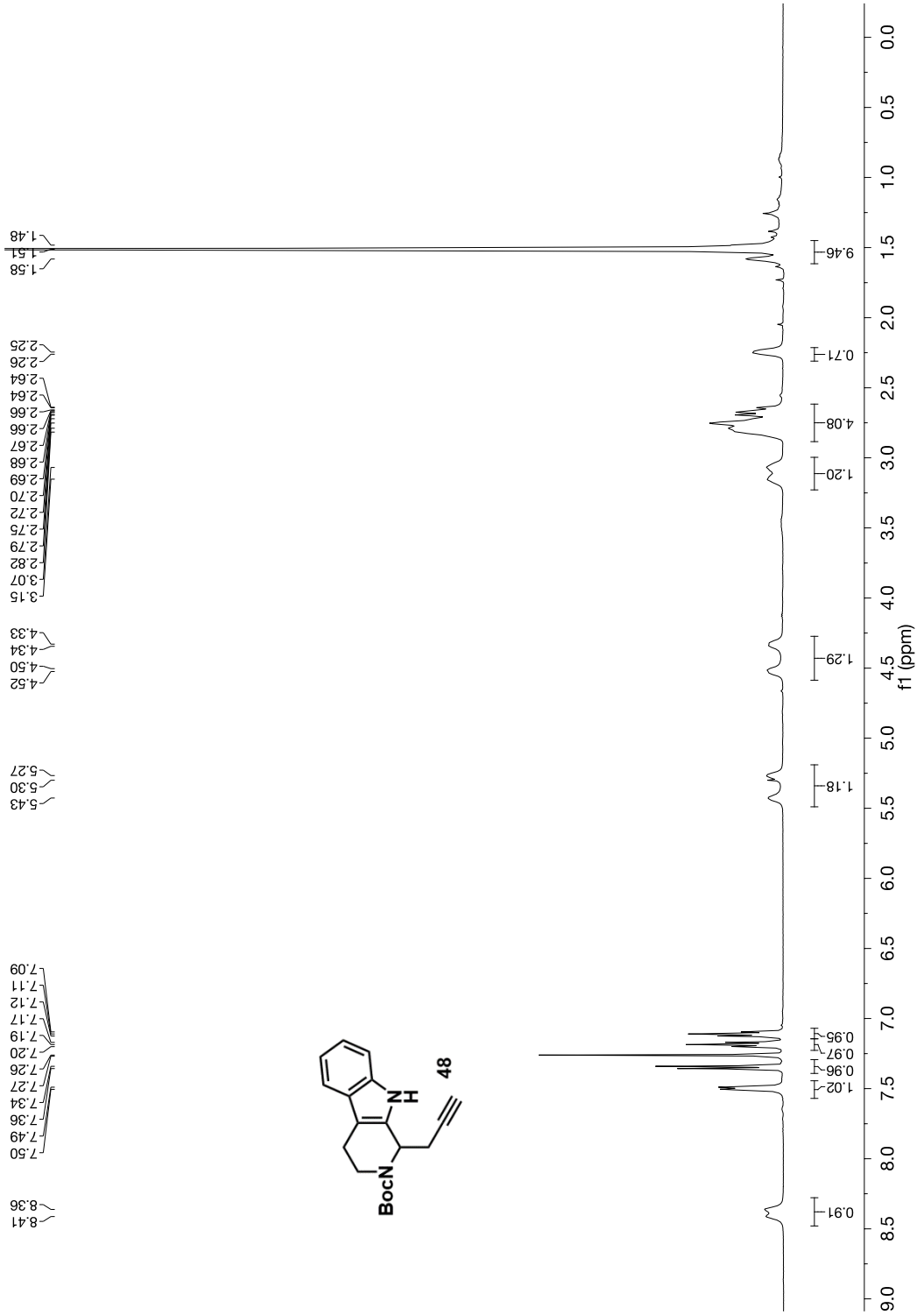

154.60
154.21
135.96
133.06
132.68
126.28
121.84
119.32
118.07
110.97
109.46
108.83
81.36
80.26
77.26
77.00
76.75
71.35
50.30
49.44
39.28
37.93
28.37
24.23
23.88
21.49
21.22
f1 (ppm)
BocN
H
N
48

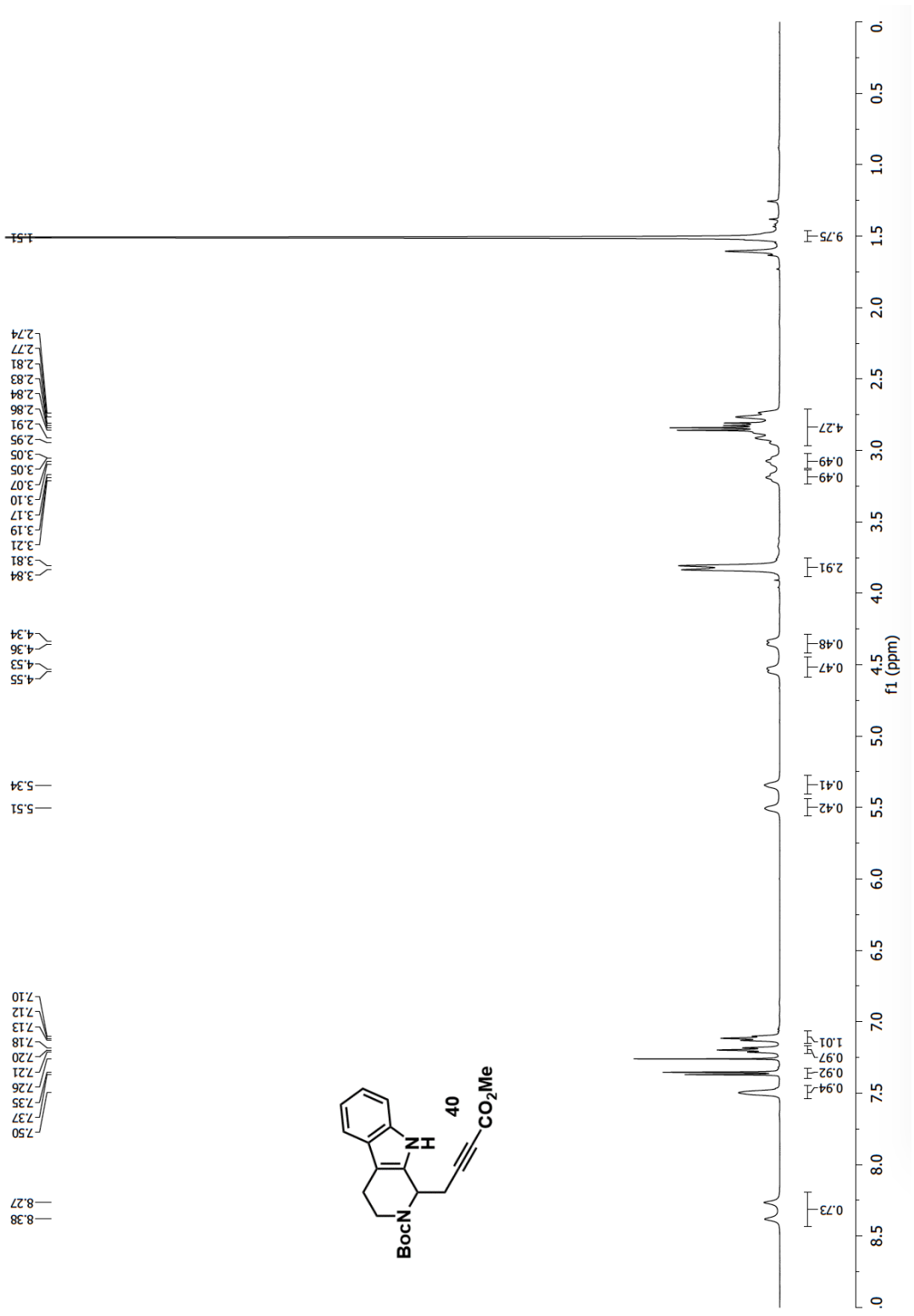
BocN
H
N
40
CO2Me
f1 (ppm)

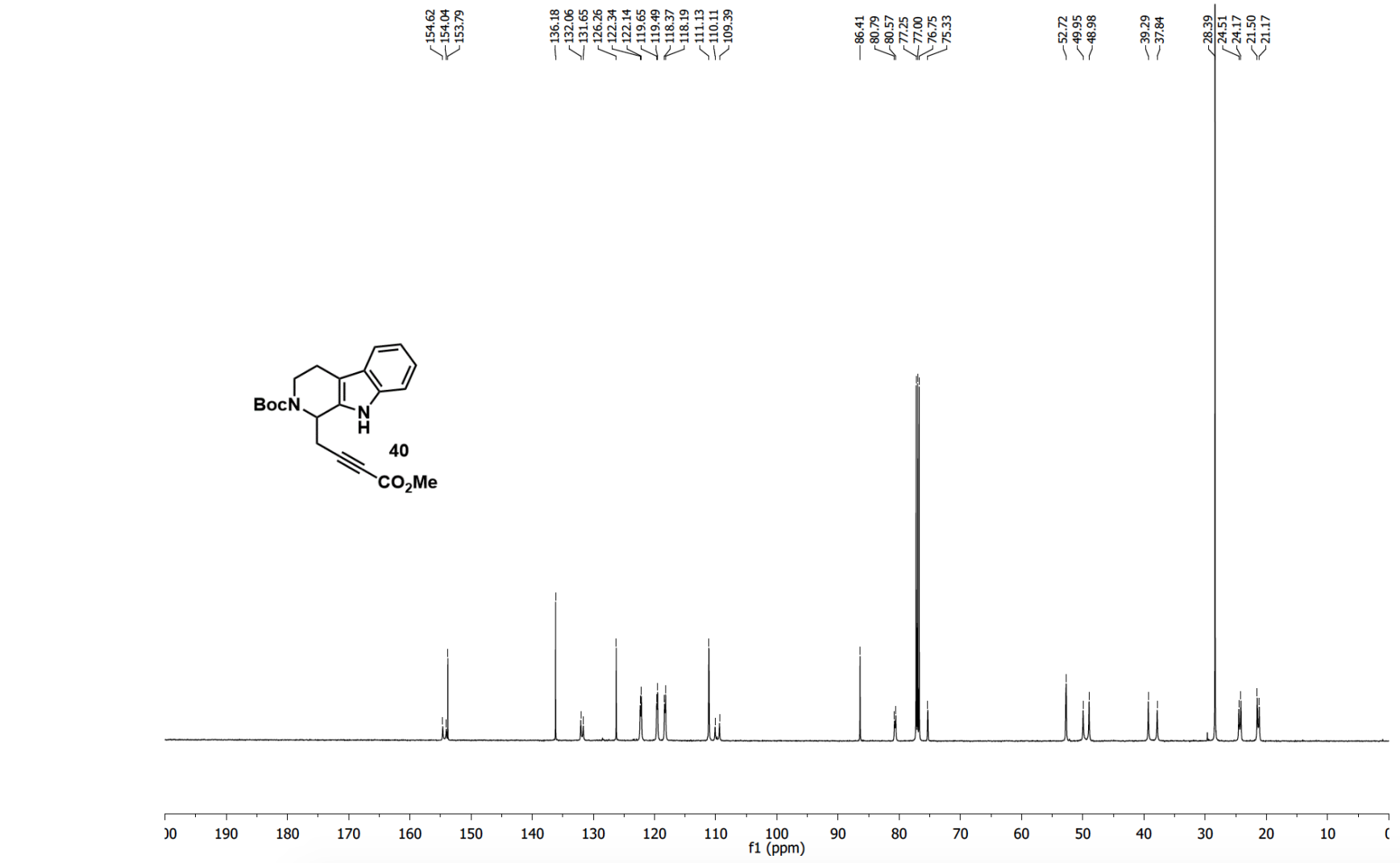
154.62
154.04
153.79
136.18
132.06
131.65
126.26
122.34
122.14
119.65
119.49
118.37
118.19
111.13
110.11
109.39
86.41
80.79
80.57
77.25
77.00
76.75
75.33
52.72
49.95
48.98
39.29
37.84
28.39
24.51
24.17
21.50
21.17
BocN
N
H
40
CO2Me
f1 (ppm)

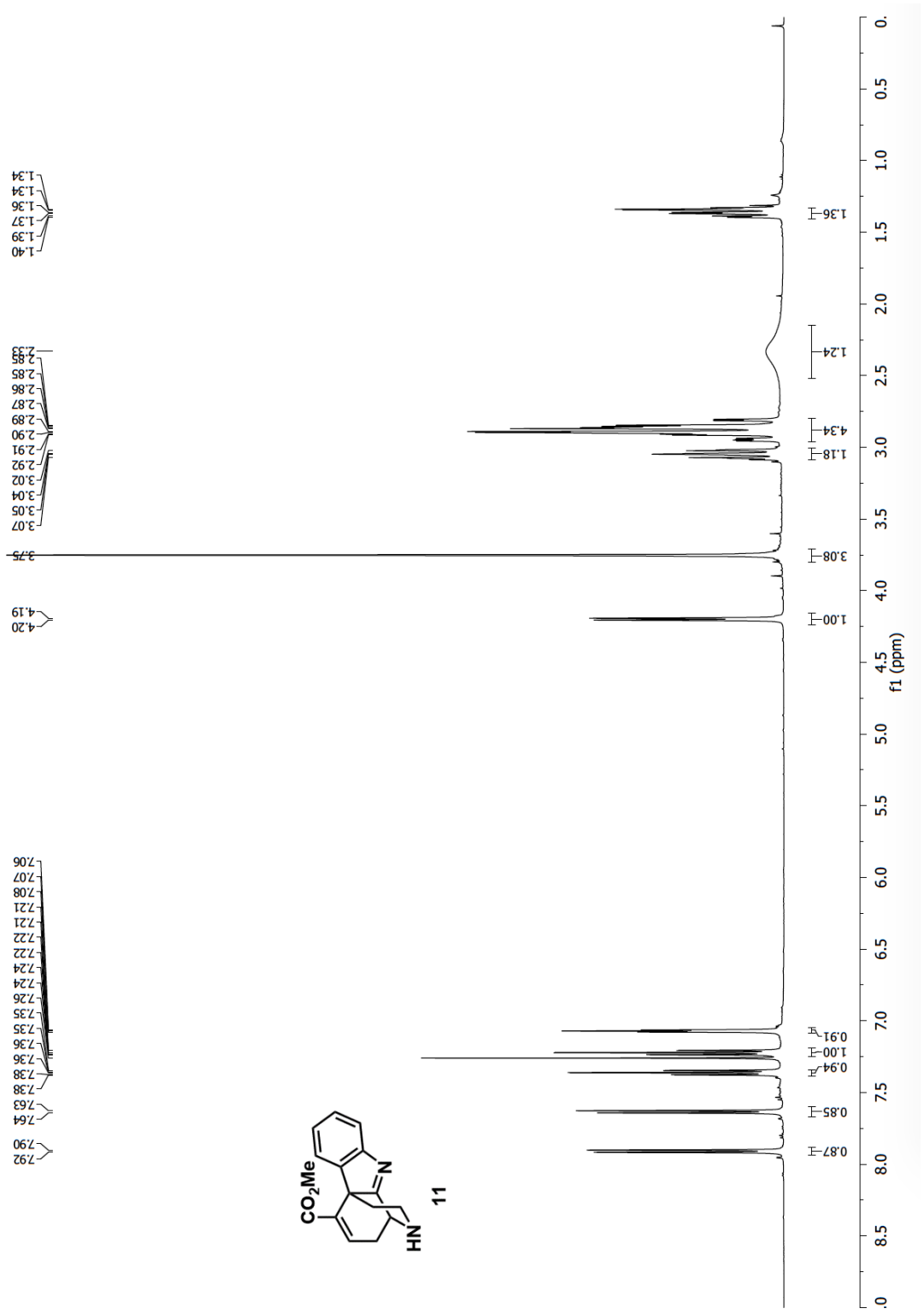
7.92
7.90
7.64
7.63
7.38
7.38
7.36
7.36
7.35
7.35
7.26
7.24
7.24
7.22
7.22
7.21
7.21
7.08
7.07
7.06
4.20
4.19
3.75
3.07
3.05
3.04
3.02
2.92
2.91
2.90
2.89
2.87
2.86
2.85
2.85
2.33
1.40
1.39
1.37
1.36
1.34
1.34
CO2Me
HN
11
0.87
0.85
0.94
1.00
0.91
1.00
3.08
4.34
1.18
1.24
1.36
f1 (ppm)

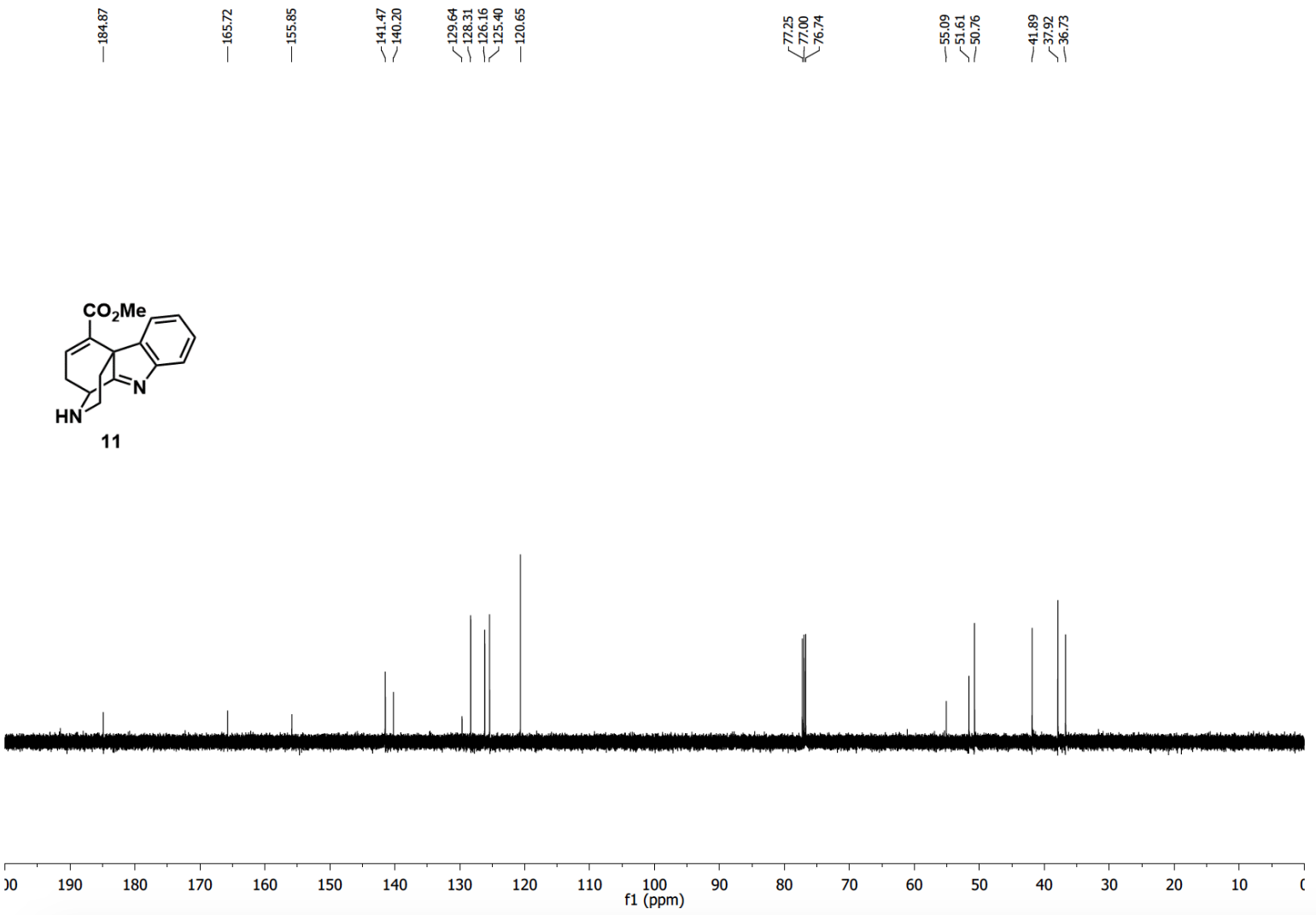
184.87
165.72
155.85
141.47
140.20
129.64
128.31
126.16
125.40
120.65
77.25
77.00
76.74
55.09
51.61
50.76
41.89
37.92
36.73
CO2Me
N
HN
11
f1 (ppm)

8.72
8.26
7.51
7.50
7.34
7.33
7.26
7.21
7.20
7.18
7.14
7.12
7.11
5.65
5.42
4.58
4.48
4.45
4.44
4.41
4.39
3.29
3.27
3.25
3.13
3.11
3.09
2.98
2.98
2.93
2.88
2.85
2.83
2.78
2.78
2.75
2.75
1.57
1.54
BocN
N
H
CO2TFE
43
0.51
0.34
0.99
1.00
1.03
1.00
0.51
0.36
3.02
0.56
0.42
4.15
9.41
f1 (ppm)

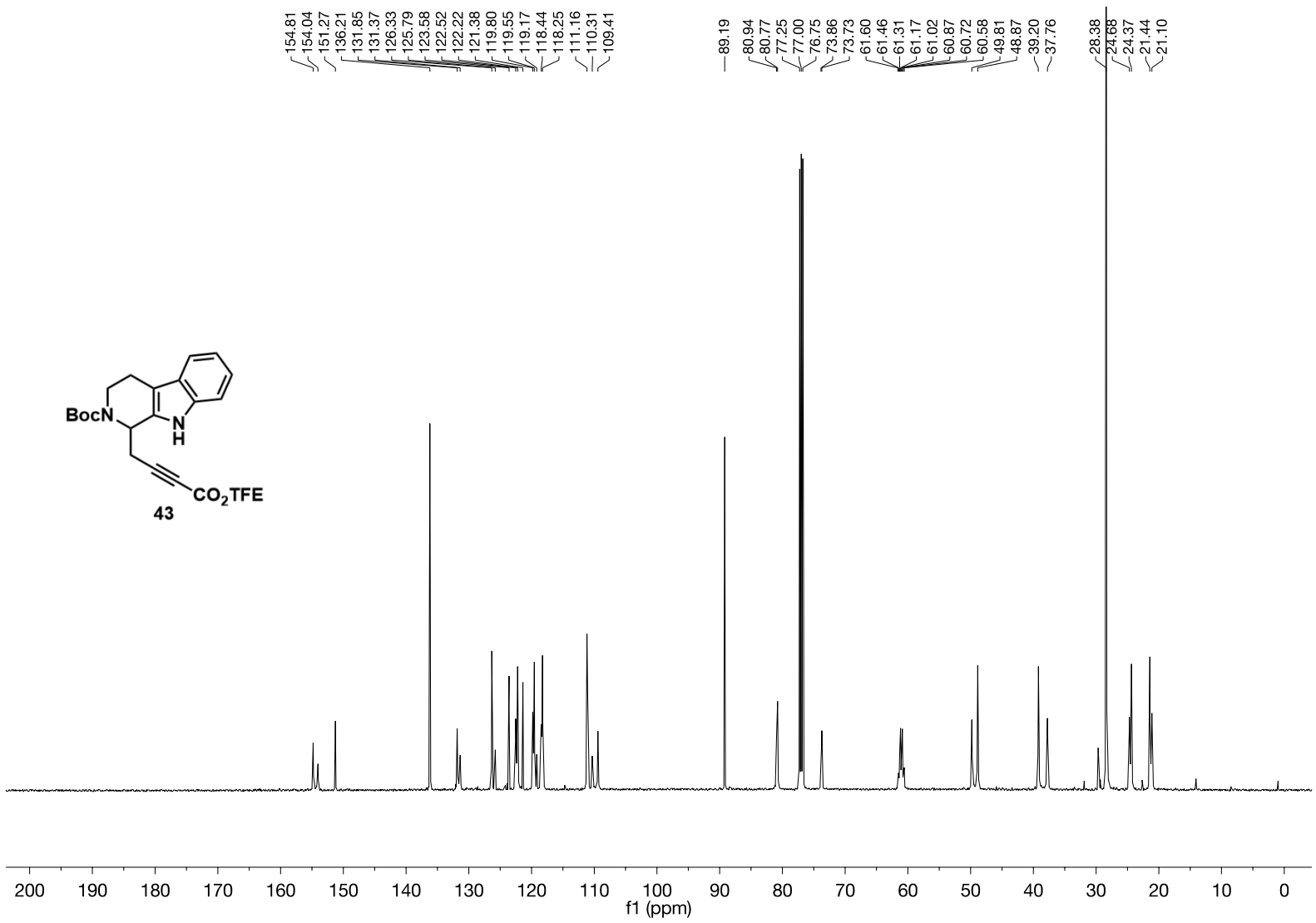
154.81
154.04
151.27
136.21
131.85
131.37
126.33
125.79
123.58
122.52
122.22
121.38
119.80
119.55
119.17
118.44
118.25
111.16
110.31
109.41
89.19
80.94
80.77
77.25
77.00
76.75
73.86
73.73
61.60
61.46
61.31
61.17
61.02
60.87
60.72
60.58
49.81
48.87
39.20
37.76
28.38
24.68
24.37
21.44
21.10
BocN
N
H
CO2TFE
43
200
190
180
170
160
150
140
130
120
110
100
90
80
70
60
50
40
30
20
10
0
f1 (ppm)

7.90
7.89
7.68
7.66
7.42
7.42
7.41
7.41
7.39
7.39
7.28
7.26
7.25
7.22
5.54
5.41
4.64
4.62
4.60
4.48
4.14
4.12
4.11
4.01
3.21
3.19
3.16
2.95
2.94
2.93
2.91
2.90
2.89
2.87
2.83
2.79
2.77
1.48
1.41
1.40
1.39
0.93
0.95
0.96
1.46
0.92
0.38
0.59
1.00
1.00
0.61
0.42
1.00
3.02
8.95
1.11
TFEO
O
N
BocN
44
10.0
9.5
9.0
8.5
8.0
7.5
7.0
6.5
6.0
5.5
5.0
4.5
4.0
3.5
3.0
2.5
2.0
1.5
1.0
0.5
0.0
f1 (ppm)

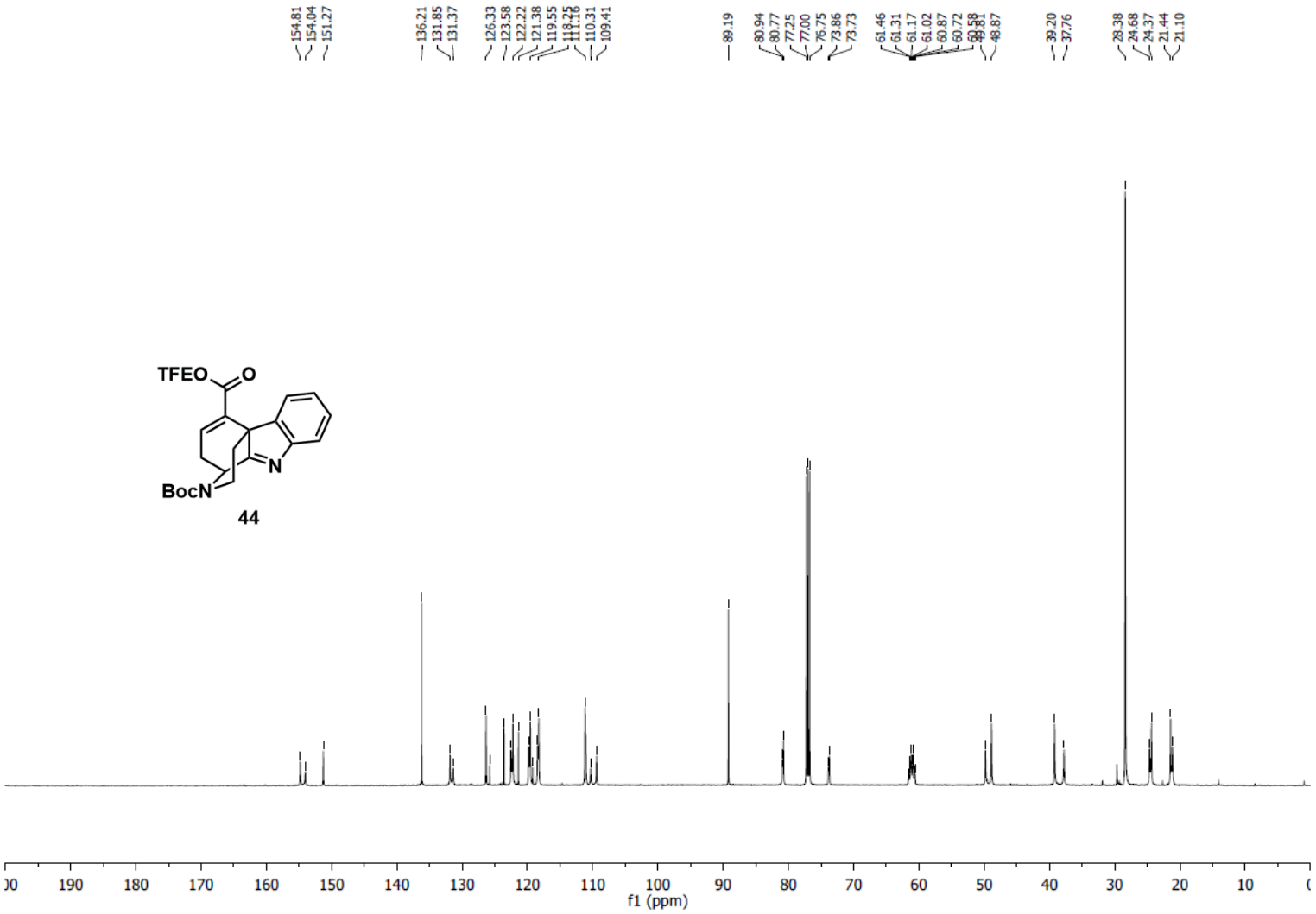
154.81
154.04
151.27
136.21
131.85
131.37
126.33
123.58
122.22
121.38
119.55
118.25
111.16
110.31
109.41
89.19
80.94
80.77
77.25
77.00
76.75
73.86
73.73
61.46
61.31
61.17
61.02
60.87
60.72
48.87
39.20
37.76
28.38
24.68
24.37
21.44
21.10
TFEO
O
N
BocN
44
f1 (ppm)

67
f1 (ppm)

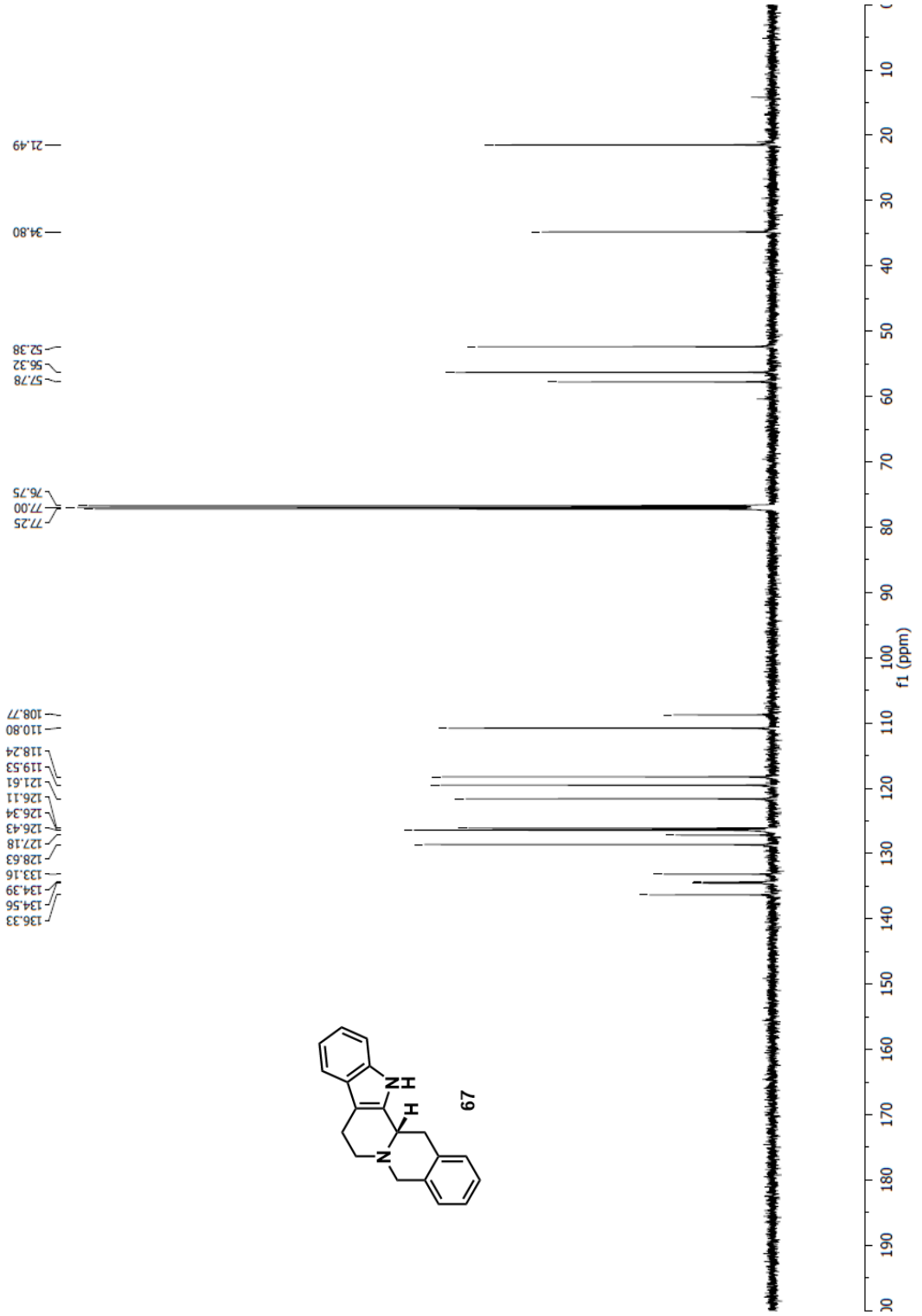
21.49
34.80
52.38
56.32
57.78
76.75
77.00
77.25
108.77
110.80
118.24
119.53
121.61
126.11
126.34
126.43
127.18
128.63
133.16
134.39
134.56
136.33
67
f1 (ppm)

2.10 HPLC Traces of Selected Intermediates

Chiral **48** as starting material (78% ee):

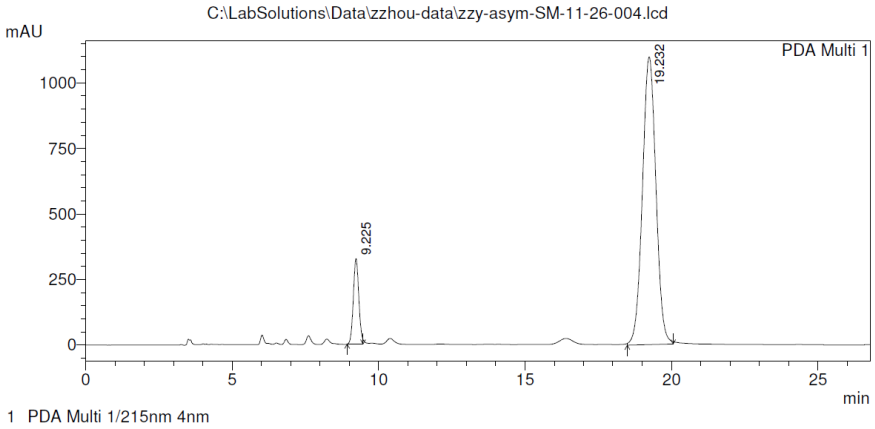

1 PDA Multi 1/215nm 4nm

PeakTable

PDA Ch1 215nm 4nm

Peak#	Ret. Time	Area	Height	Area %	Height %
1	9.225	4224216	325410	10.721	22.871
2	19.232	35178451	1097413	89.279	77.129
Total		39402667	1422823	100.000	100.000

Rac-**67**:

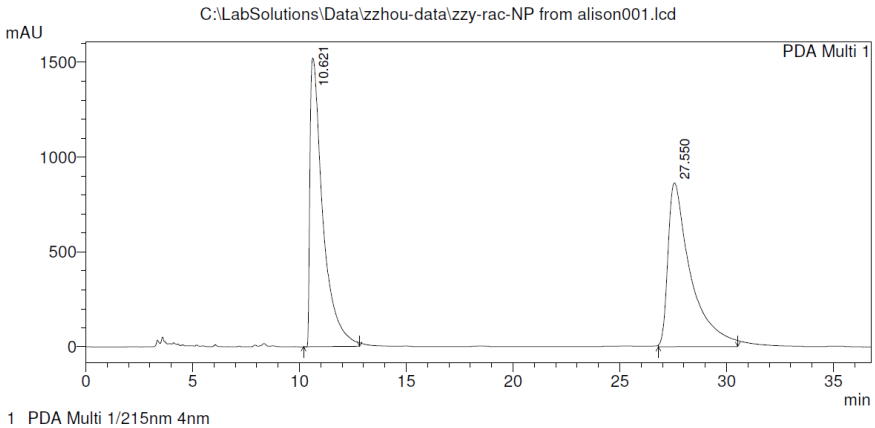

1 PDA Multi 1/215nm 4nm

PeakTable

PDA Ch1 215nm 4nm

Peak#	Ret. Time	Area	Height	Area %	Height %
1	10.621	63931398	1522288	50.109	63.813
2	27.550	63652538	863257	49.891	36.187
Total		127583936	2385545	100.000	100.000

(–)-**67** (74% ee)

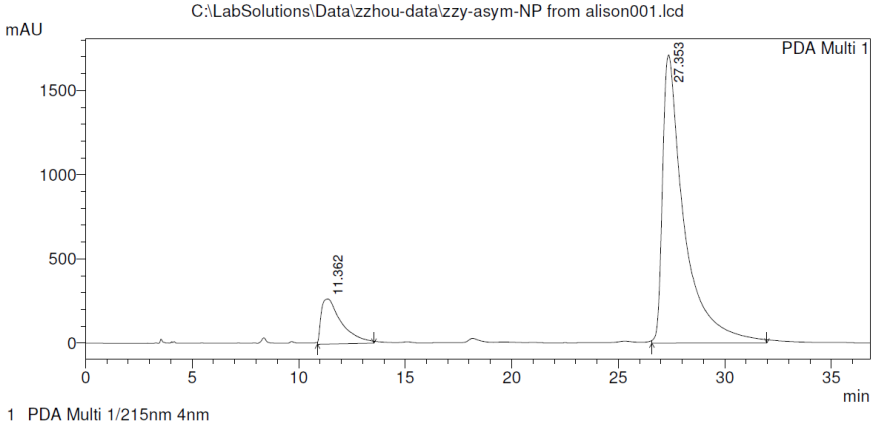

1 PDA Multi 1/215nm 4nm

PeakTable

PDA Ch1 215nm 4nm

Peak#	Ret. Time	Area	Height	Area %	Height %
1	11.362	17772109	266990	12.831	13.504
2	27.353	120734102	1710165	87.169	86.496
Total		138506211	1977155	100.000	100.000

Chapter 3 Total Synthesis of (+)-Arborisidine

3.1 Isolation, Proposed Biosynthesis and Biological Activity

Arborisidine (**1**) is a monoterpenoid indole alkaloid isolated in 2016 from *Kopsia Arborea* blume, by Kam and coworkers (Figure 3.1)[1]. Its structure was assigned via 1D and 2D NMR spectra, which revealed a novel pentacyclic caged scaffold containing an indolizidine and a fully substituted cyclohexanone moiety. The specific caged polycyclic structure quickly drew our attention, as our lab has been continuously interested in related indole alkaloid natural products with such complexity, including strictamine (**2**)[2] and arboridinine (**3**)[3], the latter being isolated from the same species and by the same group[4]. Of notes, the densely substituted cyclohexanone core (Figure 3.1) as well as the presence of an *aza*-quaternary stereocenter can pose considerable synthetic challenges, as is discussed below in our own exploration.

Figure 3.1 Arborisidne, its structural feature, and related natural products

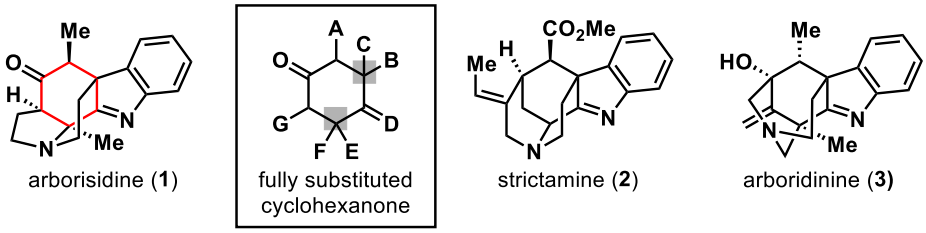

The isolation team proposed a biosynthesis pathway of arborisidine, starting from pericine (**4**, Scheme 3.1)[1]. They first proposed the epoxidation of alkene, which then triggers a transannular Friedel-Crafts type cyclization to generate the caged precursor **6**. A subsequent oxidative fragmentation is initiated by oxidation of the tertiary amine, followed by the hydrolysis of iminium **8** to give intermediate **9**. An intramolecular hydroamination then sets the ultimate ring junction, and an epimerization of **11** would provide **1**, presumably driven by thermaldynamics.

Scheme 3.1 Proposed biosynthesis pathway of arborisidine (**1**)

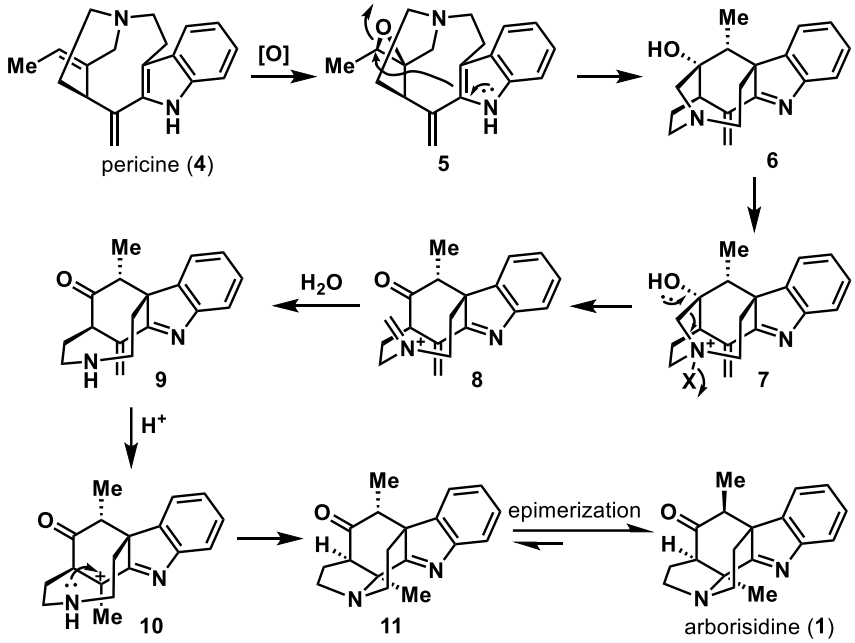

Although the authors didn't observe any appreciable cytotoxicity of **1** when it was tested against KB, PC-3, A549, HCT116, and HT-29 cells, there was a patent describing the *in vivo* antitumor activity of **1** against gastric cancer in a mice model, in combination with pimelautide[5].

3.2 Previous Work on the Synthetic Study of Arborisidine

To date, there has been only one synthetic study of arborisidine published in 2018, from Qin and coworkers[6]. Their synthetic route started with compound **12**, the same intermediate in their own strictamine synthesis[7]. In 11 steps they could access the enone substrate **13** which was then deprotected to release the free primary amine **14**, which underwent an *aza*-Michael addition in pure CH_2Cl_2 and could further be trapped in the same pot as the chloroacetamide **16**. However, the late-stage intramolecular alkylation was fruitless, with the only product being the *retro-aza*-Michael addition, a phenomenon we have also observed in our early studies[8].

Scheme 3.2 Previous synthetic study of arborisidine (**1**)

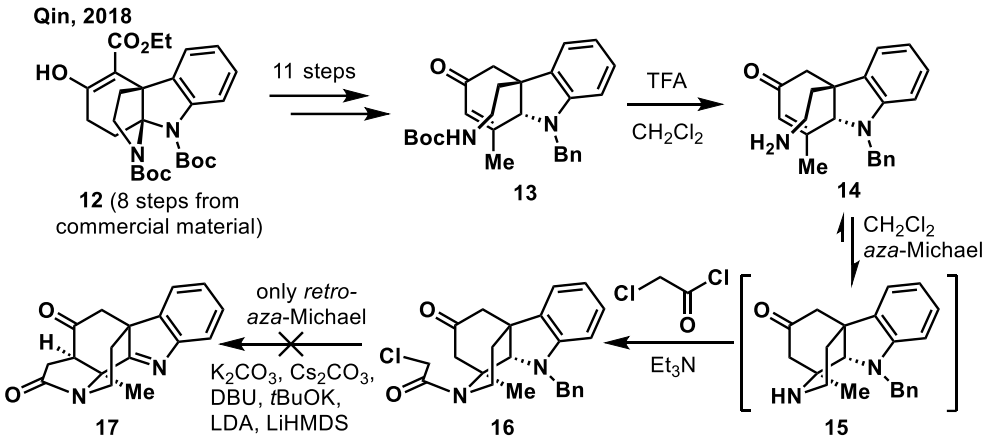

3.3 Early Approach with Late-Stage C-C Bond Formation

Based on our previous success in the concise formal synthesis of strictamine[2], we designed a similar strategy in our first generation retrosynthetic analysis (Scheme 3.3). Following an intramolecular alkylation disconnection (similar to Scheme 3.2), we proposed a 2-chloroethyl amine substrate **18**, which could be further traced back to the protected amine **19**. The hydroxyl moiety in **19** could be introduced via regioselective hydroboration of **20**, which could in turn be synthesized through a similar *6-endo*-dig cyclization of the corresponding amine/amide **21** that was accessible from the propargyl addition to ketimine **22**.

Scheme 3.3 Initial retrosynthetic analysis

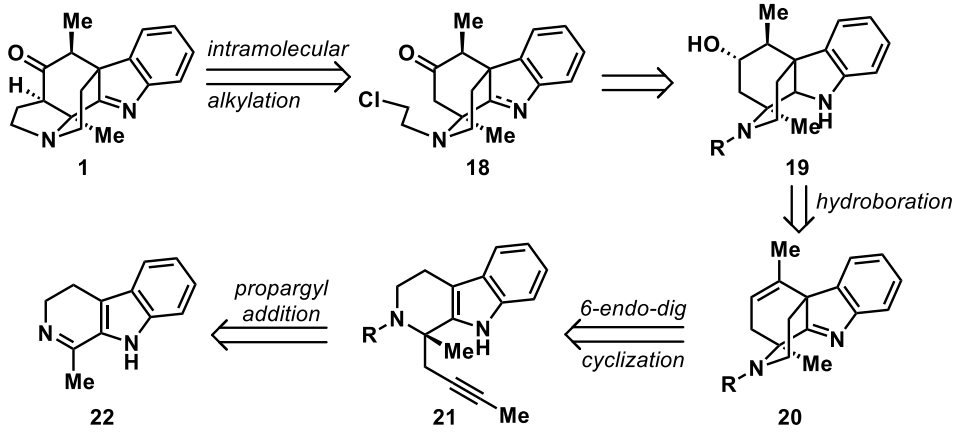

In the forward sense, we commenced to probe the reactivity of ketimine **22**. Due to the low reactivity of **22** against nucleophilic additions, we finally used Grignard reagent **23**, as well as $BF_3{\cdot}OEt_2$ as promoter to achieve the desired **24** after protection with TFAA in a scalable manner, albeit in low yield. The subsequent *6-endo*-dig cyclization of amide **24** was first discovered by my coworker, Alison Gao, using catalytic Ph_3PAuCl and 1 equivalent $AgBF_4$ in methanol[8]. Considering the weak Lewis basicity of the TFA-amide, the loading of both gold (I) and $AgBF_4$ were adjusted to 10 mol% without significant change in yield. Alison had further established a concise route, after numerous failures, to access the unstable 2-chloroethyl amine **28**[8] (Scheme 3.4).

Scheme 3.4 Preparation of chloroethyl amine **28**

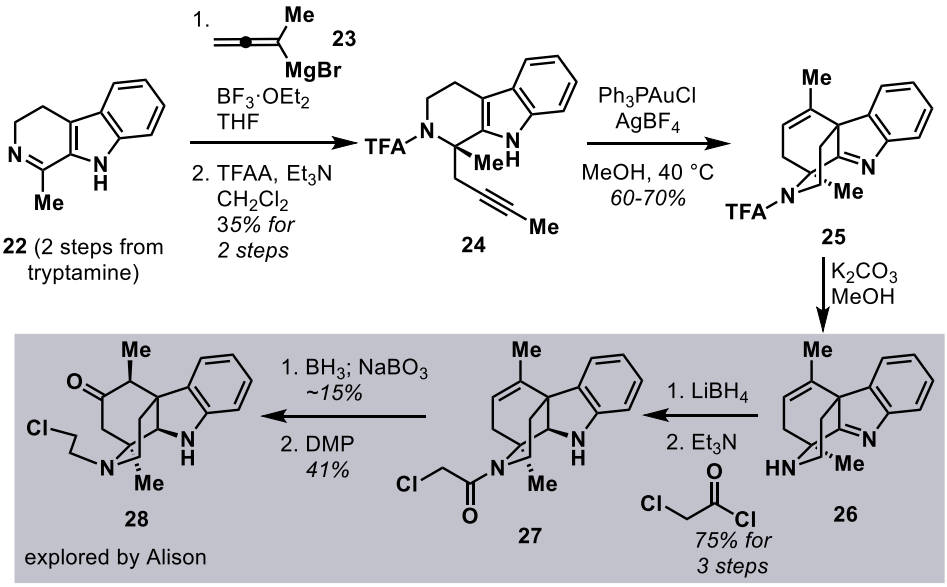

Inspired by a recent example of a formal [3+2] cycloaddition between 2-chloroethyl amide **29** and Michael acceptor **30** using KO^tBu in DMF (Scheme 3.5, top)[9], we were hoping to achieve enhanced reactivity for the final intramolecular alkylation step with this condition, but only observed S_{N2} product, **33**. The rapid

formation of **33** (within one hour) might imply a fast equilibrium of aziridinium (**34**) formation in solution, which would preclude the intramolecular alkylation due to the mismatched orientation of the σ* orbital of aziridium C-N bond and the lone pair of the enolate anion (if formed). Other base screening didn't provide any trace of desired product, although there have been a few reports on similar types of intramolecular cyclizations[10]. On the other hand, Alison had also attempted intermolecular alkylations for **28** and other related substrates without any success, possibly because of steric hindrance and lability of the substrates themselves, as *retro-aza*-Michael products were commonly seen in those cases[8].

Scheme 3.5 Failed intramolecular alkylation of **28** indicating the formation of aziridium intermediate

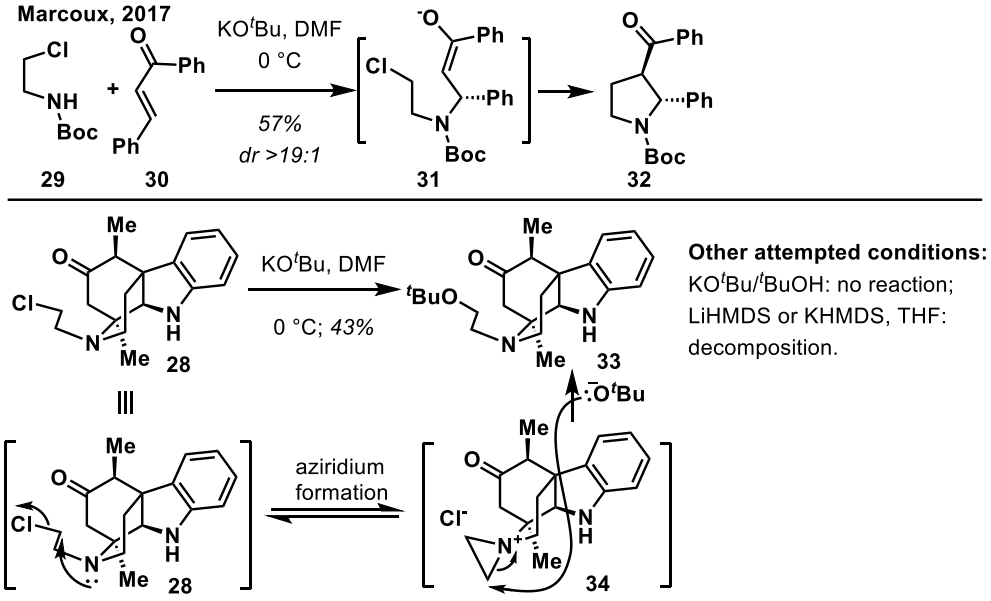

Given the instability of this type of β-aminoketone substrates, we decided to revise our retrosynthesis and introduce the ketone moiety after the formation of pyrrolidine through hydroboration of the corresponding alkene **35**. Intermediate **35** could be formed via an intramolecular allylic C–H insertion of a metal-carbene complex

generated from its diazo precursor **36**, which would ultimately be traced back to the same tetracyclic intermediate **20** (Scheme 3.6).

Scheme 3.6 Revised retrosynthetic analysis

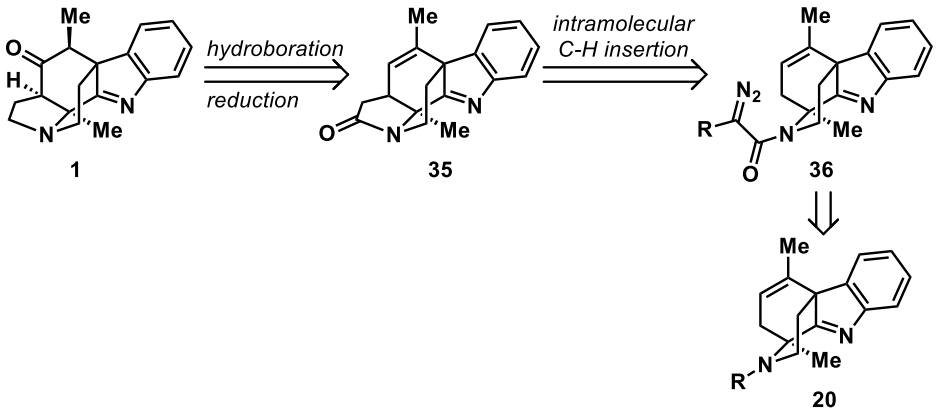

While the direct coupling between amine **26** and activated ester **38**[11] gave a messy mixture, a diazo-transfer protocol[12] worked perfectly with the corresponding methyl malonyl amide **40** to give the desired diazo amide **41**. To our delight, the subsequent Rhodium-catalyzed carbene C–H insertion of **41** took place smoothly with Rh_2[(*S*)-DOSP]$_4$[13] as catalyst, providing the product that was initially assigned as **42** with high yield. It is noteworthy that although the chiral Rh_2[(*S*)-DOSP]$_4$ was used with racemic starting material, its enantiomer worked equally efficiently and there seemed to be no kinetic resolution based on the full conversion of starting material. However, a later X-ray single crystal diffraction analysis of **42** revealed its actual structure as β-lactam **43**, indicating that instead of the desired allylic C–H insertion, the reaction of **41** proceeded exclusively at the α-position of the amide, a preference that was previously observed in various diazoacetoacetamide analogues[14].

Scheme 3.7 Installation of diazo side chain and Rh-catalyzed carbene C-H insertion

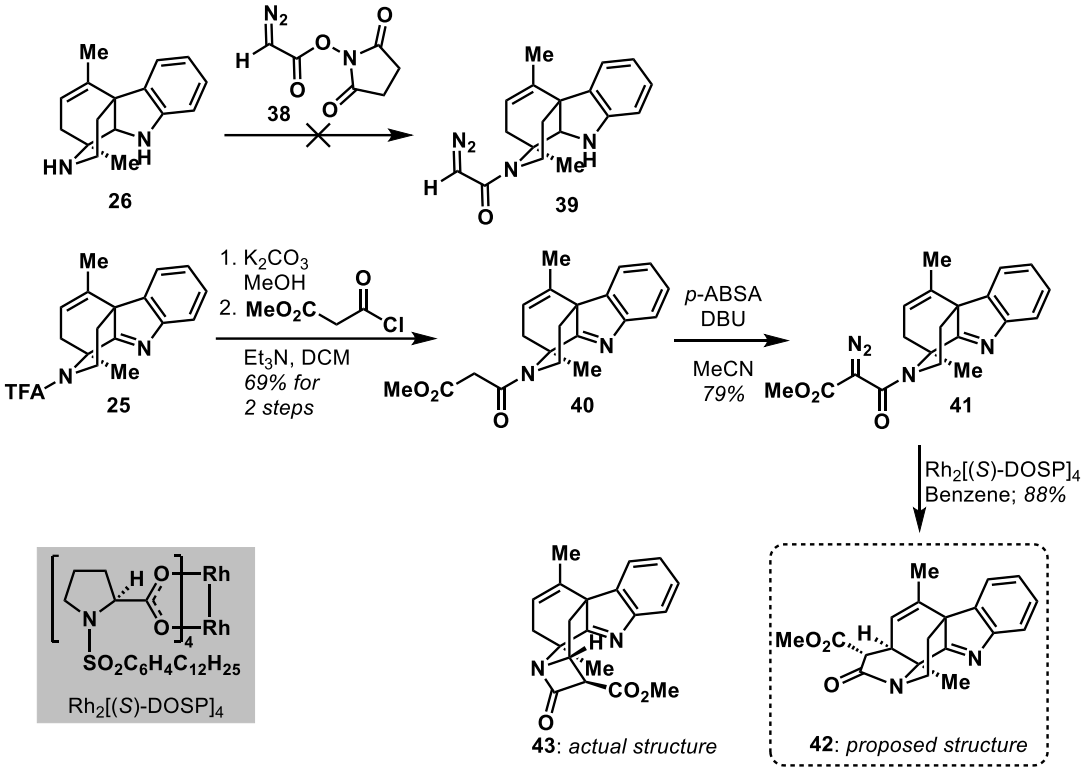

The formation of highly strained β-lactam **43** could be rationalized via its conformational restraint (Figure 3.2). Due to the planar, sp^2-hybridized nature of the amide, the Rhodium carbene complex in intermediate **44** would be pointed away from the desired allylic C–H bond, which made it impossible to form the four-membered transition state set for σ-metathesis and C–H insertion at such position. The presence of the *aza*-quaternary carbon would further lock its *trans*-configuration[14c], making the reactive site closer to the α-amide proton, thus facilitating the β-lactam formation. Such rigidity could be further validated via the crystal structure of **43**.

Figure 3.2 Conformation analysis of Rh-carbene complex **44** and crystal structure of **43**

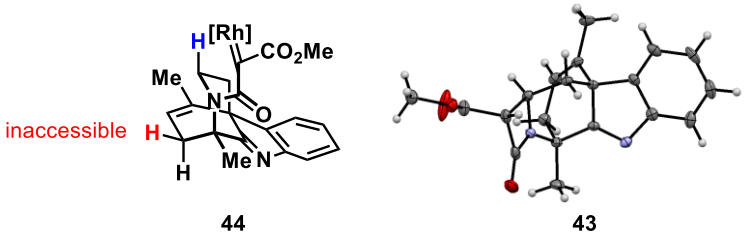

3.4 Late-Stage C-N Bond Formation and Total Synthesis of Racemic Arborisidine

3.4.1 Initial Attempts of Diastereoselective Additions to Ketimines

The global failures regarding late-stage C-C bond formation had prompted us to find a different solution to the construction of the pyrrolidine ring. We turned our attention to a late-stage C-N bond formation, which would allow for the alignment of both reactive centers in close proximity and would potentially have a greater chance to succeed. The challenger, however, was to find the suitable intermediate **45** with the right pre-installed substituent (Scheme 3.8).

Scheme 3.8 3rd generation retrosynthetic analysis

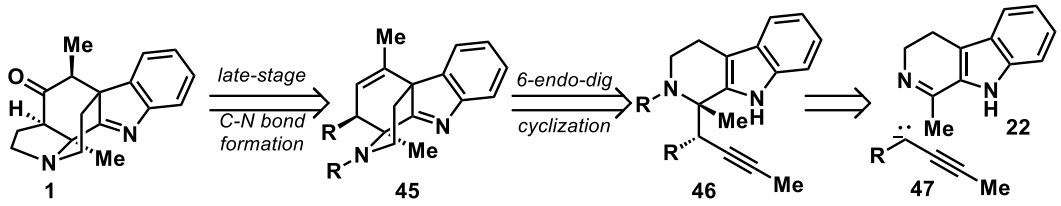

We first proposed to access **45** through the corresponding *6-endo*-dig cyclization of **46** bearing vicinal stereocenters, which could be introduced via a diastereoselective propargylation of ketimine **22**. Considering the relatively low reactivity and limited studies of propargylic nucleophiles (**47**) compared to allylic nucleophiles, we decided to explore the diastereoselective allylation of **22** instead (Scheme 3.9). There was a promising precedent reported by Szabo and coworkers employing 3-substituted allyl boronic acid **50** as nucleophile[15]. However, trace products were formed during our trials with either allyl boronic acid **52**[16] or BPin **53**[17]. We also attempted a direct Grignard addition given our previous experience with **24**, but due to the fast *E/Z* isomerization of Grignard reagent **54**[18] and their similarly low

reactivity, the allylated product **55** was isolated in low yield and essentially no diastereoselectivity.

Scheme 3.9 Model study: diastereoselective allylation of **48**

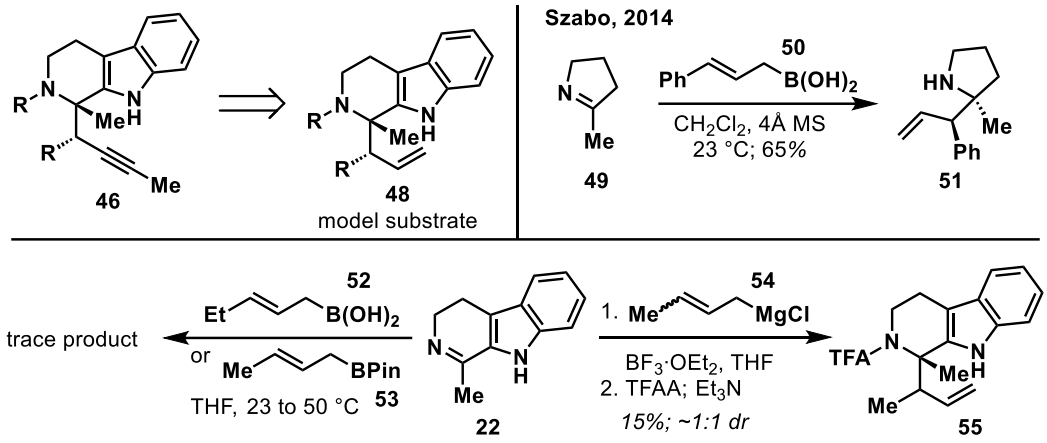

Although there might be room for further optimizations, extra steps would still be required to introduce the alkyne moiety, impairing the overall step-economy of the synthesis. The replacement of the sp^3 stereocenter in **46** to a sp^2 carbon, however, would potentially solve such problems (Scheme 3.10), by both avoiding the puzzling diastereoselectivity issue and offering versatile routes to access the enyne-type intermediate **56** (direct addition to ketimine with alkenyl lithium, cross coupling, dehydration, etc.).

Scheme 3.10 Evolution of intermediate **46** into **56**

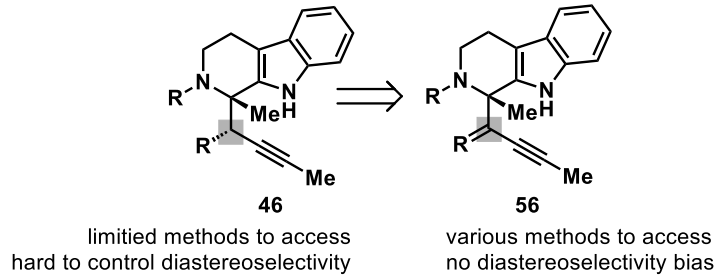

3.4.2 *6-Endo*-Dig Cyclization of 1,1-Enyne

Based on our analysis above, a 4th generation retrosynthetic analysis was proposed (Scheme 3.11). The pyrrolidine ring would be formed through either N-

tethered cyclization or intermolecular one-carbon elongation of **57**. Diene **57** could be prepared via a similar *6-endo*-dig cyclization of the corresponding enyne **58**. Particularly, the methylene moiety in enyne **58** could come from the methyl ketone in **59**, which would lead us to a Pictet-Spengler product of tryptamine (**60**) and symmetrical 2,3-butadione (**61**) with no regioselectivity bias.

Scheme 3.11 4th generation retrosynthetic analysis

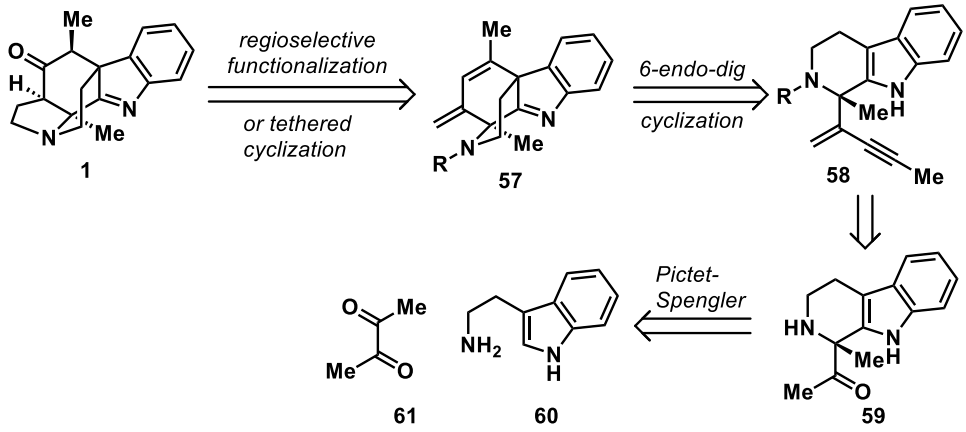

Aminoketone **59** was easily available through a Pictet-Spengler reaction of **60** and **61** in MeOH with 1 equivalent of TFA[19]. In the presence of excessive 1-propynl lithium, the nucleophilic addition occurred rapidly producing the tertiary propargyl alcohol **62**, which could be then converted into the corresponding enyne **63** with TFAA as both a dehydrating reagent and a protecting reagent for the free amine. The enyne **63** was then subjected to the *6-endo*-dig cyclization condition we developed before and a 10 mol% loading of gold catalyst/silver salt was found to be beneficial to such a substrate, producing the desired diene **64** in >70% yield (Scheme 3.12). All the steps here could be performed on gram scale, ensuring a good quantity of material supply.

Scheme 3.12 Preparation of diene **64** through *6-endo*-dig cyclization

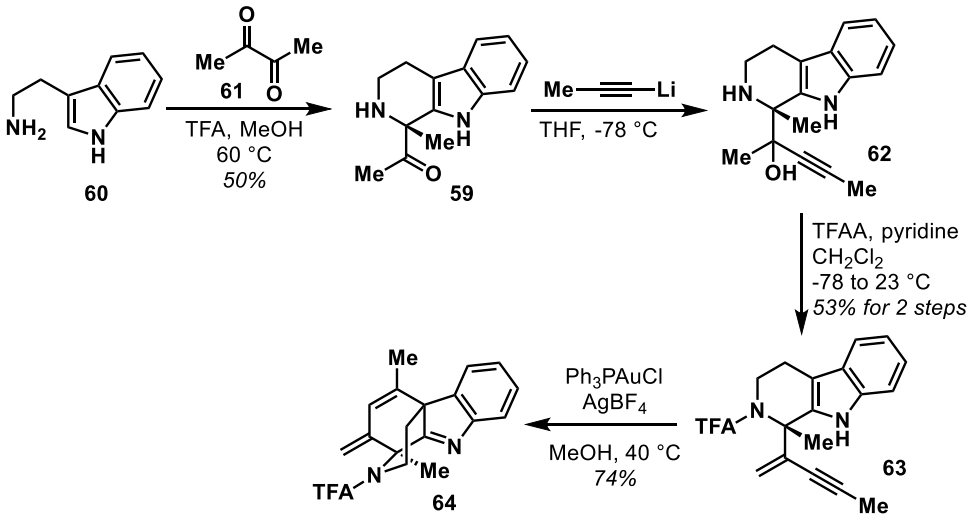

3.4.3 Intramolecular, Tethered Cyclization Strategy

With the diene **64** in hand, we were eager to try the tethered, intramolecular cyclization since it took advantage of proximity between the amine nitrogen and the exocyclic alkene and also dictated the regio- and facial selectivity of the cyclization. A recent publication from Baskaran and coworkers using nitro group as nitrile-N-oxide precursor to perform intramolecular [3+2] cycloaddition[20] (Scheme 3.13, top) came into our mind, since it provided the desired ring size as we pursued, and the nitro-containing side chain should be easily installed via Michael addition. Indeed, the Michael addition worked beautifully after deprotection of **64**, with 2-acetoxyl nitroethane (**67**)[21] serving as the precursor for the highly reactive nitroethylene. The product **68** could be then trapped in the same pot with the addition of excessive Boc_2O and catalytic DMAP, forging the dehydration and subsequent [3+2] cycloaddition of **69**, between the *in situ* formed nitrone moiety and terminal alkene. Unexpectedly, the resultant isoxazoline **70** was further converted, in the presence of DMAP, to the

corresponding Boc enamide **71** and acetyl enamide **72**, in which the acetyl group came from *retro*-Michael addition of **67**.

Scheme 3.13 Intramolecular [3+2] cycloaddition of **68**

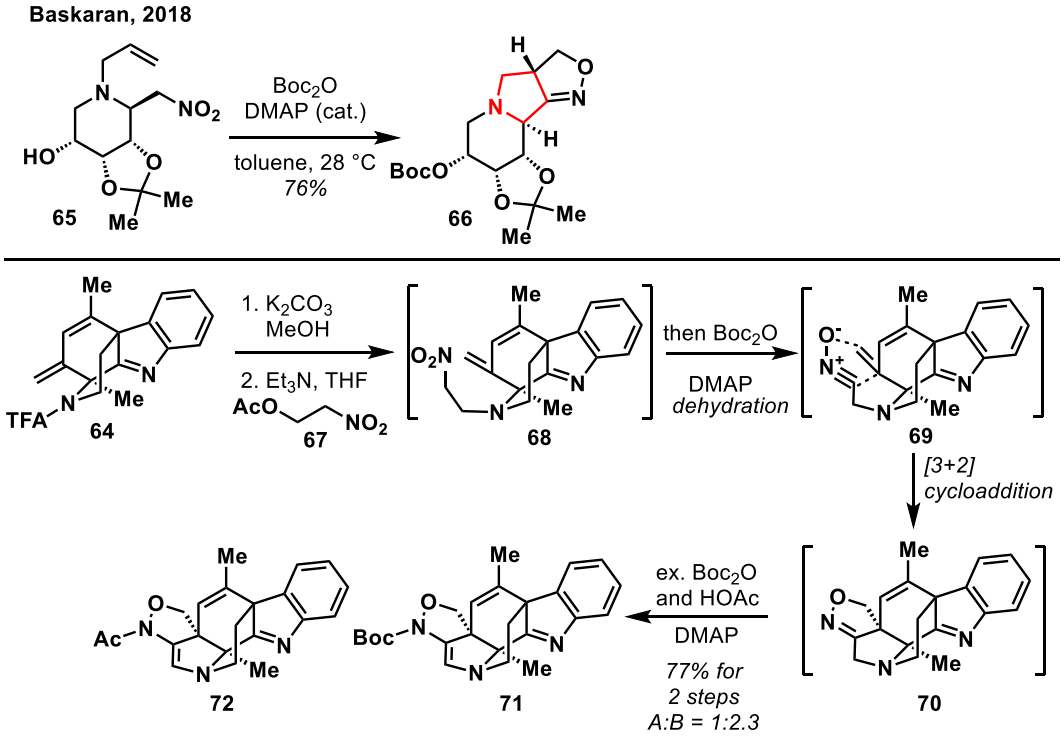

The next task would be the cleavage of the N-O bond in **71** (or **72**), removal of the pendant hydroxymethyl group via deformylation or decarboxylation, and a few oxidation state adjustments. However, the N-O cleavage within the complicate, densely functionalized skeleton of **71** turned out to be challenging, as most conventional methods (Table 3.1, entry 1-6)[22] failed to generate any desired product. Fortunately, $Mo(CO)_6$ [23]worked to convert **71** cleanly into a product which we thought to be **73**. The condition was further improved by a more reactive pre-formed $Mo(CO)_3(MeCN)_3$ complex[24] (Table 3.1, entry 9), giving **73** in a modest yield. Such condition also worked well with acetyl enamide **72** with similar yield. However, again, the actual structure of "**73**" turned out to be the rearranged product **74**, which was confirmed by X-ray diffraction analysis.

Table 3.1 Screening of the conditions for N-O cleavage in **71** and unexpected rearrangement

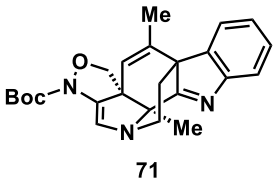

71

conditions

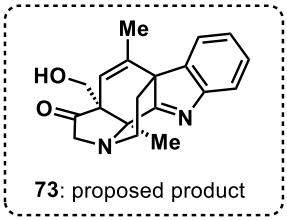

73: proposed product

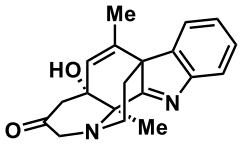

74: rearranged product

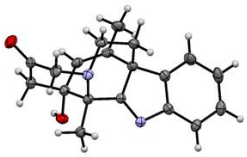

entry	conditions	results
1	Zn, HOAc, 23 °C	messy mixture
2	Zn, TFA, 23 °C	messy mixture
3	SmI_2, THF, 0 to 23 °C	messy mixture
4	Raney Ni, THF, 23 °C	alkene reduction
5	$RuCl_3$, Zn-Cu, EtOH, 100 °C	no reaction
6	Fe, NH_4Cl, EtOH/H_2O, 80 °C	decomposition
7	$Mo(CO)_6$, MeOH, 85 °C	decomposition
8	$Mo(CO)_6$, MeCN/H_2O, 85 °C	38% **73** (**74**)
9	$Mo(CO)_3(MeCN)_3$ MeCN/H_2O/CH_2Cl_2, 23 °C	59% **73** (**74**)

The mechanism for the formation of **74** is proposed in Scheme 3.14. The first step would be oxidative addition to the N-O bond by Mo(0) species, as expected; a partial hydrolysis of resultant **75** would then follow to form the alkoxyl Mo(II) complex **76**. A subsequent Wagner-Meerwein rearrangement of **76** would take place, possibly triggered by the Lewis acidity of the Mo(II) species[25], to generate a more stable tertiary allylic carbocation **77**, which could be ultimately terminated by water to give **74**. Based on this mechanism, we also attempted to add thiophenol to trap the carbocation **77**, but only observed full decomposition. Further elaborations on the rearranged product **74** regarding protection of tertiary alcohol or ring contraction have been unsuccessful.

Scheme 3.14 Proposed mechanism of rearrangement

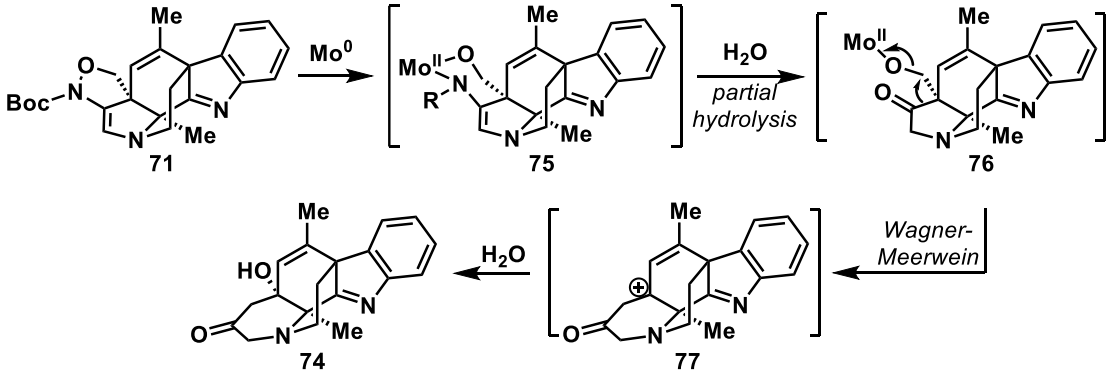

3.4.4 Intermolecular Regio- & Diastereoselective Functionalization Strategy

Bearing in mind the unexpected rearrangement in the tethered cyclization route, we then turned our attention to the intermolecular regioselective functionalization of diene **64**, noting that the terminal position should be the least hindered and most electron-rich. We first attempted radical addition to **64** with electrophilic, carbon-centered radical species[26] (Table 3.2), which ideally would attach the one carbon unit directly onto the molecule at the desired position. These efforts were met with frustration, as decomposition was prevalent under most conditions, probably due to an uncontrolled termination of the radical adduct and intolerance of sensitive functional groups (such as TFA-amide or indolenine) under harsh conditions.

Table 3.2 Attempted radical addition of diene **64**

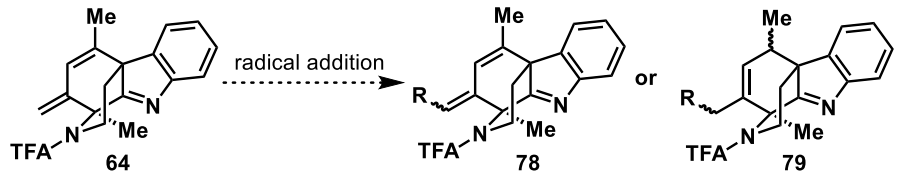

entry	reagents	solvents	temperature	R =	results
1	H_2NNHCO_2Me, FePc, air	THF	65 °C	CO_2Me	decomposition
2	H_2NNHCO_2Me, FePc, air	CH_2Cl_2	23 °C	CO_2Me	no reaction
3	H_2NNHCO_2Me, FePc, TBHP	MeCN	23 °C	CO_2Me	epoxide formation
4	$TMSCH_2MgCl$, O_2	Et_2O	23 °C	CH_2TMS	decomposition
5	Cl_3CCN, CuCl, dppf	dioxane	100 °C	CCl_2CN	decomposition
6	Cl_3CCN, Et_3B, TTMSS	CH_2Cl_2	23 °C	CCl_2CN	unknown product; <10% yield

We then turned to a more indirect method through bromination of **64** and subsequent carbonylation or S_{N2} reaction with cyanide. Luckily, when the bromination of **64** was tested with bromine and pyridine, we could obtain the corresponding vinyl bromide **80** in 30% yield as a single regio- and diastereomer (Table 3.4, entry 1). Such reaction had shown strong reactivity-dependence on the accompanying base, as Et_3N failed to deliver any product (Table 3.3, entry 2) and stronger base as DBU likely favored the formation of a 1,4-addition product **81** (X could be bromide or hydroxyl group, not determined, Table 3.3, entry 3). Since the addition of bromine might not be accurate and excess bromine might impair the reaction, we chose a structurally well-defined bromonium complex, bis(2,4,6-trimethylpyridine)bromonium hexafluoro-phosphate[27] {$[Br(coll)_2]PF_6$, Table 3.3, entry 4} as the brominating source and that indeed improved the yield to 50%. The detailed role of pyridine bases was not fully understood, but based on the observations of different behaviors across various organic bases, we hypothesized that it might serve as a ligand to mitigate the reactivity of the bromonium species, as well as controlling the regioselective deprotonation producing

the vinyl bromide **80**, through transition state **82** (see Table 3.3) in which the weak pyridine-bromonium association had oriented the base closer to the exocyclic methylene proton.

Table 3.3 Screening of conditions for bromination of diene **80**

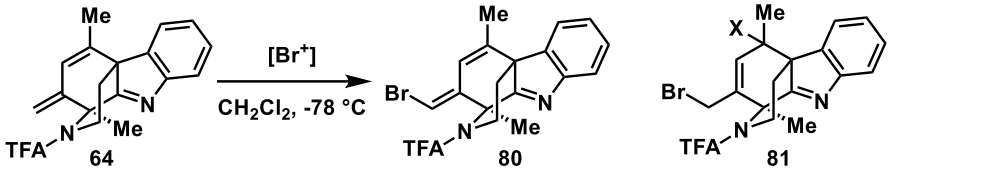

entry	[Br+] reagents	results
1	Br_2, pyridine	30% **80**
2	Br_2, Et_3N	no reaction
3	Br_2, DBU	**81** (tentative)
4	$[Br(coll)_2]PF_6$	50% **80**

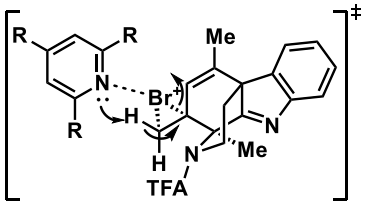

82 (R = H, Me)
proposed transition state

We further performed a one-pot bromination/carbonylation sequence employing the optimized condition reported by Buchwald and coworkers which would be tolerant to different heterocycles[28] (Scheme 3.15). We were delighted to achieve an even higher yield compared to the single bromination step, indicating the potential of this one-pot process in transforming both the vinyl bromide **80** and possibly the minor, elusive, unstable allyl bromide **84** into the desired dienoate **83**.

Scheme 3.15 One-pot bromination/carbonylation to produce ester **83**

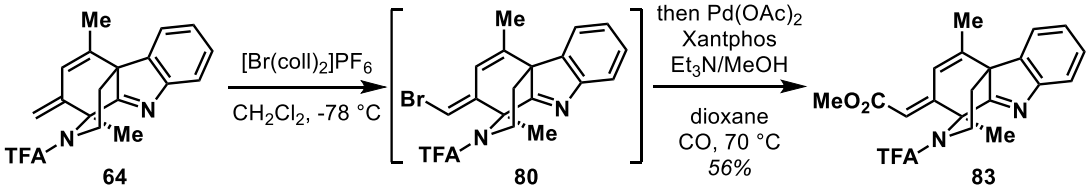

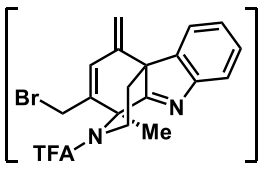

84 (not isolable)

After obtaining the dienoate **83**, we then sought to explore the regio- and diastereoselective 1,4-reduction. The diastereoselectivity would likely be well-controlled since the *Re*-face of the diene in **83** was shielded by the 2-ethyleneamino bridge on top (Figure 3.3, left). The regioselectivity, on the other hand, was proposed by carefully comparing the difference in steric environments between the β- and δ-position (Figure 3.3, right) of **83**: More sp^3 substituents (2 versus 1) at the δ-position might make it more sterically hindered compared to its β-position.

Figure 3.3 Selectivity analysis of 1,4-reduction of **83**

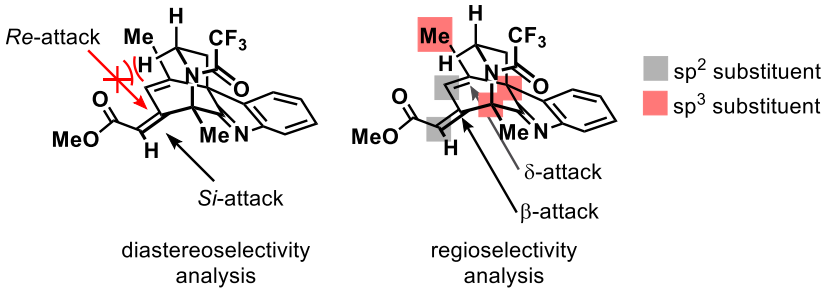

Although such analysis seemed promising, the desired selectivity (along with reactivity) was hard to achieve in practice. The presence of the reduction-sensitive trifluoroacetamide had precluded the use of harsh reduction conditions such as Birch reduction, while M_2B[29] (metal boride alloy, Table 3.4, entry 1), Mg metal[30] (Table 3.4, entry 4) and CuH complex[31] (Table 3.4, entry 5) simply didn't give any conversion regarding conjugate reduction of **83**; Traditional heterogeneous hydrogenation (Table 3.4, entry 3) provided non-selective mixtures along with imine reduction. Interestingly, when **83** was subjected to Raney Ni reduction[32] (Table 3.4, entry 2), the 1,6-reduction product **86** (structure confirmed by X-ray crystallography) predominated owing to the single-electron transfer (SET) mechanism[32]. We then turned our attention to the hydrogen-atom-transfer (HAT) reduction pioneered by Magnus[33a,b] and Shenvi[33c].

While the TBHP-activation condition (Table 3.4 entry 6) failed to provide any product except epoxide formation, we were able to fish out a trace amount of desired product **85** (Table 3.5, entry 1) without other identifiable region- and diastereoisomers.

Table 3.4 Initial screening for the 1,4- over 1,6-reduction of **83**

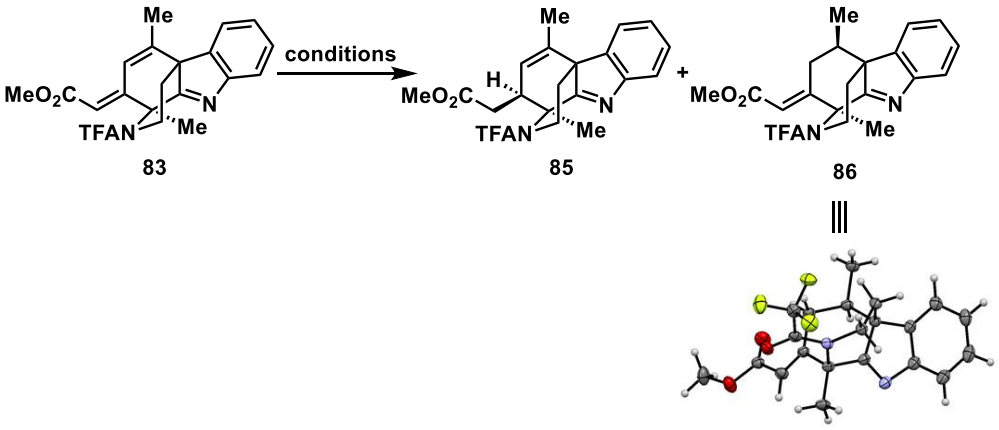

entry	reagents	solvents	temperature	results
1	$NaBH_4$, MCl_2 (M = Co, Ni, Cu)	EtOH	23 to 60 °C	no reaction
2	Raney Ni	THF	23 °C	86% (**25**:**26** = 10:1)
3	H_2, Pd/C or $Pd(OH)_2$/C	MeOH or EtOAc	23 °C	mixture of **25** and **26** with imine reduction
4	Mg	MeOH	23 to 60 °C	no reaction
5	$Cu(OAc)_2$, dppbz, PMHS, ^{t}BuOH	toluene	23 to 60 °C	no reaction
6	$Mn(dpm)_3$ (5%), $PhSiH_3$, TBHP[f]	^{i}PrOH	23 °C	low coversion; epoxide formation

Although the initial hint was appealing, subsequent optimization (Table 3.5) revealed that it was a considerably sluggish process. Importantly, trace air was found to be crucial to the reaction, as a strict air-free condition (Table 3.5, entry 3) resulted in even lower yield and much slower reaction rate, as compared to a non-degassed protocol (Table 3.5, entry 2). We reasoned that the role of trace air might be as an activator of the manganese (III) complex, as similar reactivity enhancement has been observed by Magnus[33b]. Methyl-diethoxylsilane[33d] showed superior yield (Table 3.5, entry 7) than phenylsilane (Table 3.5, entry 6) at lower catalyst loading, but the reaction

rate in the former case was significantly slower and the yield could not be further improved by increasing catalyst loading, so we returned to phenysilane. Other alkoyxlsilanes, such as $(PhSiH_2)_2O$ or $PhSiH_2(O^iPr)$[33e] (used crude) gave comparable or lower yields than phenylsilane. Heating was detrimental to the reaction (Table 3.5, entry 4) as it also promoted the alcoholysis of phenylsilane into inactive siloxane species. Ultimately a 50 mol% catalyst loading (Table 3.5, entry 10) was introduced to realize a reasonable yield. Importantly, phenylsilane needed to be added iteratively to promote full conversion of starting material **83**, especially on large scale.

Table 3.5 Screening of the conditions in regioselective 1,4-reduction of **85**

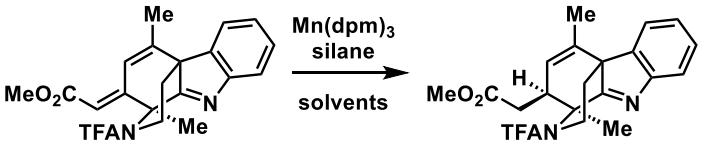

83 **85**

entry[a]	catalyst (%mol)	silane	solvents	temperature	yield (%)[b]
1	5	$PhSiH_3$	DCE/^{i}PrOH (3:1)	23 °C	trace
2	20	$PhSiH_3$	DCE/^{i}PrOH (3:1)	23 °C	20
3[c]	20	$PhSiH_3$	DCE/^{i}PrOH (3:1)	23 °C	<20%[d]
4	20	$PhSiH_3$	DCE/^{i}PrOH (3:1)	60 °C	no reaction
5	20	$PhSiH_3$	DCE/^{i}PrOH (1:1)	23 °C	25
6	20	$PhSiH_3$	CH_2Cl_2/MeOH (1:1)	23 °C	no reaction
7	20	$Me(EtO)_2SiH$	DCE/^{i}PrOH (1:1)	23 °C	31
8	20	$Me(EtO)_2SiH$	DCE/^{i}PrOH (1:1)	60 °C	43
9	50	$Me(EtO)_2SiH$	DCE/^{i}PrOH (1:1)	60 °C	42
10	50	$PhSiH_3$	DCE/^{i}PrOH (1:1)	23 °C	53
11	100	$PhSiH_3$	DCE/^{i}PrOH (1:1)	23 °C	50

[a] Conditions: substrate (0.05 mmol), $Mn(dpm)_3$, silane (3 equiv), solvents (0.05 M), temperature as shown, 12-48 h; [b] isolated yield; [c] thorough degas and reaction run in argon atmosphere; [d] extremely slow (>72 h).

After achieving an effective and selective 1,4-reduction, the TFA group was easily removed under methanolic $NaBH_4$ with partial imine reduction (Scheme 3.16). The subsequent lactam formation didn't occur in THF at elevated temperature, but we

observed a partial conversion of free amine **87** in heated methanol (near reflux). Further increasing the temperature resulted in full conversion of **87** (Scheme 3.16, entry 3).

Scheme 3.16 Deprotection and lactam formation of **85**

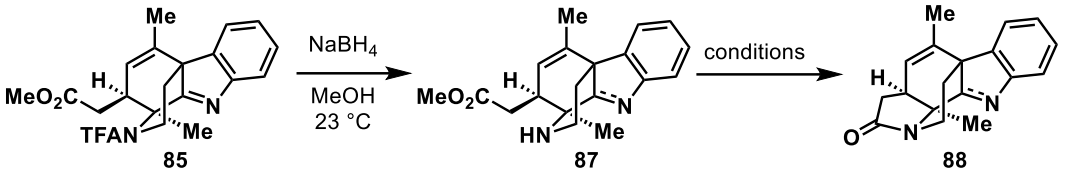

entry	conditions	results[a]
1	THF, 60 °C	No reaction
2	MeOH, 60 °C	incomplete conversion
3	MeOH, 100 °C (sealed tube)	full conversion

[a] Judged by TLC analysis

This reaction sequence was further modified into a one-pot process (Scheme 3.17), taking care that excessive $NaBH_4$ had to be fully consumed by MeOH before raising to higher temperature in sealed tube. If not, the remaining $NaBH_4$ would react with MeOH fiercely at elevated temperature leading to rapid H_2 evolution, which ultimately would cause explosion. The one-pot process maintained a similar yield of **88** as the single 1,4-reduction step and also simplified the purification, as excess silane and byproduct siloxane would always contaminate the rather non-polar **85**, but could be easily removed from more polar lactam **88**.

Scheme 3.17 One-pot 1,4-reduction/deprotection/lactam formation sequence

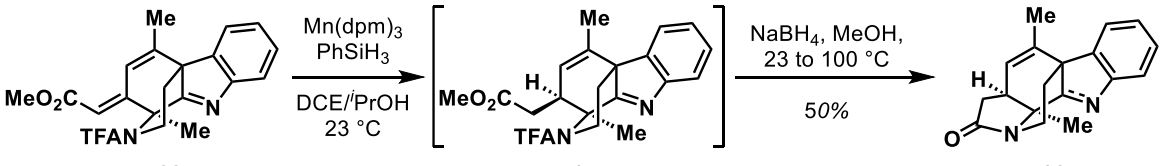

Having established the framework of arborisidine, we then set to execute the final-stage hydroboration as well as reduction of lactam **88**, both of which could be realized through the treatment with BH_3·THF complex. After oxidative quench with

basic H_2O_2, the crude **90** was further oxidized with iodosobenzene (PhIO)[34] to generate **89** in 50% yield. Dess-Martin oxidationof **89** gave arborisidine (**1**) cleanly in good yield; indeed, the crude reaction mixture was clean enough to exhibit almost every signal of natural arborisidine in the ^{1}H NMR spectrum.

Scheme 3.18 Late-stage transformation to arborisidine (**1**) and design of one-pot operation

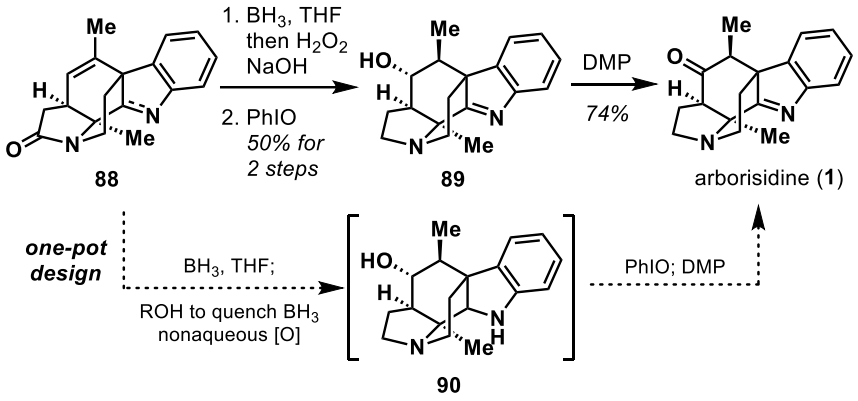

We then thought about further improving this late-stage transformation through the design of a one-pot process (Scheme 3.18), which would minimize the loss in workup and purification of the highly polar intermediate **90**. To achieve this, the excess borane would need to be quenched by either an alcohol or water; a non-aqueous oxidant would be necessary for the oxidation of the alkylborane species; the "quenching" reagent had to be compatible with the following oxidant (PhIO and DMP). Trimethylamine N-oxide (Me_3NO) was the first oxidant of choice[35]. Since we were using the dihydrate adduct of Me_3NO, water was used as the quenching reagent of borane in exact stoichiometry, as excessive water would also hydrolyze DMP and thwart the oxidation. The sequential addition of PhIO and DMP/$NaHCO_3$ was proven to be critical; although excess DMP could slowly oxidize the amine into the imine, it gave a much lower yield due to the potential decomposition of the product or reaction intermediate with longer reaction time.

By combining all of these observations, we finally devised a one-pot operation (Scheme 3.19): After treating with excess BH_3·THF (5 equivalent), water and $Me_3NO·2H_2O$ was added successively and the reaction mixture was then heated to effect the oxidation of alkylborane **91** into **90**. The solvent was then removed and replaced by CH_2Cl_2, and iodosobenzene was added followed by Dess-Martin periodane to give the natural product, arborisidine (**1**), along with recovered alcohol **89**, in a combined yield of >70%. The recovered **89** could then be oxidized back to **1** as described in Scheme 3.18. We also collected the crystal of **1** thanks to the accumulated quantities of synthetic sample (around 40 mg in total) and its structure was further confirmed via X-ray crystallography (Scheme 3.19). At this point, we completed a 7-step total synthesis of (±)-arborisidine (**1**)[35].

Scheme 3.19 One-pot operation of hydroboration/sequential oxidation to obtain arborisidine (**1**)

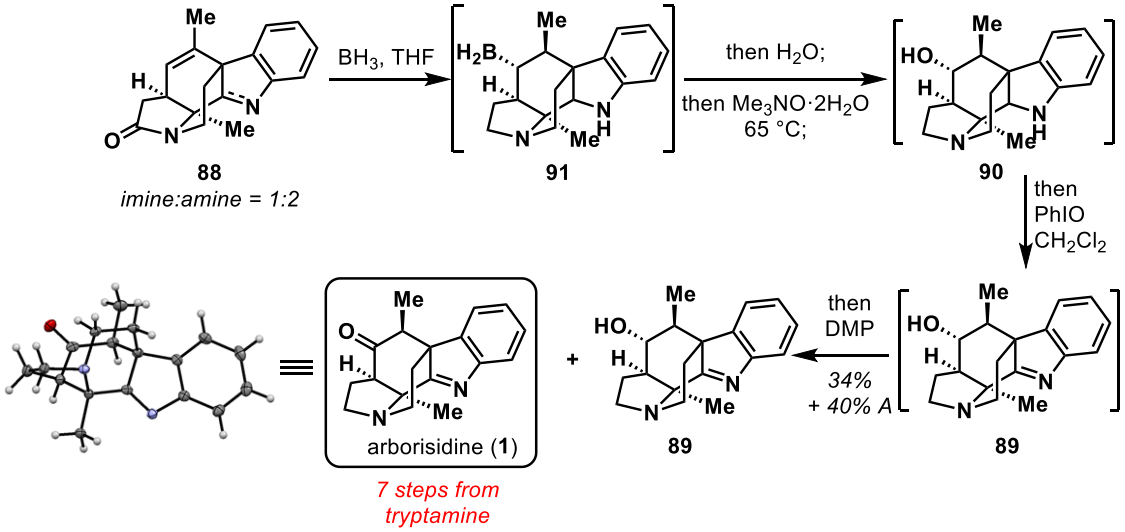

3.5 Asymmetric Total Synthesis of (+)-Arborisidine

With the route of racemic arborisidine secured, we started to work on the asymmetric total synthesis of (+)-arborisidine [(+)-**1**], which would be accessed from

asymmetric aminoketone **59**. The methods of asymmetric synthesis of **59** were summarized in Scheme 3.20: the most efficient way would be the direct asymmetric Pictet-Spengler reaction between tryptamine (**60**) and 2,3-butadione (**61**), which could also be the most challenging choice, given few examples on asymmetric Pictet-Spengler reactions of ketones in a general sense; On the other side, placing additional stereocenters in the tryptamine moiety (either chiral auxiliaries on the amine or tryptophan derivatives, **62**) could induce certain levels of diastereoselectivity. Besides, the specific enantiomer might also be accessible via chemical resolution (kinetic resolution or separation of diastereomers from racemic **59** or its derivatives).

Scheme 3.20 General plan for the asymmetric synthesis of **59**

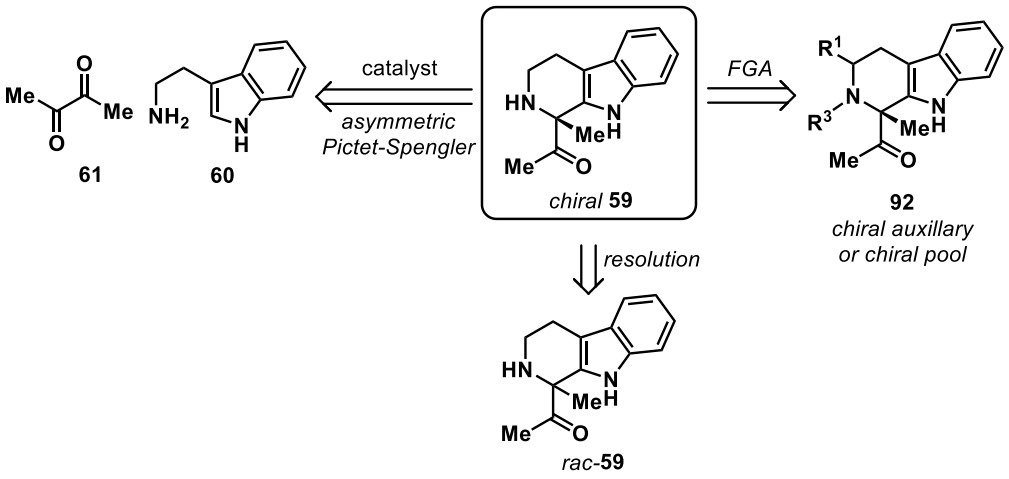

3.5.1 Initial Attempts on Asymmetric Pictet-Spengler Reaction on Tryptamine Derivatives

Because of the significantly lower reactivity of ketones versus aldehydes in the Pictet-Spengler reaction, along with increased *Z/E* isomeric bias regarding their corresponding imine formation, there were only limited examples in the asymmetric Pictet-Spengler reactions of tryptamine (**60**) with ketones[36,37] (Scheme 3.21). Besides

early examples using chiral hydrogen-bonding thiourea catalyst **99**[36a] or stoichiometric silicon-based Lewis acid **100** [37a], the chiral phosphoric acids (**101**-**103**) were most commonly used in those cases. It is worthy pointing out that all the substrates involved here were "well-engineered" as either tethered ketones (**93**, **94**)[36] that could form cyclic acyl iminium species or electron-deficient α-keto amides (**95**-**98**)[37]; there was no studies with other types of ketones, such as α-diketones.

Scheme 3.21 Previous cases of asymmetric Pictet-Spengler reaction between tryptamine and ketones

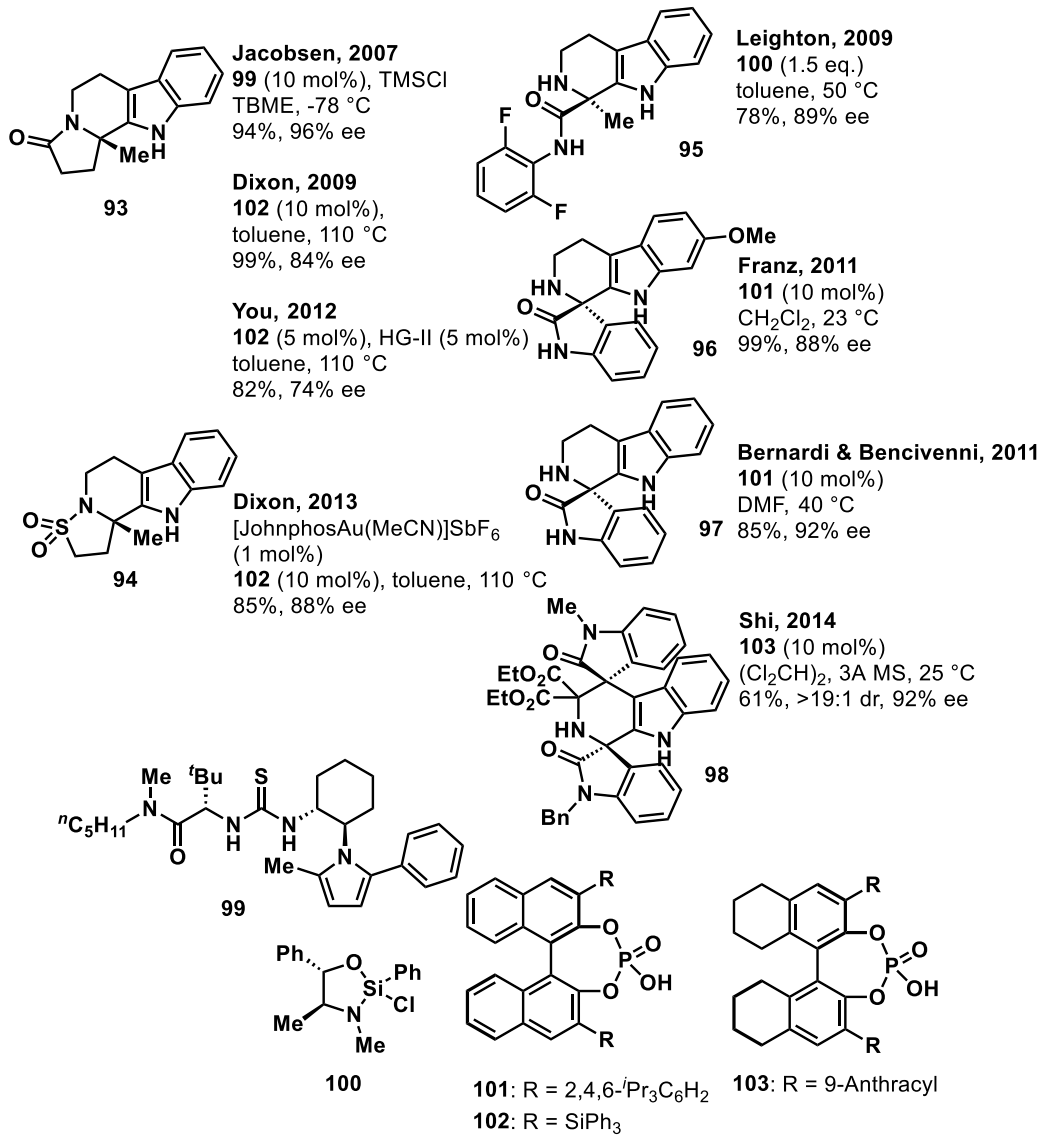

In a recent total synthesis of (+)-penganumine A (**104**)[38] from Zhu and coworkers, the last step was a daunting Pictet-Spengler/hydroamination cascade

reaction (Scheme 3.22) using 4-methoxyl tryptamine (**105**) and α-keto lactam **106** in the presence chiral thiourea catalyst **107** providing good enantioselectivity.

Scheme 3.22 Asymmetric total synthesis of (+)-penganumine A (**104**)

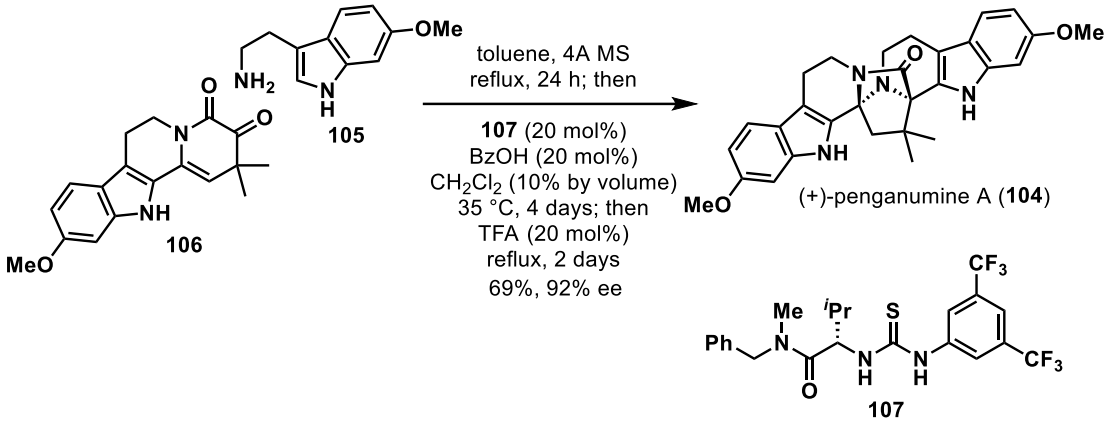

With all of these precedent in mind, we first tried to develop the catalytic Pictet-Spengler reaction using different achiral Brønsted acids and Lewis acids (Scheme 3.23). Low yield (<10%) was observed as tryptamine was poorly soluble in most solvents and likely formed insoluble oligomers over time if the reaction didn't proceed. Switching to methanol as solvent, however, would likely be detrimental for the asymmetric catalysis, due to its Lewis basicity (deactivating Lewis acid catalysts) and the peripheral hydrogen bonds. On the other hand, the use of stoichiometric chiral "catalysts" would not be practical since it was the first step of the synthesis. Since the *de novo* development of a catalytic solution was not our priority, we started seeking other methods to achieve an asymmetric synthesis of **59**.

Scheme 3.23 Attempts in catalytic Pictet-Spengler reaction of **60** and **61**

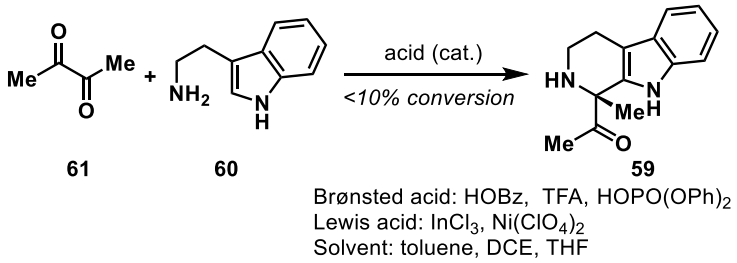

The chiral auxiliary strategy was then tested. We chose the traditional α-N-phenylethyl substitution in **108** for chiral induction[39]. However, the presence of this bulky auxiliary had significantly impaired its reactivity towards Pictet-Spengler reaction with **61**, as no reaction occurred under identical condition that worked on tryptamine.

Scheme 3.24 Attempts in Pictet-Spengler reaction of **108** and **61**

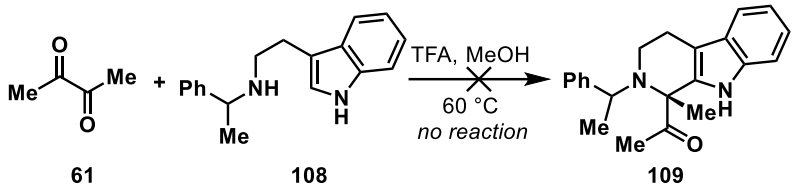

61 **108** **109**

An alternative method to obtain chiral **59** would be a CBS reduction[40] of racemic **110** via kinetic resolution[40c], since the two substituents of the ketone in **110** exhibited considerably different sizes and the two enantiomers would potentially be reduced at different rates. However, the racemic TFA-amide **110** reacted extremely slowly with Me-CBS catalyst **111** even at room temperature (23 °C) with 20% catalyst loading and the ee value of the remaining ketone **110** was found to be <5%.

Scheme 3.25 Attempts in kinetic resolution of *rac*-**110**

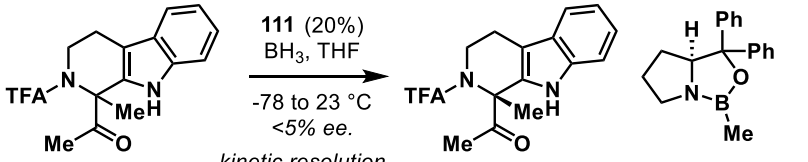

rac-**110** **110** **111**: (*S*)-Me-CBS

3.5.2 Asymmetric Pictet-Spengler Reaction on Tryptophan Derivatives and Attempted Decarboxylation

Realizing the difficulties in the asymmetric Pictet-Spengler reaction of tryptamine (**60**, and its derivatives), we quickly turned to tryptophan derivatives as starting materials[41], since the α-ester group could be wiped out through

decarboxylation, thus serving as a traceless chiral auxiliary. The reaction between *D*-tryptophan methyl ester hydrochloride **112** and 2,3-butadione (**61**) worked nicely, giving an excellent yield and modest dr value of 1.9 : 1 on decagram scale and the major diastereomer **113** (structure confirmed via X-ray diffraction analysis of its enantiomer) could be easily collected via the combination of crystallization and column chromatography. **113** was promptly hydrolyzed into the corresponding carboxylate **115**, but attempts to protect **113** as **116** with excess Boc_2O and DMAP failed to give any conversion, which might be rationalized by the existence of neighboring ketone and ester groups being both electron-withdrawing and sterically hindered, thus diminishing the nucleophilicity and accessibility of the amine. Thus, we decided to explore the decarboxylation process on the derivatives of **115** with free amine moiety.

Scheme 3.26 Diastereoselective Pictet-Spengler reaction of tryptophan derivative **112** and **61**

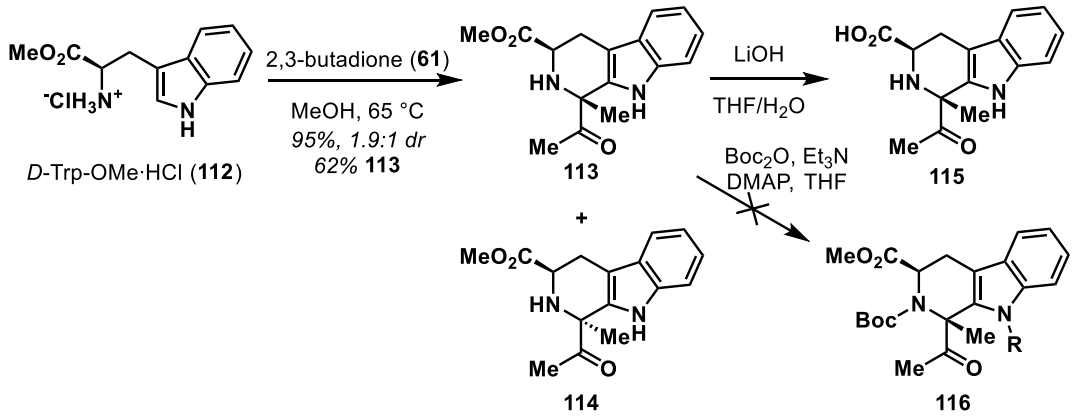

Photoredox decarboxylation conditions were first explored, but we didn't observe the formation of **59** with either oxidation[42a,b] of carboxylate **115** with 4CzIPN (**119**)[42c] or reduction of redox-ester **117** with $Ru(bpy)_3^{2+}$[42d]; instead, the aromatized compound harmalane **120** was the only identifiable product in the reaction mixture. We also tried to perform the Ni-catalyzed decarboxylation[43] of redox ester **117** as reported

by Baran and coworkers recently, but didn't see any conversion of the starting material. An ultimate backup plan of Barton decarboxylation was then executed and the light-sensitive crude **118** was directly subjected to the decarboxylation reaction with UV light irradiation[44] and tert-dodecyl thiol as the hydride source. We could isolate up to 19% of the desired decarboxylation product **59** but it was contaminated with unknown impurities and the reaction had poor reproducibility.

Scheme 3.27 Attempts in decarboxylation of **115** and its derivatives

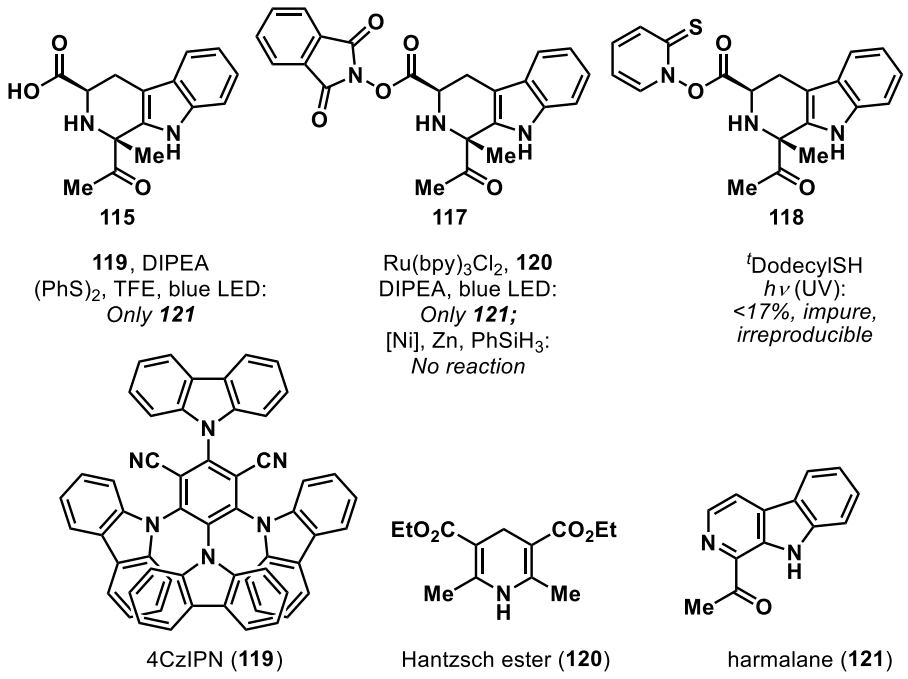

The puzzling, ubiquitous failure in the decarboxylation of **115** and its derivatives had led to a more detailed analysis of the mechanism (Scheme 3.28). When the carboxyl radical **122** was generated, the decarboxylation would generate an α-amino alkyl radical **123**. While the desired hydrogen abstraction (or hydrogen atom transfer, HAT) of radical **123** might be slow, a much faster single electron transfer (SET) could also occur owing to the fact that such types of radicals are prone to oxidation ($E_{1/2}$ = -1.03 V vs. SCE for $Me_2NCH_2\cdot$[45]) in the presence of potential oxidants such as disulfide

(in the case of Barton decarboxylation) or photocatalysts ($Ru(bpy)_3^{2+}$ or **119**) in the reaction mixture. Such irreversible oxidation would form the protonated iminium **124**, which could tautomerize into enamine **125** and further trigger the following deacylation and finally lead to the full aromatization into harmalane **121**.

Scheme 3.28 Mechanism of decarboxylation and aromatization of **115** and its derivatives

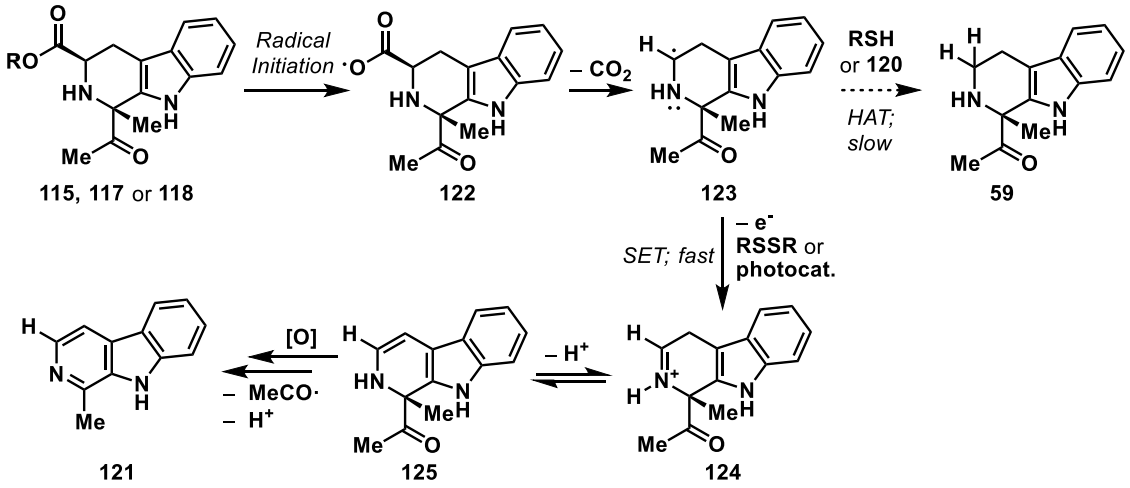

3.5.3 Exploration on Chemoselective Reductive Decyanation

As the direct decarboxylation proved to be problematic, we took a further detour of reductive decyanation[46] through a retro-Strecker process. The preparation of α-amino nitrile **127** was rather straightforward using a one-pot transamidation/ dehydration sequence[47] in excellent yield. The following reductive decyanation, however, had to take place with the ketone moiety intact, as early attempts to oxidize the alcohol **128** back to **59** had never succeeded, likely due to the existing, oxidant-sensitive free amine and free indole. Such a prerequisite would perclude the use of strong reductants, even $NaBH_4$.

Scheme 3.29 Preparation of α-amino nitrile **127**

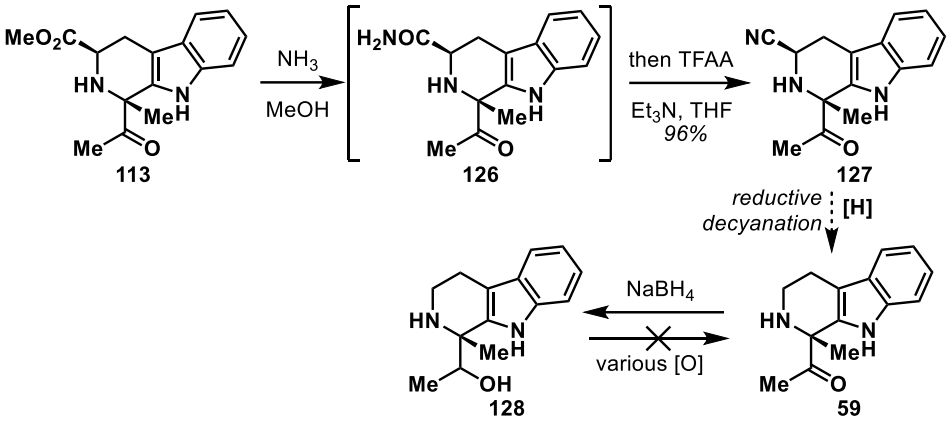

Our first strategy was to combine reductive amination reagents with acid additives that activates nitrile groups. Gratifyingly, with $ZnCl_2$ and $NaBH_3CN$[48], the desired product **59** could be obtained in 29% yield (Table 3.6, entry 1). However, prolonging reaction time resulted in the emergence of over-reduction product **128**; as did the use of methanol as solvent (Table 3.6, entry 2). Other Lewis acid/Brønsted acid[49] or reductant[50] combinations (Table 3.6, entry 3-6) were less effective and **121** was a commonly seen byproduct. We also attempted several other conditions that were claimed to selectively cleave the nitrile group in α-amino nitriles (Table 3.6, entry 8-10) and the results were not satisfactory, except for entry 8[51] with only desired **59** (in low yield), byproduct **121** and full consumption of starting material **127** without over-reduction. The use of Meerwein's salt to activate the nitrile group[52] (Table 3.6, entry 13) had also failed. Alternatively, a chemoselective reductant, $NaBH(HFIP)_3$[53] (Table 3.6, entry 14), which was reported to reduce only aldehydes in the presence of ketones, gave only ketone-reduction product **129**.

Table 3.6 Initial screening for conditions of reductive decyanation of **127**

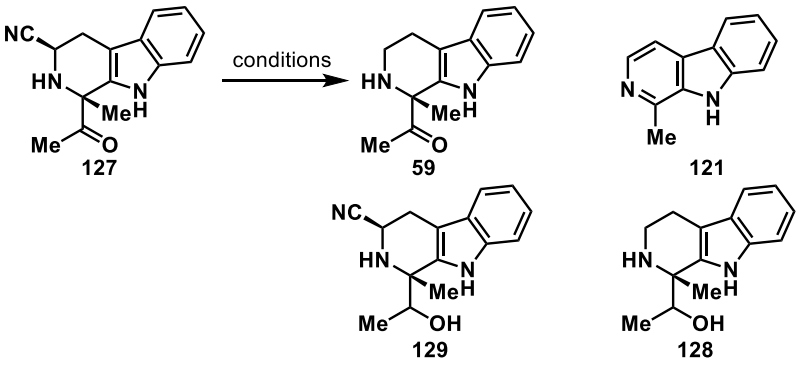

entry	reagents	solvents	temperature	results
1	$ZnCl_2$, $NaBH_3CN$	THF	23 °C	29% **59**; mainly **128** after 48 h
2	$ZnCl_2$, $NaBH_3CN$	MeOH	23 °C	**128**
3	$Cu(OAc)_2$, $NaBH_3CN$	THF	23 °C	trace **59**; mainly **121** and **127**
4	$FeSO_4$, $NaBH_3CN$	THF	23 °C	trace **59**; mainly **121** and **127**
5	$AgNO_3$, $NaBH_3CN$	THF	23 °C	trace **59**; mainly **121** and **127**
6	HOAc, $NaBH_3CN$	THF	23 °C	trace **59**; mainly **121** and **127**
7	HOAc, $NaBH_3CN$	THF or MeOH	65 °C	**128**
8	$NaBH_3CN$	THF/MeOH	65 °C	<20% **59**, mainly **121**
9	Raney Ni	THF	65 °C	decomposition
10	BH_3, w or w/o $NaBH_4$ (cat.)	THF	23 °C	**59** + **128**
11	9-BBN	THF	23 °C	trace **59**; mainly **127**
12	9-BBN	THF	65 °C	trace **59**; mainly **121** and **127**
13	Et_3SiH, $Me_3O^+BF_4^-$	CH_2Cl_2	23 °C	No reaction
14	$NaBH(HFIP)_3$	THF	23 °C	**129**

Encouraged by the initial result of $NaBH_3CN$ (see also Table 3.7, entry 1) in heated MeOH, we sought to figure out the ways to hamper the byproduct formation. A thorough degas of the reaction system along with additional BHT as a radical scavenger (Table 3.7, entry 2), however, didn't suppress the formation of **121**, which implied that the aromatization went through a redox-neutral pathway. Inspired by the mechanism of *retro*-Benzoin coupling[54], we wondered if the free cyanide anion, expelled from **127**, could catalyze a similar *retro-aza*-Benzoin coupling through the formation of a transient ketone-cyanohydrin intermediate **130**.

Table 3.7 Optimization of Conditions for reductive decyanation of **127**

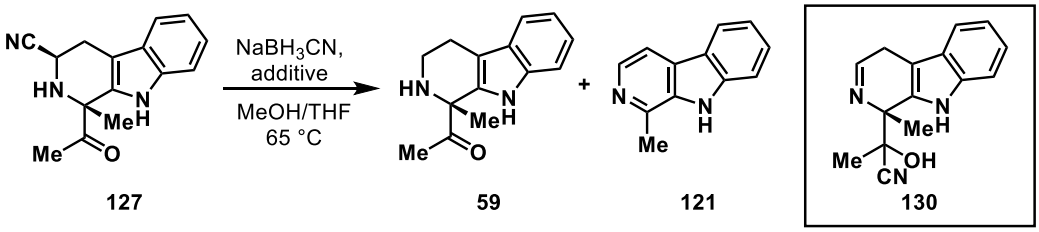

127 **59** **121** **130**

entry[a]	additive	reaction time (h)	yield (%)[b]
1	none	8	<20[c]
2	BHT	8	ND[c]
3	C_6H_5CHO	3	50
4	C_6H_5CHO	8	56
5	4-$MeOC_6H_4CHO$	8	42
6	4-ClC_6H_4CHO	8	46
7	4-$CF_3C_6H_4CHO$	8	69
8	4-$CF_3C_6H_4CHO$[d,e]	8	71
9	4-$NO_2C_6H_4CHO$	8	0[c]
10	BnOH	8	13[c]

[a] Conditions: substrate (0.2 to 0.3 mmol), $NaBH_3CN$ (2.0 equiv, 1.0 M in THF), additive (3.0 equiv), MeOH (0.1 M), 65 °C; [b] isolated yield; [c] the major product is **121**; [d] performed on 5 mmol scale; [e] 2.6 equiv of aldehyde was used.

With this assumption in mind, a "cyanide scavenger" would be demanded to inhibit the formation of ketone-cyanohydrin **130**. Aromatic aldehydes were then selected as the "scavenger", considering their higher reactivity compared to ketones during the cyanohydrin formation equilibrium, and that they would not be entangled with other reactants in the system or undergo self-aldol reaction. Pleasingly, by simply adding benzaldehyde (Table 3.7, entry 3), we could boost the yield of **59** to 50% and saw a further increase in yield with prolonged reaction time. Further screening of aldehydes revealed that a more electron-deficient 4-trifluoromethylbenzaldehyde (Table 3.7, entry 7, 8) provided an optimal yield that was reproducible on gram scale. Moving forward in that direction, 4-nitrobenzaldehyde (Table 3.7, entry 9), however, gave no desired product, possibly due to the fact that this aldehyde was rapidly reduced by $NaBH_3CN$ and thus not able to quench the cyanide. It is noteworthy that although

the aldehydes were partially reduced at the end of the reaction, the control experiment using benzyl alcohol (Table 3.7, entry 10) showed no yield improvement, which served as an indirect evidence for the "cyanide scavenger" effect of such aldehydes.

This chemoselective reductive decyanation allowed for a scalable access to the asymmetric aminoketone **59** in only 3 steps from D-tryptophan derivative **112** (Scheme 3.30) and we were able to complete the asymmetric total synthesis of (+)-arborisidine in another 6 steps[35] with the same route shown before.

Scheme 3.30 Asymmetric total synthesis of (+)-arborisidine [(+)-**1**]

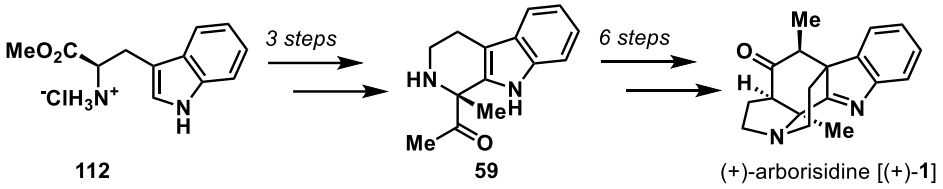

112 **59** (+)-arborisidine [(+)-**1**]

To further understand and validate such "cyanide scavenger" effect and the mechanism of aromatization into **121**, we conducted two experiments: with a large excess of benzaldehyde as additive, we could observe the signal of the benzaldehyde cyanohydrin **131** in the ^{1}H NMR of the crude mixture (Scheme 3.31, left); merely heating nitrile **127** in CD_3OD without any reductant gave a mixture of the starting material, the aromatized **121** and a trace of lactonitrile **132** (2-hydroxylpropionitrile) as indicated by the ^{1}H NMR spectrum (Scheme 3.31, right).

Scheme 3.31 Mechanistic evidence of "cyanide scavenger" effect

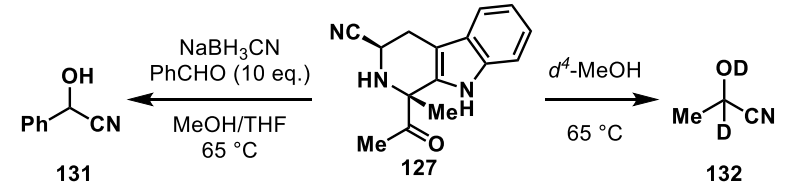

131 crude ^{1}H NMR **127** **132** crude ^{1}H NMR

Based on these data, we have proposed the mechanisms of reductive decyanation and competing aromatization in Scheme 3.32: the intermediate iminium

133 could be effectively trapped by BH_3CN^- to give the desired product **59**, but the wandering CN^- could also attack the ketone in **133** to form the elusive intermediate **130** which would undergo a *retro-aza*-Benzoin condensation with aromatization as driving force and extrude the lactonitrile **136**. The aldehyde additive **134**, indeed, would form the cyanohydrin **135** much more facile than the ketone **133**, thus preventing the aromatization pathway and favor the desired reduction to **59**.

Scheme 3.32 Proposed mechanism for reductive decyanation and competing aromatization

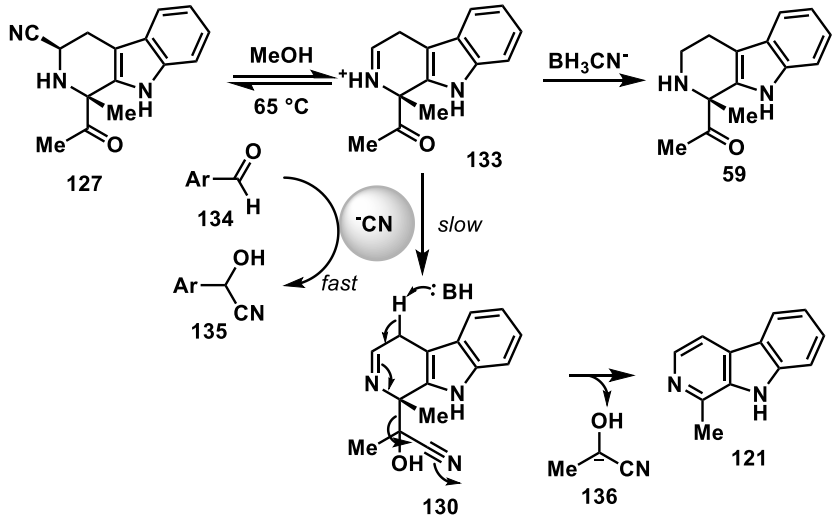

3.6 Conclusion

In this chapter, we have accomplished the first total synthesis of (+)-arborisidine (**1**) within 10 steps (7-step racemic, 9-step asymmetric), after considerable efforts and detours, based on a series of unique transformations, including the gold-catalyzed *6-endo*-dig cyclization, the regio- and diastereoselective functionalization of diene, and the one-pot hydroboration/sequential oxidation. The asymmetric Pictet-Spengler reaction of tryptophan derivatives in combination with "cyanide scavenger" strategy in the chemoselective decyanation had also allowed for easy access to

asymmetric 1,1-disubstituted 3,4-dihydro β-carboline, which could benefit us in the asymmetric synthesis of other indole alkaloids and pharmaceutically important molecules.

3.7 Experimental Details

General Procedures. All reactions were carried out under an argon atmosphere with dry solvents under anhydrous conditions, unless otherwise noted. Dry tetrahydrofuran (THF), toluene, acetonitrile, and dichloromethane (CH_2Cl_2) were obtained by passing commercially available pre-dried, oxygen-free formulations through activated alumina columns. Yields refer to chromatographically and spectroscopically (^1H and ^{13}C NMR) homogeneous materials, unless otherwise stated. Reagents were purchased at the highest commercial quality and used without further purification, unless otherwise stated. Reactions were magnetically stirred and monitored by thin-layer chromatography (TLC) carried out on 0.25 mm E. Merck silica gel plates (60F-254) using UV light as visualizing agent, and an ethanolic solution of phosphomolybdic acid and cerium sulfate, and heat as developing agents. Macherey-Nagel® silica gel (60, academic grade, particle size 0.040–0.063 mm) was used for flash column chromatography. The lactam formation reaction was performed using a Biotage microwave tube. Preparative thin-layer chromatography separations were carried out on 0.50 mm E. Merck silica gel plates (60F-254). NMR spectra were recorded on Bruker 500 MHz instruments and calibrated using residual undeuterated solvent as an internal reference. The following abbreviations were used to explain the multiplicities:

s = singlet, d = doublet, t = triplet, br = broad, app = apparent. IR spectra were recorded on a Perkin-Elmer 1000 series FT-IR spectrometer. High-resolution mass spectra (HRMS) were recorded on a Waters Synapt G2-Si mass spectrometer using ESI (Electrospray Ionization) at the University of Chicago Mass Spectrometry Laboratory, and Agilent 6244 Tof-MS using ESI (Electrospray Ionization) at the University of Chicago Mass Spectroscopy Core Facility. High-pressure liquid chromatography (HPLC) was performed on a Shimadzu Prominence UFLC System, using column ChiralPak® AD-H (0.46 cm × 25 cm).

Amide 24: To a solution containing carboline **22** (1.88 g, 10.2 mmol, 1.0 equiv) in THF (70 mL) was added BF_3•OEt_2 (2.36 mL, 15.3 mmol, 1.5 equiv) and a freshly prepared solution of Grignard reagent **23** (30.6 mL, freshly prepared from 2-butnyl bromide and magnesium, 1 M in diethyl ether, 3.0 equiv) successively at 0 °C. The reaction was then allowed to warm to 23 °C and stirred for 12 h. Upon completion, the reaction contents were quenched with saturated potassium sodium tartrate (100 mL) and CH_2Cl_2 (100 mL) and stirred at 23 °C for 1 h. The layers were separated and the aqueous layer was extracted with CH_2Cl_2 (3 × 100 mL). The combined organic layers were then dried (Na_2SO_4), filtered, and concentrated to give the crude product that was further dissolved in CH_2Cl_2 (100 mL). To this solution was added Et_3N (1.24 mL, 15.3 mmol, 1.5 equiv) and TFAA (1.70 mL, 29.012.2 mmol, 1.2 equiv) successively at 23 °C and reaction mixture was stirred at 23 °C for 1 h. Upon completion, the reaction contents were quenched by the addition of saturated aqueous $NaHCO_3$ (50 mL) and the

contents were transferred to a separatory funnel, diluting with CH_2Cl_2 (100 mL). The layers were separated and the aqueous layer was extracted with CH_2Cl_2 (3 × 100 mL). The combined organic layers were dried (Na_2SO_4), filtered, and concentrated. The resultant crude product was purified by flash chromatography (silica gel, EtOAc/hexanes, 1:20→1:15→1:10) to give amide **24** (1.19 g, 35% yield over two steps) as a yellow solid. **24**: R_f = 0.56 (silica gel, EtOAc/hexanes, 1/4); ^{1}H NMR (500 MHz, $CDCl_3$) δ 8.22 (br, s, 1 H), 7.52 (d, *J* = 7.8 Hz, 1 H), 7.38 (d, *J* = 8.1 Hz, 1 H), 7.24–7.21 (m, 1 H), 7.15 (t, *J* = 7.0 Hz, 1 H), 3.88–3.78 (m, 2 H), 3.27 (dd, *J* = 16.3, 2.3 Hz, 1 H), 3.11 (dd, *J* = 16.4, 2.4 Hz, 1 H), 2.91 – 2.87 (m, 2 H), 1.91 (s, 3 H), 1.77 (t, *J* = 2.4 Hz, 3 H).

Alkene 25: To a flask charged with Ph_3PAuCl (49.5 mg, 0.10 mmol, 0.10 equiv) and silver(I) tetrafluoroborate (34.4 mg, 0.10 mmol, 0.10 equiv) was added MeOH (6 mL) and the resultant mixture was stirred at 23 °C for 15 min. The suspension was then transferred to a solution of **24** (0.341 g, 1.02 mmol, 1.0 equiv) in MeOH (10 mL) at 23 °C. The resultant mixture was then warmed to 40 °C and stirred at that temperature for 7.5 h. Upon completion, the reaction mixture was quenched by the addition of saturated aqueous $NaHCO_3$ (20 mL) and the contents were transferred to a separatory funnel, diluting with CH_2Cl_2 (50 mL). The layers were separated and the aqueous layer was extracted with CH_2Cl_2 (3 × 25 mL). The combined organic layers were then dried (Na_2SO_4), filtered, and concentrated. The resulting crude product was purified by flash chromatography (silica gel, EtOAc/hexanes, 1:15→1:10) to give diene

25 (0.210 g, 62% yield) as a yellow solid. The yield ranged from 60% to 70% depending on the scale and purity of starting material **24**. **25**: R_f = 0.61 (silica gel, EtOAc/hexanes, 1/4); ^{1}H NMR (500 MHz, $CDCl_3$) δ 7.68 (d, *J* = 7.7 Hz, 1 H), 7.49 (d, *J* = 7.4 Hz, 1 H), 7.39 (td, *J* = 7.7, 1.1 Hz, 1 H), 7.28–7.24 (m, 1 H), 5.25 (dd, *J* = 3.1, 1.4 Hz, 1 H), 4.02 (dd, *J* = 18.2, 4.0 Hz, 1 H), 3.91 (dd, *J* = 14.7, 5.9 Hz, 1 H), 2.90 (td, *J* = 14.2, 4.8 Hz, 1 H), 2.48 (td, *J* = 13.2, 6.0 Hz, 1 H), 2.26–2.21 (m, 1 H), 1.99 (dd, *J* = 13.1, 4.8 Hz, 1 H), 1.96 (s, 6 H).

Ether 33. To a solution of substrate **28** (5.0 mg, 0.016 mmol, 1.0 equiv, obtained from Alison) in DMF (0.5 mL) was added KO^{t}Bu (1.0 M in THF, 0.03 mL, 0.03 mmol, 1.9 equiv) at 0 °C. The reaction mixture was stirred at 0 °C for 1 h. Upon completion, the reaction contents were quenched by the addition of saturated aqueous $NaHCO_3$ (5 mL) and the contents were transferred to a separatory funnel, diluting with EtOAc (10 mL). The layers were separated and the aqueous layer was extracted with EtOAc (3 × 5 mL). The combined organic layers were then washed with water (5 × 5 mL), dried (Na_2SO_4), filtered, and concentrated. The resultant crude product was purified by preparative TLC (silica gel deactivated with Et_3N, EtOAc/hexanes, 1:1,) to give **33** (2.4 mg, 43%) as a colorless oil. **33**: ^{1}H NMR (500 MHz, $CDCl_3$) δ 7.11–7.04 (m, 2 H), 6.85–6.80 (m, 2 H), 4.06 (d, *J* = 12.1 Hz, 1 H), 3.94 (d, *J* = 12.2 Hz, 1 H), 3.85 (s, 1 H), 3.70–3.66 (m, 1 H), 3.64 (s, 1H), 3.48–3.38 (m, 1 H), 3.12 (dd, *J* = 12.4, 3.4 Hz, 1 H), 2.33 (ddd, *J* = 14.0, 11.8, 7.7 Hz, 1 H), 2.00 (dd, *J* = 14.2, 5.8 Hz, 1 H),

1.74–1.69 (m, 1 H), 1.61 (s, 1 H), 1.55 (s, 3 H), 1.42–1.37 (m, 1 H), 0.97 (d, J = 6.7 Hz, 3 H).

Amide 40: To a solution of **25** (0.576 g, 1.72 mmol, 1.0 equiv) in MeOH (8 mL) at 23 °C was added solid K_2CO_3 (0.700 g, 5.07 mmol, 2.9 equiv). The resultant suspension was then heated to 60 °C and stirred at that temperature for 4 h. Upon completion, the reaction contents were quenched by the addition of saturated aqueous $NaHCO_3$ (10 mL) and the resultant mixture was transferred to a separatory funnel, diluting with CH_2Cl_2 (50 mL). The layers were separated and the aqueous layer was extracted with CH_2Cl_2 (3 × 50 mL). The combined organic layers were then dried (Na_2SO_4), filtered, and concentrated to give the crude amine **26** (0.417 g,) as a yellow solid that was used directly in the next step without further purification. To a solution of crude **26** (0.207 g, 0.85 mmol assuming 100% pure, 1.0 equiv) in CH_2Cl_2 (6 mL) was added Et_3N (0.18 mL, 1.27 mmol, 1.5 equiv) and methyl malonyl chloride (0.091 mL, 0.85 mmol, 1.0 equiv) at 23 °C. The reaction mixture was stirred at 23 °C for 1.5 h. Upon completion, the reaction contents were quenched by the addition of saturated aqueous $NaHCO_3$ (20 mL) and the contents were transferred to a separatory funnel, diluting with CH_2Cl_2 (20 mL). The layers were separated and the aqueous layer was extracted with CH_2Cl_2 (3 × 20 mL). The combined organic layers were then dried (Na_2SO_4), filtered, and concentrated. The resultant crude product was purified by flash chromatography (silica gel, EtOAc/hexanes, 1:5→1:3→1:1) to give **40** (0.202 g, 69% for 2 steps from **25**) as a light yellow oil. **40**: R_f = 0.10 (silica gel, EtOAc/hexanes, 1/2);

^{1}H NMR (500 MHz, $CDCl_3$) δ 7.67 (d, *J* = 7.8 Hz, 1 H), 7.47 (d, *J* = 7.3 Hz, 1 H), 7.36 (t, *J* = 7.5 Hz, 1 H), 7.23 (t, *J* = 7.5 Hz, 1 H), 5.26 (d, *J* = 2.8 Hz, 1 H), 4.12 (dd, *J* = 18.0, 4.4 Hz, 1 H), 3.76 (s, 3 H), 3.61 (dd, *J* = 14.4, 5.9 Hz, 1 H), 3.48 (s, 2 H), 2.92 (td, *J* = 13.8, 4.9 Hz, 1 H), 2.46 (td, *J* = 13.0, 6.1 Hz, 1 H), 2.18 (d, *J* = 18.0 Hz, 1 H), 1.95 (s, 3 H), 1.94 (s, 3 H), 1.91–1.90 (m, 1 H).

Diazoamide 41: To a solution of **40** (0.173 g, 0.50 mmol, 1.0 equiv) in MeCN (4 mL) was added DBU (0.15 mL, 1.0 mmol, 2.0 equiv) and *p*-ABSA (0.144 g, 0.6 mmol, 1.2 equiv) at 23 °C. The reaction mixture was stirred at 23 °C for 14 h. Upon completion, the reaction contents were quenched by the addition of saturated aqueous $NaHCO_3$ (10 mL) and the contents were transferred to a separatory funnel, diluting with CH_2Cl_2 (20 mL). The layers were separated and the aqueous layer was extracted with CH_2Cl_2 (3 × 20 mL). The combined organic layers were then dried (Na_2SO_4), filtered, and concentrated. The resultant crude product was purified by flash chromatography (silica gel, EtOAc/hexanes, 1:10→1:5→1:4) to give **41** (0.143 g, 79%) as a light yellow solid. **41**: R_f = 0.42 (silica gel, EtOAc/hexanes, 1/2); ^{1}H NMR (500 MHz, $CDCl_3$) δ 7.68 (d, *J* = 7.8 Hz, 1 H), 7.48 (d, *J* = 7.3 Hz, 1 H), 7.37 (td, *J* = 7.6, 0.9 Hz, 1 H), 7.23 (td, *J* = 7.5, 0.9 Hz, 1 H), 5.32–5.31 (m, 1 H), 3.83–3.78 (m, 1 H), 3.78 (s, 3 H), 3.63 (ddd, *J* = 14.0, 5.8, 2.9 Hz, 1 H), 3.05 (ddd, *J* = 14.0, 11.0, 5.0 Hz, 1 H), 2.89–2.84 (m, 1H), 2.28–2.23 (m, 1 H), 2.01 (s, 3 H), 1.98 (s, 3 H), 1.76 (ddd, *J* = 12.7, 4.9, 2.9 Hz, 1 H).

Lactam 43: To a solution of **41** (0.161 g, 0.44 mmol, 1.0 equiv) in dry, degassed benzene (8 mL) was added Rh_2[(S)-DOSP]$_4$ (16.8 mg, 0.0088 mmol, 0.02 equiv) at 23 °C under argon atmosphere. The reaction was stirred at 23 °C for 8 h. Upon completion, the reaction contents were concentrated and the resultant crude product was purified by flash chromatography (silica gel, EtOAc/hexanes, 1:10→1:5→1:2) to give **43** (0.132 g, 88%) as a white solid. **43**: R_f = 0.22 (silica gel, EtOAc/hexanes, 1/2); ^{1}H NMR (500 MHz, $CDCl_3$) δ 7.72 (d, *J* = 7.8 Hz, 1 H), 7.47 (d, *J* = 7.5 Hz, 1 H), 7.41 (t, *J* = 7.2 Hz, 1 H), 7.29–7.26 (m, 1 H), 5.61 (s, 1 H), 4.25 (ddd, *J* = 10.8, 4.3, 2.1 Hz, 1 H), 3.79 (s, 3 H), 3.56 (d, *J* = 2.0 Hz, 1 H), 2.93–2.88 (m, 1 H), 2.86 (dd, *J* = 12.9, 4.3 Hz, 1 H), 2.05 (s, 3 H), 1.94 (s, 3 H), 1.33 (dd, *J* = 12.7, 11.1 Hz, 1 H).

Aminoketone 59. Prepared using a modified procedure from that reported in the literature by Kuehne.[19] A 100 mL round-bottom flask was charged with tryptamine **60** (9.60 g, 60.0 mmol, 1.0 equiv) and anhydrous methanol (200 mL). Upon dissolution, TFA (4.50 mL, 60.0 mmol, 1.0 equiv) and 2,3-butadione **61** (5.80 mL, 66.0 mmol, 1.1 equiv) were added sequentially and the solution was stirred at 60 °C for 20 h. The reaction contents were then cooled to 23 °C, the solvent was removed under reduced pressure, and the residue was partitioned between saturated aqueous $NaHCO_3$ (200 mL) and CH_2Cl_2 (400 mL). The layers were separated and the aqueous layer was extracted with CH_2Cl_2 (3 × 200 mL). The combined organic layers were then dried (Na_2SO_4), filtered, and concentrated. The resultant crude product was purified by flash chromatography (silica gel, CH_2Cl_2/MeOH, 1:0→50:1→20:1) to give aminoketone **59**

(6.90 g, 50%) as a brown foam. All spectroscopic data matched that reported in the literature[19]. **59**: R_f = 0.44 (silica gel, acetone/hexanes, 1/1); IR (film) ν_{max} 3328, 2924, 1706, 1453, 1350, 1298, 742 cm^{-1}; ^1H NMR (500 MHz, $CDCl_3$) δ 8.24 (s, 1 H), 7.49 (d, *J* = 7.8 Hz, 1 H), 7.35 (d, *J* = 8.1 Hz, 1 H), 7.17 (t, *J* = 7.5 Hz, 1 H), 7.10 (t, *J* = 7.3 Hz, 1 H), 3.34–3.31 (m, 1 H), 3.02 (dt, *J* = 12.8, 6.3 Hz, 1 H), 2.79–2.71 (m, 1 H), 2.35 (s, 3 H), 1.57 (s, 3 H); ^{13}C NMR (125 MHz, $CDCl_3$) δ 213.2, 136.2, 133.6, 126.8, 122.0, 119.3, 118.3, 111.0, 109.9, 63.5, 41.2, 25.6, 25.4, 22.5; HRMS (ESI) calcd for $C_{14}H_{17}N_2O^+$ [M + H^+] 229.1335, found 229.1336.

Enyne 63. To a solution of 1-bromo-1-propene (both *cis* and *trans* isomers, 4.50 mL, 52.6 mmol, 4.0 equiv) in THF (100 mL) at –78 °C was slowly added *n*-BuLi (42.0 mL, 105 mmol, 8.0 equiv). The reaction contents were then stirred at –78 °C for another 1.5 h.[55] To this freshly prepared 1-propynyl lithium solution at –78 °C was added a solution of **59** (3.00 g, 13.2 mmol, 1.0 equiv) in THF (100 mL) over 20 min via cannula. Once the addition was complete, the reaction contents were then stirred at –78 °C for an additional 2 h. Upon completion, the reaction contents were quenched by the addition of saturated aqueous $NaHCO_3$ (100 mL) and the contents were transferred to a separatory funnel, diluting with CH_2Cl_2 (100 mL). The layers were separated and the aqueous layer was extracted with CH_2Cl_2 (3 × 100 mL). The combined organic layers were then dried (Na_2SO_4), filtered, and concentrated to give **62** (3.50 g) as a crude red oil which was carried forward without any additional purification. Pressing forward, to so-obtained **62** (3.50 g) was dissolved in CH_2Cl_2 (100 mL), cooled to –78 °C, and pyridine (3.72 mL, 46.0 mmol, 3.5 equiv) and TFAA (4.03 mL, 29.0 mmol, 2.2 equiv)

were added sequentially dropwise, with the color of the original red-orange solution darkening during the process. The resultant solution was then allowed to warm to 23 °C over 2 h. Upon completion, the reaction contents were quenched by the addition of 0.5 M HCl (50 mL) and the contents were transferred to a separatory funnel, diluting with CH_2Cl_2 (100 mL). The layers were separated and the aqueous layer was extracted with CH_2Cl_2 (3 × 100 mL). The combined organic layers were then washed with $NaHCO_3$ (2 × 50 mL) and then dried (Na_2SO_4), filtered, and concentrated. The resultant crude product was purified by flash chromatography (silica gel, EtOAc/hexanes, 1:20→1:15→1:13) to give enyne **63** (2.43 g, 53% yield over two steps) as a yellow solid. **63**: R_f = 0.41 (silica gel, EtOAc/hexanes, 1/4); IR (film) ν_{max} 3366, 2919, 2232, 1688, 1439, 1202, 1148, 744 cm^{-1}; ^1H NMR (500 MHz, $CDCl_3$) δ 7.75 (s, 1 H), 7.53 (d, *J* = 7.8 Hz, 1 H), 7.35 (d, *J* = 8.1 Hz, 1 H), 7.21 (t, *J* = 7.6 Hz, 1 H), 7.15 (t, *J* = 7.3 Hz, 1 H), 5.59 (s, 1 H), 5.55 (s, 1 H), 4.05 (dt, *J* = 13.1, 4.8 Hz, 1 H), 3.82–3.79 (m, 1 H), 3.00 (ddd, *J* = 15.2, 8.0, 4.0 Hz, 1 H), 2.90 (ddd, *J* = 15.3, 5.8, 3.8 Hz, 1 H), 1.97 (s, 3 H), 1.81 (s, 3 H); ^{13}C NMR (125 MHz, $CDCl_3$) δ156.5 (q, *J* = 35.3 Hz), 136.1, 135.0, 134.5, 126.4, 122.5, 119.9, 118.5, 118.4, 114.5 (q, *J* = 287.5 Hz), 111.3, 109.2, 88.0, 63.6, 43.4 (d, *J* = 3.8 Hz), 22.9, 21.2, 4.0; HRMS (ESI) calcd for $C_{19}H_{18}F_3N_2O^+$ [M + H^+] 347.1366, found 347.1378.

Diene 64. To a flask charged with Ph_3PAuCl (0.198 g, 0.40 mmol, 0.10 equiv) and silver(I) tetrafluoroborate (77.9 mg, 0.40 mmol, 0.10 equiv) was added MeOH (10 mL) and the resultant mixture was stirred at 23 °C for 15 min. The suspension was then transferred to a solution of **63** (1.38 g, 3.98 mmol, 1.0 equiv) in MeOH (70 mL) at 23 °C.

The resultant mixture was then warmed to 40 °C and stirred at that temperature for 17 h. Upon completion, the reaction mixture was quenched by the addition of saturated aqueous $NaHCO_3$ (100 mL) and the contents were transferred to a separatory funnel, diluting with CH_2Cl_2 (200 mL). The layers were separated and the aqueous layer was extracted with CH_2Cl_2 (3 × 150 mL). The combined organic layers were then dried (Na_2SO_4), filtered, and concentrated. The resulting crude product was purified by flash chromatography (silica gel, EtOAc/hexanes, 1:20→1:15) to give diene **64** (1.02 g, 74% yield) as a yellow solid. **64**: R_f = 0.44 (silica gel, EtOAc/hexanes, 1/4); IR (film) ν_{max} 2940, 1700, 1436, 1199, 1140 cm^{-1}; ^1H NMR (500 MHz, $CDCl_3$) δ 7.67 (d, *J* = 7.7 Hz, 1 H), 7.49 (d, *J* = 7.4 Hz, 1 H), 7.38 (t, *J* = 7.6 Hz, 1 H), 7.26 (t, *J* = 7.5 Hz, 1 H), 5.87 (s, 1 H), 5.52 (s, 1 H), 5.29 (s, 1 H), 3.90 (dd, *J* = 14.7, 5.4 Hz, 1 H), 3.08–3.02 (m, 1 H), 2.49 (td, *J* = 12.8, 5.8 Hz, 1 H), 2.11 (s, 3 H), 2.02 (s, 3 H), 1.99 (ddd, *J* = 13.1, 4.7, 1.5 Hz, 1 H).; ^{13}C NMR (125 MHz, $CDCl_3$) δ 185.6, 155.4 (q, *J* = 35.5 Hz), 154.9, 142.5, 142.0, 137.4, 128.5, 126.1, 125.7, 123.6, 121.8, 116.8, 116.0 (q, *J* = 289.4 Hz), 65.3, 57.3, 43.3 (d, *J* = 3.8 Hz), 33.7, 19.2, 14.2; HRMS (ESI) calcd for $C_{19}H_{18}F_3N_2O^+$ [M + H^+] 347.1366, found 347.1379.

Isoxazolines 71 and 72. To a solution of **64** (0.417 mg, 1.2 mmol, 1.0 equiv) in MeOH (5 mL) at 23 °C was added solid K_2CO_3 (0.670 g, 4.8 mmol, 4.0 equiv). The resultant suspension was then heated to 60 °C and stirred at that temperature for 4 h. Upon completion, the reaction contents were quenched by the addition of saturated aqueous $NaHCO_3$ (10 mL) and the resultant mixture was transferred to a separatory funnel, diluting with CH_2Cl_2 (50 mL). The layers were separated and the aqueous layer

was extracted with CH_2Cl_2 (3 × 50 mL). The combined organic layers were then dried (Na_2SO_4), filtered, and concentrated to give the crude amine which was dissolved in THF (20 mL). To this solution was added Et_3N (0.83 mL, 6.0 mmol, 5.0 equiv) and 2-acetoxy nitroethane[21] (0.176 g, 1.3 mmol, 1.1 equiv) sequentially at 23 °C. The reaction contents were then stirred at 23 °C for 2 h. Upon completion as indicated by TLC analysis, 4-DMAP (29.0 mg, 0.24 mmol, 0.2 equiv) and Boc_2O (0.523 g, 2.4 mmol, 2.0 equiv) were added sequentially at 23 °C. The reaction contents were then stirred at 23 °C for 20 h, at which time a second portion of 4-DMAP (30.0 mg, 0.24 mmol, 0.2 equiv) and Boc_2O (0.670 g, 3.1 mmol, 2.6 equiv) were added sequentially. The reaction contents were stirred at 23 °C for a further 7 h. Upon completion, the reaction contents were quenched by the addition of saturated aqueous $NaHCO_3$ (10 mL) and transferred to a separatory funnel, diluting with CH_2Cl_2 (50 mL). The layers were then separated, and the aqueous layer was then extracted with CH_2Cl_2 (3 × 50 mL). The combined organic layers were dried (Na_2SO_4), filtered, and concentrated. The resultant residue was purified by flash chromatography (silica gel, acetone/hexanes, 1/10 →1/5→1/2) to afford *t*-butyl carbamate **71** (0.261 g, 54% yield) as a yellow solid and acetamide **72** (0.095 g, 23% yield) as a brown solid. **71**: R_f = 0.54 (silica gel, acetone/hexanes, 1/1); IR (film) ν_{max} 2980, 2936, 1770, 1738, 1370, 1238, 1150, 1051 cm^{-1}; ^1H NMR (500 MHz, $CDCl_3$) δ 7.73 (d, *J* = 7.8 Hz, 1H), 7.47 (d, *J* = 7.3 Hz, 1H), 7.40 (t, *J* = 7.6 Hz, 1H), 7.27–7.24 (m, 1H, overlap with $CDCl_3$), 6.47 (s, 1H), 6.37 (s, 1H), 4.20 (d, *J* = 18.0 Hz, 1H), 3.44 (d, *J* = 18.2 Hz, 1H), 2.59–2.45 (m, 3H), 2.01 (s, 3H), 1.80 (s, 3H), 1.56 (s, 9H), 1.52 (dd, *J* = 13.7, 6.5 Hz, 1H); ^{13}C NMR (125 MHz, $CDCl_3$) δ 184.6,

155.6, 155.4, 153.0, 152.1, 140.4, 140.1, 130.1, 128.6, 125.4, 124.1, 121.6, 108.7, 83.8, 58.2, 57.5, 49.8, 47.7, 38.7, 27.8, 21.8, 20.2; HRMS (ESI) calcd for $C_{24}H_{28}N_3O_3^+$ [M + H^+] 406.2125, found 406.2132.

72: R_f = 0.42 (silica gel, acetone/hexanes, 1/1); IR (film) ν_{max} 2923, 2850, 1764, 1596, 1437, 1366, 1197 cm^{-1}; ^1H NMR (500 MHz, $CDCl_3$) δ 7.69 (d, *J* = 7.9 Hz, 1H), 7.44 (d, *J* = 7.3 Hz, 1H), 7.37 (t, *J* = 7.5 Hz, 1H), 7.23 (t, *J* = 7.3 Hz, 1H), 6.46 (s, 1H), 6.31 (s, 1H), 4.17 (d, *J* = 18.0 Hz, 1H), 3.41 (d, *J* = 18.0 Hz, 1H), 2.56– 2.52 (m, 1H), 2.49–2.42 (m, 2H), 2.19 (s, 3H), 1.99 (s, 3H), 1.78 (s, 3H), 1.53–1.47 (m, 1H); ^{13}C NMR (125 MHz, $CDCl_3$) δ184.3, 168.3, 156.1, 155.4, 153.3, 140.7, 139.8, 130.0, 129.9, 128.5, 125.4, 124.0, 121.5, 108.4, 58.0, 57.3, 49.6, 47.6, 38.5, 21.7, 20.1, 19.5; HRMS (ESI) calcd for $C_{21}H_{23}N_3O_2^+$ [M + H^+] 348.1707, found 348.1713.

Rearrangement product 74. A suspension of $Mo(CO)_6$ (0.264 g, 1.0 mmol, 4.0 equiv) in MeCN (3 mL) was heated to 85 °C and stirred at that temperature for 3 h, during which time the reaction mixture solution color turned to blackish-yellow. The resultant Mo-containing solution was then cooled to 23 °C and a solution of **71** (0.100 g, 0.25 mmol, 1.0 equiv) in CH_2Cl_2 (1 mL) and water (0.4 mL) was added concurrently. The resultant solution immediately turned to dark red. The reaction contents were further stirred at 23 °C for 1 h. Upon completion, the reaction contents were quenched by the addition of water (10 mL) and then transferred to a separatory funnel, diluting with CH_2Cl_2 (50 mL). The layers were separated and the aqueous layer was extracted with CH_2Cl_2 (3 × 50 mL). The combined organic layers were dried (Na_2SO_4), filtered, and concentrated. The resultant crude residue was purified by flash chromatography

(silica gel, acetone/hexanes, 1/5 →1/3→1/1) to give rearrangement product **74** (45.1 mg, 59% yield) as a brown foam. **74**: R_f = 0.31 (silica gel, acetone/hexanes, 1/1); IR (film) ν_{max} 3357, 1719, 1594, 1447, 1377, 1194 cm^{-1}; ^1H NMR (500 MHz, $CDCl_3$) δ 7.74 (d, *J* = 7.6 Hz, 1 H), 7.48 (d, *J* = 7.3 Hz, 1 H), 7.42 (t, *J* = 7.6 Hz, 1 H), 7.29 – 7.26 (m, 1 H), 5.66 (s, 1 H), 3.88 (d, *J* = 15.7 Hz, 1 H), 3.08 (d, *J* = 15.7 Hz, 1 H), 2.96–2.89 (m, 1 H), 2.88 (d, *J* = 15.3 Hz, 1 H), 2.80–2.74 (m, 2 H), 2.21 (d, *J* = 12.7 Hz, 1 H), 1.94 (s, 6 H), 1.56 (d, *J* = 20.0 Hz, 1 H), 1.35 (td, *J* = 13.0, 4.7 Hz, 1 H); ^{13}C NMR (125 MHz, $CDCl_3$) δ 206.8, 185.1, 155.1, 139.8, 136.0, 132.4, 128.6, 125.6, 123.9, 121.6, 80.0, 62.0, 58.3, 57.0, 50.3, 47.1, 30.9, 19.6, 16.2; HRMS (ESI) calcd for $C_{19}H_{21}N_2O_2^+$ [M + H^+] 309.1598, found 309.1599.

Dienoate 83 and bromide 80. To a solution of **64** (0.155 g, 0.45 mmol, 1.0 equiv) in CH_2Cl_2 (4.5 mL) was added $Br(coll)_2PF_6$ (0.214 g, 0.46 mmol, 1.02 equiv) at –78 °C. The resulting solution was stirred at –78 °C for 30 min and then was allowed to warm to 23 °C over 30 min. Upon completion, the reaction contents were concentrated directly and $Pd(OAc)_2$ (2.0 mg, 0.009 mmol, 0.02 equiv) and Xantphos (10.4 mg, 0.018 mmol, 0.04 equiv) were added. The entire mixture was then dissolved in a combination of 1,4-dioxane (2 mL), MeOH (1 mL), and Et_3N (1 mL). The solution was sparged with CO (bubbled using a needle and balloon) for 5 min and then heated to 70 °C and stirred at that temperature for 13 h under a CO atmosphere. Upon completion, the reaction contents were concentrated directly and the resulting crude product was purified by flash chromatography (silica gel, EtOAc/hexanes, 1:15→1:12→1:10). The co-eluting collidine (2,4,6-trimethylpyridine) in the desired

fractions was further removed by re-dissolving the mixture in EtOAc, washing with 0.5 M HCl and saturated aqueous $NaHCO_3$ sequentially, drying (Na_2SO_4), and concentrating to give pure **83** (0.101 g, 56% yield) as a white solid. **83**: R_f = 0.29 (silica gel, EtOAc/hexanes, 1/4); IR (film) ν_{max} 2949, 1737, 1701, 1631, 1437, 1208, 113, 1143 cm^{-1}; ^1H NMR (500 MHz, $CDCl_3$) δ 7.67 (d, *J* = 7.7 Hz, 1 H), 7.51 (d, *J* = 7.4 Hz, 1 H), 7.40 (dd, *J* = 11.1, 4.2 Hz, 1 H), 7.29 (t, *J* = 7.5 Hz, 1 H), 7.14 (s, 1 H), 6.13 (s, 1 H), 3.97 (dd, *J* = 14.8, 6.0 Hz, 1 H), 3.68 (s, 3 H), 3.10–3.04 (m, 1 H), 2.56 (td, *J* = 13.0, 6.2 Hz, 1 H), 2.16 (s, 3 H), 2.08 (s, 3 H), 2.00 (dd, *J* = 13.3, 4.1 Hz, 1 H); ^{13}C NMR (125 MHz, $CDCl_3$) δ183.8, 166.4, 155.6 (q, *J* = 35.9 Hz), 154.9, 149.9, 144.3, 141.7, 128.8, 126.5, 123.6, 122.0, 121.8, 121.7, 116.7, 115.9 (q, *J* = 289.0 Hz), 66.0, 57.5, 51.4, 43.5(d, *J* = 3.6 Hz), 33.1, 19.8, 13.9; HRMS (ESI) calcd for $C_{21}H_{20}F_3N_2O_3^+$ [M + H^+] 405.1421, found 405.1433.

The vinyl bromide **80** could also be isolated upon removal of CH_2Cl_2 after first step, and purified via flash chromatography (silica gel, EtOAc/hexanes, 1:20→1:15), with its appearance being that of a white solid. **80**: R_f = 0.42 (silica gel, EtOAc/hexanes, 1/4); IR (film) ν_{max} 2940, 1701, 1438, 1200, 11431129, 1062 cm^{-1}; ^1H NMR (500 MHz, $CDCl_3$) δ 7.68 (d, *J* = 7.7 Hz, 1 H), 7.51 (d, *J* = 7.3 Hz, 1 H), 7.40 (t, *J* = 7.6 Hz, 1 H), 7.31–7.26 (m, 1 H), 6.63 (s, 1 H), 6.24 (s, 1 H), 3.91 (dd, *J* = 14.4, 5.2 Hz, 1 H), 3.05 (td, *J* = 14.5, 4.4 Hz, 1 H), 2.51 (td, *J* = 13.0, 5.9 Hz, 1 H), 2.10 (s, 6 H), 2.03–2.00 (m, 1 H).; ^{13}C NMR (125 MHz, $CDCl_3$) δ 184.4, 155.6 (q, *J* = 35.7 Hz), 154.8, 141.7, 141.0, 137.8, 128.8, 126.4, 123.7, 122.1, 122.0, 115.9 (q, *J* = 289.2 Hz), 110.2, 65.5, 57.2,

43.3 (d, J = 3.5 Hz), 33.4, 19.8, 14.2; HRMS (ESI) calcd for $C_{19}H_{17}BrF_3N_2O^+$ [M + H^+] 425.0471, found 425.0485.

1,6-Reduction Product 86. To a solution of **83** (0.040 g, 0.10 mmol, 1.0 equiv) in THF (2.5 mL) was added a suspension of Raney Nickel (0.200 g, washed three times with deionized water and three times with THF and then weighed) in THF (1 mL). The resultant reaction mixture was then stirred at 23 °C for 1.5 h under a H_2 atmosphere maintained by a standard balloon. Upon completion, the suspension was filtered through Celite® and the filtrate was concentrated. The resulting crude product was purified by flash chromatography (silica gel, EtOAc/hexanes, 1:15→1:10→1:8) to give **86** and **85** (34.4 mg, 86% combined yield, 10:1 ratio of **86** and **85** as indicated by ^{1}H NMR analysis) as a colorless oil. **86**: R_f = 0.34 (silica gel, EtOAc/hexanes, 1/4); IR (film) ν_{max} 2929, 2854, 1721, 1699, 1437, 1195, 1170, 1141 cm^{-1}; ^{1}H NMR (500 MHz, $CDCl_3$) δ 7.67 (d, J = 7.7 Hz, 1 H), 7.44 (d, J = 7.4 Hz, 1 H), 7.39 (t, J = 7.6 Hz, 1 H), 7.28–7.26 (m, 1 H), 6.11 (s, 1 H), 3.99 (dd, J = 14.4, 4.0 Hz, 1 H), 3.91 (dd, J = 14.1, 3.4 Hz, 1 H), 3.67 (s, 3 H), 2.80 (td, J = 14.1, 3.1 Hz, 1 H), 2.58 (td, J = 13.8, 4.9 Hz, 1 H), 2.05–2.03 (m, 4 H), 1.93 (t, J = 13.5 Hz, 1 H), 1.32 (d, J = 6.6 Hz, 3 H), 1.23–1.18 (m, 1 H); ^{13}C NMR (125 MHz, $CDCl_3$) δ 185.8, 166.4, 157.0, 155.1 (q, J = 35.7 Hz), 154.3, 145.8, 128.5, 126.3, 122.8, 122.0, 117.0, 116.0 (q, J = 288.8 Hz), 68.4, 57.3, 51.4, 43.4 (d, J = 3.4 Hz), 41.8, 29.0, 27.9, 15.6, 14.8; HRMS (ESI) calcd for $C_{21}H_{22}F_3N_2O_3^+$ [M + H^+] 407.1577, found 407.1571.

Lactam 88 and ester 85. To a microwave reaction tube containing **83** (0.182 g, 0.45 mmol, 1.0 equiv) and $Mn(dpm)_3$ (0.136 g, 0.22 mmol, 0.5 equiv) was added *i*-PrOH (2.3 mL) and 1,2-dichloroethane (2.3 mL) sequentially at 23 °C. Once full dissolution had occurred, $PhSiH_3$ (0.086 mL, 0.90 mmol, 2.0 equiv) was added, at which point the reaction mixture turned into bright yellow after 5 min. The resultant reaction mixture was stirred at 23 °C with the addition of further aliquots of $PhSiH_3$ (0.043 mL, 0.45 mmol, 1.0 equiv) after 10 h and 17 h to promote conversion. In total 3 portion of $PhSiH_3$ (0.17 mL, 1.80 mmol, 4.0 equiv) were added. After being stirring for 22 h from the beginning, the reaction had reached to full conversion as indicated by TLC analysis, and the reaction contents were concentrated directly and re-dissolved in MeOH (4 mL). Solid $NaBH_4$ (0.171 g, 4.52 mmol, 10 equiv) was then added and the reaction mixture was stirred at 23 °C for 1 h. The microwave reaction tube was then sealed with microwave cap and the reaction mixture was heated to 100 °C in an oil bath and stirred for 9 h at that temperature. Upon completion, the reaction contents were cooled down to 23 °C and quenched by the sequential addition of saturated aqueous $NaHCO_3$ (10 mL), 1 M aqueous Rochelle's salt solution (10 mL) and saturated NaCl (10 mL). The reaction contents were then transferred to a separatory funnel, diluting with CH_2Cl_2 (50 mL). The layers were separated and the aqueous layer was extracted with CH_2Cl_2 (3 × 50 mL). The combined organic layers were then dried (Na_2SO_4), filtered, and concentrated. The resulting crude product was purified by flash chromatography (silica gel, EtOAc/hexanes, 1:3→1:1→1:2, then EtOAc/acetone/ hexanes, 1:1:1) to give a mixture of compound **88** (62.5 mg, 50% combined yield, 1:2

ratio of **88-imine** and **88-amine** as indicated by ^{1}H NMR analysis) as a light yellow solid. The mixture of **88** was normal subjected to the next step directly without further separation. The ratio of imine/amine varied from ~7:1 to 1:2 depending on the scale and reaction time at 100 °C. **88-imine**: R_f = 0.45 (silica gel, acetone/hexanes, 1/1); IR (film) ν_{max} 2927, 1687, 1389, 1378, 1133, 1077, 745 cm^{-1}; ^{1}H NMR (500 MHz, $CDCl_3$) δ 7.67 (d, *J* = 7.7 Hz, 1 H), 7.45 (d, *J* = 7.4 Hz, 1 H), 7.37 (t, *J* = 7.3 Hz, 1 H), 7.26–7.23 (m, 1 H), 5.04 (s, 1 H), 4.12–4.05 (m, 1 H), 3.05 (br s, 1 H), 2.97 (dd, *J* = 15.9, 6.0 Hz, 1 H), 2.64–2.53 (m, 2 H), 2.17 (d, *J* = 15.9 Hz, 1 H), 1.93–1.90 (m, 4 H), 1.74 (s, 3 H); ^{13}C NMR (125 MHz, $CDCl_3$) δ 188.1, 176.6, 155.2, 142.4, 139.0, 128.3, 125.8, 124.2, 124.2, 121.3, 63.2, 56.2, 50.8, 36.9, 36.3, 36.2, 20.2, 17.6; HRMS (ESI) calcd for $C_{18}H_{19}N_2O^+$ [M + H$^+$] 279.1492, found 279.1503.

88-amine: R_f = 0.41 (silica gel, acetone/hexanes, 1/1); IR (film) ν_{max} 2927, 1676, 1464, 1399, 1133, 1080, 744 cm^{-1}; ^{1}H NMR (500 MHz, $CDCl_3$) δ 7.13 (d, *J* = 7.3 Hz, 1 H), 7.09 (t, *J* = 7.8 Hz, 1 H), 6.85 (t, *J* = 7.3 Hz, 1 H), 6.77 (d, *J* = 7.8 Hz, 1 H), 5.12 (s, 1 H), 4.11 (dd, *J* = 14.0, 9.2 Hz, 1 H), 3.90 (s, 1 H), 3.79 (s, 1 H), 3.00–2.93 (m, 1 H), 2.87–2.80 (m, 2 H), 2.33 (dd, *J* = 22.4, 9.5 Hz, 1 H), 2.02–1.95 (m, 2 H), 1.46 (s, 3 H), 1.44 (s, 3 H); ^{13}C NMR (125 MHz, $CDCl_3$) δ176.4, 149.9, 134.0, 133.8, 127.8, 124.5, 123.1, 120.2, 111.7, 68.1, 60.4, 46.4, 41.3, 36.4, 32.8, 30.3, 22.2, 18.2; HRMS (ESI) calcd for $C_{18}H_{21}N_2O^+$ [M + H$^+$] 281.1648, found 281.1660.

The 1,4-reduction intermediate **85** could also be isolated using the same workup protocol and purified via flash chromatography (silica gel, EtOAc/hexanes, 1:15→1:12→1:10), with its appearance being that of a colorless oil. **85**: R_f = 0.34 (silica

gel, EtOAc/hexanes, 1/4); IR (film) ν_{max} 2952, 1736, 1702, 1438, 1200, 1143 cm^{-1}; ^1H NMR (500 MHz, $CDCl_3$) δ 7.76 (d, *J* = 7.7 Hz, 1 H), 7.51 (d, *J* = 7.4 Hz, 1 H), 7.43 (t, *J* = 7.2 Hz, 1 H), 7.29 (t, *J* = 7.1 Hz, 1 H), 5.58 (s, 1 H), 3.85 (d, *J* = 13.6 Hz, 1 H), 3.74 (s, 3 H), 3.68–3.62 (m, 1 H), 3.13 (dd, *J* = 16.0, 2.8 Hz, 1 H), 3.03 (d, *J* = 11.3 Hz, 1 H), 2.39 (dd, *J* = 16.0, 11.5 Hz, 1 H), 2.32 (d, *J* = 13.4 Hz, 1 H), 2.22 (s, 3 H), 1.92 (s, 3 H), 1.42 (td, *J* = 13.1, 4.4 Hz, 1 H); ^{13}C NMR (125 MHz, $CDCl_3$) δ 183.6, 172.3, 157.9 (q, *J* = 34.6 Hz), 154.5, 140.3, 131.4, 128.7, 128.1, 125.9, 123.8, 122.0, 116.5 (q, *J* = 289.4 Hz), 64.2, 56.5, 52.0, 48.4, 41.2 (d, *J* = 4.2 Hz), 34.9, 32.5, 21.0, 19.8; HRMS (ESI) calcd for $C_{21}H_{22}F_3N_2O_3^+$ [M + H^+] 407.1577, found 407.1575.

Alcohol 89. To a flask charged with **27** (mixture of amine and imine, 15.2 mg, 0.054 mmol, 1.0 equiv) was added BH_3•THF (1.08 mL, 1.0 M in THF, 1.08 mmol, 20.0 equiv) at 23 °C. After stirring the resultant reaction mixture at 23 °C for 12 h, the reaction was quenched by the addition of 1 M NaOH (2 mL) and 10% H_2O_2 (2 mL) and further stirred for 1 h. The mixture was then were transferred to a separatory funnel, diluting with CH_2Cl_2 (10 mL). The layers were separated and the aqueous layer was extracted with CH_2Cl_2 (3 × 5 mL). The combined organic layers were then dried (Na_2SO_4), filtered, and concentrated to give crude **90** that was dissolved in CH_2Cl_2 (2 mL). To this solution was added iodosobenzene (15.0 mg, 0.068 mmol, 1.3 equiv) at 23 °C. The reaction mixture was then stirred at 23 °C for 2 h, filtered through Celite®, and concentrated. The resulting crude product was purified by flash chromatography (silica gel, CH_2Cl_2/MeOH, 20:1→10:1) to give **89** (7.7 mg, 50% yield) as a yellow oil. **89**: R_f = 0.10 (silica gel, CH_2Cl_2/MeOH, 10/1); IR (film) ν_{max} 3347, 2929, 1587, 1453,

1374, 1038, 1014, 748 cm^{-1}; ^{1}H NMR (500 MHz, $CDCl_3$) δ 7.71 (d, *J* = 7.6 Hz, 1 H), 7.40–7.35 (m, 2 H), 7.20 (t, *J* = 7.4 Hz, 1 H), 3.56 (t, *J* = 8.9 Hz, 1 H), 3.48 (t, *J* = 9.4 Hz, 1 H), 3.03 (dd, *J* = 18.0, 10.2 Hz, 1 H), 2.71–2.65 (m, 1 H), 2.55 (dt, *J* = 14.2, 8.5 Hz, 2 H), 2.46–2.37 (m, 1 H), 2.14 (dd, *J* = 12.9, 7.1 Hz, 1 H), 2.06 (t, *J* = 6.1 Hz, 1 H), 1.75 (d, *J* = 14.2 Hz, 1 H), 1.55 (s, 3 H), 1.34 (d, *J* = 6.4 Hz, 3 H), 1.18–1.12 (m, 1 H); ^{13}C NMR (125 MHz, $CDCl_3$) δ 191.9, 155.2, 146.2, 128.0, 125.0, 123.4, 121.4, 76.0, 64.2, 58.4, 56.2, 51.7, 48.6, 47.5, 31.7, 27.9, 24.0, 13.8; HRMS (ESI) calcd for $C_{18}H_{23}N_2O^+$ [M + H^+] 283.1805, found 283.1814.

One-pot procedure to prepare arborisidine (1). To a flask charged with a mixture of imine and amine variants of **88** (imine/amine = 1:2, 57.1 mg, 0.20 mmol, 1.0 equiv) was added BH_3•THF (1.03 mL, 1.0 M in THF, 1.03 mmol, 5.0 equiv) at 23 °C. After stirring the resultant reaction mixture at 23 °C for 12 h, water (7 μL, 0.41 mmol, 2.0 equiv) in THF (0.5 mL) and Me_3NO•$2H_2O$ (25.0 mg, 0.22 mmol, 1.1 equiv) were added sequentially. The reaction contents were then heated to 65 °C and stirred for 2 h. Upon completion, the reaction contents were then concentrated directly to dryness, re-dissolved in CH_2Cl_2 (2 mL) and PhIO (67.5 mg, 0.31 mmol, 1.5 equiv) was added at 23 °C. The reaction mixture was then stirred at 23 °C for 2.5 h, after which solid $NaHCO_3$ (86.5 mg, 1.03 mmol, 5.0 equiv) and Dess–Martin periodinane (0.130 g, 0.31 mmol, 1.5 equiv) were added sequentially. The reaction mixture was stirred at 23 °C for 1 h. Upon completion, the reaction contents were quenched by the addition of saturated aqueous $NaHCO_3$ (5 mL) and saturated aqueous $Na_2S_2O_3$ (5 mL) and

stirred at 23 °C for 15 min. The mixture was then were transferred to a separatory funnel, diluting with CH_2Cl_2 (20 mL). The layers were separated and the aqueous layer was extracted with CH_2Cl_2 (3 × 20 mL). The combined organic layers were then dried (Na_2SO_4), filtered, and concentrated. The resulting crude product was purified by flash chromatography (silica gel, acetone/EtOAc/hexanes, 0:1:1→1:0:1→2:0:1, then CH_2Cl_2/MeOH, 20:1→10:1) to give arborisidine (**1**, 19.7 mg, 34% yield) as a yellow oil and alcohol **89** (23.0 mg, 40% yield) as a brown foam. **1**: R_f = 0.44 (silica gel, CH_2Cl_2/MeOH, 10/1); IR (film) ν_{max} 2979, 2938, 1699, 1591, 1452, 1374, 1273, 1207, 1020, 767, 749 cm^{-1}; ^1H NMR (500 MHz, $CDCl_3$) δ 7.80 (d, *J* = 7.8 Hz, 1 H), 7.46–7.42 (m, 2 H), 7.27–7.24 (m, 1 H), 3.31–3.25 (m, 1 H), 2.90–2.81 (m, 3 H), 2.67 (d, *J* = 8.7 Hz, 1 H), 2.43 (d, *J* = 14.2 Hz, 1 H), 2.36–2.30 (m, 1 H), 2.18 (t, *J* = 12.6 Hz, 1 H), 2.07 (q, *J* = 6.4 Hz, 1 H), 1.63 (s, 3 H), 1.50 (d, *J* = 4.0 Hz, 1 H), 1.45 (d, *J* = 6.7 Hz, 3 H); ^{13}C NMR (125 MHz, $CDCl_3$) δ 210.5, 186.2, 154.9, 144.3, 128.5, 125.5, 122.9, 121.7, 65.5, 57.5, 56.3, 52.2, 52.0, 47.9, 30.0, 27.6, 21.1, 10.2; HRMS (ESI) calcd for $C_{18}H_{21}N_2O^+$ [M + H^+] 281.1648, found 281.1657. All spectroscopic data matched the natural sample reported by the isolation team[1] as denoted below in Table 3.8 and 3.9.

Oxidation of 89 to 1. To a vial charged with **89** (8.3 mg, 0.029 mmol, 1.0 equiv) was added CH_2Cl_2 (1 mL). Upon dissolution, solid $NaHCO_3$ (12.4 mg, 0.148 mmol, 5.0 equiv) and Dess–Martin periodinane (12.5 mg, 0.029 mmol, 1.0 equiv) were added sequentially at 23 °C. The reaction mixture was then stirred at 23 °C for 1 h.

Upon completion, the reaction contents were quenched by the addition of saturated aqueous $NaHCO_3$ (1 mL) and saturated aqueous $Na_2S_2O_3$ (1 mL) and then were transferred to a separatory funnel, diluting with CH_2Cl_2 (10 mL). The layers were separated and the aqueous layer was extracted with CH_2Cl_2 (3 × 10 mL). The combined organic layers were then dried (Na_2SO_4), filtered, and concentrated. The resulting crude product was purified by flash chromatography (silica gel, acetone/EtOAc/hexane, 0:1:0→1:0:1) to give arborisidine (**1**, 6.1 mg, 74% yield) as a yellow oil, identical in all respects to the sample characterized above.

Table 3.8 ^{1}H NMR data comparison of synthetic arborisidine (**1**) with natural **1**

^{1}H NMR (in $CDCl_3$)	
Synthetic **1** (500 MHz)	Natural **1** (600 MHz)
7.80 (d, *J* = 7.8 Hz, 1 H)	7.80 (d, *J* = 8 Hz, 1 H)
7.46–7.42 (m, 2 H)	7.45 (m, 1 H)
	7.43 (m, 1 H)
7.27–7.24 (m, 1 H)	7.26 (m, 1 H)
3.31–3.25 (m, 1 H)	3.29 (m, 1 H)
2.90–2.81 (m, 3 H)	2.86 (m, 3 H)
2.67 (d, *J* = 8.7 Hz, 1 H)	2.67 (d, *J* = 9 Hz, 1 H)
2.43 (d, *J* = 14.2 Hz, 1 H)	2.43 (dt, *J* = 14, 4 Hz, 1 H)
2.36–2.30 (m, 1 H)	2.35 (m, 1 H)
2.18 (t, *J* = 12.6 Hz, 1 H)	2.18 (ddd, *J* = 14, 12, 4 Hz, 1 H)
2.07 (q, *J* = 6.4 Hz, 1 H)	2.08 (q, *J* = 7 Hz, 1 H)
1.63 (s, 3 H)	1.63 (s, 3 H)
1.50 (d, *J* = 4.0 Hz, 1 H)*	1.48 (ddd, *J* = 14, 12, 5 Hz, 1 H)
1.45 (d, *J* = 6.7 Hz, 3 H)	1.45 (d, *J* = 7 Hz, 3 H)

* the rest of the peak was on the shoulder of peak 1.45.

Table 3.9 ^{13}C NMR data comparison of synthetic arborisidine (**1**) with natural **1**

^{13}C NMR (in $CDCl_3$)	
Synthetic **1** (125 MHz)	Natural **1** (150 MHz)
210.5	210.5
186.2	186.2
154.9	155.0
144.3	144.3
128.5	128.6
125.5	125.5
122.9	122.9
121.7	121.7
65.5	65.6
57.5	57.6
56.3	56.3
52.2	52.2
52.0	52.1
47.9	48.0
30.0	30.0
27.6	27.7
21.1	21.2
10.2	10.2
77.0 (t, $CDCl_3$)	N/A (t, $CDCl_3$)

Ester 113 and **114**. A 250 mL round-bottom flask was charged with *D*-tryptophan methyl ester hydrochloride (**112**, 10.0 g, 39.0 mmol, 1.0 equiv) and anhydrous MeOH (130 mL). Upon dissolution, 2,3-butadione (**61**, 8.50 mL, 96 mmol, 2.5 equiv) was added and the solution was stirred at 65 °C for 20 h. The reaction contents were then cooled to 23 °C and the reaction contents were partitioned between

saturated aqueous $NaHCO_3$ (100 mL) and CH_2Cl_2 (100 mL). The layers were separated and the aqueous layer was extracted with CH_2Cl_2 (3 × 150 mL). The combined organic layers were then dried (Na_2SO_4), filtered, and concentrated. A portion of the major diastereomer **113** was collected (0.77 g) as white crystalline solid via trituration and washing with EtOAc. The remaining solution was concentrated again and the residue was purified by flash chromatography (silica gel, EtOAc/hexanes, 1:9→1:3→1:1) to give **114** (as minor diastereomer, 3.73 g, 33% yield) as a yellow solid and **113** (6.00 g, 6.77 g in combination of sample obtained above, 62% yield) as a light-yellow solid. **113**: R_f = 0.37 (silica gel, EtOAc/hexanes, 1/1); $[\alpha]_D^{25}$ = –17.1° (c = 0.39, $CHCl_3$); IR (film) ν_{max} 3329, 1726, 1709, 1432, 1355, 745 cm^{-1}; ^1H NMR (500 MHz, $CDCl_3$) δ 8.42 (s, 1 H), 7.49 (d, *J* = 7.8 Hz, 1 H), 7.35 (d, *J* = 8.1 Hz, 1 H), 7.19 (t, *J* = 7.6 Hz, 1 H), 7.11 (t, *J* = 7.4 Hz, 1 H), 3.86 (s, 3 H), 3.73 (dd, *J* = 11.0, 4.1 Hz, 1 H), 3.13 (dd, *J* = 15.3, 4.1 Hz, 1 H), 2.79 (dd, *J* = 15.3, 11.0 Hz, 1 H), 2.38 (s, 3 H), 1.60 (s, 3 H); ^{13}C NMR (125 MHz, $CDCl_3$) δ213.1, 173.4, 136.6, 133.3, 126.5, 122.3, 119.6, 118.2, 111.2, 108.7, 63.2, 54.5, 52.3, 26.7, 26.2, 25.3; HRMS (ESI) calcd for $C_{16}H_{19}N_2O_3^+$ [M + H^+] 287.1390, found 287.1396. The relative configuration of major diastereomer **113** was confirmed by single crystal X-ray diffraction analysis of its enantiomer (obtained as major diastereomer from L-tryptophan methyl ester hydrochloride with comparable yield and d.r.).

114: R_f = 0.63 (silica gel, EtOAc/hexanes, 1/1); $[\alpha]_D^{25}$ = –65.3 (c = 0.56, $CHCl_3$); IR (film) ν_{max} 3374, 1735, 1710, 1437, 1350, 1225, 745 cm^{-1}; ^1H NMR (500 MHz, $CDCl_3$) δ 8.19 (s, 1 H), 7.51 (d, *J* = 7.8 Hz, 1 H), 7.32 (d, *J* = 8.1 Hz, 1 H), 7.19

(t, *J* = 7.5 Hz, 1 H), 7.12 (t, *J* = 7.4 Hz, 1 H), 3.95 (d, *J* = 10.5 Hz, 1 H), 3.85 (s, 3 H), 3.21 (dd, *J* = 15.0, 2.4 Hz, 1 H), 2.90 (dd, *J* = 14.7, 11.1 Hz, 1 H), 2.36 (br, s, 1 H), 2.29 (s, 3 H), 1.64 (s, 3 H); ^{13}C NMR (125 MHz, $CDCl_3$) δ 211.7, 173.3, 136.4, 133.0, 126.7, 122.4, 119.7, 118.3, 111.2, 108.7, 64.1, 52.7, 52.3, 25.5, 25.5, 24.3; HRMS (ESI) calcd for $C_{16}H_{18}N_2O_3Na^+$ [M + Na^+] 309.1210, found 309.1219.

Nitrile 127. To a flask containing **113** (6.00 g, 21.0 mmol, 1.0 equiv) at 23 °C was added a solution of NH_3 in MeOH (7 M, 150 mL) and the resulting solution was stirred at 23 °C for 15 h. Upon completion, the reaction contents were concentrated to dryness and connected to a vacuum line for 5 min to remove trace NH_3, after which time the resultant residual **126** was dissolved in THF (200 mL). To this solution was added Et_3N (6.19 mL, 42.0 mmol, 2.0 equiv) and TFAA (2.92 mL, 21.0 mmol, 1.0 equiv) at 23 °C and the resultant solution was stirred for 1 h at that temperature. At that time, a second portion of Et_3N (3.09 mL, 21.0 mmol, 1.0 equiv) and TFAA (1.46 mL, 10.5 mmol, 0.5 equiv) was added and the solution was further stirred at 23 °C for 1.5 h. Upon completion, the reaction was quenched by the addition of 0.5 M HCl (100 mL) and the contents were transferred to a separatory funnel, diluting with EtOAc (100 mL). The layers were separated and the organic layer was washed with saturated aqueous $NaHCO_3$ (2 × 100 mL), dried (Na_2SO_4), filtered, and concentrated. The resultant crude product was purified by flash chromatography (silica gel, EtOAc/hexanes, 1:10→1:7→1:3) to give nitrile **127** (5.11 g, 96% yield) as a yellow solid. **127**: R_f = 0.45 (silica gel, EtOAc/hexanes, 1/1); $[\alpha]_D^{25}$ = –14.9° (c = 0.49, $CHCl_3$); IR (film) ν_{max} 3347, 1709, 154, 1375, 1354, 1305 1253, 744 cm^{-1}; ^{1}H NMR (500 MHz, $CDCl_3$) δ 8.20 (s,

1H), 7.49 (d, *J* = 7.8 Hz, 2 H), 7.37 (d, *J* = 8.1 Hz, 1 H), 7.22 (t, *J* = 7.7 Hz, 2 H), 7.14 (t, *J* = 7.4 Hz, 1 H), 4.13 (d, *J* = 4.1 Hz, 1 H), 3.21 (dd, *J* = 15.3, 4.5 Hz, 1 H), 3.12 (dd, *J* = 15.3, 7.6 Hz, 1 H), 2.31 (s, 3 H), 2.13 (d, *J* = 6.0 Hz, 1 H), 1.71 (s, 3 H); ^{13}C NMR (125 MHz, $CDCl_3$) δ 211.0, 136.6, 132.0, 126.2, 122.9, 120.2, 120.1, 118.3, 111.3, 107.0, 63.6, 42.7, 27.1, 25.4, 25.0; HRMS (ESI) calcd for $C_{15}H_{16}N_3O^+$ [M + H^+] 254.1288, found 2554.1287.

Aminoketone (–)-**59**. To a flask containing **127** (1.41 g, 5.57 mmol, 1.0 equiv) and 4-trifluoromethyl benzaldehyde (2.50 g, 14.4 mmol, 2.6 equiv) was added MeOH (56 mL). Upon dissolution, a solution of $NaBH_3CN$ (1.0 M in THF, 11.2 mL, 11.2 mmol, 2.0 equiv) was added and the solution was then warmed to 65 °C and stirred at that temperature for 8 h. Upon completion, the reaction contents were cooled to 23 °C and transferred to a separatory funnel, diluting with saturated aqueous $NaHCO_3$ (50 mL) and CH_2Cl_2 (100 mL). The layers were separated and the aqueous layer was extracted with CH_2Cl_2 (3 × 100 mL). The combined organic layers were then dried (Na_2SO_4), filtered, and concentrated. The resultant crude product was purified by flash chromatography (silica gel, EtOAc/hexanes, 1:3→1:1) to give aminoketone (–)-**59** (0.91 g, 71% yield) as a brown foam. All spectroscopic data were in full agreement with the racemic compound. (–)-**59**: $[\alpha]_D^{25}$ = –19.1° (c = 0.12, $CHCl_3$).

Chiral **110**. To a solution of (–)-**59** (0.346 g, 1.52 mmol, 1.0 equiv) in CH_2Cl_2 (7 mL) were added pyridine (0.15 mL, 1.82 mmol, 1.5 equiv) and TFAA (0.21 mL, 1.52 mmol, 1.0 equiv) sequentially. The resultant solution was stirred at 23 °C for 40

min. Upon completion, the reaction contents were quenched by the addition of 0.5 M HCl (5 mL) and the contents were transferred to a separatory funnel, diluting with CH_2Cl_2 (10 mL). The layers were separated and the aqueous layer was extracted with CH_2Cl_2 (3 × 10 mL). The combined organic layers were then washed with $NaHCO_3$ (2 × 5 mL) and then dried (Na_2SO_4), filtered, and concentrated. The resultant crude product was purified by flash chromatography (silica gel, EtOAc/hexanes, 1:20→1:15) to give **110** (0.395 g, 75% yield) as a light yellow solid. **110**: R_f = 0.48 (silica gel, EtOAc/hexanes, 1/4); ^{1}H NMR (500 MHz, $CDCl_3$) δ7.87 (s, 1 H), 7.53 (d, *J* = 7.8 Hz, 1 H), 7.34 (d, *J* = 8.2 Hz, 1 H), 7.26–7.23 (m, 1 H), 7.16 (t, *J* = 7.4 Hz, 1 H), 4.43 (d, *J* = 13.3 Hz, 1 H), 3.54–3.49 (m, 1 H), 3.12–3.04 (m, 2 H), 1.87 (s, 3 H), 1.84 (s, 3 H). The chiral material was prepared as described above using (–)-**59** (4.6 mg, 0.020 mmol, 1.0 equiv) to afford chiral **110** (4.9 mg, 70%) with its appearance being a light yellow solid. All spectroscopic data were in full agreement with the racemic compound. The enantiopurity was determined using chiral HPLC (AD-H column, 9:1 hexanes/*i*-PrOH, 1 mL/min) and found to be 99% ee.

Enyne (+)-**63.** Prepared as described above using (–)-**59** (1.50 g, 6.59 mmol) to afford (+)-**63** (1.21 g, 53% yield) as a yellow solid. All spectroscopic data were in full agreement with the racemic compound. (+)-**63**: $[\alpha]_D^{25}$ = +26.3° (*c* = 0.07, $CHCl_3$).

Diene (+)-**64.** Prepared as described above using chiral **63** (0.311 g, 0.90 mmol) to afford chiral (+)-**64** (0.264 g, 74% yield) as a light yellow foam. All

spectroscopic data were in full agreement with the racemic compound. (+)-**64**: $[\alpha]_D^{25}$ = +144° (*c* = 0.24, $CHCl_3$).

Dienoate (+)-**83.** Prepared as described above using (+)-**64** (0.177 g, 0.51 mmol) to afford (+)-**83** (0.129 g, 62% yield) as a light yellow solid. All spectroscopic data were in full agreement with the racemic compound. (+)-**83**: $[\alpha]_D^{25}$ = +11.8° (*c* = 0.23, $CHCl_3$).

Lactam (+)-**88.** Prepared as described above using chiral (+)-**83** (81.1 mg, 0.20 mmol) to afford (+)-**88-imine** (20.1 mg, 36% yield) as a yellow oil and (+)-**88-amine**(13.7 mg, 24% yield) as a light yellow solid. All spectroscopic data were in full agreement with the racemic compounds. (+)-**88-imine**: $[\alpha]_D^{21}$ = +27.4° (*c* = 0.20, $CHCl_3$). (+)-**88-amine**: $[\alpha]_D^{21}$ = +40.1° (*c* = 0.34, $CHCl_3$).

Arborisidine (+)-1 and alcohol (+)-89. Prepared as described above using (+)-**88** (imine/amine = 1.5:1, 9.0 mg, 0.032 mmol, 1.0 equiv) to afford arborisidine (+)-**1** (3.3 mg, 36% yield) as a yellow oil and alcohol (+)-**89** (1.0 mg, 11% yield) as a brown oil. All spectroscopic data were in full agreement with the racemic compounds. (+)-**1**: $[\alpha]_D^{25}$ = +14.2° (*c* = 0.08, $CHCl_3$). (+)-**89**: $[\alpha]_D^{25}$ = +18.9°(*c* = 0.05, $CHCl_3$). Note: lower combined yields have also been observed alone with small-scale racemic material experiments, presumably due to the inefficient PhIO oxidation, since the precipitated boronic acid and insoluble PhIO would stick onto the inner wall of reaction tubes and thus might prevent sufficient contact with substrates.

3.8 References

[1] Wong, S.-P.; Chong, K.-W.; Lim, K.-H.; Lim, S.-H.; Low, Y.-Y.; Kam, T.-S. *Org. Lett*. **2016**, *18*, 1618.

[2] Smith, M. W.; Zhou, Z.; Gao, A. X.; Shimbayashi, T.; Snyder, S. A. *Org. Lett*. **2017**, *19*, 1004.

[3] Gan, P.; Pitzen, J.; Qu, P.; Snyder, S. A. *J. Am. Chem. Soc.* **2018**, *140*, 919.

[4] Wong, S. P.; Gan, C. Y.; Lim, K. H.; Ting, K. N.; Low, Y. Y.; Kam, T. S. *Org. Lett.* **2015**, *17*, 3628.

[5] Zhuang, H.; Wei, S. Medicine composition for inhibiting stomach cancer. Chinese Patent CN106540237A, **2016**.

[6] Chen, Z.; Xiao, T.; Song, H.; Qin, Y. *Chin. J. Org. Chem.* **2018**, *38*, 2427.

[7] Xiao, T.; Chen, Z.; Deng, L.; Zhang, D.; Liu, X.-Y.; Song, H.; Qin, Y. *Chem. Commun.* **2017**, *53*, 12665.

[8] Gao, A. X. Ph.D. Dissertation, The Scripps Research Institute, Jupiter, FL, **2017**.

[9] Shi, Q.; Meehan, M. C.; Galella, M.; Park, H.; Khandelwal, P.; Hynes, J. Jr.; Dhar, T. G. M.; Marcoux, D. *Org. Lett.* **2018**, *20*, 337.

[10] (a) Huang, P.-Q.; Huang, S.-Y.; Gao, L.-H.; Mao, Z.-Y.; Chang, Z.; Wang, A.-E. *Chem. Commun.* **2015**, *51*, 4576; (b) Granger, B. A.; Jewett, I. T.; Butler, J. D.; Hua, B.; Knezevic, C. E.; Parkinson, E. I.; Hergenrother, P. J.; Martin, S. F. *J. Am. Chem. Soc.* **2013**, *135*, 12984; (c) Granger, B. A.; Jewett, I. T.; Butler, J. D.; Martin, S. F. *Tetrahedron*, **2014**, *70*, 4094.

[11] Ouihia, A.; Rene, L.; Guilhem, J.; Pascard, C.; Badet, B. *J. Org. Chem.* **1993**, *58*, 1641.

[12] Baum, J. S.; Shook, D. A.; Davies, H. M.; Smith, H. D. *Synth. Commun.* **1987**, *17*, 1709.

[13] Davies, H.M., Ren, P. and Jin, Q. *Org. Lett.* **2001**, *3*, 3587.

[14] (a) Doyle, M. P.; Shanklin, M. S.; Oon, S. M.; Pho, H. Q.; Van der Heide, F. R.; Veal, W. R. *J. Org. Chem.* **1988**, *53*, 3384; (b) Doyle, M. P.; Taunton, J.; Pho, H. Q. *Tetrahedron Lett.* **1989**, *30*, 5397; (c) Wee, A. G. H.; Liu, B.; Zhang, L. *J. Org. Chem.* **1992**, *57*, 4404.

[15] Alam, R.; Das, A.; Huang, G.; Eriksson, L.; Himo, F.; Szabó, K. J. *Chem. Sci*. **2014**, *5*, 2732.

[16] Raducan, M.; Alam, R.; Szabó, K. J. *Angew. Chem., Int. Ed.* **2012**, *51*, 13050.

[17] Zhang, P.; Roundtree, I. A.; Morken, J. P. *Org. Lett.* **2012**, *14*, 1416.

[18] Hutchison, D.A., Beck, K.R., Benkeser, R.A. and Grutzner, J.B. *J. Am. Chem. Soc.* **1973**, *95*, 7075.

[19] Kuehne, M. E. Process for the preparation of (+,-) vincadifformine and other related pentacyclic derivatives. European Patent EP0011059A1, **1978**.

[20] Prasad, S. S.; Baskaran, S. *J. Org. Chem.* **2018**, *83*, 1558.

[21] López, R.; Zalacain, M.; Palomo, C. *Chem. Eur. J.* **2011**, *17*, 2450.

[22] (a) Kozikowski, A. P.; Adamczyk, M. *Tetrahedron Lett.* **1982**, *23*, 3123; (b) Chiara, J. L.; Destabel, C.; Gallego, P.; Marco-Contelles, J. *J. Org. Chem.* **1996,** *61*, 359; (c)

Jiang, D.; Chen, Y. *J. Org. Chem.* **2008**, *73*, 9181; (d) Fukuzawa, H.; Ura, Y.; Kataoka, Y. *J. Organomet. Chem.* **2011**, *696*, 3643
[23] (a) Baraldi, P. G.; Barco, A.; Benetti, S.; Manfredini, S.; Simoni, D. 1987. Ring cleavage of 3, 5-disubstituted 2-isoxazolines by molybdenum hexacarbonyl and water to β-hydroxy ketones. *Synthesis* **1987**, 276; (b) Cicchi, S.; Goti, A.; Brandi, A.; Guarna, A.; De Sarlo, F. 1990. *Tetrahedron Lett.* **1990**, *31*, 3351.
[24] (a) Tate, D. P.; Knipple, W. R.; Augl, J. M. *Inorg. Chem.* **1962**, *1*, 433; (b) Kobayashi, T.; Nitta, M. *Bull. Chem. Soc. Jpn.* **1985**, *58*, 152; (c) Guarna, A.; Guidi, A.; Goti, A.; Brandi, A.; De Sarlo, F. *Synthesis* **1989**, 175.
[25] For a similar $Mo(CO)_6$ mediated rearrangement of epoxides, see: Alper, H.; Des Roches, D.; Durst, T.; Legault, R. *J. Org. Chem.* **1976**, 41, 3611.
[26] (a) Nobe, Y.; Arayama, K.; Urabe, H. *J. Am. Chem. Soc. 2005*, *127*, 18006; (b) Taniguchi, T.; Sugiura, Y.; Zaimoku, H.; Ishibashi, H. *Angew. Chem. Int. Ed*. **2010**, *49*, 10154; (c) Kamijo, S.; Yokosaka, S.; Inoue, M. *Tetrahedron* **2012**, *68*, 5290.
[27] Homsi, F.; Robin, S.; Rousseau, G. *Org. Synth.* **2000**, *77*, 206.
[28] Martinelli, J. R.; Watson, D. A.; Freckmann, D. M. M.; Barder, T. E.; Buchwald, S. L. *J. Org. Chem.* **2008**, *73*, 7102.
[29] (a) Ma, J.; Yin, W.; Zhou, H.; Liao, X.; Cook, J. M. *J. Org. Chem*. **2009**, *74*, 264; (b) Renata, H.; Zhou, Q.; Dünstl, G.; Felding, J.; Merchant, R. R.; Yeh, C.-H.; Baran, P. S. *J. Am. Chem. Soc.* **2015**, *137*, 1330. (c) Hugelshofer, C. L.; Magauer, T. *J. Am. Chem. Soc.* **2015**, *137*, 3807.
[30] (a) Zarecki, A.; Wicha, J. *Synthesis*, **1996**, 455; (b) Gabriëls, S.; Van Haver, D.; Vandewalle, M.; De Clercq, P.; Viterbo, D. *Eur. J. Org. Chem.* **1999**, 1803.
[31] Baker, B. A.; Boskovic, Z. V.; Lipshutz, B. H. *Org. Lett.* **2008**, *10*, 289.
[32] Barrero, A. F.; Alvarez-Manzaneda, E. J.; Chahboun, R.; Meneses, R. *Synlett* **1999**, *10*, 1663.
[33] (a) Magnus, P.; Waring, M. J.; Scott, D. A. *Tetrahedron Lett.* **2000**, *41*, 9731; (b) Magnus, P.; Payne, A. H.; Waring, M. J.; Scott, D. A.; Lynch, V. *Tetrahedron Lett.* **2000**, *41*, 9725; (c) Iwasaki, K.; Wan, K. K.; Oppedisano, A.; Crossley, S. W. M.; Shenvi, R. A. *J. Am. Chem. Soc.* **2014**, *136*, 1300; (d) Gao, A. X.; Hamada, T.; Snyder, S. A. *Angew. Chem. Int. Ed.* **2016**, *55*, 10301; (e) Obradors, C.; Martinez, R. M.; Shenvi, R. A. J. *Am. Chem. Soc.* **2016**, *138*, 4962.
[34] (a) Muller, P.; Gilabert, D. *Tetrahedron* **1988**, *44*, 7171; (b) Larsen, J.; Jorgensen, K. A. *J. Chem. Soc., Perkin Trans. 2* **1992**, 1213.
[35] Zhou, Z.; Gao, A. X. Snyder, S. A. *J. Am. Chem. Soc.* **2019**, *141*, 7715.
[36] (a) Raheem, I. T.; Thiara, P. S.; Peterson, E. A.; Jacobsen, E. N. *J. Am. Chem. Soc.* **2007**, *129*, 13404; (b) Muratore, M. E.; Holloway, C. A.; Pilling, A. W.; Storer, R. I.; Trevitt, G.; Dixon, D. J. *J. Am. Chem. Soc.* **2009**, *131*, 10796; (c) Holloway, C. A.; Muratore, M. E.; Storer, R. I.; Dixon, D. J. *Org. Lett.* **2010**, *12*, 4720; (d) Cai, Q.; Liang, X.-W.; Wang, S.-G.; Zhang, J.-W.; Zhang, X.; You, S.-L. *Org. Lett*. **2012**, *14*, 5022; (e) Gregory, A. W.; Jakubec, P.; Turner, P.; Dixon, D. J. *Org. Lett.* **2013**, *15*, 4330.
[37] (a) Bou-Hamdan, F. R.; Leighton, J. L. *Angew. Chem., Int. Ed.* **2009**, *48*, 2403; (b) Badillo, J. J.; Silva-García, A.; Shupe, B. H.; Fettinger, J. C.; Franz, A. K. *Tetrahedron Lett.* **2011**, *52*, 5550; (c) Duce, S.; Pesciaioli, F.; Gramigna, L.; Bernardi, L.; Mazzanti,

A.; Ricci, A.; Bartoli, G.; Bencivenni, G. *Adv. Synth. Catal.* **2011**, *353*, 860; (d) Dai, W.; Lu, H.; Li, X.; Shi, F.; Tu, S. J. *Chem. -Eur. J.* **2014**, *20*, 11382.
[38] Piemontesi, C.; Wang, Q.; Zhu, J. *J. Am. Chem. Soc.* **2016**, *138*, 11148.
[39] (a) Soe, T.; Kawate, T.; Fukui, N.; Hino, T.; Nakagawa, M. *Heterocycles* **1996**, *42*, 347; (b) Kawate, T.; Yamanaka, M.; Nakagawa, M. *Heterocycles* **1999**, 50, 1033.
[40] (a) Corey, E. J.; Bakshi, R. K.; Shibata, S. *J. Am. Chem. Soc.* **1987**, *109*, 5551; (b) Corey, E. J.; Bakshi, R. K.; Shibata, S. *J. Am. Chem. Soc.* **1987**, *109*, 7925; (c) Tarr, J. C.; Johnson, J. S. *J. Org. Chem.* **2010**, *75*, 3317.
[41] (a) Horiguchi, Y.; Nakamura, M.; Saitoh, T.; Sano, T. *Chem. Pharm. Bull.* **2003**, *51*, 1368; (b) Kulkarni, A. S.; Shingare, R. D.; Dandela, R.; Reddy, D. R. *Eur. J. Org. Chem.* **2018**, 6453.
[42] (a) Cassani, C.; Bergonzini, G.; Wallentin, C.-J. *Org. Lett.* **2014**, *16*, 4228; (b) Griffin, J. D.; Zeller, M. A.; Nicewicz, D. A. *J. Am. Chem. Soc.* **2015**, *137*, 11340; (c) Luo, J.; Zhang, J. *ACS Catal.*, **2016**, ***6*** , 873; (d) Yang, J.; Zhang, J.; Qi, Li.; Hu, C.; Chen, Y. *Chem. Commun.* **2015**, *51*, 5275.
[43] Qin, T.; Malins, L. R.; Edwards, J. T.; Merchant, R. R.; Novak, A. J. E.; Zhong, J. Z.; Mills, R. B.; Yan, M.; Yuan, C.; Eastgate, M. D.; Baran, P. S. *Angew. Chem. Int. Ed.* **2017**, *56*, 260.
[44] (a) Barton, D. H. R.; Crich, D.; Motherwell, W. B. *J. Chem. Soc. Chem. Commun.* **1983**, 939; (b) Barton, D. H. R.; Crich, D.; Motherwell, W. B. *Tetrahedron* **1985**, *41*, 3901.
[45] Wayner, D. D. M.; Dannenberg, J. J.; Griller, D. *Chem. Phys. Lett.* **1986**, *131*, 189.
[46] For a recent review, see: Mattalia, J.-M. R. Beilstein *J. Org. Chem.* **2017**, *13*, 267.
[47] Pellegrini, C.; Weber, M.; Borschberg, H.-J. *Helv. Chim. Acta* **1996**, *79*, 151.
[48] Kim, S.; Oh, C. H.; Ko, J. S.; Ahn, K. H.; Kim, Y. J. *J. Org. Chem.* **1985,** *50*, 1927;
[49] (a) Agami, C.; Couty, F.; Evano, G. *Org. Lett.* **2000**, *2*, 2085. (b) Amos, D. T.; Renslo, A. R.; Danheiser, R. L. *J. Am. Chem. Soc.* **2003**, *125*, 4970; (c) Meyer, N.; Werner, F.; Opatz, T. *Synthesis* **2005**, 945.
[50] (a) Abdel-Magid, A. F.; Carson, K. G.; Harris, B. D.; Maryanoff, C. A.; Shah, R. D. *J. Org. Chem.* **1996,** *61*, 3849; (b) François, D., Poupon, E., Lallemand, M.C., Kunesch, N. and Husson, H. P. *J. Org. Chem.* **2000,** *65*, 3209; (c) Li, J., Zhao, H., Jiang, X., Wang, X., Hu, H., Yu, L. and Zhang, Y. *Angew. Chem. Int. Ed.* **2015**, *54*, 6306.
[51] Baldwin, J. E.; Spring, D. R.; Whitehead, R. C. *Tetrahedron Lett.* **1998**, *39*, 5417.
[52] Fry, J. L. *J. Chem. Soc., Chem. Commun.* **1974**, 45.
[53] Kuroiwa, Y.; Matsumura, S.; Toshima, K. *Synlett* **2008**, 2523.
[54] Miyashita, A.; Suzuki, Y.; Okumura, Y.; Higashino, T. *Chem. Pharm. Bull.* **1996**, *44*, 252.
[55] Toussaint, D.; Suffert, J. *Org. Synth.* **1999**, *76*, 214.

3.9 NMR Spectra of Selected Intermediates

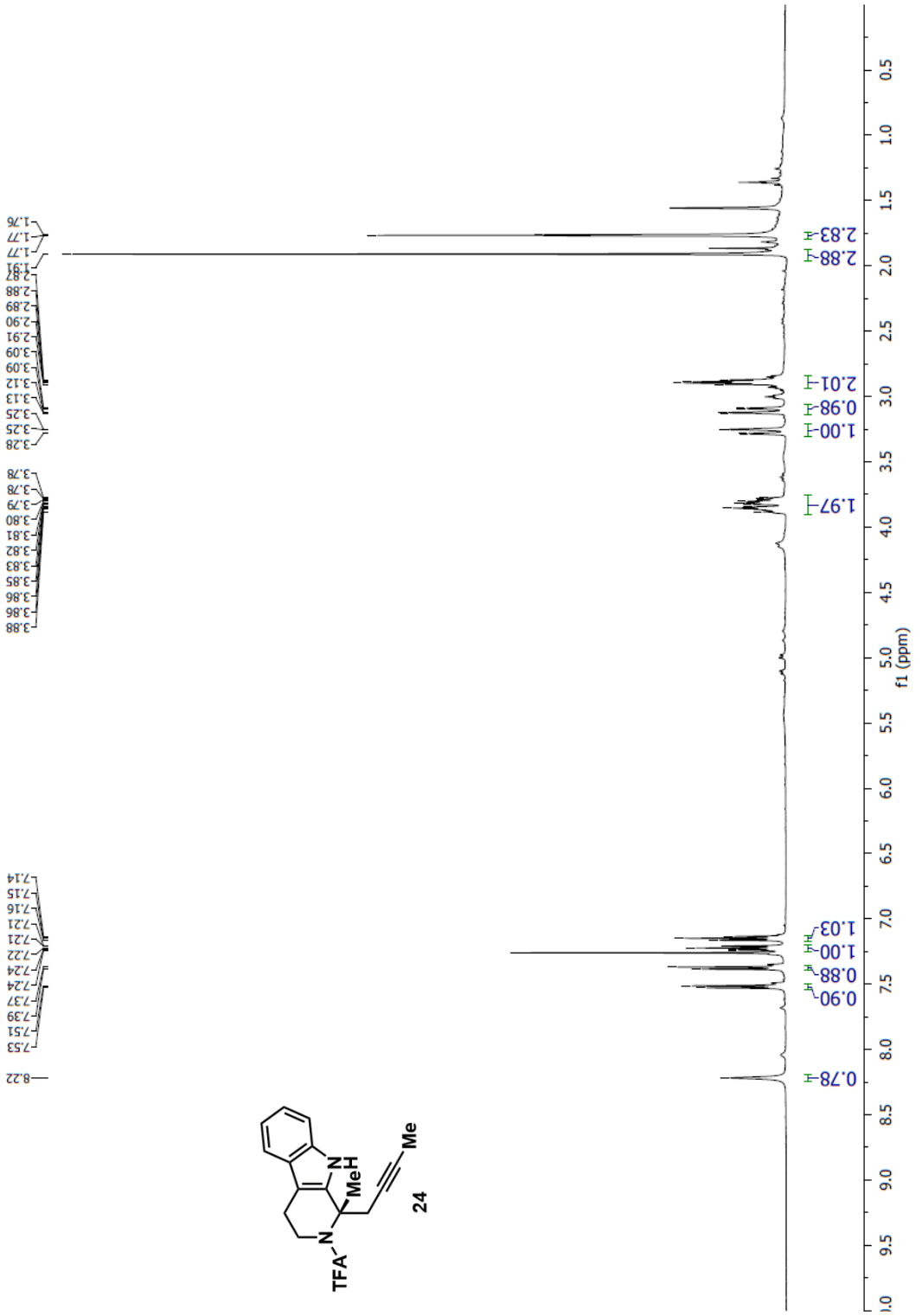

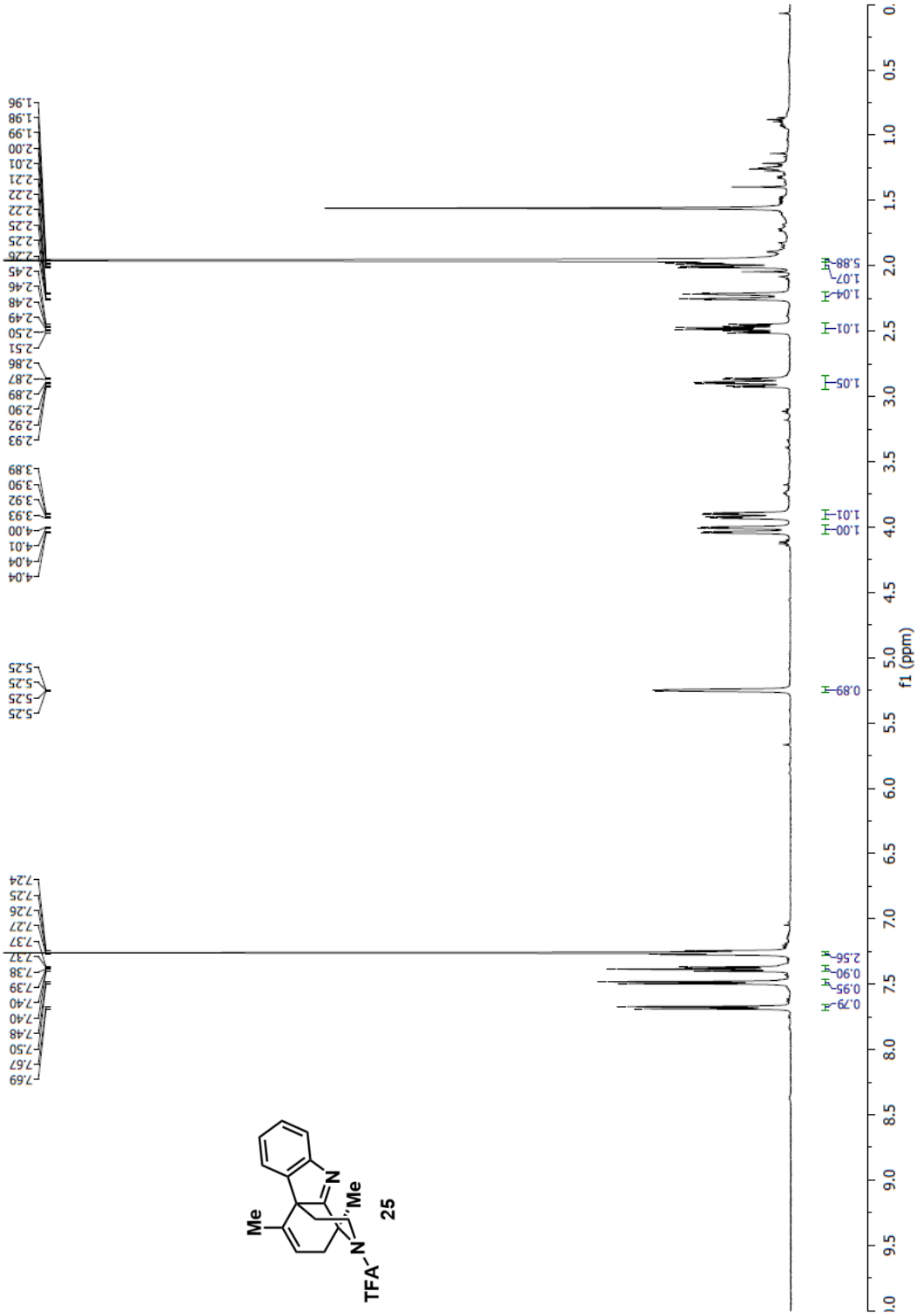
Me
N
Me
N
TFA
25
f1 (ppm)

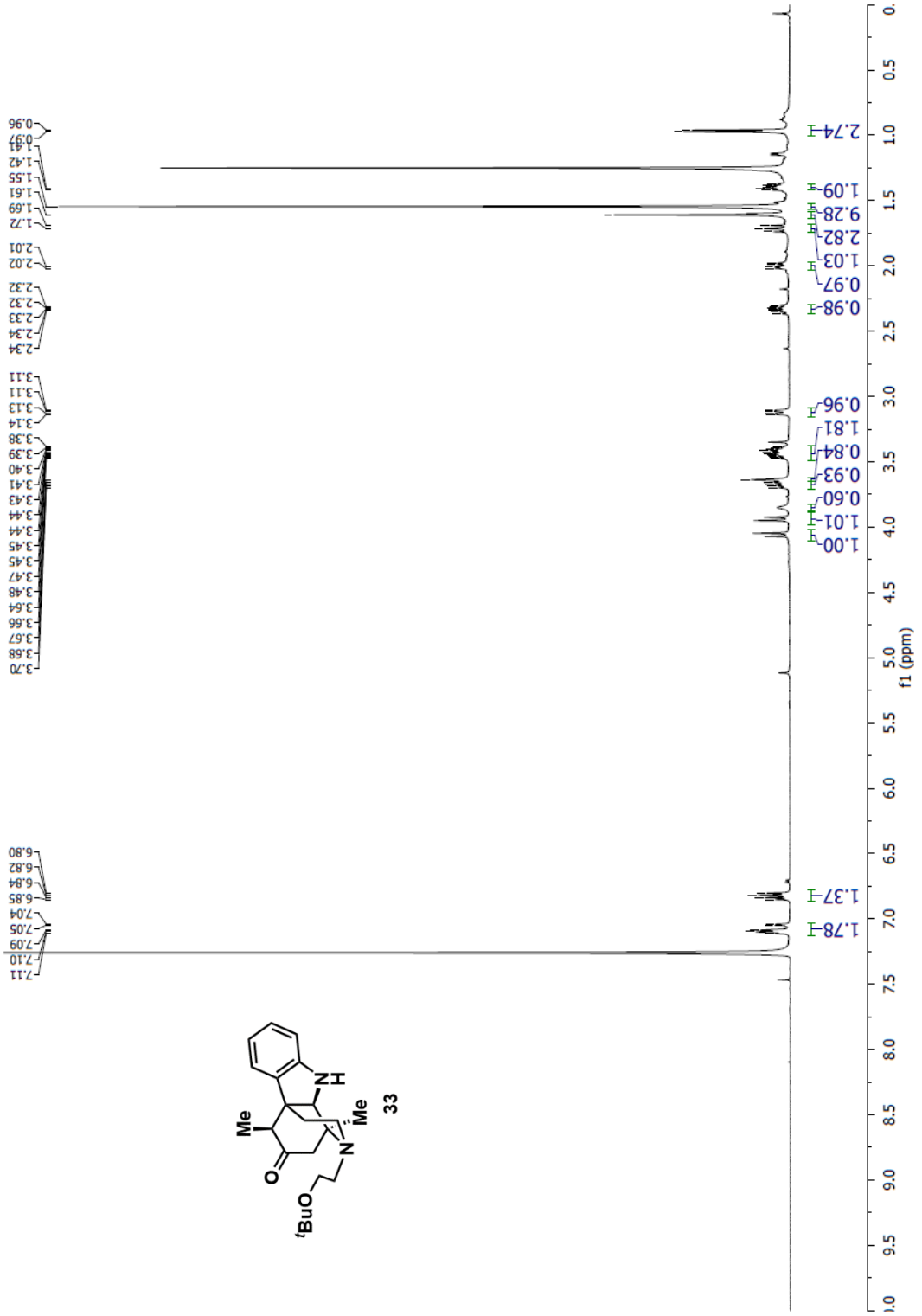
7.11
7.10
7.09
7.05
7.04
6.85
6.84
6.82
6.80
3.70
3.68
3.67
3.66
3.64
3.48
3.47
3.45
3.45
3.44
3.44
3.43
3.41
3.40
3.39
3.38
3.14
3.13
3.11
3.11
2.34
2.34
2.33
2.32
2.32
2.02
2.01
1.72
1.69
1.61
1.55
1.42
1.41
0.97
0.96
1.78
1.37
2.74
1.09
9.28
2.82
1.03
0.97
0.98
0.96
1.81
0.84
0.93
0.60
1.01
1.00
Me
Me
O
N
N
H
OtBu
33
f1 (ppm)

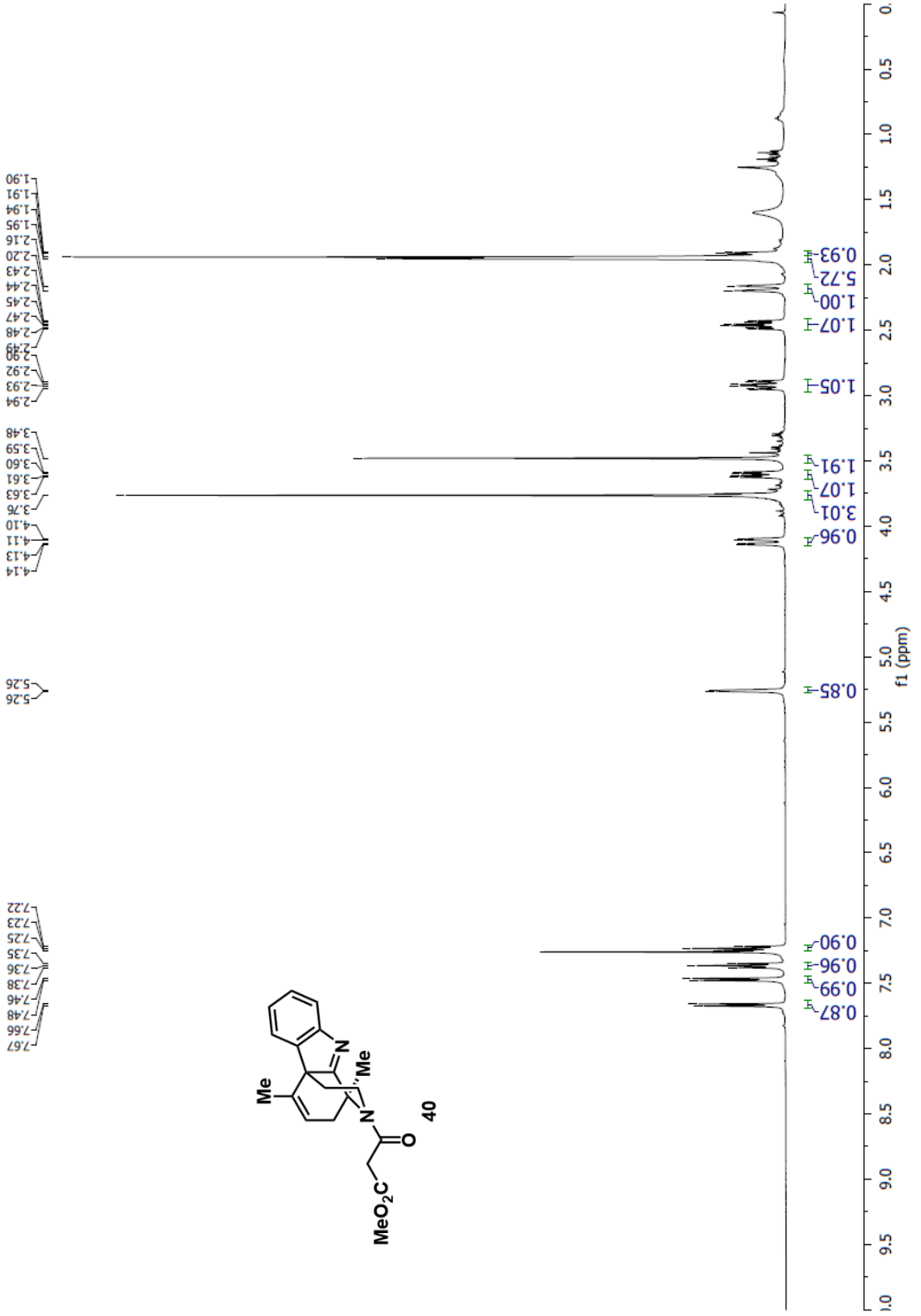
Me
N
Me
N
O
MeO2C
40
f1 (ppm)

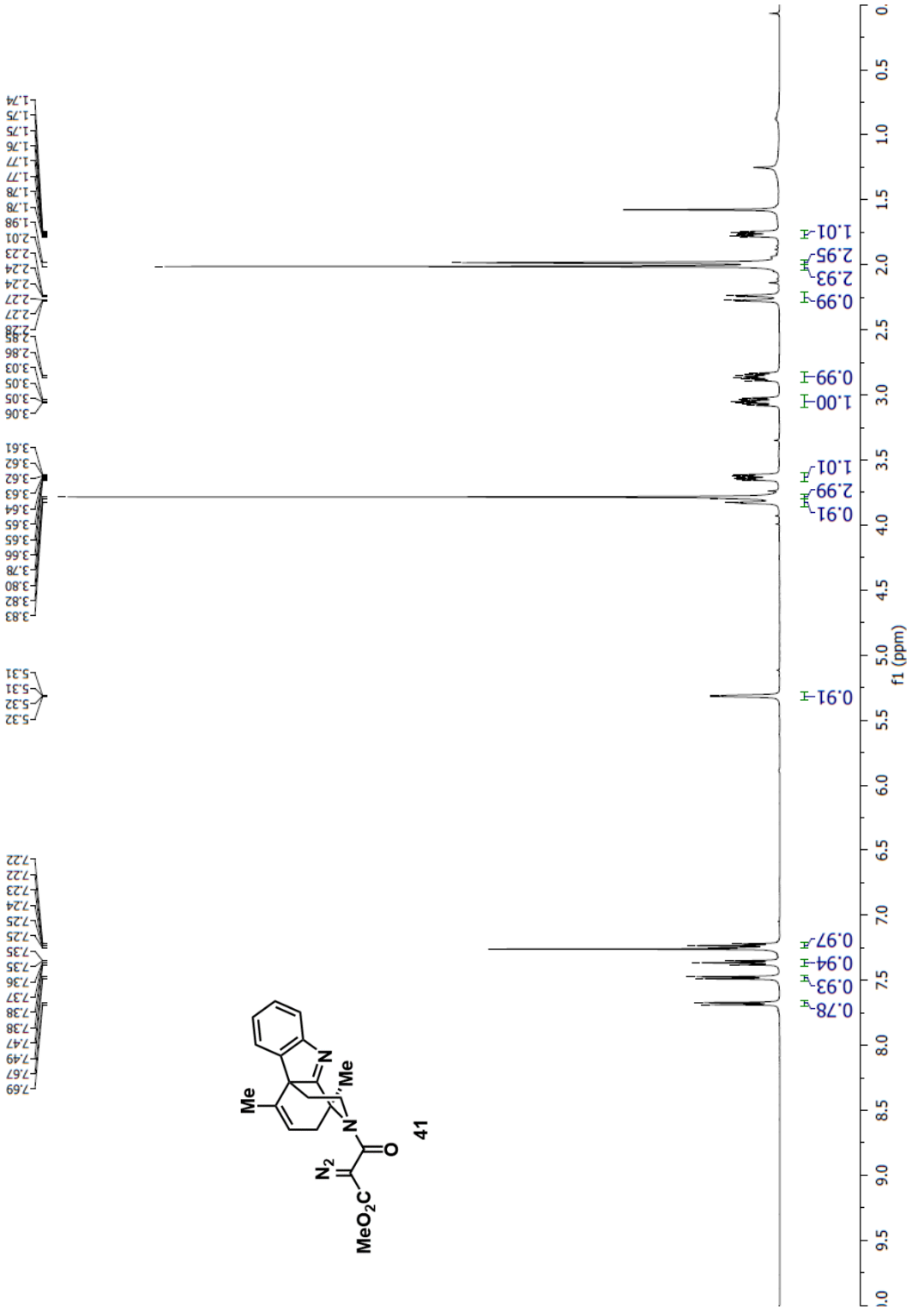
41
Me
Me
N
N
O
N2
MeO2C
f1 (ppm)

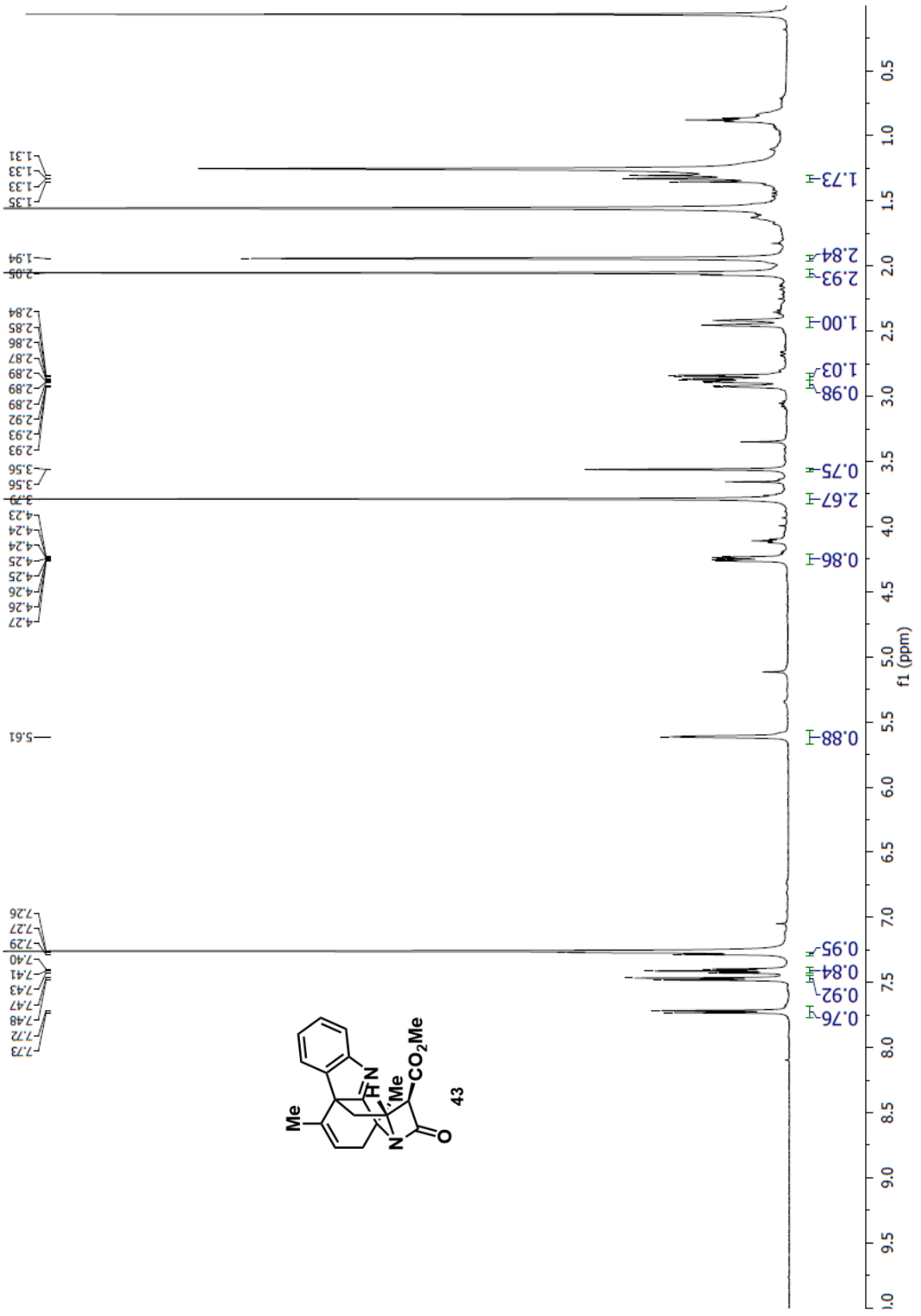
Me
N
H
Me
CO2Me
N
O
43
f1 (ppm)

8.24
7.50
7.49
7.36
7.34
7.26
7.19
7.17
7.16
7.11
7.10
7.08
3.34
3.33
3.32
3.31
3.03
3.02
3.00
2.76
2.75
2.74
2.35
1.57
CDCl3
0.82
0.89
0.96
0.94
0.92
1.00
1.03
2.09
2.89
3.09
f1 (ppm)
59
HN
Me
O
MeH
N

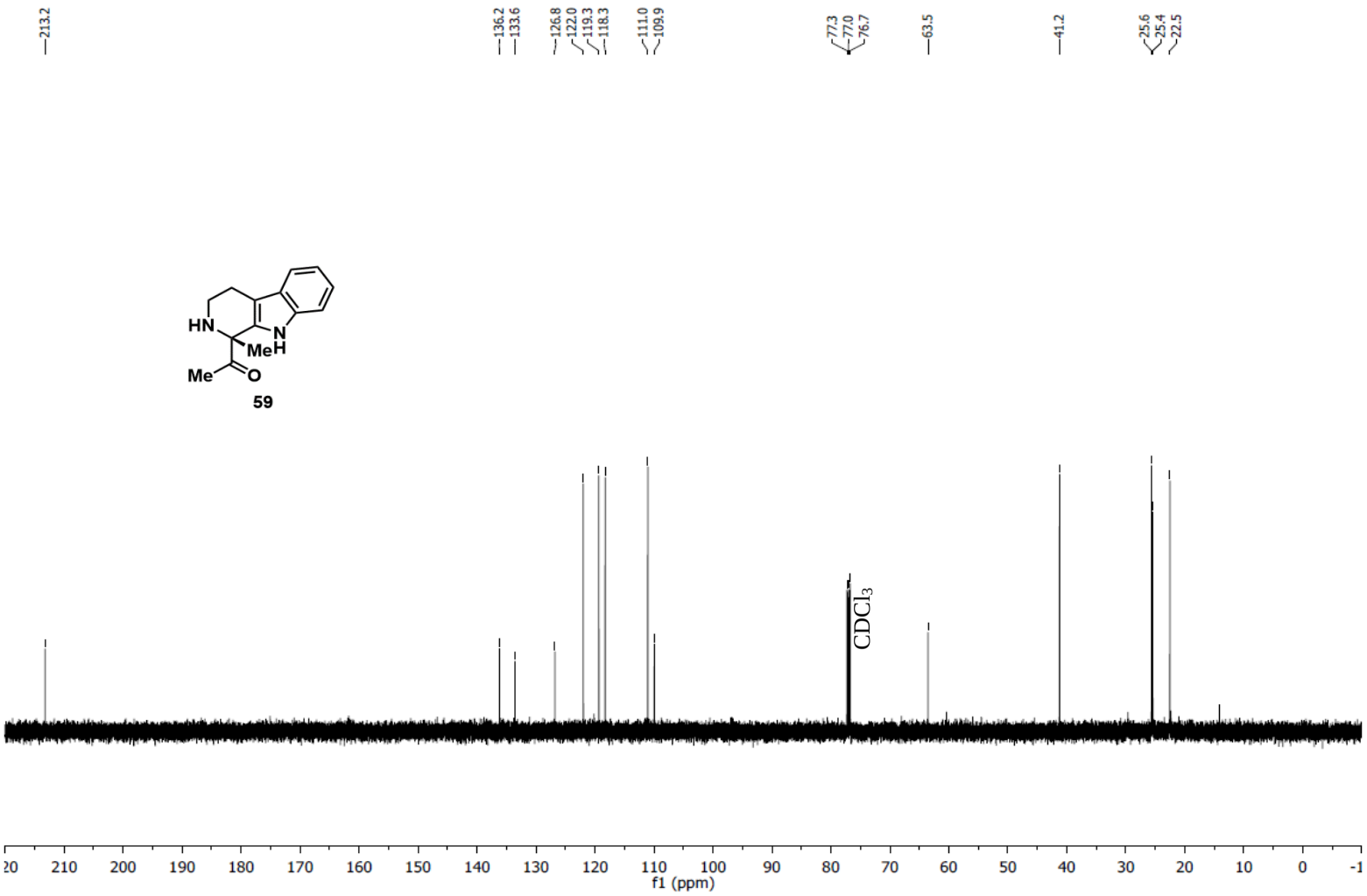
213.2
136.2
133.6
126.8
122.0
119.3
118.3
111.0
109.9
77.3
77.0
76.7
63.5
41.2
25.6
25.4
22.5
HN
N
H
Me
Me
O
59
CDCl3
f1 (ppm)

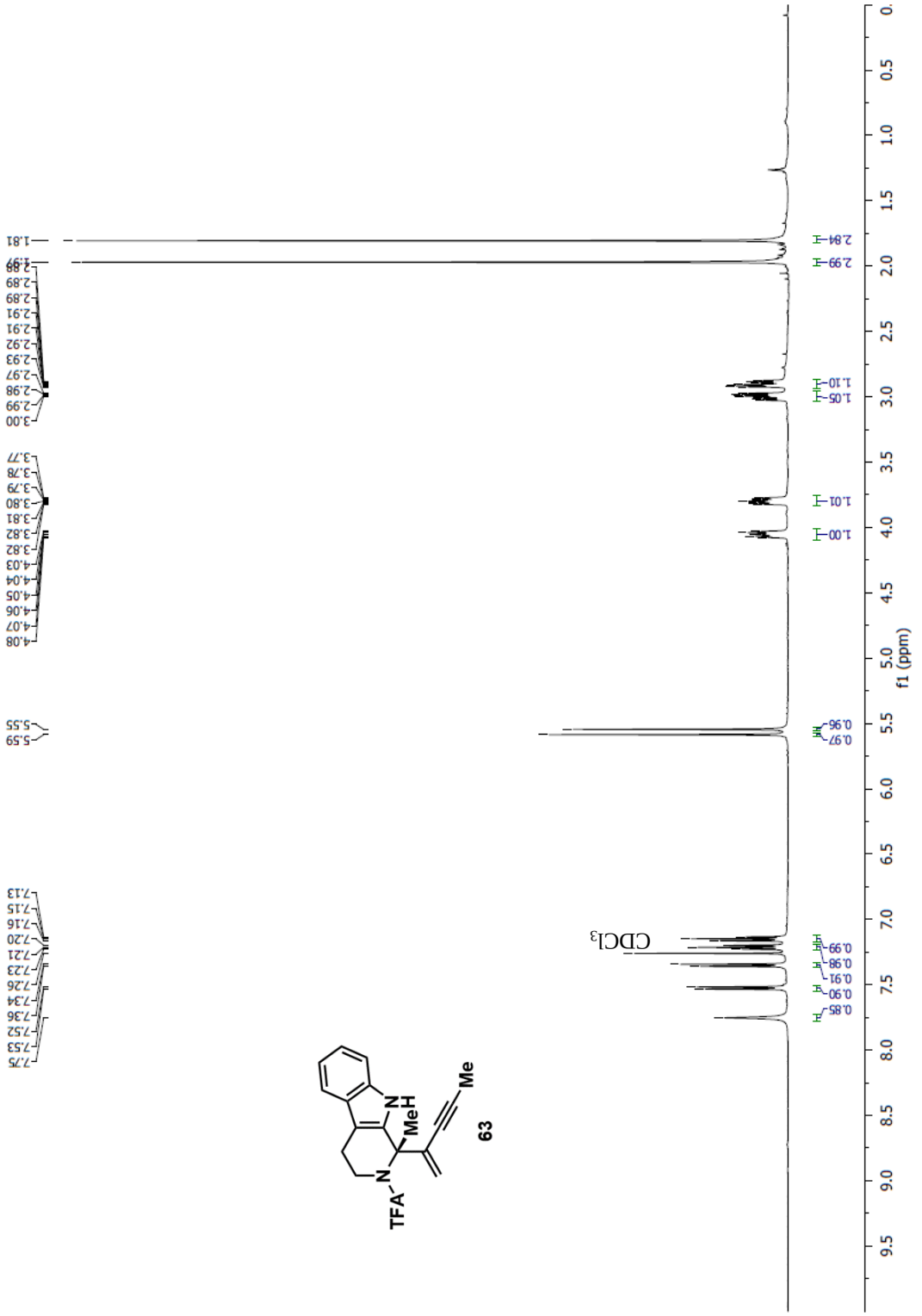
CDCl3
f1 (ppm)
TFA
N
MeH
Me
63

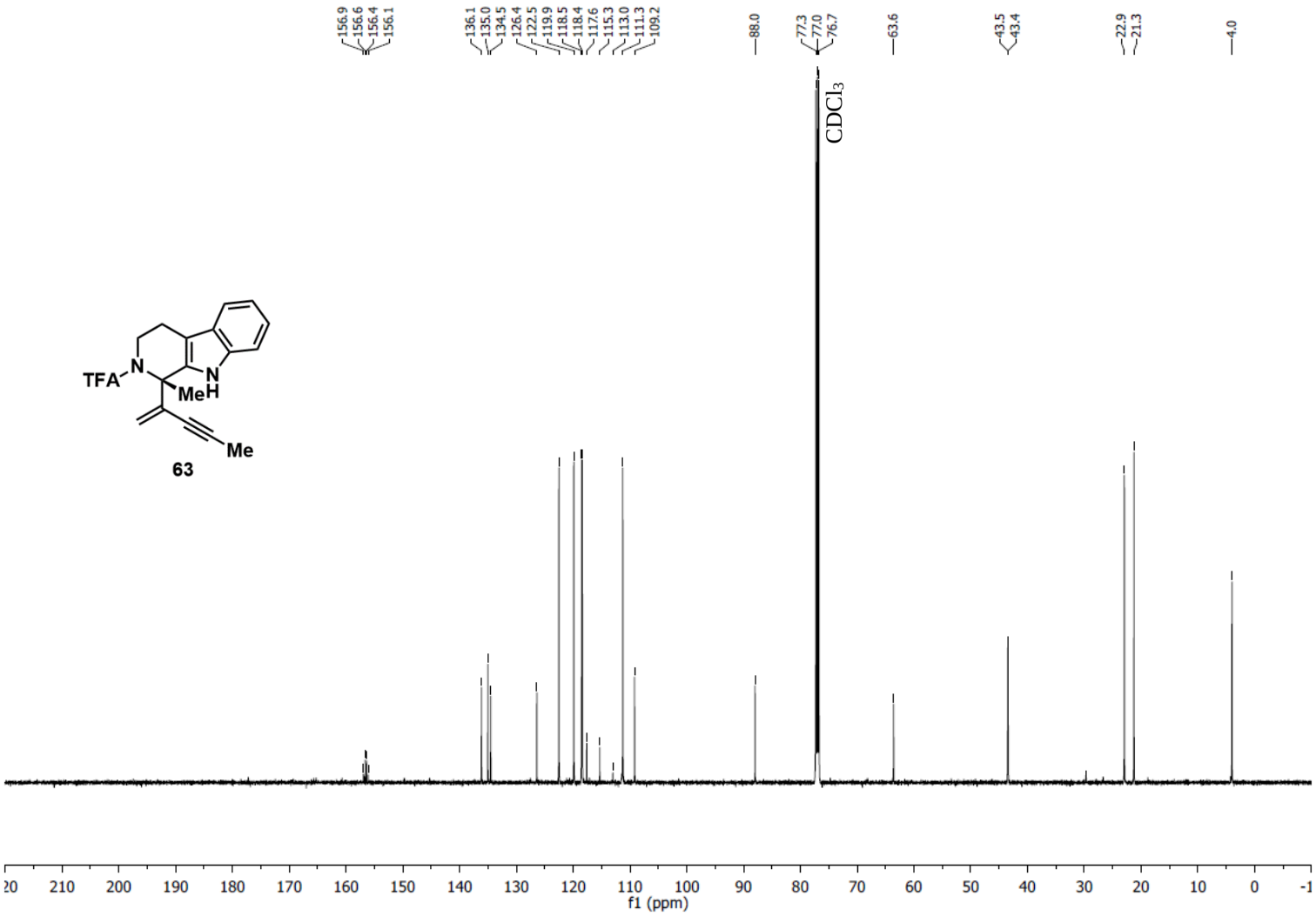
156.9
156.6
156.4
156.1
136.1
135.0
134.5
126.4
122.5
119.9
118.5
118.4
117.6
115.3
113.0
111.3
109.2
88.0
77.3
77.0
76.7
63.6
43.5
43.4
22.9
21.3
4.0
CDCl3
TFA
N
N
MeH
Me
63
f1 (ppm)

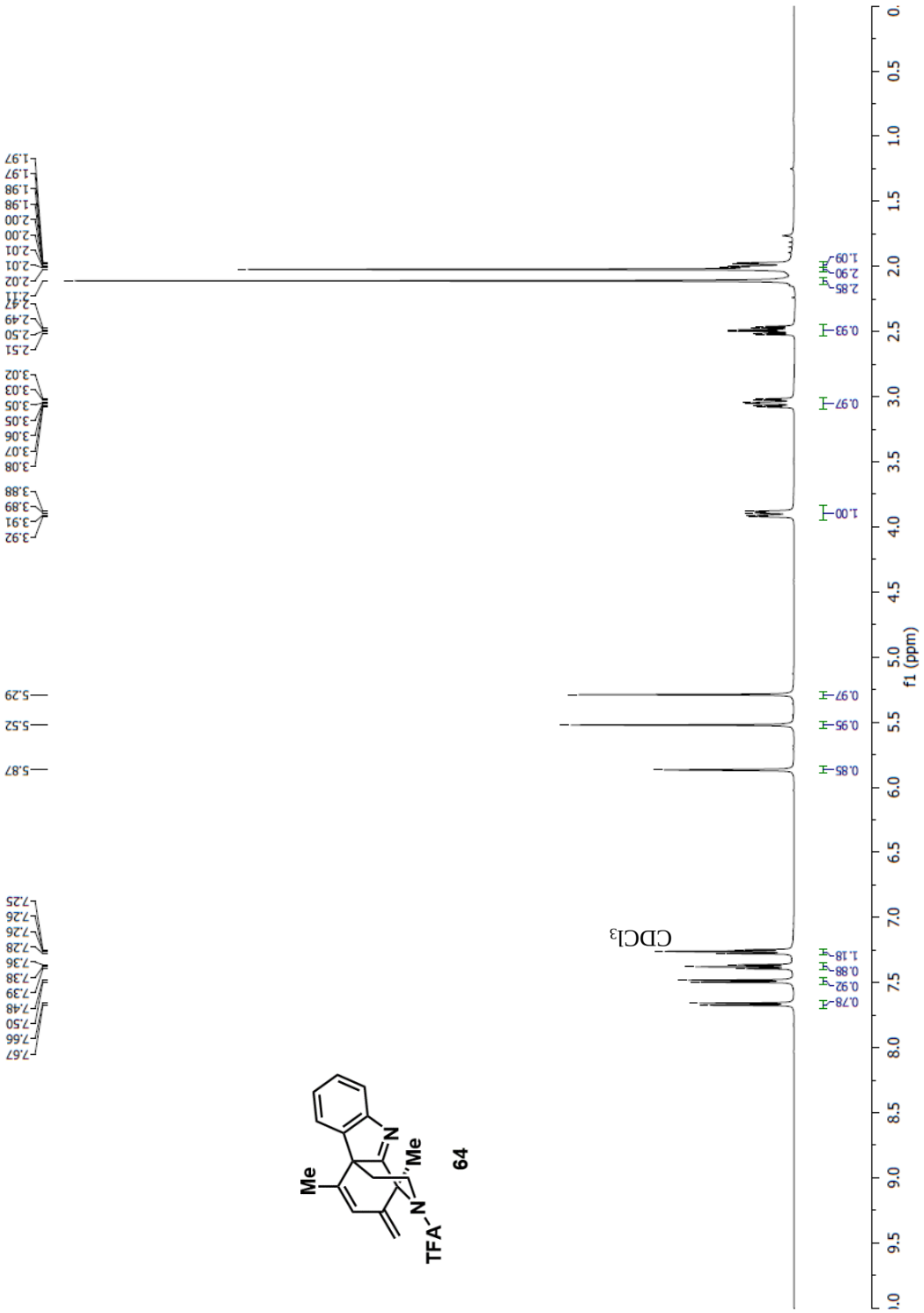
CDCl3
Me
N
Me
N
TFA
64
f1 (ppm)

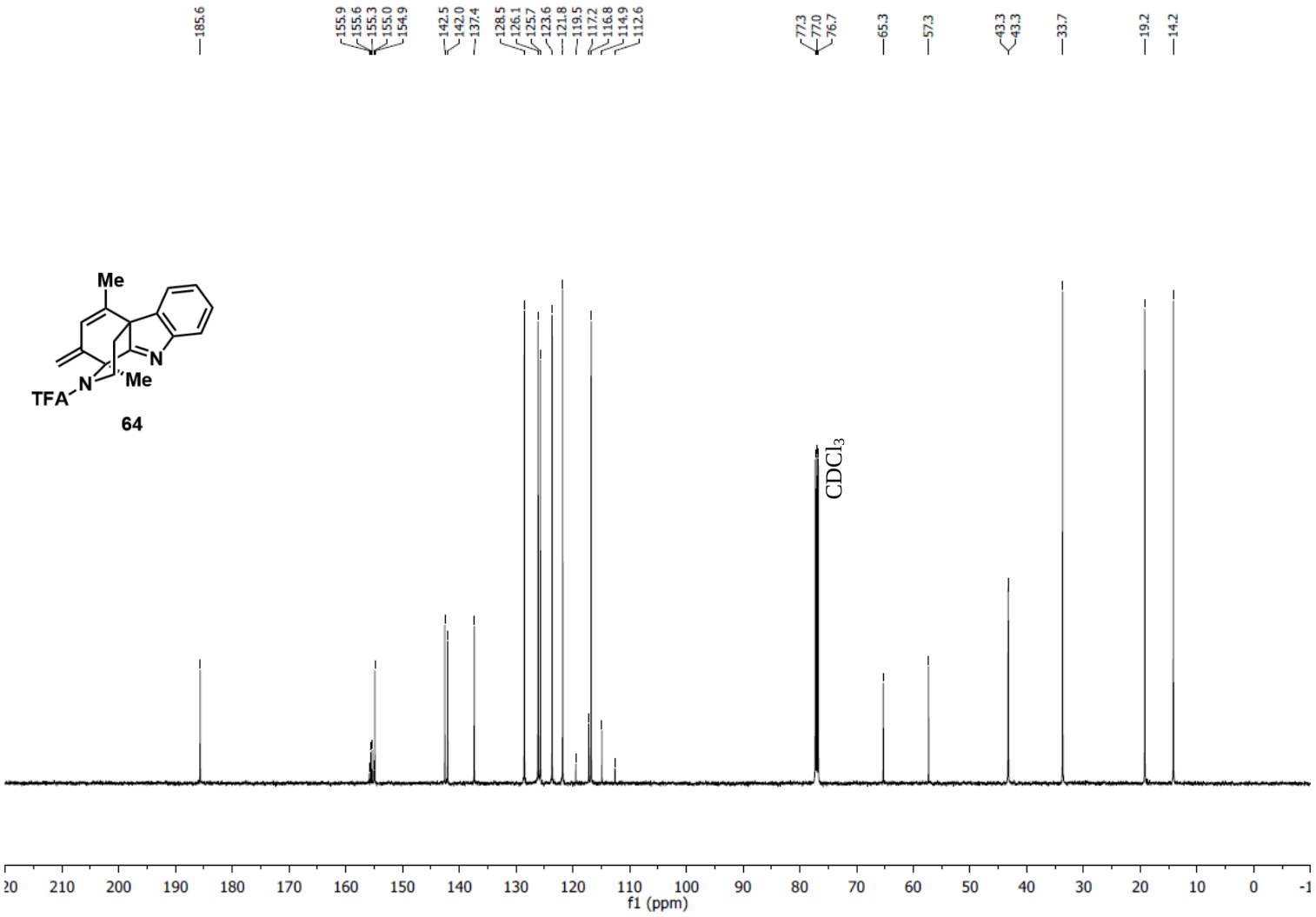
185.6
155.9
155.6
155.3
155.0
154.9
142.5
142.0
137.4
128.5
126.1
125.7
123.6
121.8
119.5
117.2
116.8
114.9
112.6
77.3
77.0
76.7
65.3
57.3
43.3
43.3
33.7
19.2
14.2
Me
N
Me
TFA
N
64
CDCl3
f1 (ppm)

CDCl3
Me
Me
N
N
O
N
Boc
71
f1 (ppm)

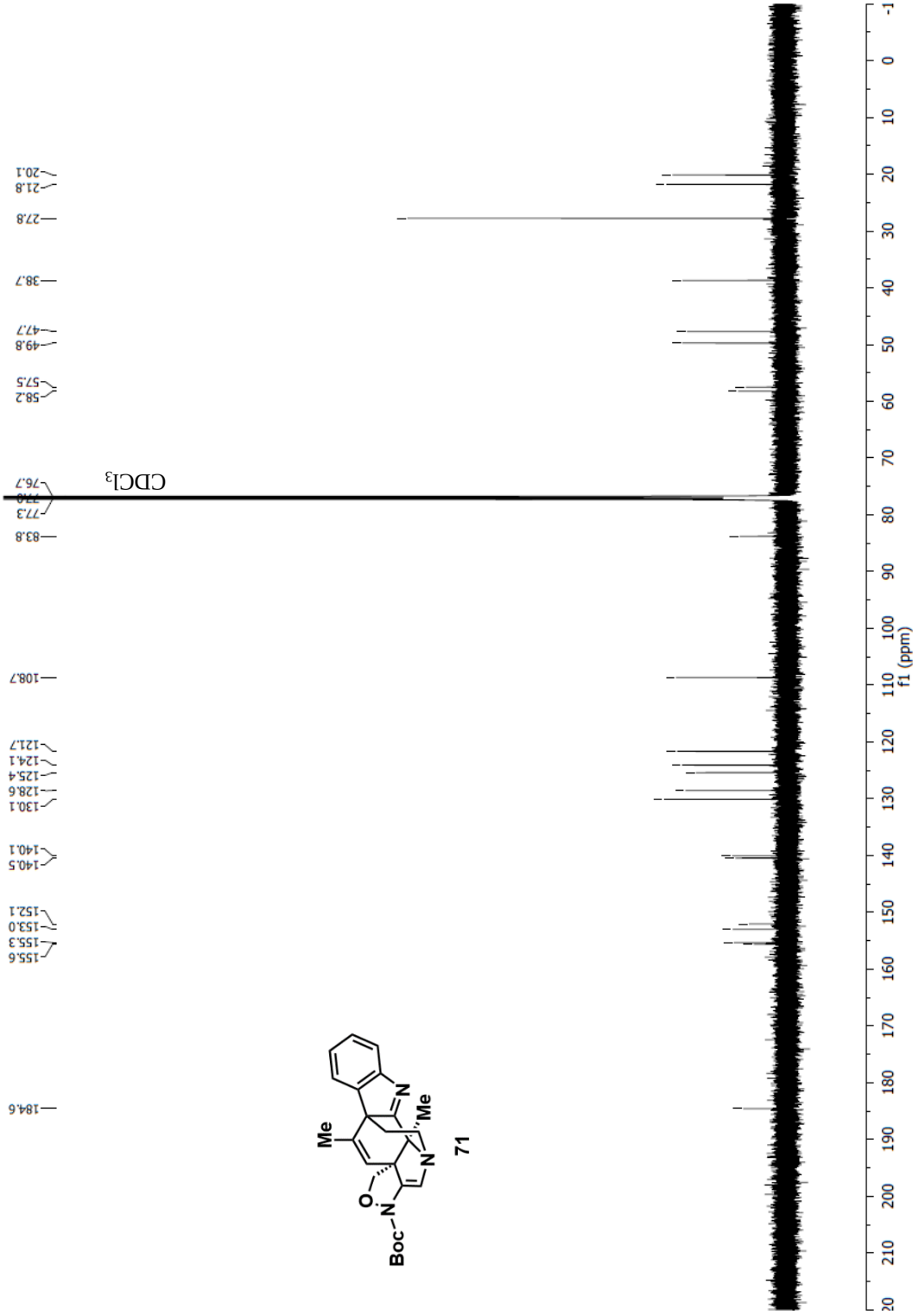
CDCl3
Me
Me
N
N
O
N
Boc
71
f1 (ppm)

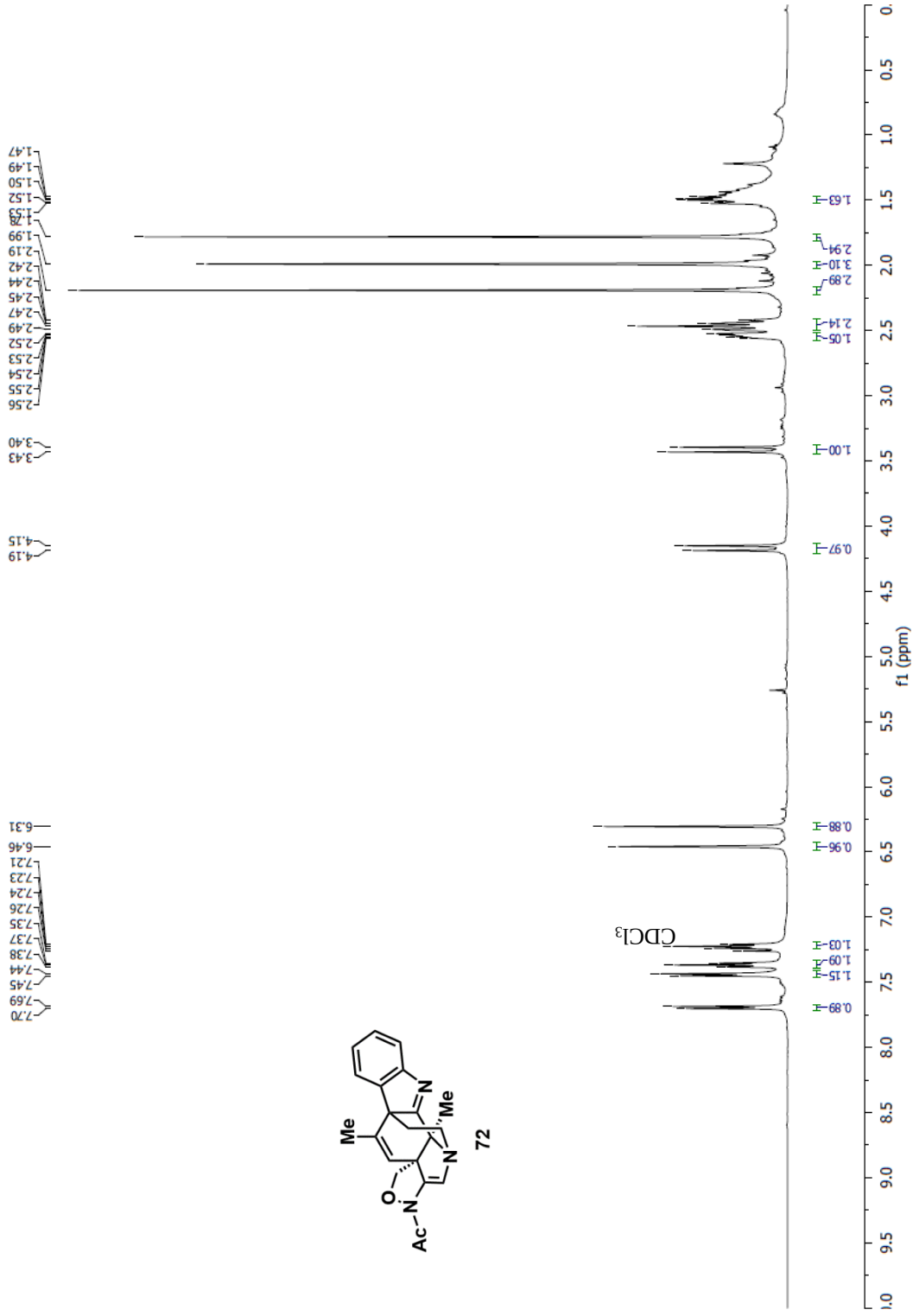
CDCl3
Me
Me
N
N
O
N
Ac
72
f1 (ppm)

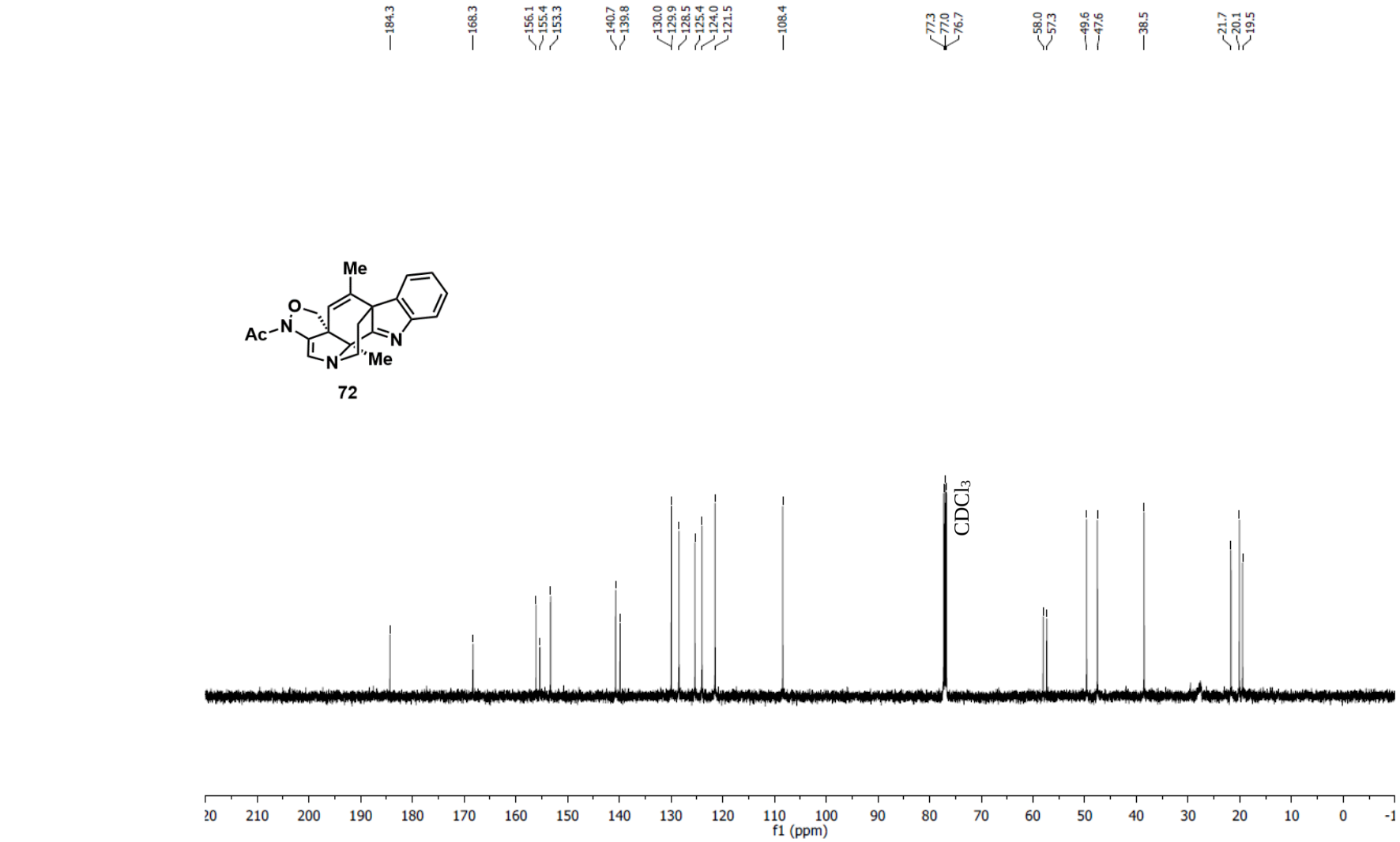
184.3
168.3
156.1
155.4
153.3
140.7
139.8
130.0
129.9
128.5
125.4
124.0
121.5
108.4
77.3
77.0
76.7
58.0
57.3
49.6
47.6
38.5
21.7
20.1
19.5
Me
O
Ac
N
N
N
Me
72
CDCl3
f1 (ppm)

7.75
7.73
7.49
7.47
7.43
7.42
7.40
7.29
7.27
7.26
5.66
3.90
3.87
3.10
3.06
2.95
2.93
2.91
2.90
2.89
2.86
2.80
2.79
2.77
2.74
2.22
2.19
1.94
1.58
1.54
1.38
1.38
1.36
1.35
1.33
1.32
CDCl3
Me
HO
N
Me
N
O
74
0.81
1.01
0.91
1.09
0.91
1.00
0.95
0.91
2.00
0.98
6.05
1.14
1.05
f1 (ppm)

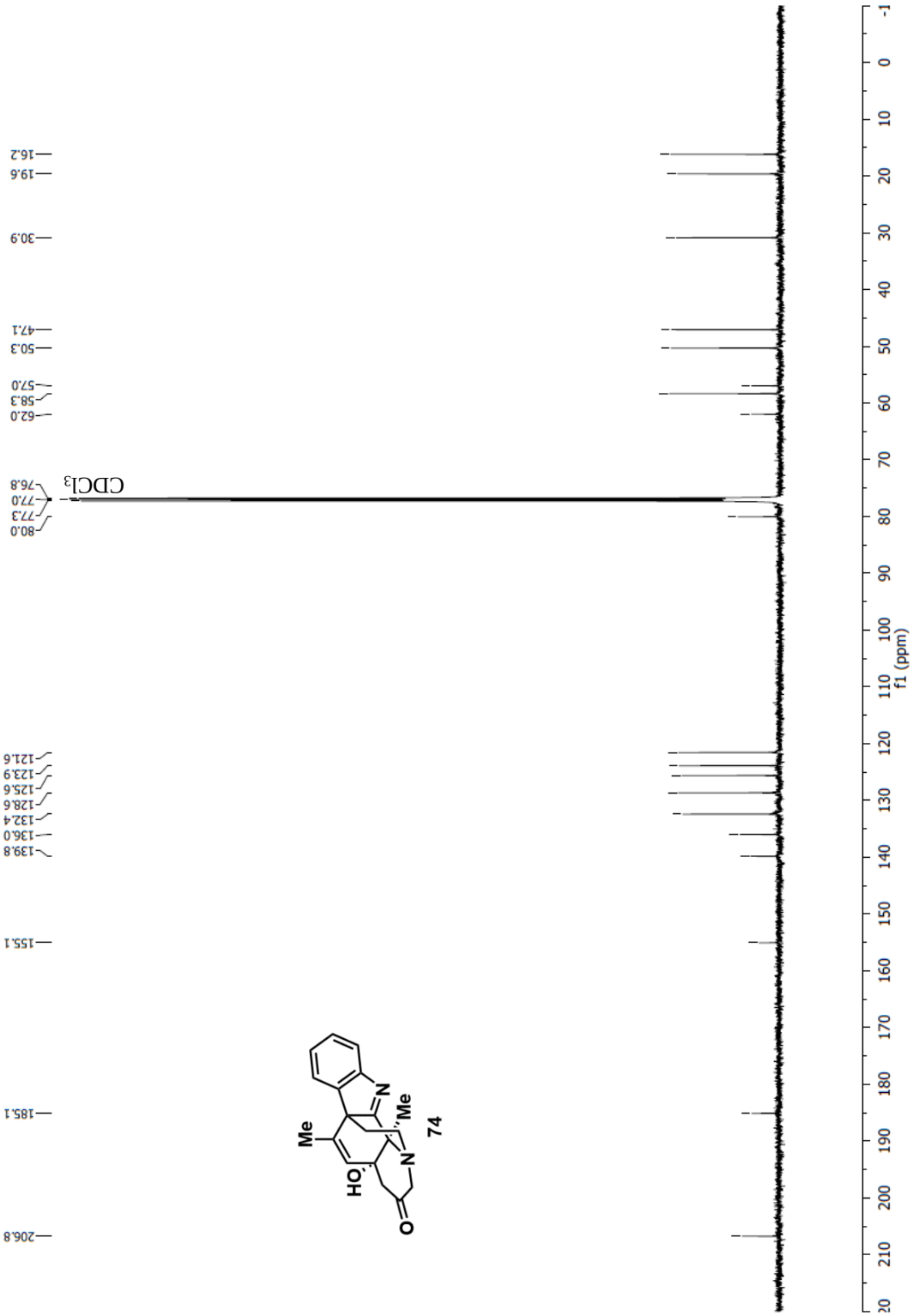
206.8
185.1
155.1
139.8
136.0
132.4
128.6
125.6
123.9
121.6
80.0
77.3
77.0
76.8
CDCl3
62.0
58.3
57.0
50.3
47.1
30.9
19.6
16.2
Me
HO
N
Me
N
O
74
f1 (ppm)

7.67
7.66
7.52
7.50
7.41
7.41
7.39
7.38
7.30
7.29
7.27
7.26
7.14
6.13
3.99
3.98
3.96
3.95
3.68
3.10
3.09
3.08
3.07
3.07
3.05
2.58
2.56
2.55
2.18
2.08
2.01
2.00
1.99
1.98
CDCl3
0.85
0.98
0.95
0.96
0.79
0.92
1.00
2.89
0.95
1.01
3.05
2.96
1.01
f1 (ppm)
Me
N
Me
N
TFA
MeO2C
83

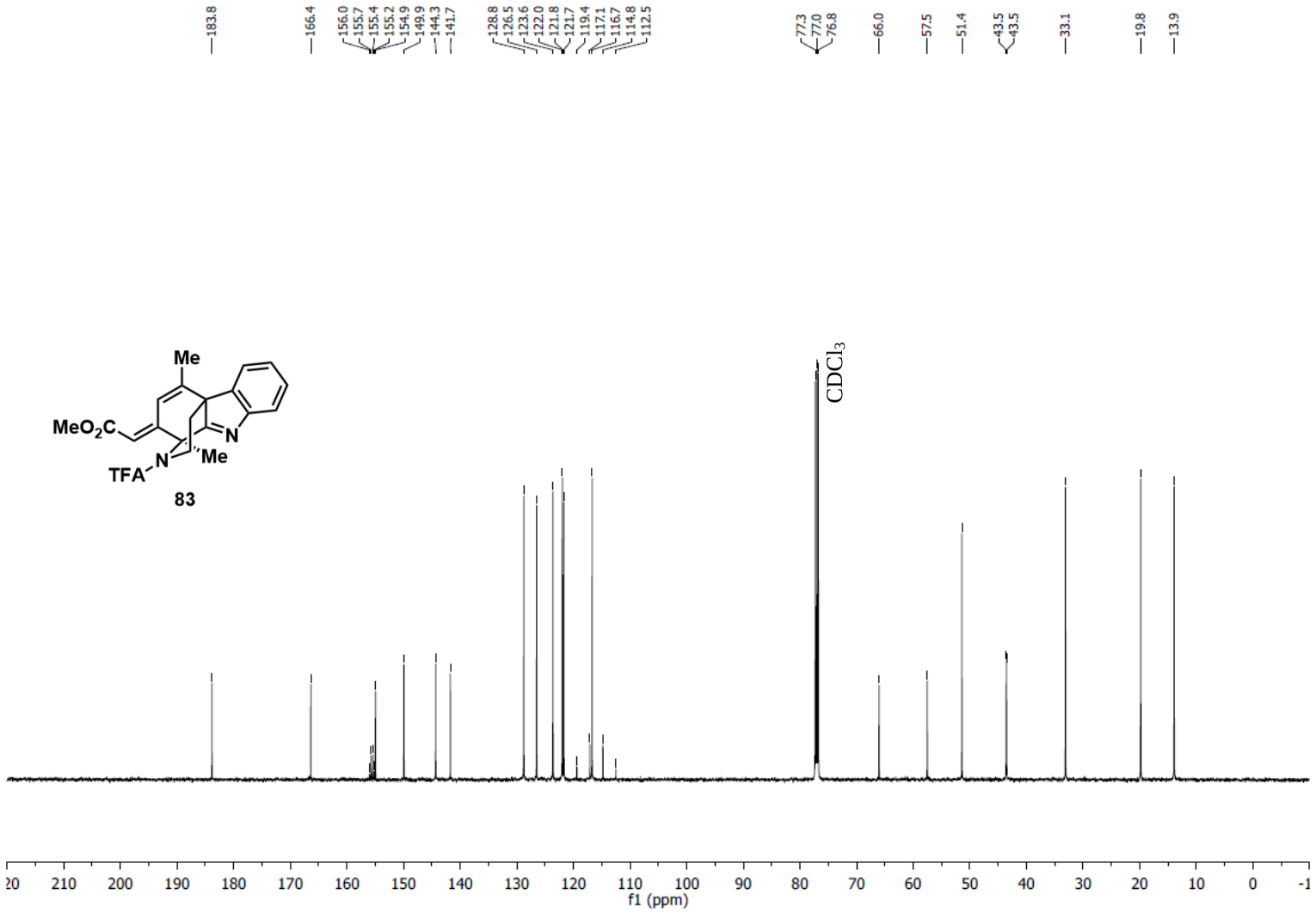
183.8
166.4
156.0
155.7
155.4
155.2
154.9
149.9
144.3
141.7
128.8
126.5
123.6
122.0
121.8
121.7
119.4
117.1
116.7
114.8
112.5
77.3
77.0
76.8
66.0
57.5
51.4
43.5
43.5
33.1
19.8
13.9
CDCl3
Me
MeO2C
N
N
Me
TFA
83
f1 (ppm)

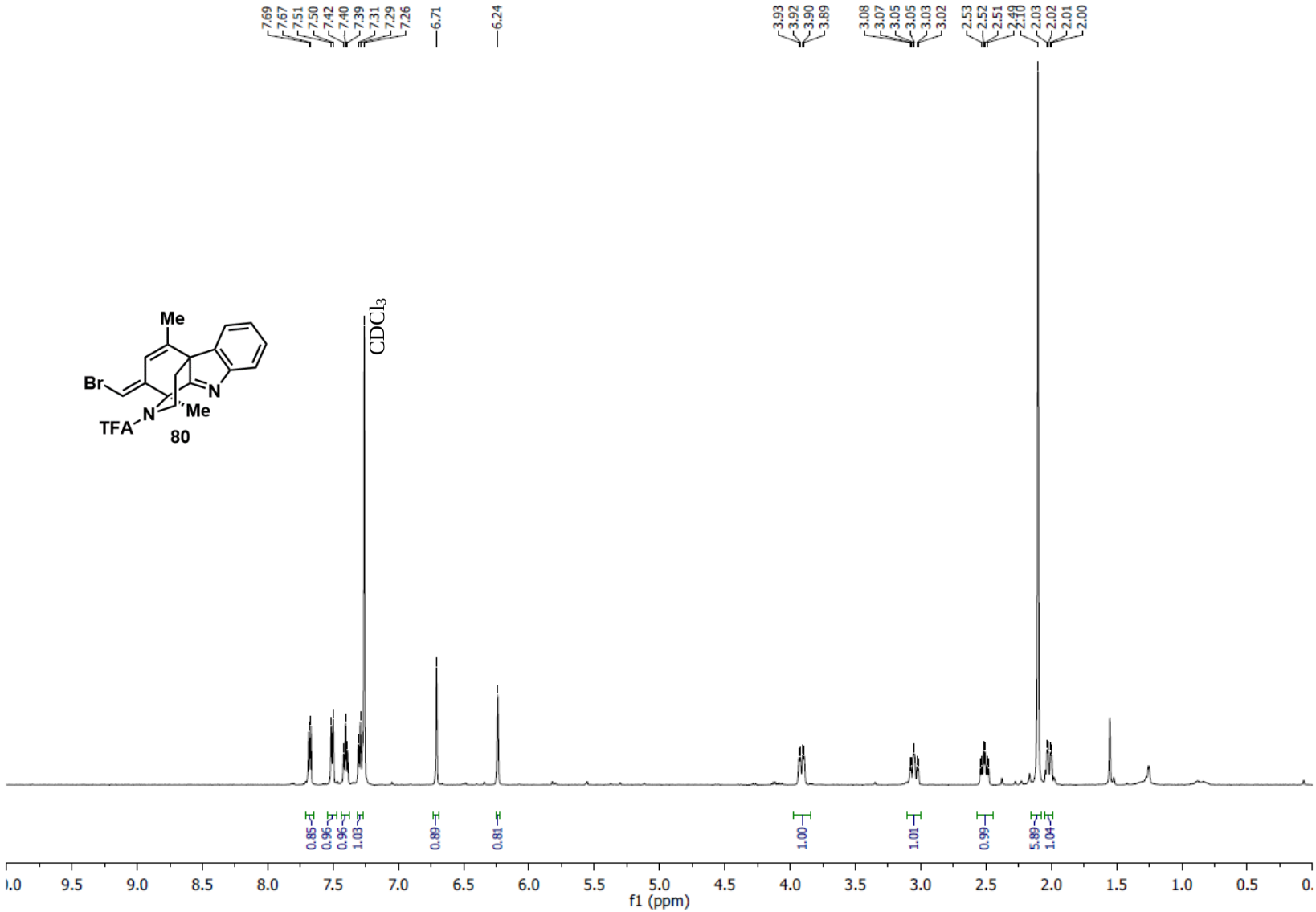
7.69
7.67
7.51
7.50
7.42
7.40
7.39
7.31
7.29
7.26
6.71
6.24
3.93
3.92
3.90
3.89
3.08
3.07
3.05
3.05
3.03
3.02
2.53
2.52
2.51
2.03
2.02
2.01
2.00
CDCl3
Me
Br
N
N
Me
TFA
80
0.85
0.96
0.96
1.03
0.89
0.81
1.00
1.01
0.99
5.89
1.04
f1 (ppm)

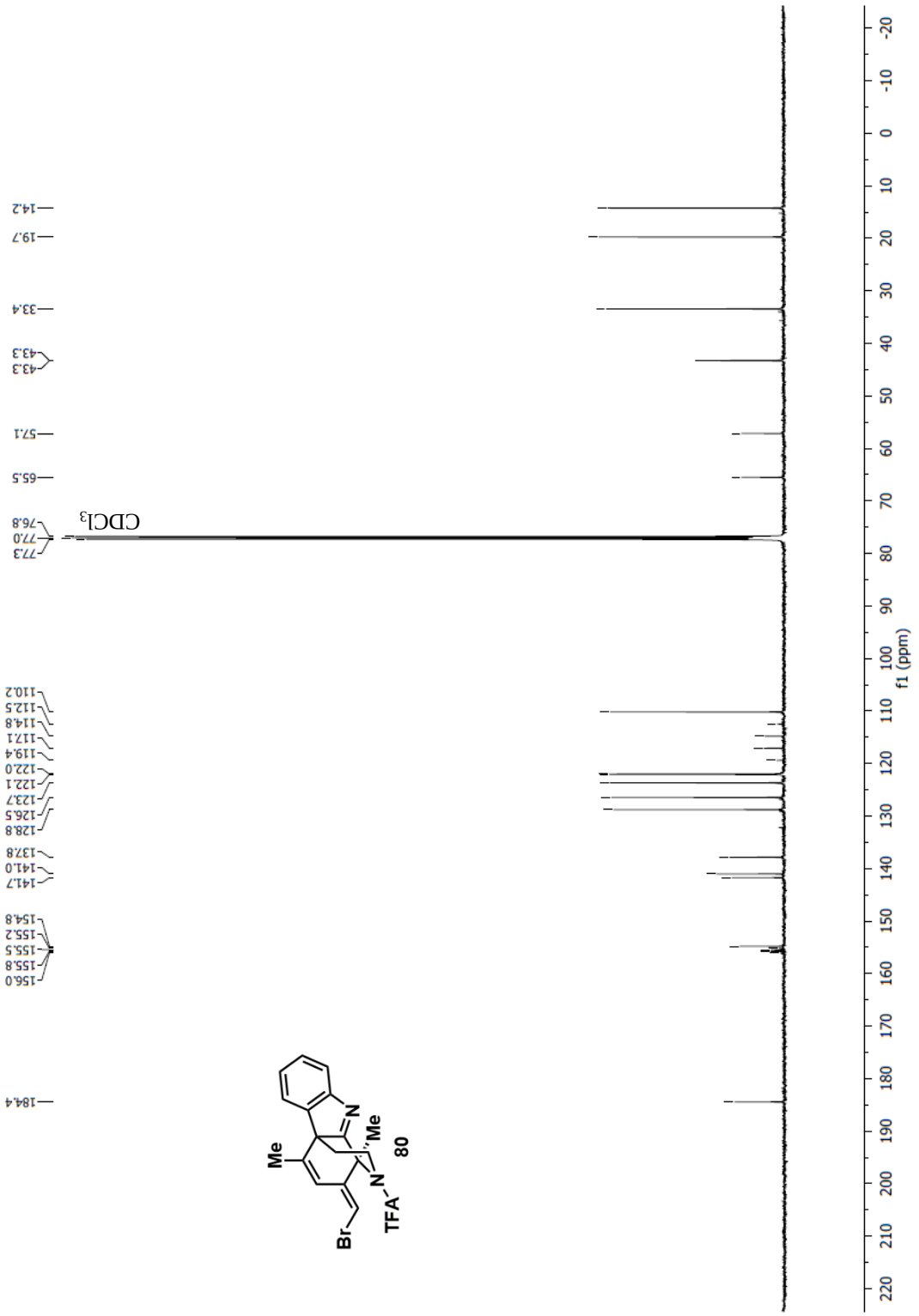
CDCl3
Me
Me
N
N
TFA
Br
80
f1 (ppm)

7.68
7.67
7.45
7.44
7.41
7.39
7.38
7.28
7.26
6.11
4.01
4.00
3.98
3.97
3.93
3.92
3.90
3.89
3.67
2.82
2.80
2.80
2.77
2.77
2.60
2.58
2.57
2.05
2.03
1.96
1.93
1.91
1.32
1.31
1.23
1.22
1.21
1.21
1.20
1.19
1.18
CDCl3
Me
N
Me
MeO2C
TFAN
86
0.80
1.01
0.99
1.31
0.92
2.88
0.99
0.98
1.00
0.98
4.14
1.15
3.05
0.98
f1 (ppm)

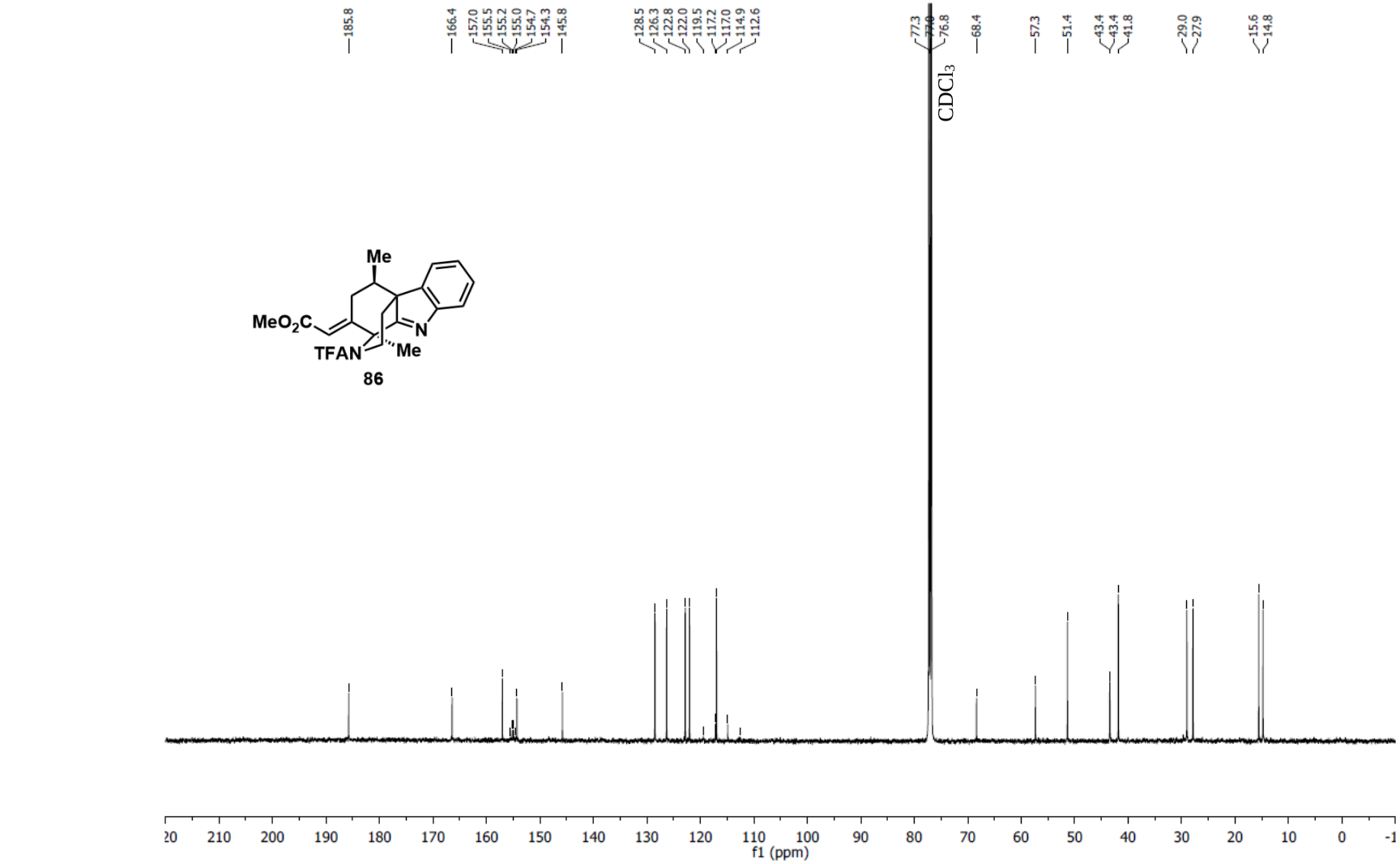
185.8
166.4
157.0
155.5
155.2
155.0
154.7
154.3
145.8
128.5
126.3
122.8
122.0
119.5
117.2
117.0
114.9
112.6
77.3
77.0
76.8
CDCl3
68.4
57.3
51.4
43.4
43.4
41.8
29.0
27.9
15.6
14.8
Me
MeO2C
N
TFAN
Me
86
f1 (ppm)

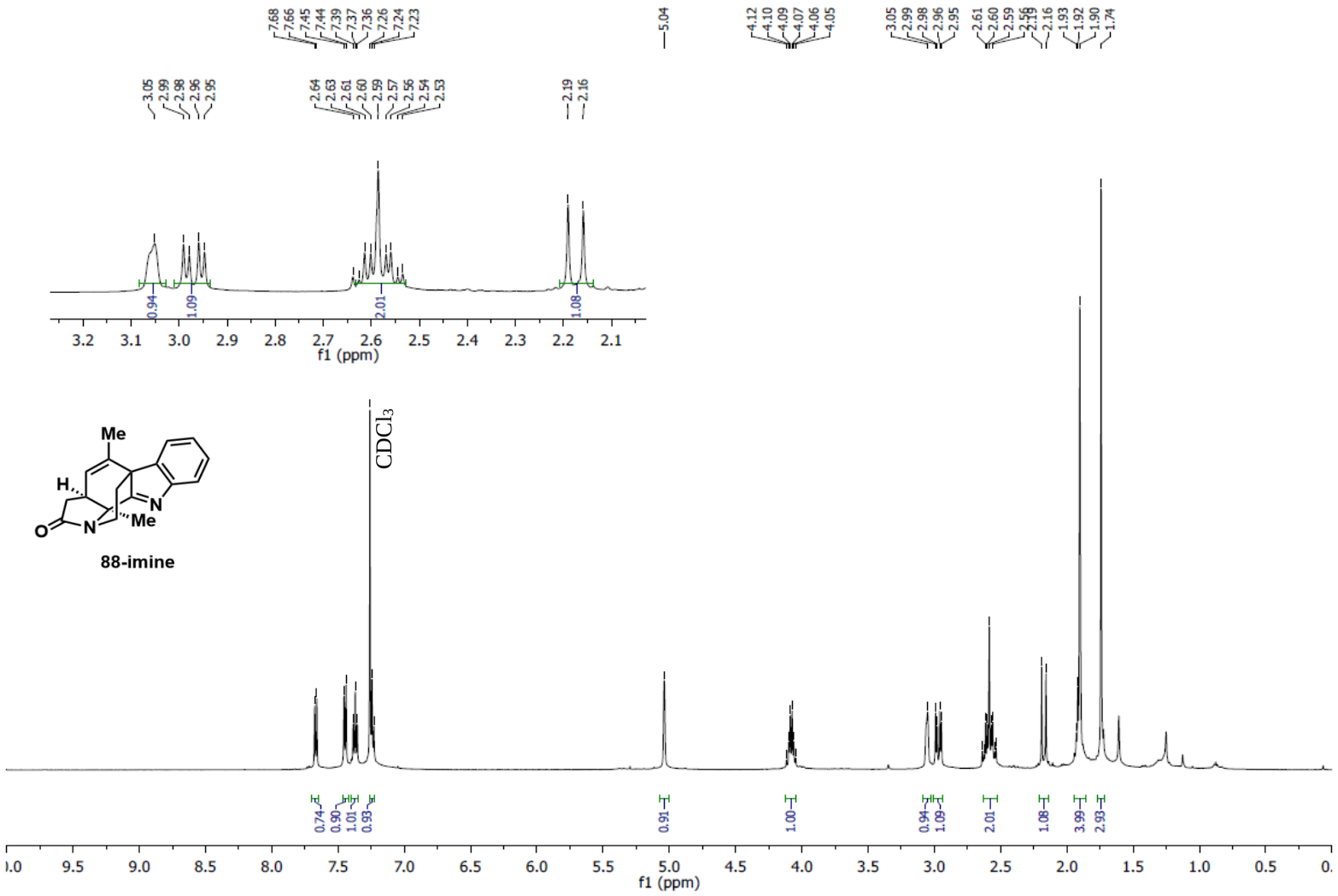
7.68
7.66
7.45
7.44
7.39
7.37
7.36
7.26
7.24
7.23
5.04
4.12
4.10
4.09
4.07
4.06
4.05
3.05
2.99
2.98
2.96
2.95
2.64
2.63
2.61
2.60
2.59
2.57
2.56
2.54
2.53
2.19
2.16
2.61
2.60
2.59
2.16
1.93
1.92
1.90
1.74
0.94
1.09
2.01
1.08
f1 (ppm)
CDCl3
Me
H
N
O
N
Me
88-imine
0.74
0.90
1.01
0.93
0.91
1.00
0.94
1.09
2.01
1.08
3.99
2.93
f1 (ppm)

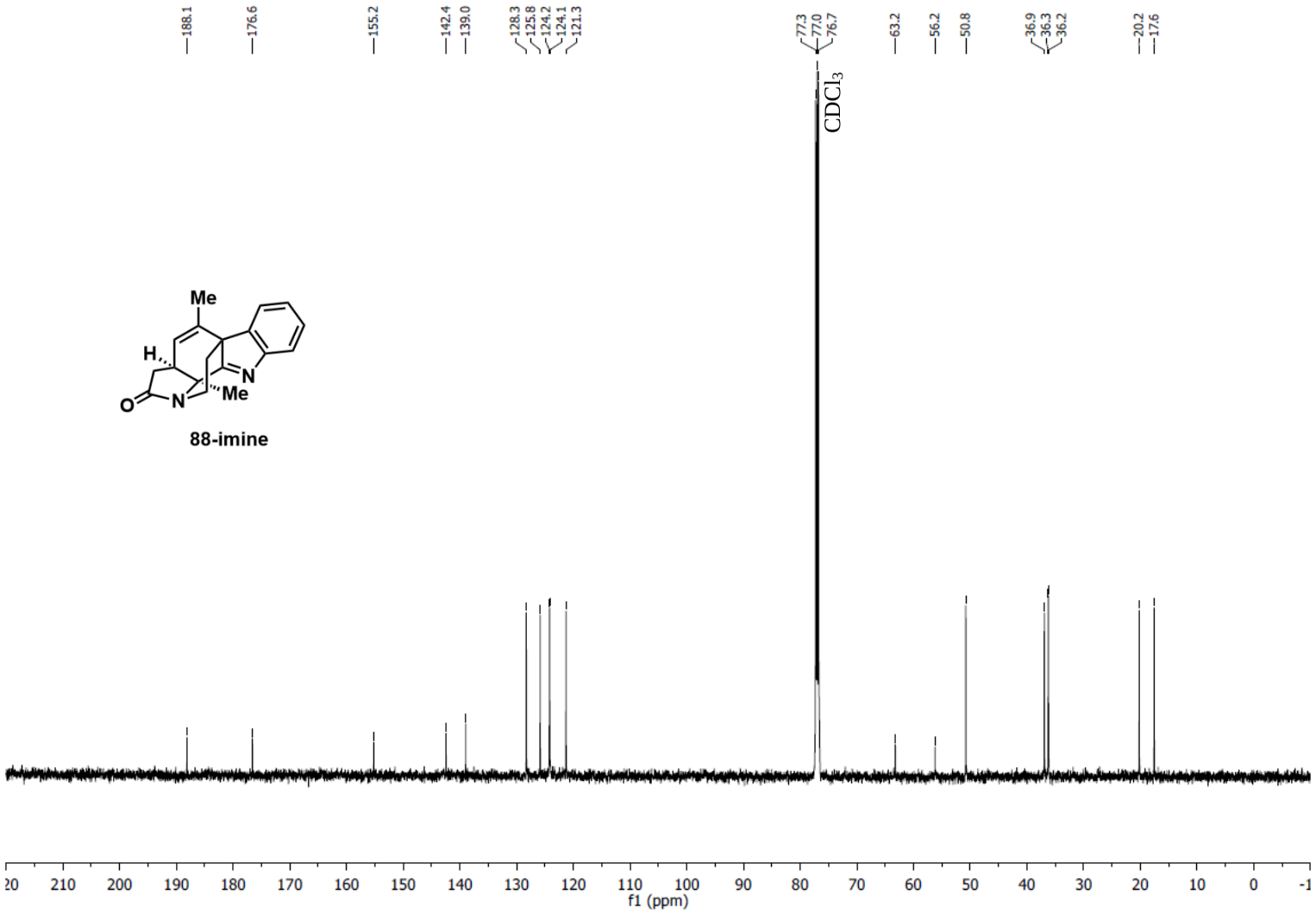
188.1
176.6
155.2
142.4
139.0
128.3
125.8
124.2
124.1
121.3
77.3
77.0
76.7
63.2
56.2
50.8
36.9
36.3
36.2
20.2
17.6
CDCl3
Me
H
N
O
N
Me
88-imine
f1 (ppm)

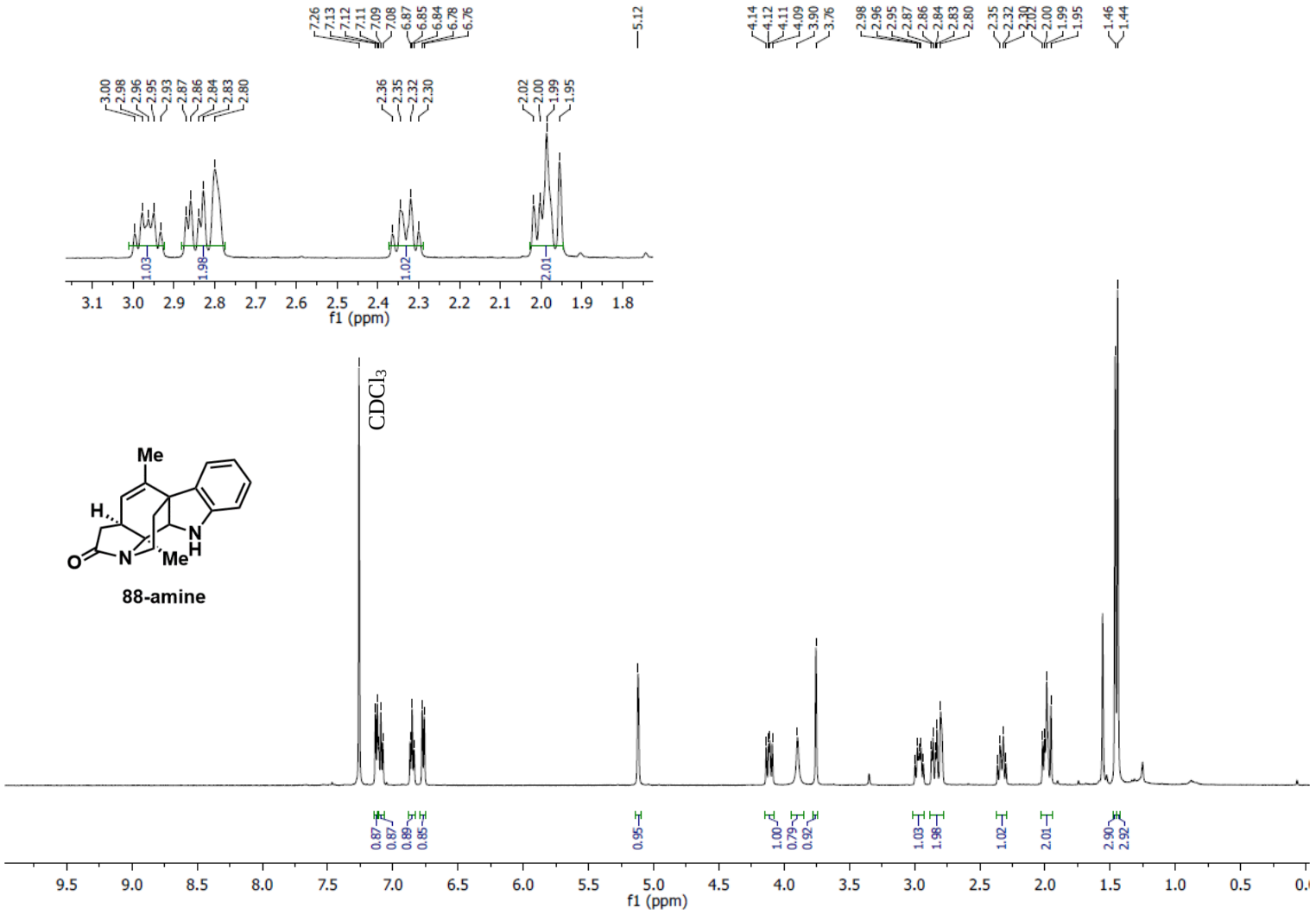
7.26
7.13
7.12
7.11
7.09
7.08
6.87
6.85
6.84
6.78
6.76
5.12
4.14
4.12
4.11
4.09
3.90
3.76
2.98
2.96
2.95
2.87
2.86
2.84
2.83
2.80
2.35
2.32
2.30
2.02
2.00
1.99
1.95
1.46
1.44
3.00
2.98
2.96
2.95
2.93
2.87
2.86
2.84
2.83
2.80
2.36
2.35
2.32
2.30
2.02
2.00
1.99
1.95
1.03
1.98
1.02
2.01
3.1 3.0 2.9 2.8 2.7 2.6 2.5 2.4 2.3 2.2 2.1 2.0 1.9 1.8
f1 (ppm)
CDCl3
Me
H
N
H
O
N
Me
88-amine
0.87
0.87
0.89
0.85
0.95
1.00
0.79
0.92
1.03
1.98
1.02
2.01
2.90
2.92
9.5 9.0 8.5 8.0 7.5 7.0 6.5 6.0 5.5 5.0 4.5 4.0 3.5 3.0 2.5 2.0 1.5 1.0 0.5
f1 (ppm)

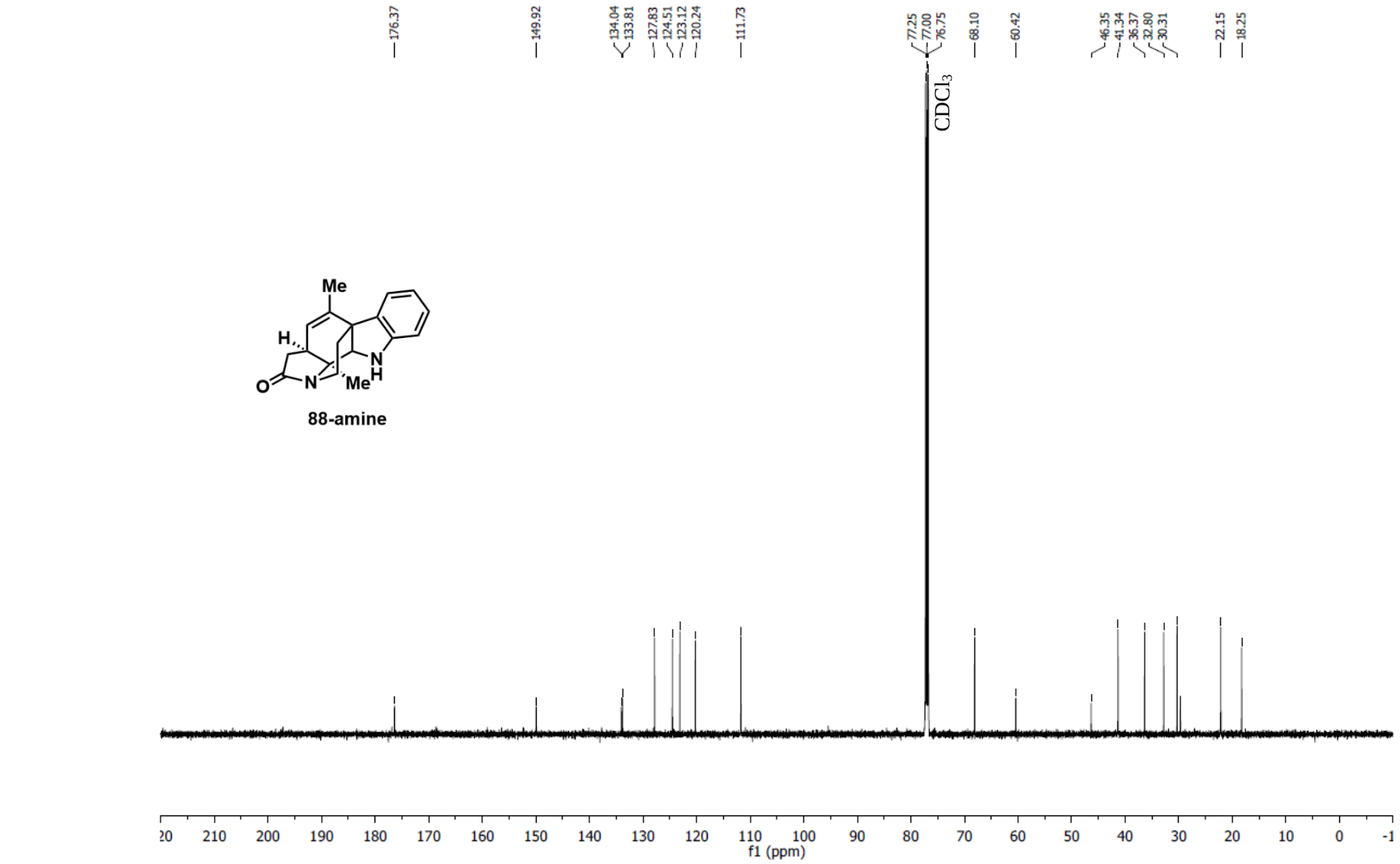
176.37
149.92
134.04
133.81
127.83
124.51
123.12
120.24
111.73
77.25
77.00
76.75
68.10
60.42
46.35
41.34
36.37
32.80
30.31
22.15
18.25
CDCl3
Me
H
N
H
O
N
Me
88-amine
f1 (ppm)

CDCl3
Me
N
Me
H
MeO2C
TFAN
85
f1 (ppm)

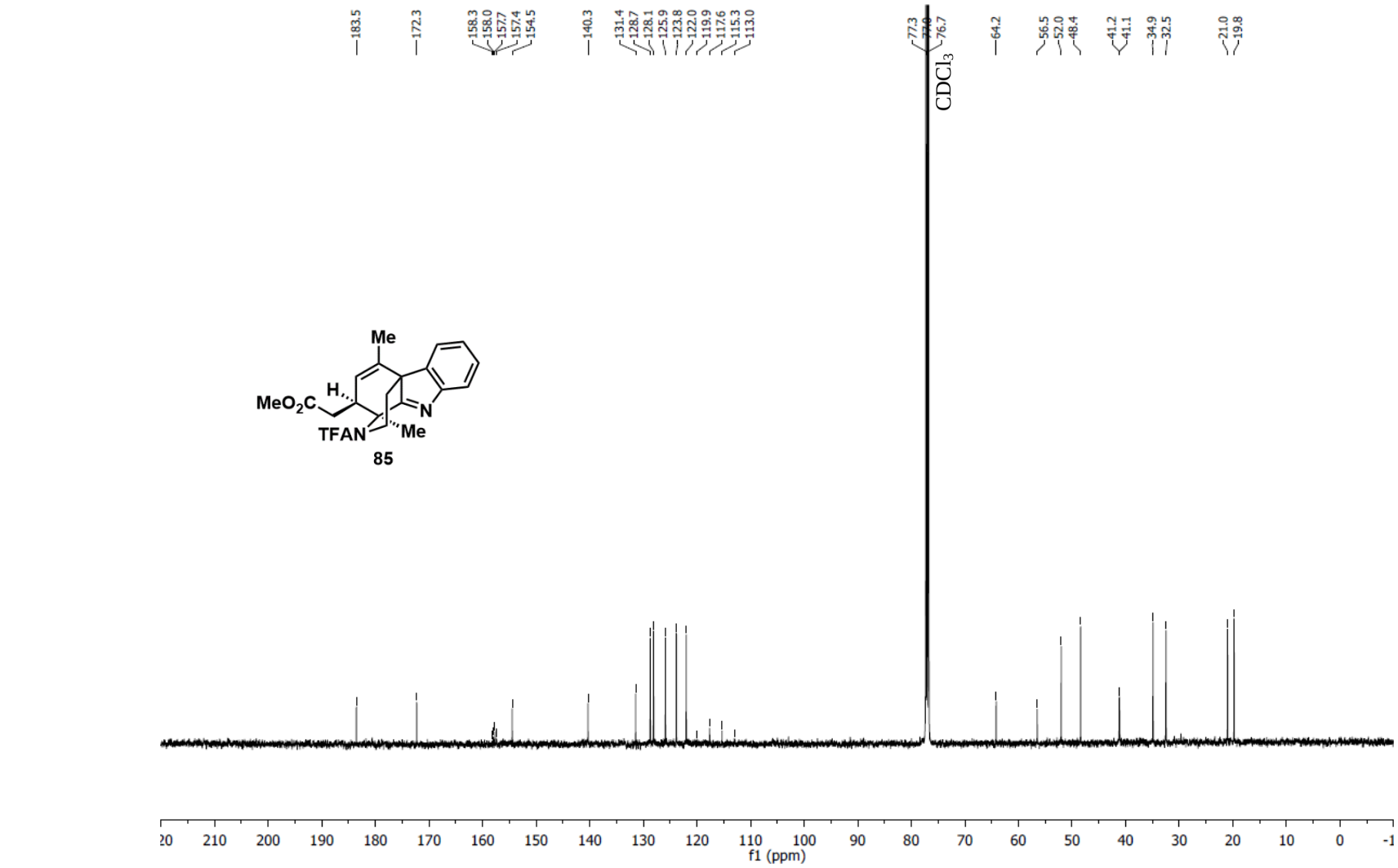
183.5
172.3
158.3
158.0
157.7
157.4
154.5
140.3
131.4
128.7
128.1
125.9
123.8
122.0
119.9
117.6
115.3
113.0
77.3
77.0
76.7
CDCl3
64.2
56.5
52.0
48.4
41.2
41.1
34.9
32.5
21.0
19.8
Me
MeO2C
H
N
TFAN
Me
85
f1 (ppm)

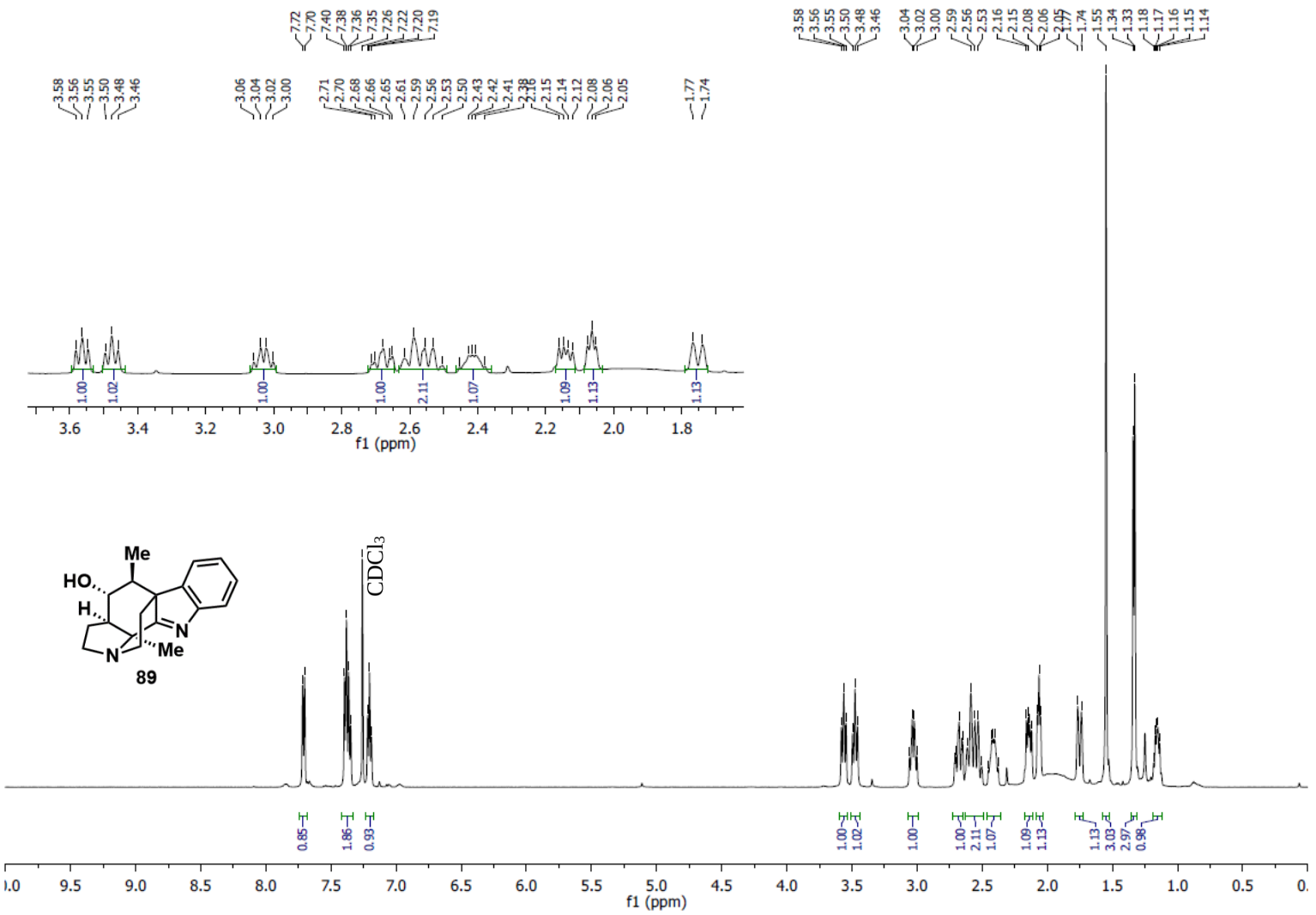
Me
HO
H
N
N
Me
89
CDCl3
f1 (ppm)

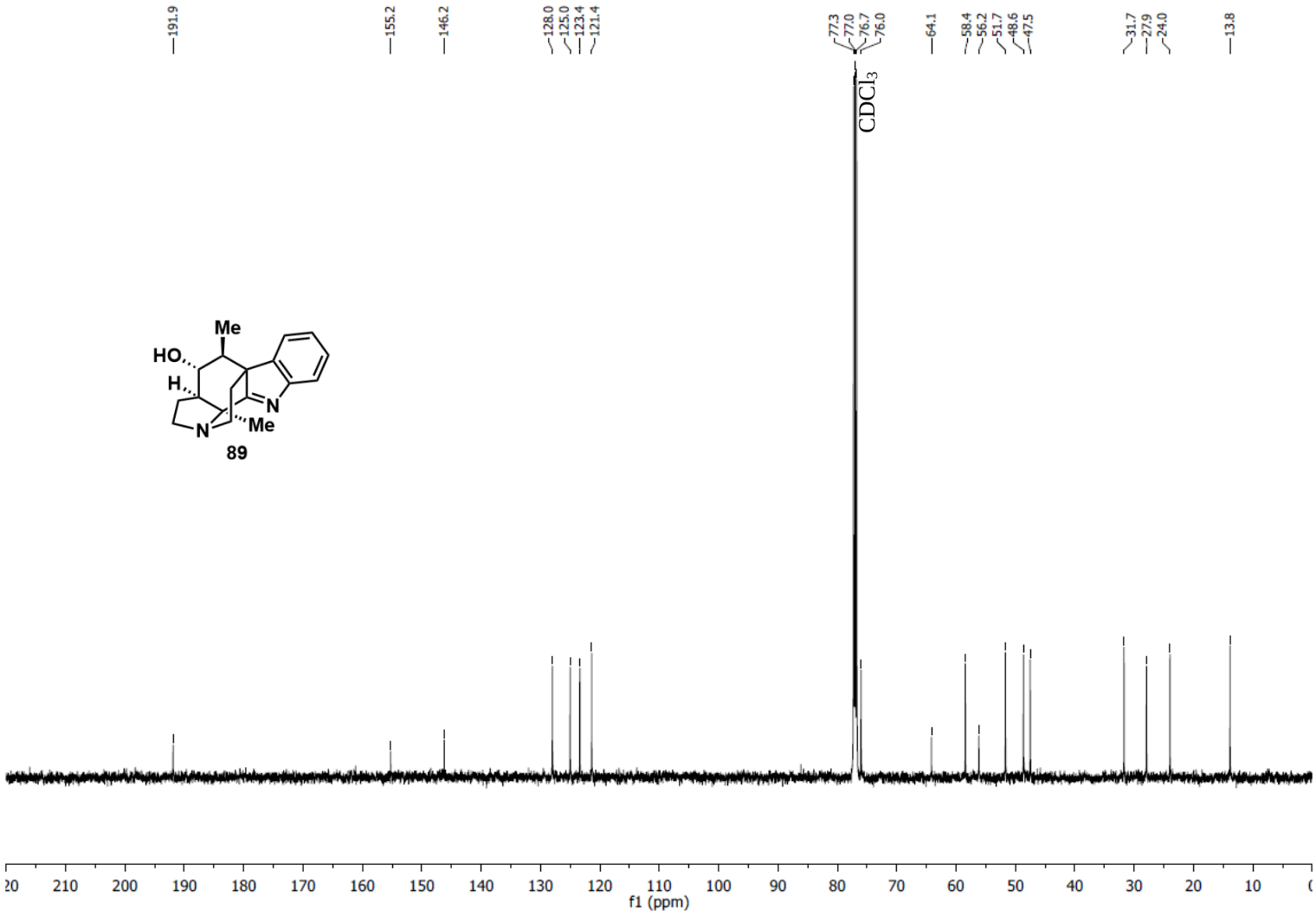
191.9
155.2
146.2
128.0
125.0
123.4
121.4
77.3
77.0
76.7
76.0
64.1
58.4
56.2
51.7
48.6
47.5
31.7
27.9
24.0
13.8
CDCl3
Me
HO
H
N
N
Me
89
f1 (ppm)

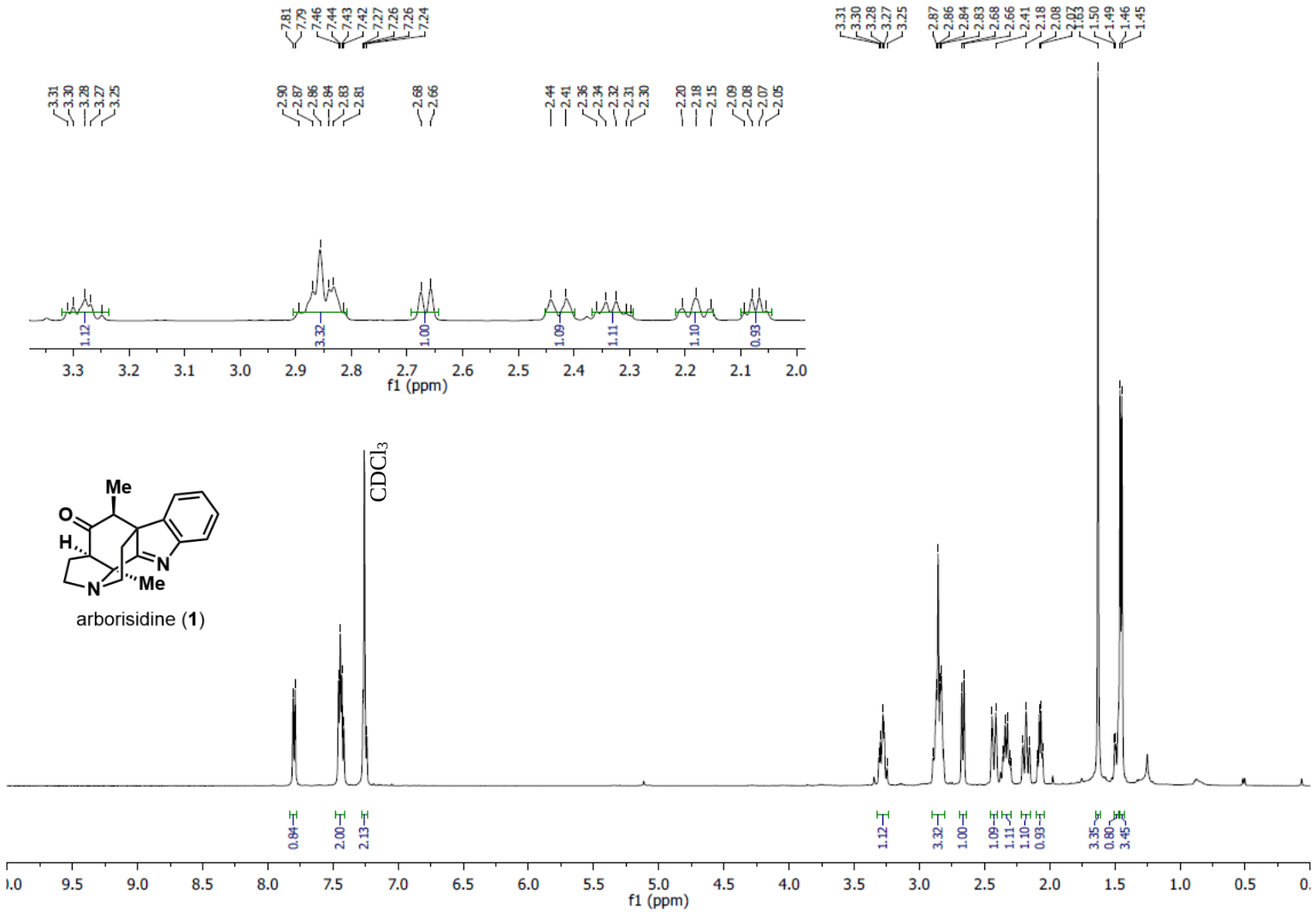
arborisidine (1)
CDCl3
f1 (ppm)

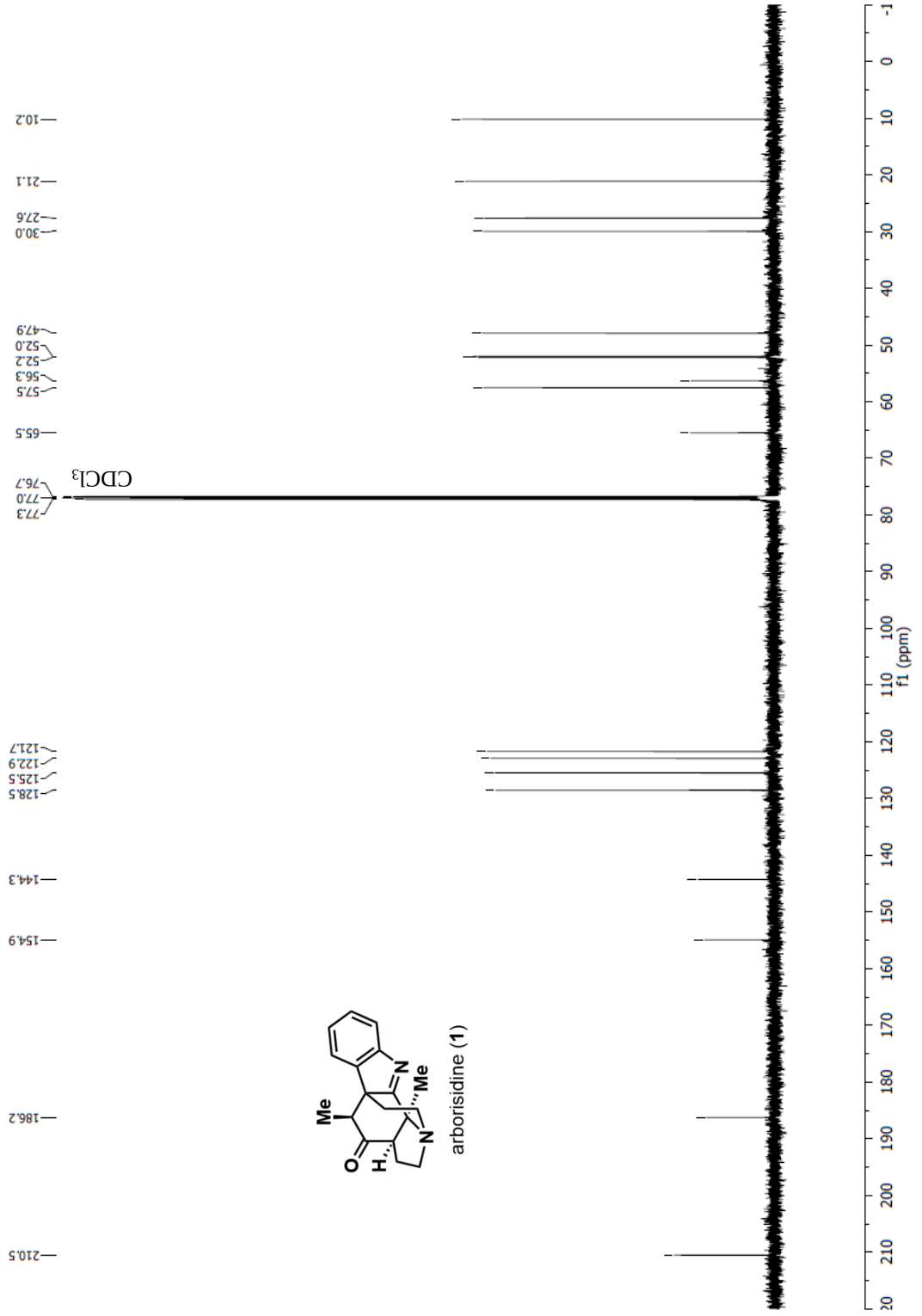
arborisidine (1)
Me
Me
N
N
O
H
CDCl3
77.3
77.0
76.7
65.5
57.5
56.3
52.2
52.0
47.9
30.0
27.6
21.1
10.2
210.5
186.2
154.9
144.3
128.5
125.5
122.9
121.7
f1 (ppm)

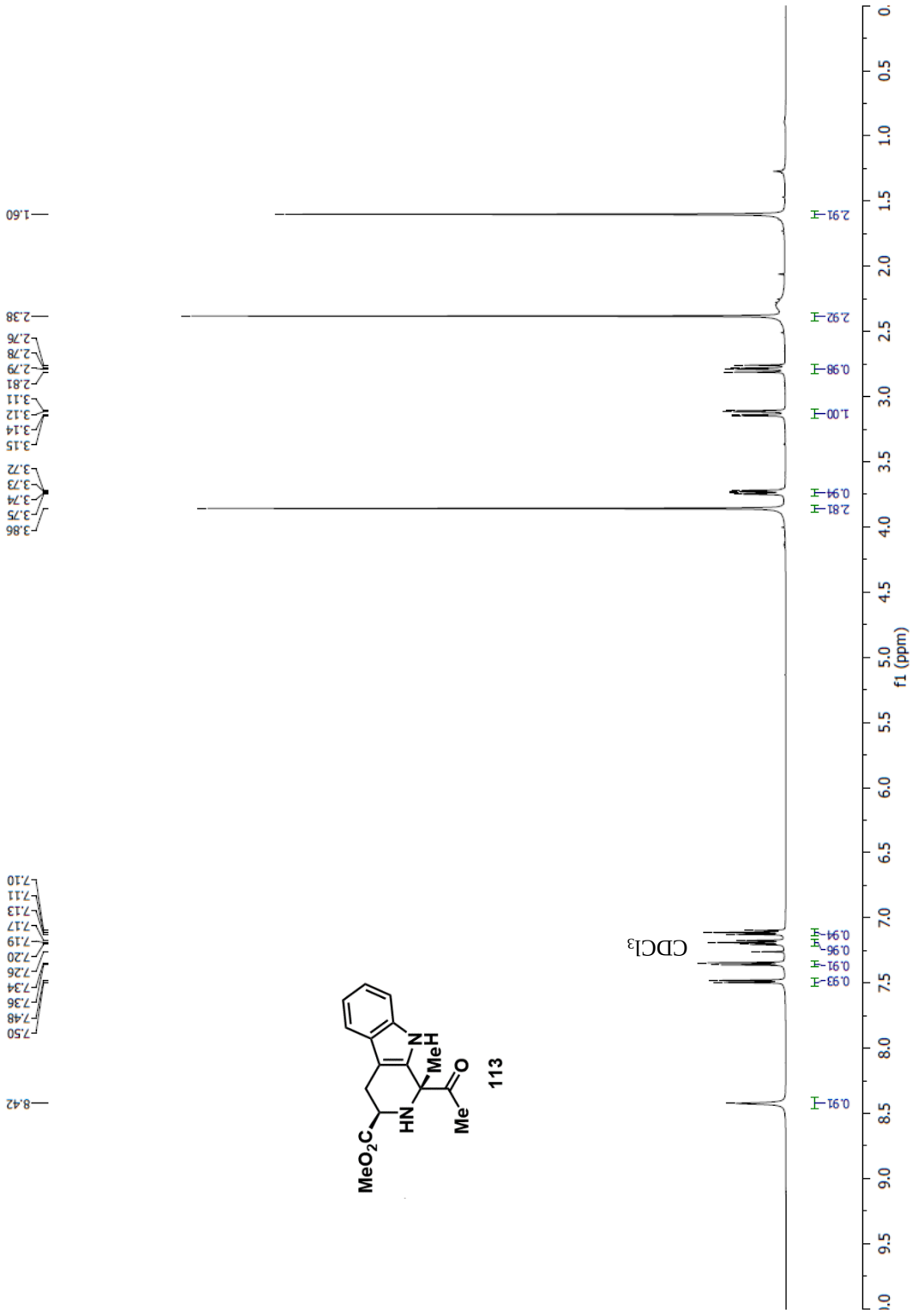
MeO2C
HN
MeH
N
O
Me
113
CDCl3
f1 (ppm)

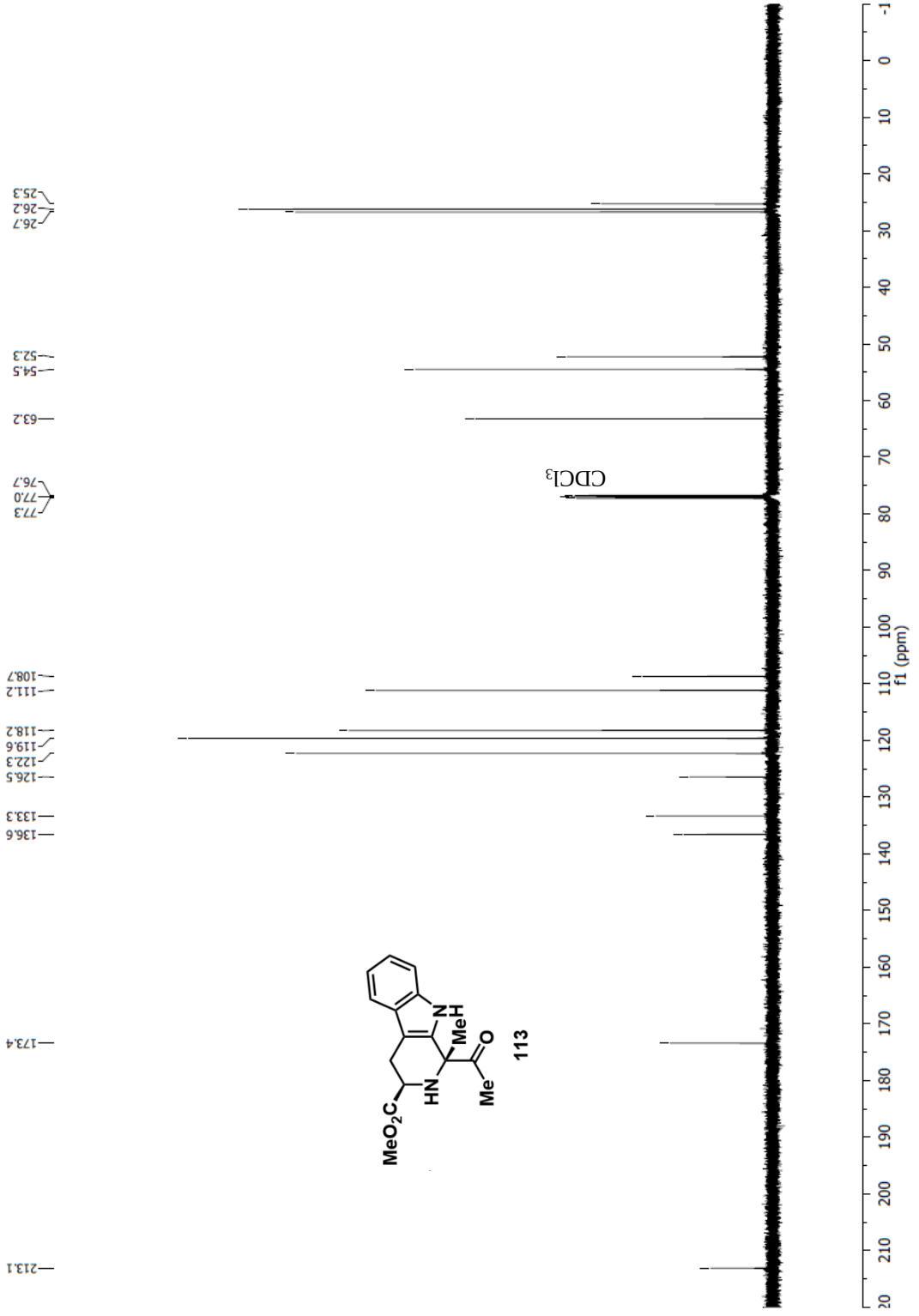
213.1
173.4
136.6
133.3
126.5
122.3
119.6
118.2
111.2
108.7
77.3
77.0
76.7
63.2
54.5
52.3
26.7
26.2
25.3
CDCl3
MeO2C
HN
N
MeH
O
Me
113
f1 (ppm)

8.19
7.52
7.50
7.33
7.32
7.26
7.20
7.19
7.17
7.13
7.12
7.10
3.96
3.94
3.85
3.22
3.22
3.19
3.19
2.93
2.91
2.90
2.88
2.36
2.29
1.64
CDCl3
MeO2C
HN
N
MeH
O
Me
114
0.85
0.88
0.88
0.92
0.93
2.80
0.95
0.98
1.00
2.87
0.95
2.99
f1 (ppm)

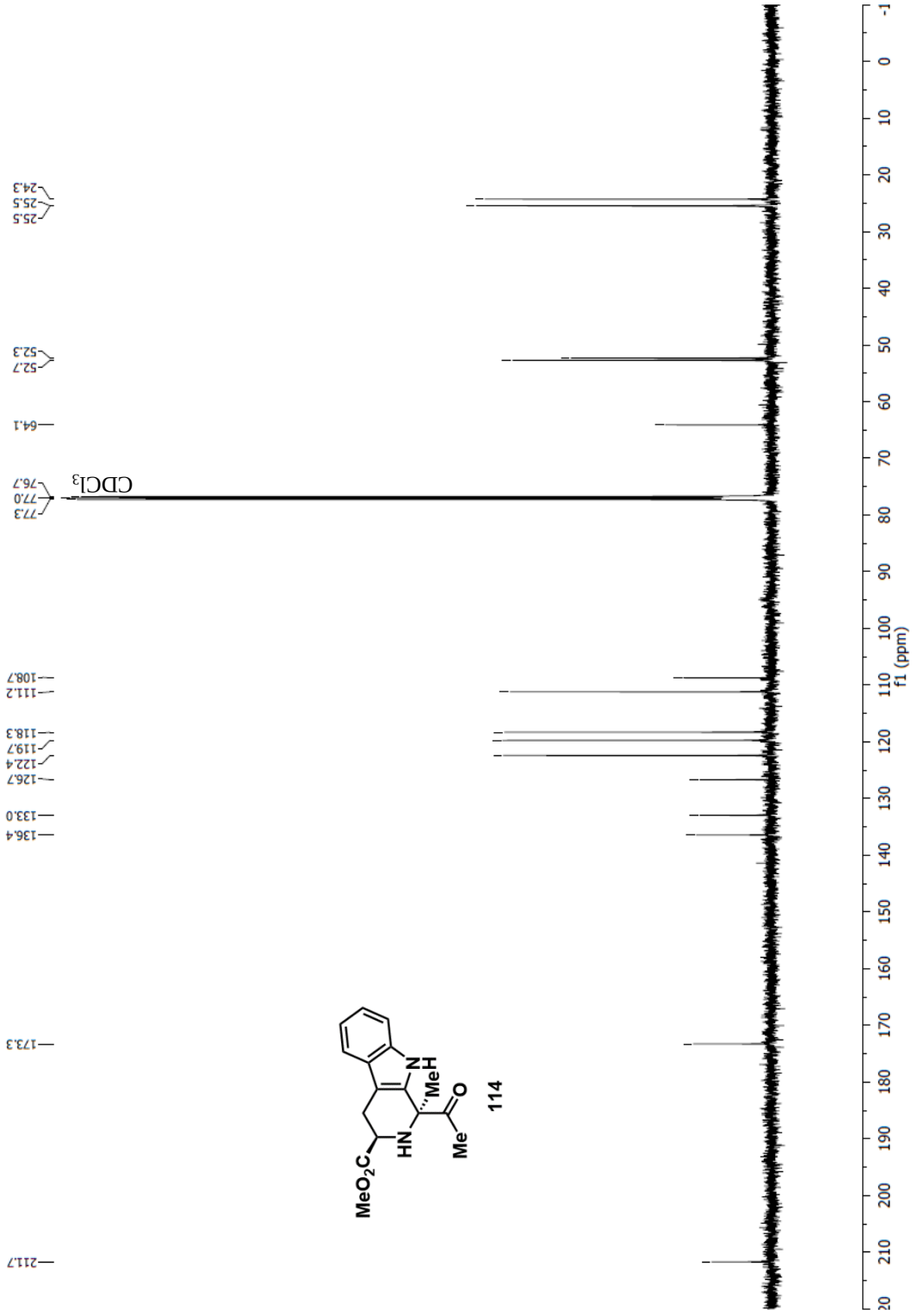
211.7
173.3
136.4
133.0
126.7
122.4
119.7
118.3
111.2
108.7
77.3
77.0
76.7
CDCl3
64.1
52.7
52.3
25.5
25.5
24.3
MeO2C
HN
N
MeH
O
Me
114
f1 (ppm)

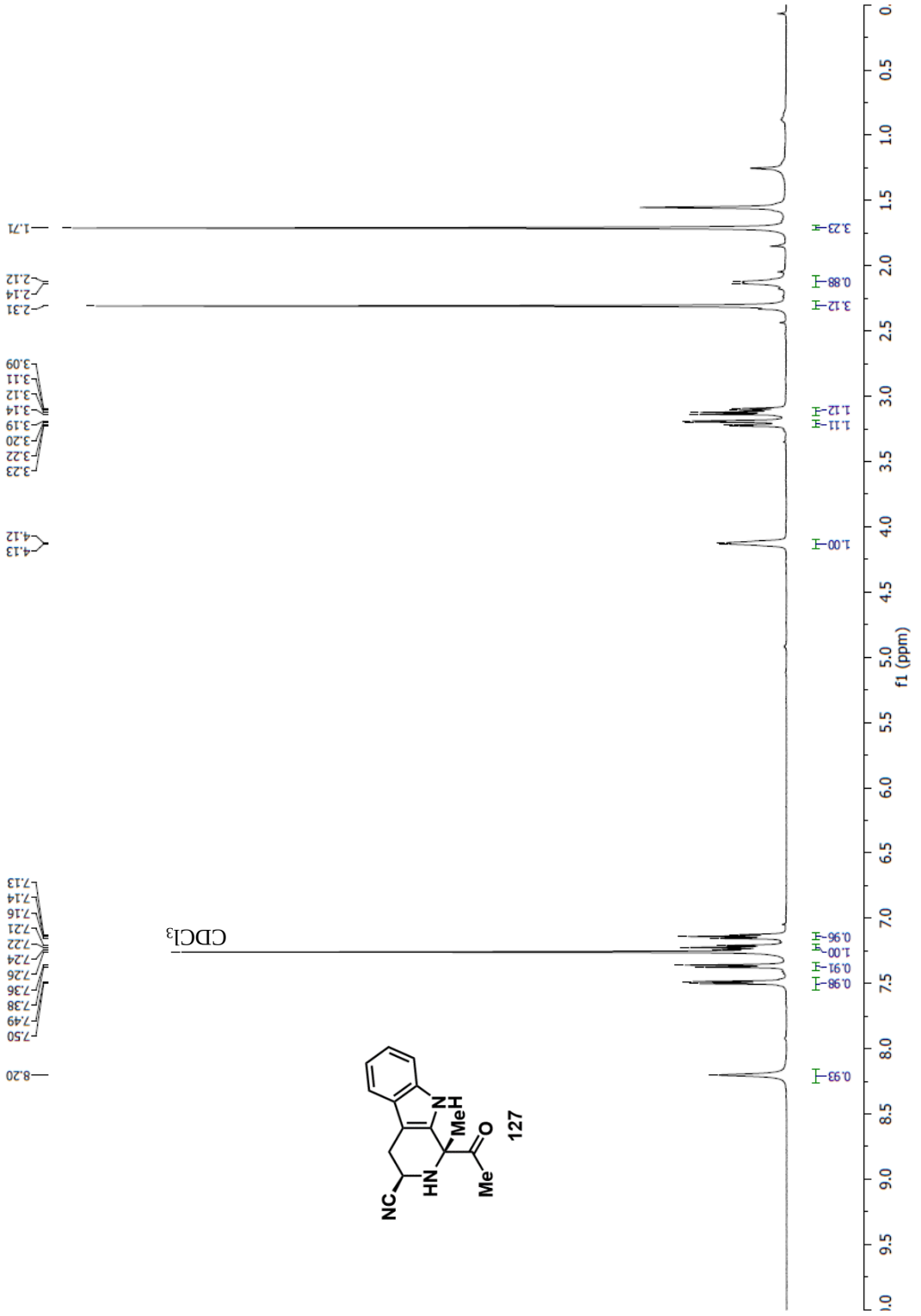
CDCl3
NC
HN
MeH
N
O
Me
127
f1 (ppm)

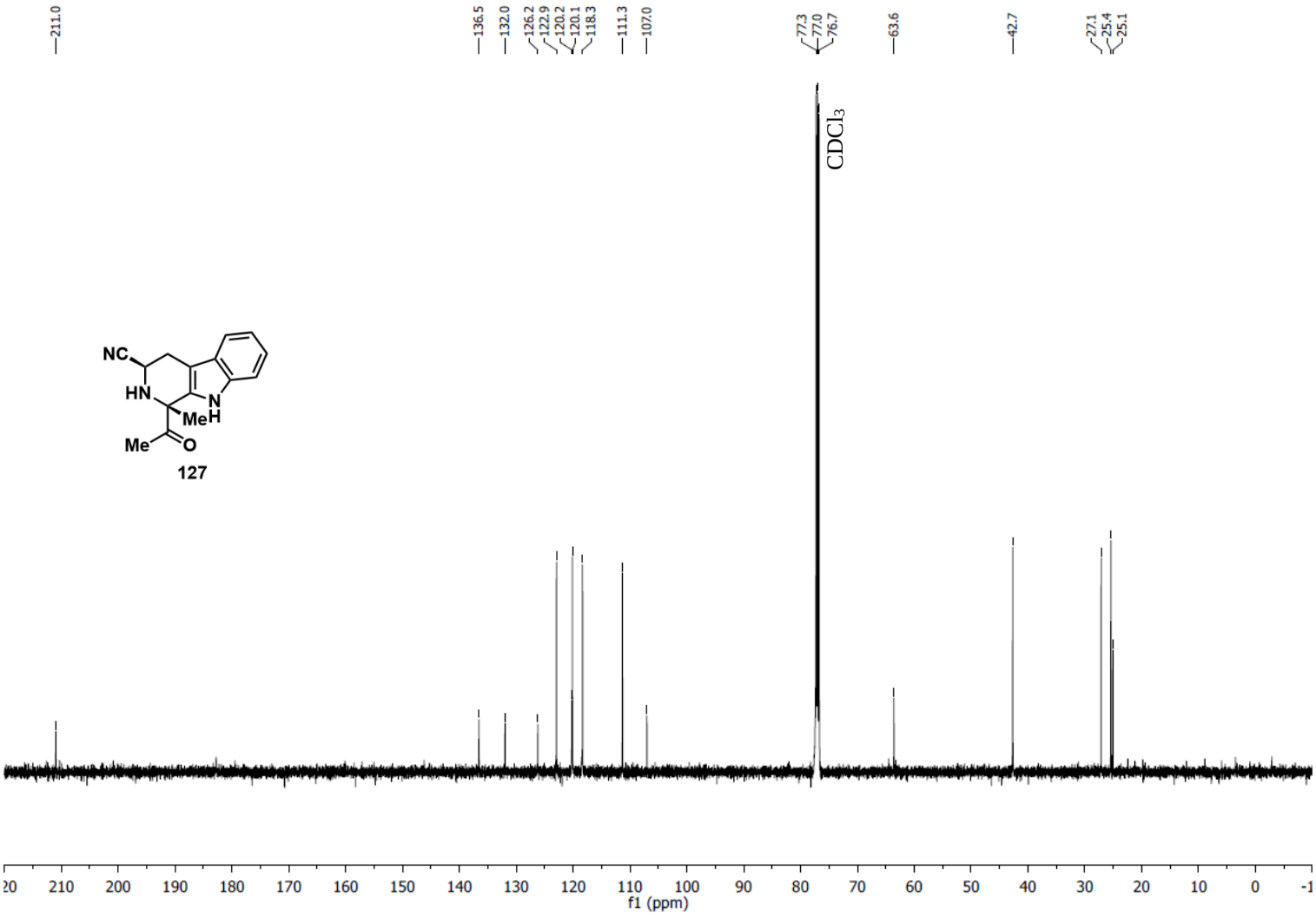
211.0
136.5
132.0
126.2
122.9
120.2
120.1
118.3
111.3
107.0
77.3
77.0
76.7
63.6
42.7
27.1
25.4
25.1
CDCl3
NC
HN
N
H
Me
Me
O
127
f1 (ppm)

3.10 HPLC traces of Selected Intermediates

rac-**110**:

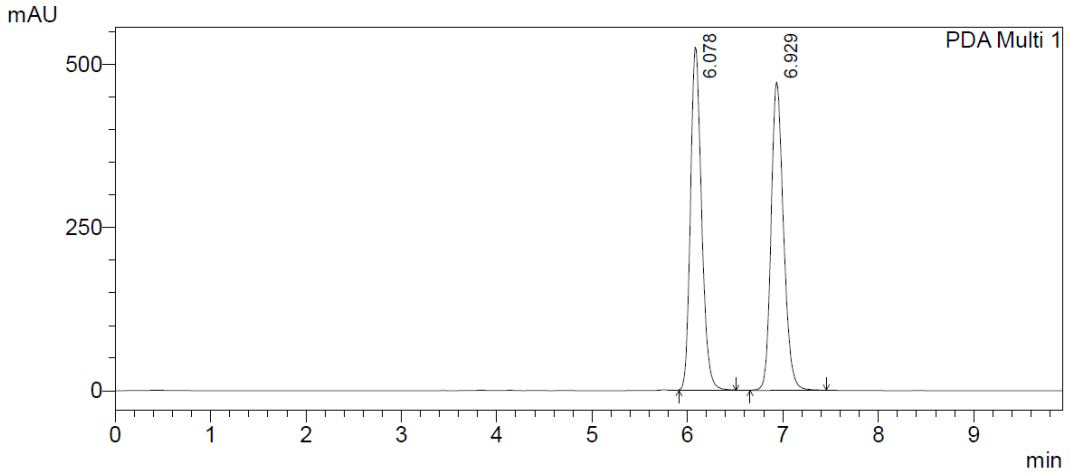

1 PDA Multi 1/254nm,4nm

PDA Ch1 254nm

Peak#	Ret. Time	Area	Area%
1	6.078	4277499	49.943
2	6.929	4287321	50.057
Total		8564820	100.000

chiral **110**:

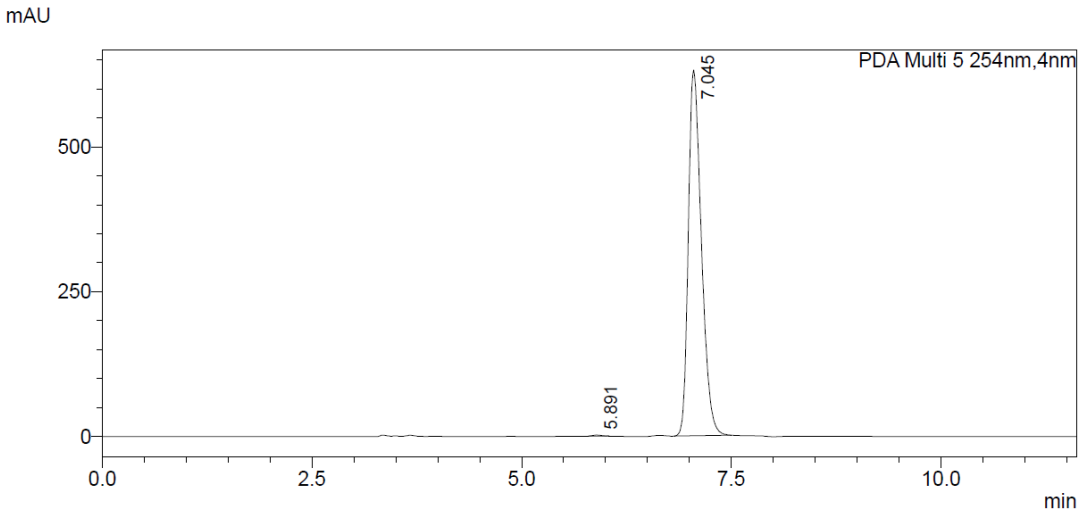

PDA Ch5 254nm

Peak#	Ret. Time	Area	Area%
1	5.891	15918	0.233
2	7.045	6826440	99.767
Total		6842358	100.000

Chapter 4 Studies toward Total Synthesis of Harziane Diterpenes

4.1 Isolation, Structural Feature and Bioactivity of Harziane Diterpenes

Harziandione (**1**), the first member of harziane diterpene family, was isolated in 1992 from *Trichoderma harzianum* (a biocontrol agent in agriculture) by Ghisalberti and coworkers[1a] and its structure was elucidated via NMR and X-ray diffraction studies, disclosing a novel tetracyclic scaffold that contains 4, 5, 6 and 7-membered rings. The absolute stereochemistry of **1** has not been resolved until 2012, when Harzianone (**2**) was isolated from *Trichoderma longibrachiatum* by Ji and coworkers[1c]. The absolution configuration of **2** was identified by the comparison of its DFT-calculated electronic circular dichroism (ECD) spectrum as well as computational optical rotation value with experimental data[1c]; the absolute configuration of **1** was further extrapolated from **2** and computational evidences in its own optical rotation. Since then, there have been other few members in this family[1] isolated from different *Trichoderma spp.* sharing the unique harziane skeleton (Figure 4.1) with at least five stereocenters, three all-carbon quaternary centers, two of which are vicinal, and diverse ring sizes of four, five, six and seven. Although their oxidation state patterns vary in a wide range at the left-half, the right-half of most harziane diterpenes is rather conserved, with either conjugated enone (such as **1**, **2**, alone with its reduced forms **15**, **16**, **17** or γ-hydroxyl enone **18**) or tertiary alcohol together with saturated cyclobutane (such as harzianol F, **11**).

Figure 4.1 Currently isolated harziane diterpene natural products

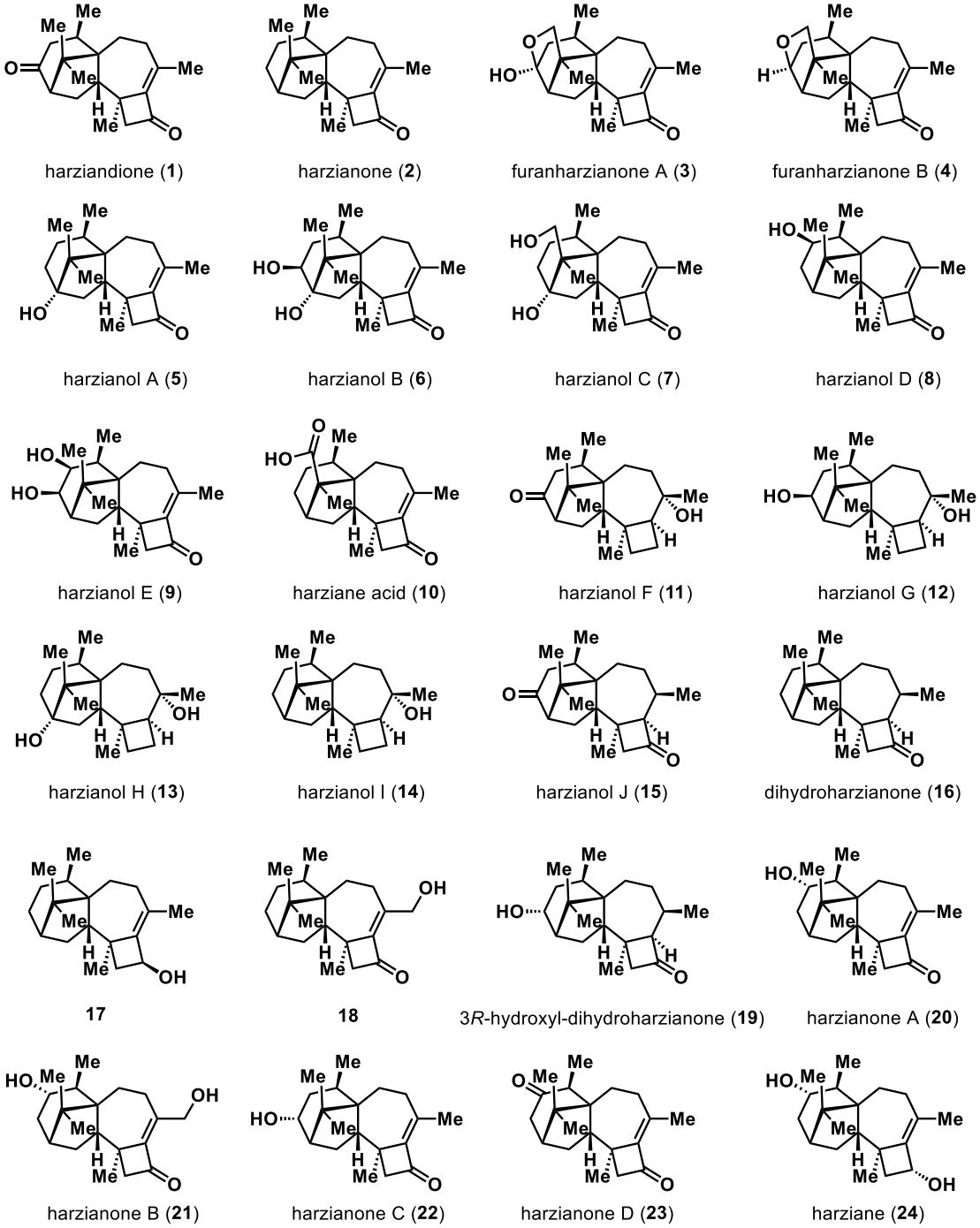

Besides structures shown above, people have also isolated other harziane diterpenes [1d,f,k,m](Figure 4.2) in the past few years that contain a butyrolactone instead of cyclobutanone, which was proposed to form biosynthetically through the Bayer-Villager oxidation of the latter moiety.

Figure 4.2 Other harziane diterpenes with lactone moiety

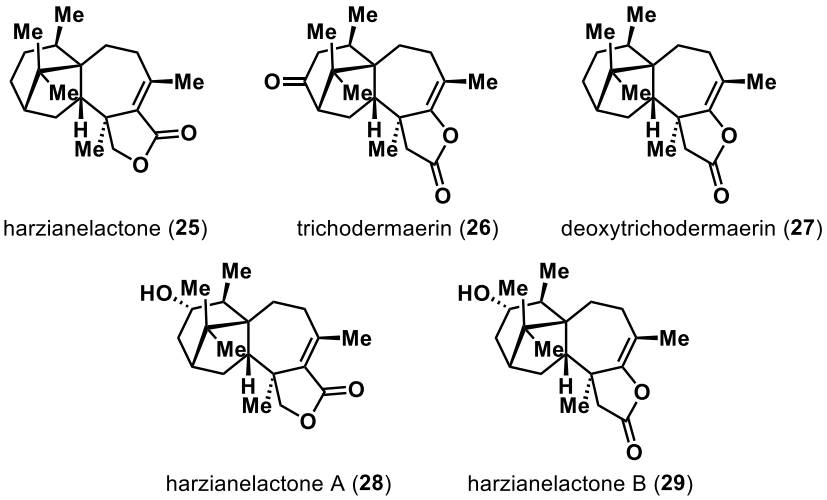

The biosynthesis of harziane diterpenes has also been studied via isotope feeding experiments by Dickschat and coworkers[2](Scheme 4.1), starting from geranylgeranyl pyrophosphate (GGPP, **32**), which undergoes a series of cyclization and 1,2-hydride migration to generate carbocation **36**. Hydration of **36** would give harzianol I (**14**) and related compounds, while elimination followed by allylic oxidation would result in harzianone (**2**), and subsequent hierarchical oxidations would provide other members, such as harzianedione (**1**).

Scheme 4.1 Proposed biosynthesis pathway of selected harziane diterpenes

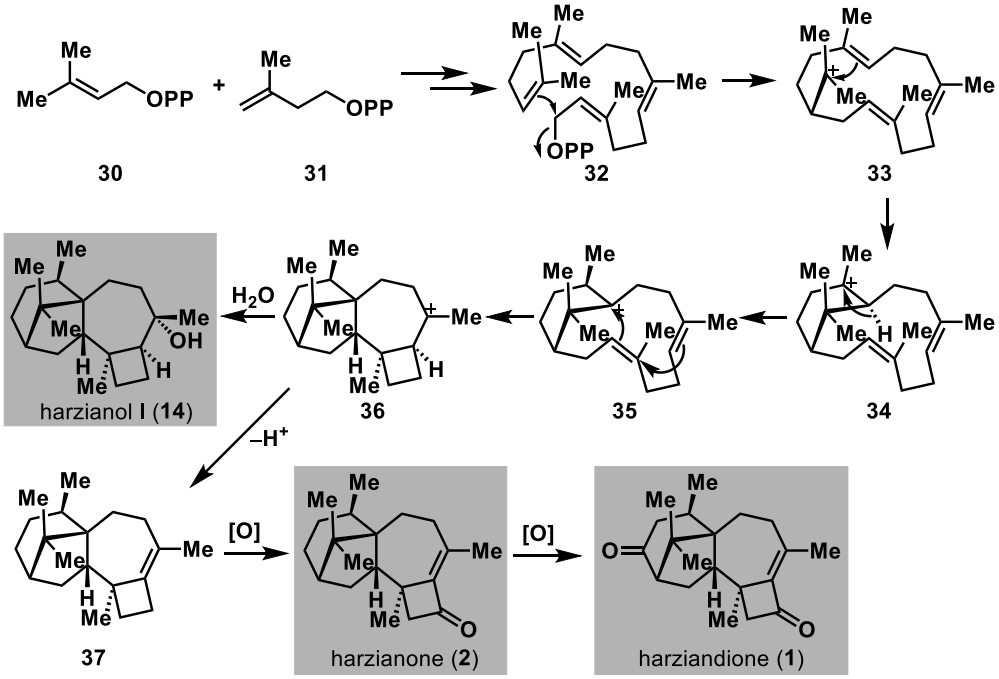

Because most harziane diterpenes were originated from *Trichoderma spp.* which had been used as plant biocontrol agents, it is not surprising that some of the them exhibit growth inhibition activities of marine phytoplankton species[1i,j,m]. In addition, a few members in this family, such as harzianol I (**14**), also exhibit antibacterial activities[1n], cytotoxicity[1e,f,n], anti-HIV activity[1g] and potent phytotoxicity against seedling growth of amaranth and lettuce[1k].

4.2 Previous Work on the Total Syntheses of Harziane Diterpenes

The total synthesis of harziane diterpenes has not been accomplished for decades until recently, when the first total synthesis of racemic harzianol I (**14**) was reported in late 2019 by Carreira and coworkers[3] (Scheme 4.2). Their synthesis started with a readily available ester **38**. Enyne **39** could be prepared in 9 steps, which underwent a gold-catalyzed cycloisomerization/ring expansion[4] to generate **40** containing the desired cyclobutane moiety with good stereocontrol. In another 7 steps, the corresponding silyl enol ether **41** was obtained which went through a one-pot reduction/hydrolysis/aldol condensation reaction to forge the left-hand bicyclic scaffold in **42**. Additional 7 steps including a formal ring expansion and Mukaiyama hydration finally gave rise to **14** which matched the isolated sample regarding their NMR spectra and they further revised the stereochemistry of **14** at the tertiary alcohol carbon position (highlighted in Scheme 4.2).

Scheme 4.2 Carreira's total synthesis of (±)-harzianol I (**14**)

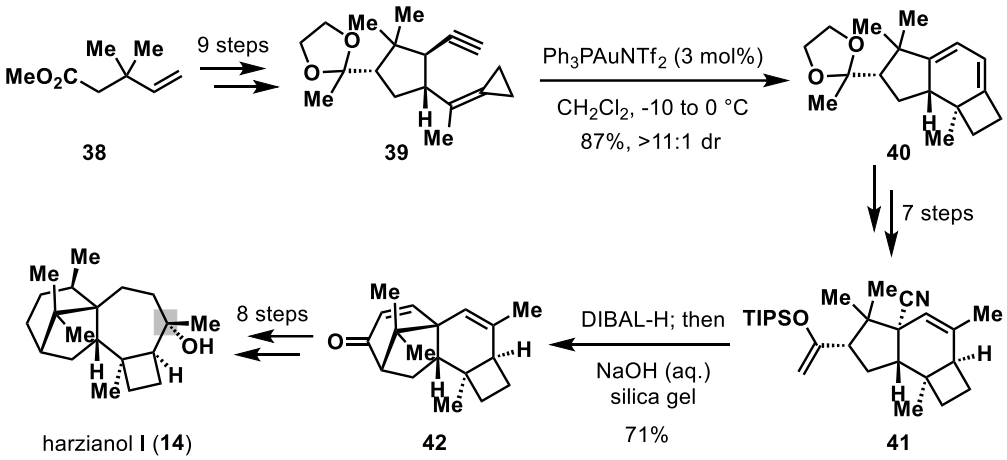

This elegant work represented a delicate implementation of gold-catalysis methodology in the realm of total synthesis. However, this method only allows for access to the saturated family of harziane diterpenes (i.e. harzianol F-I, **11**-**14**). Herein, we would like to present our efforts in pursuing a unified strategy with a late-stage diversification of cyclobutene moiety to achieve the syntheses of different types of harziane diterpene natural products.

4.3 Model Studies of Gold-Catalyzed [2+2] Cycloaddition

While the intriguing skeleton of harziane diterpenes could potentially inspire disconnections from various angles, we were initially more interested in the rapid build-up of the right half 7-4 fused bicyclic unit in harzianedione (**1**). Intuitively, we proposed a ketene [2+2] cycloaddition to generate such ring junction, but the tethering 7-membered ring had raised significant concerns since there was no precedent for such a transformation; the closest examples only involved the formation of 6-4 and 5-4 fused bicyclic compounds[5].

Scheme 4.3 General disconnection and related example of gold-catalyzed [2+2] cycloaddition

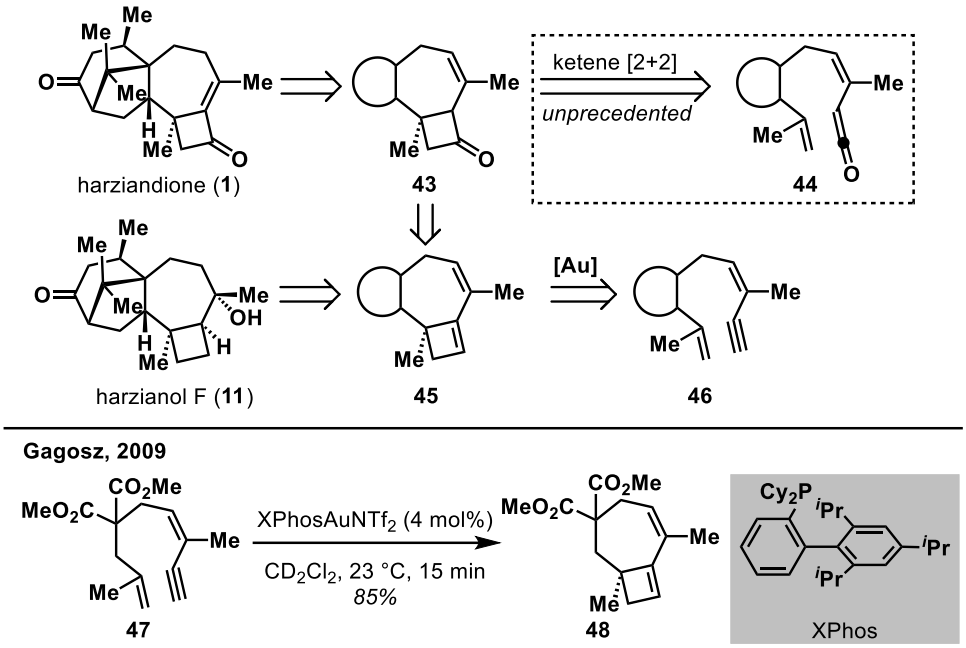

We then turned our attention into metal-catalyzed [2+2] cycloaddition of 1,n-enynes, with the early examples disclosed by Trost and coworkers in 1988 using Pd(II) catalyst[6]. A number of other π-acids, including Pt(II), Au(I), Ga(III) and Ru(II), were later exploited in such type of reactions[7]. Of particular notes, Gagosz and coworkers have discovered that the *cis*-enyne could rapidly undergo the [2+2] cycloaddition in the presence of catalytic $XPhosAuNTf_2$ [8](Scheme 4.3); the high resemblance of intermediate **45** and **48** offered an opportunity for us to incorporate this reaction into our retrosynthesis.

The left-hand bicyclic [3.2.1] scaffold of **1** and **11** could thus be disconnected through an aldol condensation (similar to the Carreira synthesis of **14**[3]), which would lead us to a monocyclic intermediate **50** (Scheme 4.4) with both the isopropenyl group and the enyne side chain pended to a 5-membered ring in a 1,2-*trans*-manner.

Scheme 4.4 Retrosynthetic analysis of **1** and **11** with proposed model substrates

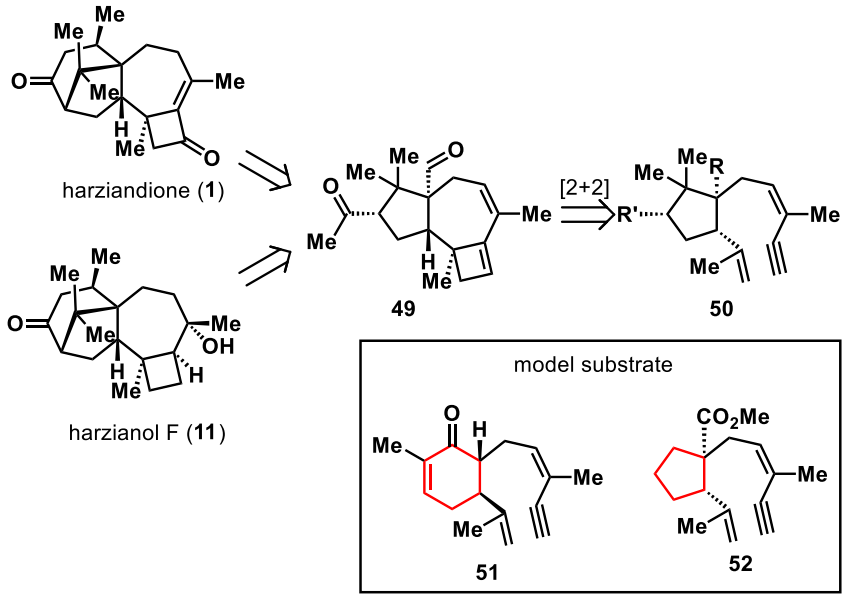

Considering the potential challenges of synthesizing intermediate **50** bearing three stereocenters and two adjacent quaternary carbons on the same ring, we decided to probe the reactivity through two model substrates, **51** and **52** to test the feasibility of enyne [2+2] cycloaddition bearing an additional ring junction with different ring sizes (Scheme 4.4). **51** and **52** could be prepared via α'-alkylation of carvone or α-alkylation of readily available 2-isopropenyl cyclopentane carboxylate **56**[9] with known enyne **54**[10], both of which would establish the key *trans*-1,2-disubstitution stereochemistry.

The syntheses of these two model substrates are shown in Scheme 4.5; note that the reduction of **52** was performed to separate it from the starting material **56**. All the reactions went smoothly with moderate to good yield. With model **51**, under the identical condition reported by Gagosz and coworkers[8] using 4 mol% XPhosAuCl and $AgNTf_2$·MeCN, we could observed a new product in 22% yield with recovered **51**. Its structure was confirmed via ^1H NMR with the signature signals of the conjugated

cyclobutene (δ=5.79, 5.57) as compared with the literature report[8], thus we would tentatively assign the structure as **55**.

Scheme 4.5 Synthesis of model substrates **51** and **57** and initial result of [2+2] cycloaddition

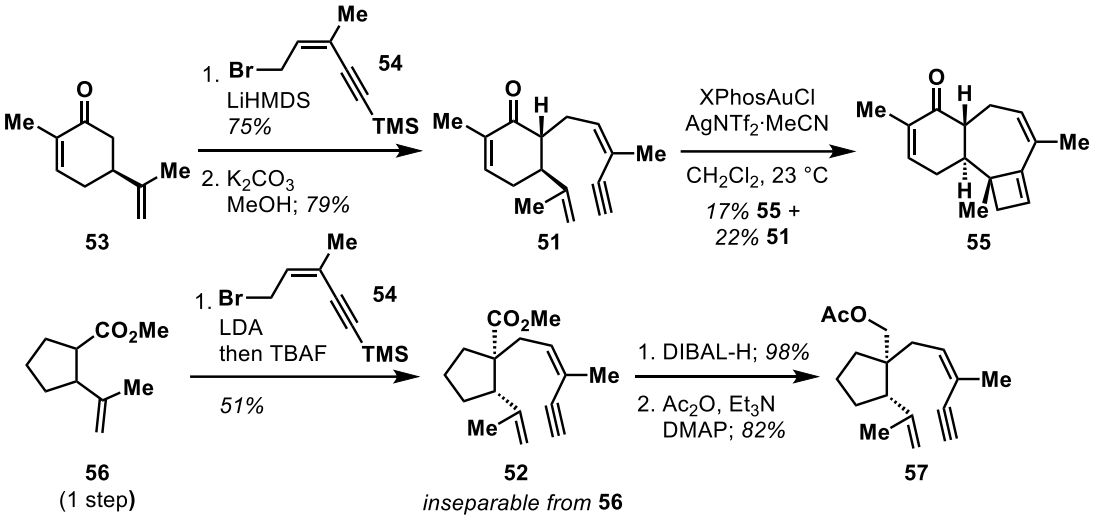

Given this encouraging result, we quickly turned our attention to enyne **57** which was more similar to the real substrate **50**. Unfortunately, in the presence of XPhosAuCl and $AgNTf_2$·MeCN (Table 4.1, entry 1), no conversion was observed; switching to a more bulky ligand, ^{t}BuXPhos[11], on the gold (I) complex, resulted in a full conversion. ^{1}H NMR analysis of the purified sample revealed that it was actually a mixture of cyclobutene **58** and triene **59**, resulting from a *retro*-4π-electrocyclization of **58**. The formation of trienes like **59** was also documented in Gagosz's report[8] with longer reaction time. Another study from Echavarren and coworkers[12] indicated that the counterion was important in the gold-catalyzed intermolecular [2+2] cycloaddition and their best catalyst was [^{t}BuXPhosAu(MeCN)]BARF. Indeed, we have also performed a brief screening of the catalyst bearing different counterions (SbF_6^- and $BARF^-$) and the results were inferior to NTf_2^-. We ultimately decided to stick to ^{t}BuXPhosAuCl and $AgNTf_2$·MeCN as our optimal catalyst combination. The

inevitable partial formation of **59** might be due to the increased ring strain of 5-7-4 fused tricyclic **58**, which led to a slower rate of [2+2] and faster rate of ring-opening to release the ring strain.

Table 4.1 Screening of reaction conditions for intramolecular [2+2] of **57**

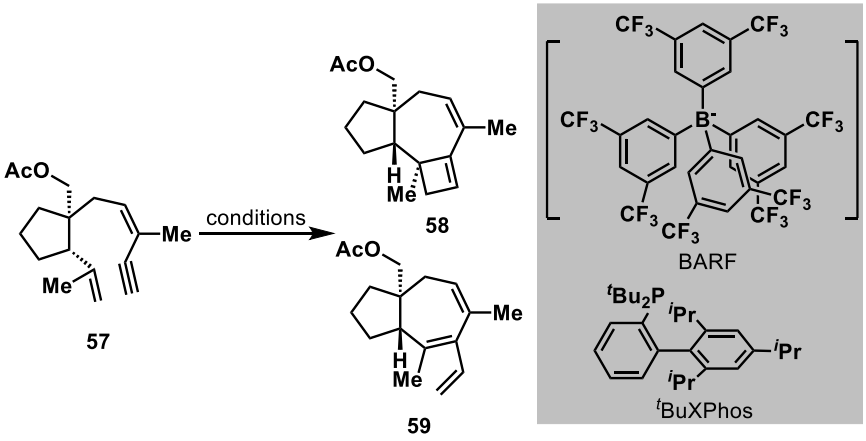

catalyst (5 mol%)	**solvent**	**temp.**	**time**	**results**
XPhosAuCl, $AgNTf_2$·MeCN	CH_2Cl_2	23 °C	12 h	no reaction
^{t}BuXPhosAuCl, $AgNTf_2$·MeCN	CH_2Cl_2	23 °C	12 h	66%; **58**:**57**:**59** = 3.3 : 2.3 : 1
^{t}BuXPhosAuCl, $AgNTf_2$·MeCN	DCE	50 °C	2 h	44%; **58**:**59** = 2.5 : 1
XPhosAuNTf$_2$	DCE	50 °C	2.5 h	36%; **58**:**59** = 2 : 1
[^{t}BuXPhosAu(MeCN)]SbF_6	DCE	50 °C	> 12 h	trace **58**
[^{t}BuXPhosAu(MeCN)]BARF	DCE	50 °C	2.5 h	35%; **58**:**57**:**59** = 5 : 1 : 2

At the same time, my coworker Phil Gemmel, a grad student in our lab, also attempted the optimal ^{t}BuXPhosAuCl/$AgNTf_2$·MeCN condition on **51** and we observed a full conversion into **55** (judged by crude NMR, estimate yield >70%). Realizing the nuance of reactivity regarding ring-size difference, we decided to pursue the 6-membered-ring tethered intermediate **60** (Scheme 4.6) via [2+2] cycloaddition of **61**, and further converted **60** into our desired **49** through ring contraction. Intermediate **61** could thus be synthesized from conjugate addition of enone **62**, which came from alkylation and reduction/elimination of dimedone derivative **63**[13].

Scheme 4.6 Revised retrosynthetic analysis with ring-contraction strategy

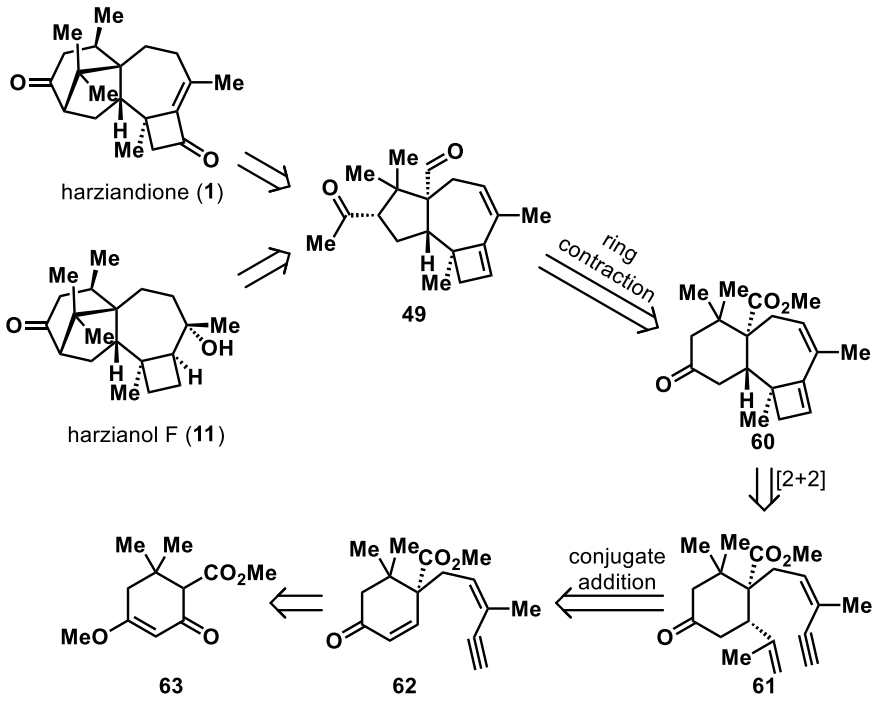

4.4 Synthesis of 6-7-4 Fused Tricyclic Intermediate

The starting material **63** could be easily accessed through α-carboxylation of dimedone methyl ether with Mander's reagent. Here, a large-scale, environmentally benevolent route was developed using condensation between methyl malonate (**66**) and mesityl oxide (**65**)[13] followed by one-pot acid-catalyzed etherification (Scheme 4.7). The subsequent α-alkylation followed by one-pot desilylation gave **64**. We then sought to perform a reduction/ hydrolysis/elimination sequence of **64**, which was found to be quite tricky: the selective 1,2-reduction could only be achieved effectively with DIBAL-H at high concentration, while other common reductant ($NaBH_4/CeCl_3$ or $LiAlH_4$) failed to provide the desired reactivity and/or selectivity. Moreover, the product bearing a β-methoxyl allylic alcohol group, was unexpectedly stable upon neutral workup and column chromatography, and could only be hydrolyzed via the

direct quench after DIBAL-H reduction by pure MsOH and subsequent concentrated HCl (aq.); the limited equivalents of water, excess acid and homogeneity of the solution were all critical to the reproducibility of this reaction. Nevertheless, we were able to accumulate the desired enone **62** in good quantities and the conjugate addition promoted by CuBr·SMe_2 took place cleanly to give a single diastereomer of **61**. The [2+2] cycloaddition of **61** took place in 85% yield with the aid of ^{t}BuXPhosAuCl/ $AgNTf_2$·MeCN (Scheme 4.7), and the structure of **60** was determined unambiguously via X-ray diffraction analysis.

Scheme 4.7 Access to 6-7-4 tricyclic intermediate **60**

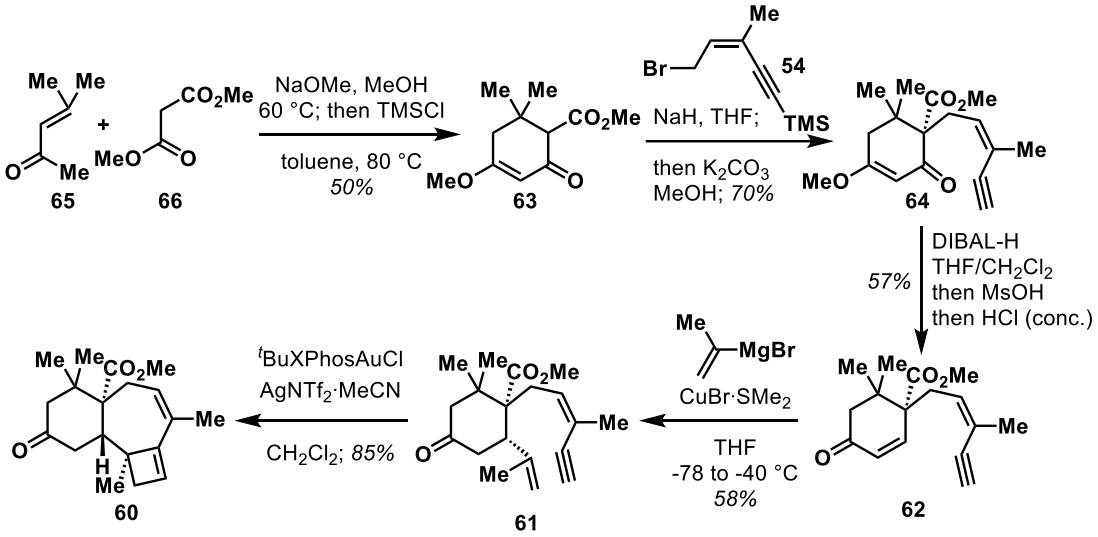

4.5 Attempted Ring Contraction and Detour

With **60** in hand, our next task was the ring contraction to generate the desired 5-membered ring. Wolff rearrangement was abandoned due to the concern of photo-lability of the cyclobutene moiety in **60**; the classic Favorskii rearrangement would involve a separate α-bromination of ketone which the reactive cyclobutene might not survive. We finally picked the PIDA-mediated Favorskii-type rearrangement[14]. The

reaction was completed within 1 hour in the presence of PIDA and KOH/MeOH (Scheme 4.8, left) to generate a single isomer **65**, but COSY and NOESY experiments of **65** suggested its structure as the undesired regioisomer. We postulated that other ring contraction method relying on α-functionalization of ketone would probably give the same regioselectivity outcome, and such selectivtiy might stem from the substantial steric difference between the two α-position of the ketone.

Scheme 4.8 Attempted ring contraction of **60** and detour of α-oxygenation

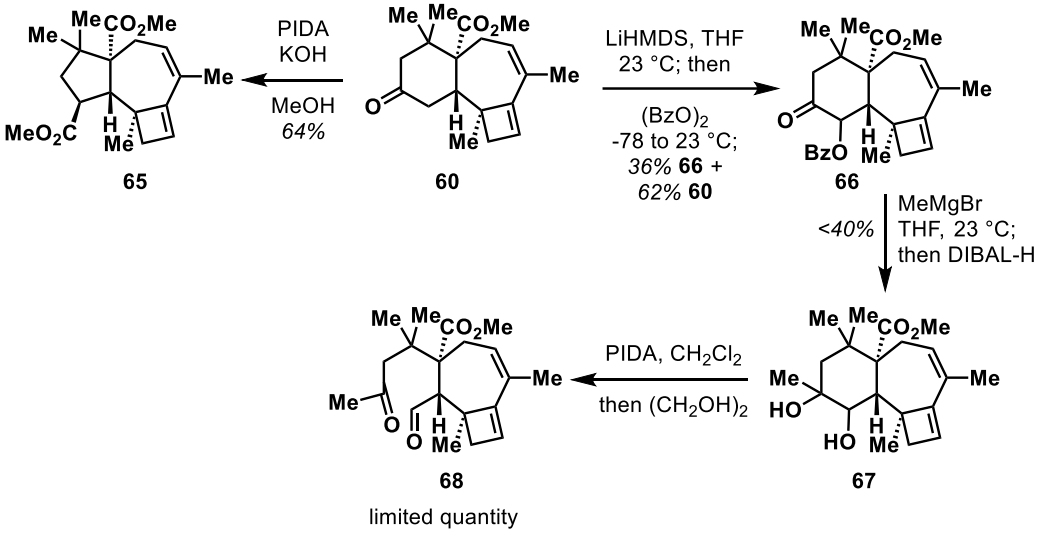

This unwanted result, however, led us to detour and exploit the existing regiospecificity. We then designed a different ring-contraction strategy involving a C-C bond cleavage and reconstruction (Scheme 4.8, right). Although the detour might take more steps, most reactions employed were orthogonal to the sensitive cyclobutene. We first attempted the α-benzoylation employing LiHMDS and benzoyl peroxide[15] as electrophile and the reaction was rather sluggish, although most unreacted starting material could be recovered. Other oxygenation reagents (Davis oxaziridine[16] or nitrosobenzene[17] with proline catalysts) failed to give any conversion, and screening of other bases, including reversible bases such as KO^{t}Bu or DBU, had not been

successful; the high temperature (23 °C) was necessary for deprotonation, since lower temperature resulted in lower conversion. Nevertheless, ketone **66** was further converted into diol **67** through Grignard addition and one-pot deprotection with DIBAL-H, although the yield was not high. Importantly, the bridgehead ester group was totally inert towards DIBAL-H reduction. The diol cleavage of **67** was then performed with PIDA[18], while common oxidants such as $NaIO_4$ was inactive to **67**. As the slight excess of PIDA had decomposed the resultant **68** by reacting with either the carbonyls or the cyclobutenes upon concentration of crude material, ethylene glycol was used as the quenching reagent; aqueous $Na_2S_2O_3$ was found ineffective.

68 was then ready for the intramolecular aldol condensation. Due to the low yields in the preceeding steps, we couldn't accumulate enough amount of **68** through this route and had to go back and optimize the α-oxygenation reaction of **60**. Conformation analysis of **60** based on its crystal structure (here drawn in its enantiomeric conformation, Figure 4.3) would provide additional hints: the presence of bridgehead ester group, bridgehead methyl group (introduced by [2+2] cycloaddition) and methylene group in the four-membered ring had created an extremely congested environment that would be hard for bases to approach and deprotonate at the ketone α-position; a pre-[2+2] intermediate with more flexible conformation of the "bridgehead" methyl group might reduce the steric constraint of such α-position.

Figure 4.3 Conformation analysis of **60**

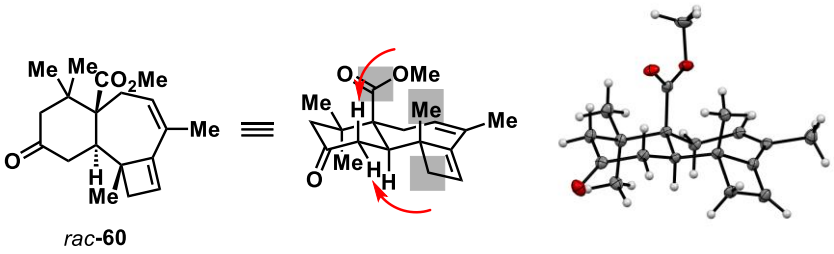

Given this hypothesis, my coworker Phil Gemmel had first tried the Rubottom oxidation of the corresponding TMS enol ether **69** and we were delighted to see full conversion of starting material upon treatment with slight excess *m*-CPBA. Further treatment with TBAF gave the desired α-hydroxy ketone **70** (Scheme 4.9).

Scheme 4.9 Pre-[2+2] α-oxygenation enabled scalable synthesis of **68**

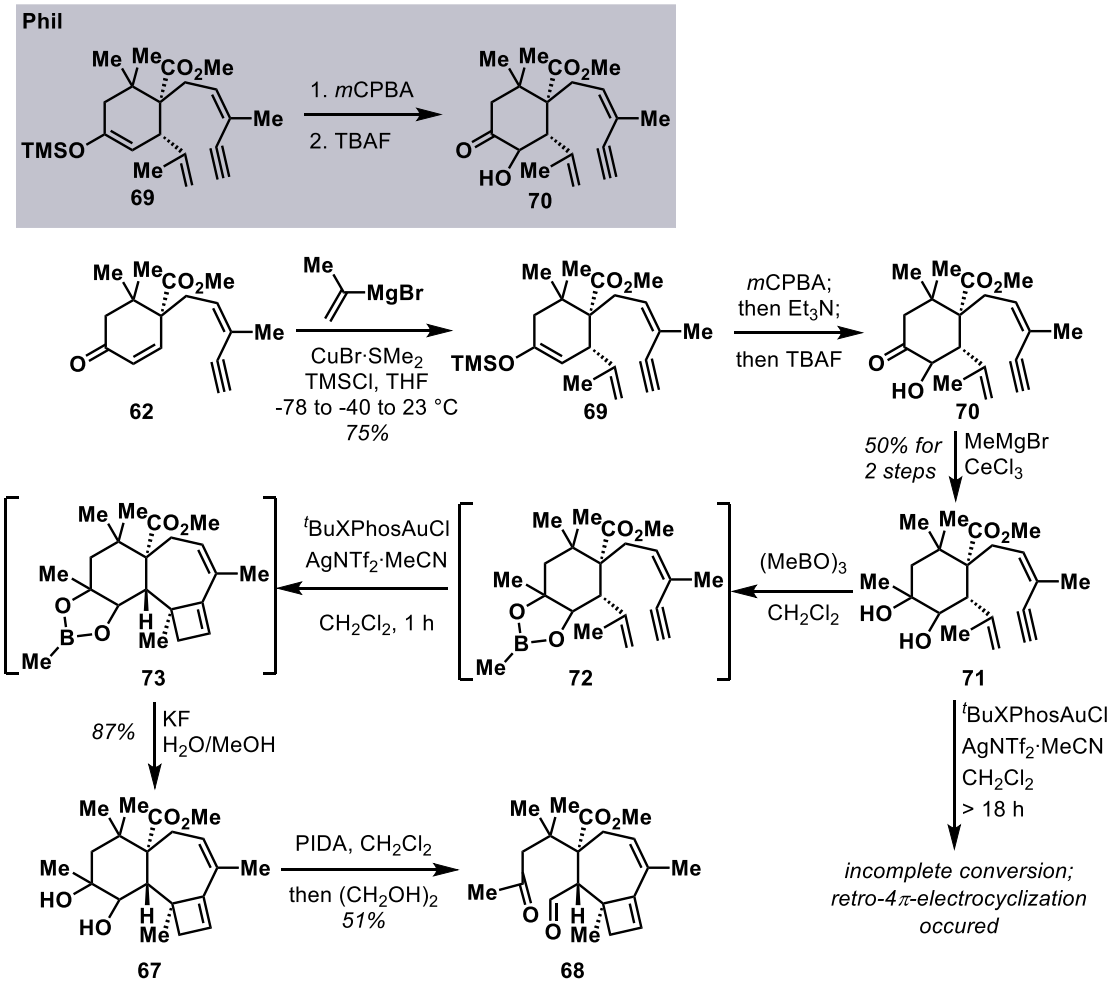

We further optimized the route by adding TMSCl at the conjugate addition of **62** to trap the thus-formed enolate as **69**, which also increased the yield[19] at the same

time. The stable TMS enol ether **69** was further taken into a one-pot Rubottom oxidation/desilylation reaction to give the desired α-hydroxyl ketone **70**, which could be transformed into diol **71** as a single diastereomer with the aid of $CeCl_3$[20] and methyl Grignard reagent. We then conducted the [2+2] cycloaddition with the naked diol moiety presented in **71** and the reaction resulted in slow and incomplete conversion, likely due to the inhibition of highly reactive cationic Au (I) by the Lewis basic alcohol (Scheme 4.9). To solve this problem, we developed a one-pot protection/cycloaddition/ deprotection sequence using $(MeBO)_3$[21] as the *in situ*, transient protecting agent; the cyclic boronate **73** was formed smoothly and could be purified separately by column chromatography, but it could be removed by homogenous KHF_2 solution to give **67** as the spectrum was identical to the product obtain from route shown in Scheme 4.8. Further treatment of **67** with PIDA would give the ketoaldehyde **68** cleanly.

The quick access of ketoaldehyde **68** had opened up great opportunities for the ring reorganization leading to the desired bicyclic[3.2.1] skeleton in our target natural products. Upon exposure to KOH/MeOH[22], **68** would be fully converted into acetal **74** instead of the aldol condensation product. Similarly, treatment of **68** with excess $NaBH_4$/MeOH resulted in the formation of the lactone moiety in **75** (Scheme 4.10). These implied that once the cyclohexane ring was cleaved, the 5-membered lactone formation was almost spontaneous under suitable conditions. On the other hand, we observed a nearly complete consumption of **68** when heated in the presence of DBU in THF, and the product was tentatively assigned as **76** (Scheme 4.10). The further validation and transformation of these intermediates are still ongoing.

Scheme 4.10 Preliminary exploration of final ring reorganization in **68**

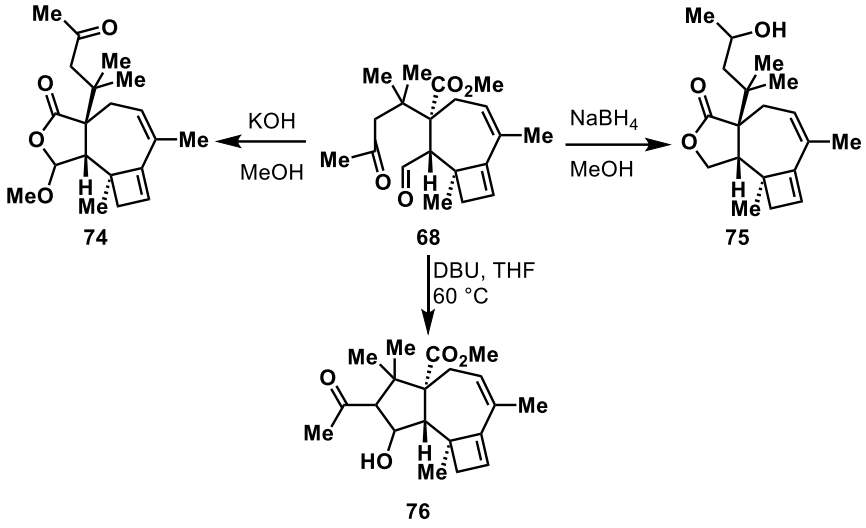

4.6 Preliminary Attempts on Diene Functionalization

We were also looking for effective transformations from the cyclobutene **45** to the functional groups presented in harziane diterpenes. This could be further separated into two types of reaction sequences based on their disparage oxidation states (Scheme 4.11): a) a regioselective 1,2-reduction of cyclobutene, followed by a formal hydration to **78**, which had been demonstrated in Carreira's synthesis[3] through Mukaiyama hydration; b) a formal *anti*-Markovnikov hydration of cyclobutene to **79**, followed by alkene migration and oxidation to generate enone **43**.

Scheme 4.11 Diversified functionalization of cyclobutene **45**

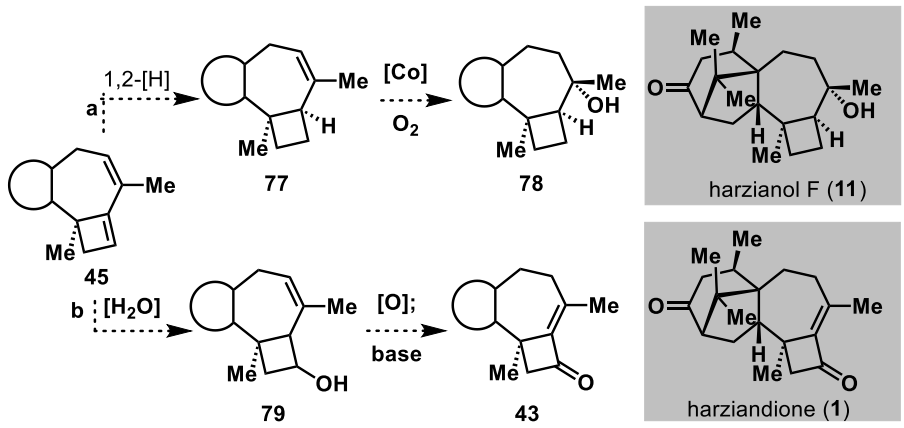

We first attempted the regioselective diene hydrogenation with **60**, considering that the hydrogenation of highly strained cyclobutene (ΔH_{hydro} = -28.5 kcal/mol for 1-methyl cyclobutene[23]) should be more favored than the cycloheptene (ΔH_{hydro} = -25.8 kcal/mol for cycloheptene[24]). However, my coworker, Phil Gemmel has found that Pd/C simply showed no selectivity with EtOAc or EtOH. Switching to other solvent (Table 4.2, entry 1) or other supported heterogeneous catalysts (Table 4.2, entry 2, 4) didn't improve the situation; other types of catalysts, such as Raney Ni[25] (Table 4.2, entry 3) or Co_2B[26] (Table 4.2, entry 5) appeared to be more reactive in the ketone reduction. Pleasingly, Phil was screening some homogeneous catalysts at the same time and $RhCl(PPh_3)_3$ in mixed solvent of toluene/MeOH (Table 4.2, entry 6) gave **82** as a single regio- and diastereoisomer in 86% yield. Unexpectedly, such condition somehow could not be steadily reproduced especially on larger scale (>20 mg) even with increased catalyst loading for unknown reasons. On the other hand, the conventional Birch reduction (Table 4.2, entry 7) gave **83** in 52% yield alone with concomitant ketone reduction. Interestingly, the ester group in **60** remained intact even with Birch reduction, further validating a highly sterically encumbered environment at the bridgehead position.

Table 4.2 Screening of reaction conditions for 1,2-hydrogenation of **60**

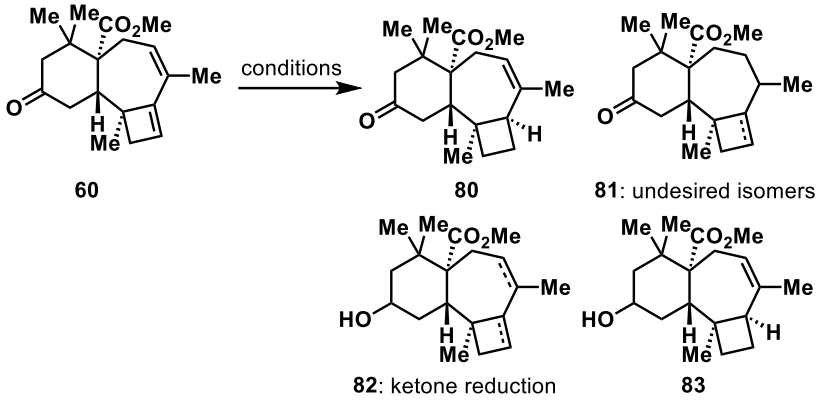

entry	conditions[a]	results
1	Pd/C, H_2, CH_2Cl_2	**80** + **81**
2	Rh/C, H_2, toluene/EtOAc (1:2)	**60** + **80** + **81**
3	Raney Ni, ^{i}PrOH, 23 to 50 °C	**60** + **82**
4	Pd/$BaSO_4$, H_2, EtOAc or EtOH	**60** + **82** + cyclobutene opening
5	$NaBH_4$, $CoCl_2 \cdot 6H_2O$, EtOH	**82**
6	$RhCl(PPh_3)_3$, H_2, toluene/MeOH	**80** (86% yield)[b]
7	Li, NH_3(l), THF/^{t}BuOH, -78 °C	**83** (52% yield)[b]

a. Reaction run at 23 °C unless specified; b. isolated yield

We also explored the *anti*-Markovnikov hydration of cyclobutene in **60**. The first choice would be hydroboration. However, treating **60** with $BH_3 \cdot$THF complex gave a complex mixture, and a $RhCl(PPh_3)_3$ catalyzed hydroboration[27] with HBPin gave no reaction at all. Upon exposure of 1 equivalent *m*CPBA, **60** could offer a single diastereomer which was not stable on silica gel, and the structure was tentatively assigned as epoxide **84**, based on its crude ^{1}H NMR spectrum. The existence of a vinyl epoxide scaffold led us to examine the Tsuji-Trost type reductions with Pd_2dba_3, PBu_3 and formic acid as hydride source[28] (Scheme 4.12, entry 1), but no reaction occurred at ambient temperature; heating to 60 °C only resulted in slow decomposition. Other conditions, including Cp_2Ti(III)-mediated epoxide opening[29] and SmI_2 reduction[30], were unsatisfactory. Given the facile full hydrogenation of diene **60**, we also designed

a one-pot hydrogenation/elimination procedure[31] (Scheme 4.12, entry 4), but a rearrangement product, **86**, was observed instead, implying that the first-step hydrogenation did not occur.

Scheme 4.12 Attempts in formal hydration of **60** and epoxide opening of **84**

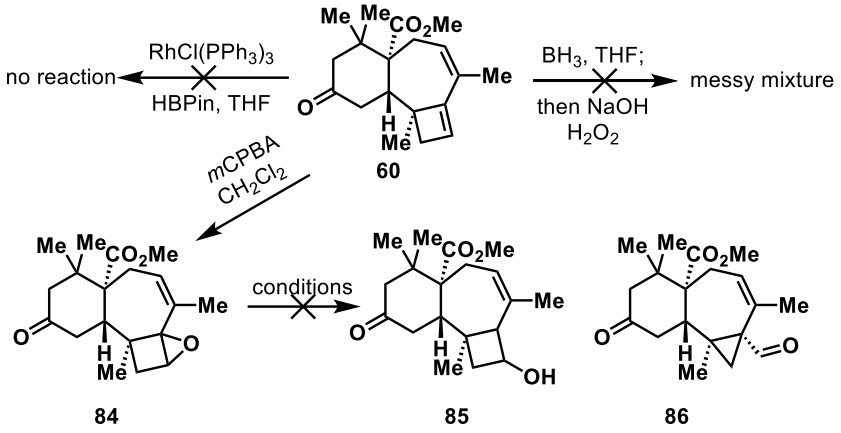

entry	conditions[a]	results
1[b]	Pd_2dba_3, P^nBu_3, HCO_2H/Et_3N, dioxane	no reaction at 23 °C; decomposition at 60 °C
2	Cp_2TiCl_2, Mn, THF/H_2O	messy mixture
3	SmI_2, THF	decomposition
4	Pd/C, H_2, EtOAc; then *p*TsOH	**86**[c]

a. Reaction run at 23 °C unless specified; b. Run by Phil; c. judged from crude ^1H NMR.

4.7 Conclusion and Future Plan

With a fast access to ketoaldehyde **68** in 10 steps (from commercially availale materials) featuring a diastereoselective conjugate addition, a regioselective Rubottom oxidation and a [2+2] cycloaddition reaction, we have secured the key framework of a 7-4 fused common intermediate with all the desired stereochemistry presented that could potentially lead to a concise and collective synthesis of a variety of harziane diterpenes, a puzzle wandering for decades and only one solution in recent time. Our next goal is to engage different condensation reactions to build up the final

bicyclo[3.2.1] skeleton in **89** (Scheme 4.13), either through a Claisen condensation of lactone **87** (or aldol condensation of its lactol) to construct the spirocycle **88**, or through aldol condensation/conjugate reduction to form the five-membered ring **90**. Considering the spatial proximity of these functional groups, the final C-C bond formation should be promising.

Scheme 4.13 Future direction on construction of bicyclic[3.2.1]moiety from **68**

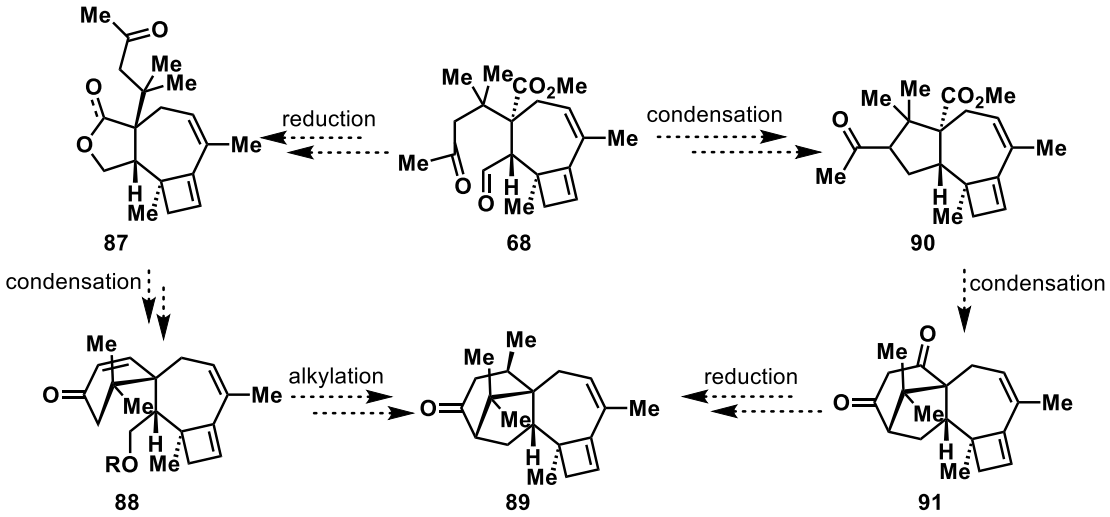

The regioselective diene reduction conditions on model **60** could then be transplanted here at **89** to access harzianol F (**11**) and related natural products. We will also test the feasibility of other reductions such as Birch reduction in the opening of epoxides (such as **84**) to generate the desired cyclobutanol functionality and access harzianone (**2**) and harziandione (**1**). Such strategy would also expand the utility of cyclic conjugated dienes as useful synthons towards the synthesis of other polycyclic natural products.

4.8 Experimental Section

General Procedures. All reactions were carried out under an argon atmosphere with dry solvents under anhydrous conditions, unless otherwise noted. Dry tetrahydrofuran (THF), toluene, acetonitrile, and dichloromethane (CH_2Cl_2) were obtained by passing commercially available pre-dried, oxygen-free formulations through activated alumina columns. Yields refer to chromatographically and spectroscopically (^1H and ^{13}C NMR) homogeneous materials, unless otherwise stated. Reagents were purchased at the highest commercial quality and used without further purification, unless otherwise stated. Reactions were magnetically stirred and monitored by thin-layer chromatography (TLC) carried out on 0.25 mm E. Merck silica gel plates (60F-254) using UV light as visualizing agent, and an ethanolic solution of phosphomolybdic acid and cerium sulfate, and heat as developing agents. Macherey-Nagel® silica gel (60, academic grade, particle size 0.040–0.063 mm) was used for flash column chromatography. The lactam formation reaction was performed using a Biotage microwave tube. Preparative thin-layer chromatography separations were carried out on 0.50 mm E. Merck silica gel plates (60F-254). NMR spectra were recorded on Bruker 500 MHz instruments and calibrated using residual undeuterated solvent as an internal reference. The following abbreviations were used to explain the multiplicities: s = singlet, d = doublet, t = triplet, br = broad, app = apparent. IR spectra were recorded on a Perkin-Elmer 1000 series FT-IR spectrometer. High-resolution mass spectra (HRMS) were recorded on a Waters Synapt G2-Si mass spectrometer using ESI (Electrospray Ionization) at the University of Chicago Mass Spectrometry Laboratory,

and Agilent 6244 Tof-MS using ESI (Electrospray Ionization) at the University of Chicago Mass Spectroscopy Core Facility.

Enyne 51: To a solution of (*S*)-carvone (0.211 mL, 1.35 mmol, 1.1 equiv) in THF (6 mL) was added LiHMDS (1.0 M in THF, 1.35 mL, 1.1 equiv) at –78 °C. The reaction contents were then stirred at –78 °C for 30 min before a solution of freshly made (*Z*)-5-trimethylsilyl-3-methyl-1-bromo-2-penten-4-yne[10] (**54**, 0.284 g, 1.23 mmol, 1.0 equiv) in THF (6 mL) was added dropwise. The reaction mixture was slowly warmed to 23 °C over 8 h while stirring was continued. Upon completion, the reaction contents were quenched by the addition of saturated aqueous NH_4Cl (20 mL) and the contents were transferred to a separatory funnel, diluting with CH_2Cl_2 (20 mL). The layers were separated and the aqueous layer was extracted with CH_2Cl_2 (3 × 20 mL). The combined organic layers were then dried (Na_2SO_4), filtered, and concentrated and the resultant crude product was purified by flash chromatography (silica gel, EtOAc/hexanes, 1:50→1:40) to give alkylated product (0.277 g, 75% yield) as a light yellow oil with R_f = 0.54 (silica gel, EtOAc/hexanes, 1/10). To a solution of such product (0.135 g, 0.45 mmol, 1.0 equiv) in MeOH (5 mL) at 23 °C was added solid K_2CO_3 (0.150 g, 1.09 mmol, 2.4 equiv). The resultant suspension was stirred for 1.5 h. Upon completion, the reaction contents were quenched by the addition of water (5 mL) and saturated aqueous NaCl (5 mL) and the resultant mixture was transferred to a separatory funnel, diluting with EtOAc (20 mL). The layers were separated and the aqueous layer was extracted with EtOAc (3 × 20 mL). The combined organic layers

were then dried (Na_2SO_4), filtered, and concentrated. The resultant crude product was purified by flash chromatography (silica gel, EtOAc/hexanes, 1:70) to give enyne **51** (81.5 mg, 79% yield) as a colorless oil. **51**: R_f = 0.48 (silica gel, EtOAc/hexanes, 1/10); ^{1}H NMR (500 MHz, $CDCl_3$) δ 6.65 (dd, *J* = 3.2, 1.7 Hz, 1 H), 5.83 (t, *J* = 7.0 Hz, 1 H), 4.84–4.83 (m, 1 H), 4.78 (s, 1 H), 3.08 (s, 1 H), 2.68–2.50 (m, 2 H), 2.50–2.46 (m, 1H), 2.44–2.38 (m, 3H), 1.83 (d, *J* = 1.1 Hz, 3 H), 1.77 (d, *J* = 1.4 Hz, 3 H), 1.73 (s, 3 H).

Cyclobutene 55: To a microwave tube containing XPhosAuCl (2.0 mg, 0.003 mmol, 0.04 equiv) was added CH_2Cl_2 (0.8 mL) and $AgNTf_2$·MeCN (1.4 mg, 0.003 mg, 0.04 equiv) at 23 °C. The resultant suspension was stirred for 15 min before a solution of **51** (18.7 mg, 0.082 mmol, 1.0 equiv) in CH_2Cl_2 (0.2 mL) was added at 23 °C. The reaction mixture was then stirred at 23 °C for 12 h and quenched with Et_3N (0.01 mL). The reaction contents were concentrated and the crude material was purified via preparative TLC (EtOAc/hexanes, 1:4) to give **55** (3.2 mg, 17% yield, 22% brsm) as a colorless oil and recovered starting material **51** (4.1 mg). **55**: R_f = 0.49 (silica gel, EtOAc/hexanes, 1/10); ^{1}H NMR (500 MHz, $CDCl_3$) δ 6.75 (d, *J* = 5.3 Hz, 1 H), 5.79 (s, 1 H), 5.57 (s, 1 H), 2.96 (ddd, *J* = 16.0, 7.2, 4.2 Hz, 1 H), 2.40 (ddd, *J* = 12.5, 8.7, 3.9 Hz, 1 H), 2.29–2.25 (m, 2 H), 2.22–2.11 (m, 4 H), 1.76–1.75 (m, 6 H), 1.20 (s, 3 H).

Acetate 57: To a solution of freshly distilled diisopropyl amine (0.168 mL, 1.15 mmol, 1.15 equiv) in THF (4 mL) was added *n*-BuLi (1.6 M in hexane, 0.72 mL, 1.2

mmol, 1.2 equiv) dropwise at -78 °C. The solution was warmed to 0 °C and stirred for 30 min before it was cooled down to -78 °C. To such solution was added ester **56** (0.185 g, 1.10 mmol, 1.1 equiv) in THF (2 mL) at –78 °C. The reaction contents were then stirred at –78 °C for 1 h before a solution of freshly made (*Z*)-5-trimethylsilyl-3-methyl-1-bromo-2-penten-4-yne[10] (**54**, 0.231 g, 1.0 mmol, 1.0 equiv) in THF (4 mL) was added dropwise. The reaction mixture was slowly warmed to 23 °C over 6 h while stirring was continued. Upon completion, TBAF (1.0 M in THF, 1.5 mL, 1.5 mmol, 1.5 equiv) was added at 23 °C and the reaction mixture was further stirred for 1 h. Then the reaction contents were quenched by the addition of saturated aqueous $NaHCO_3$ (10 mL) and the contents were transferred to a separatory funnel, diluting with CH_2Cl_2 (15 mL). The layers were separated and the aqueous layer was extracted with CH_2Cl_2 (3 × 15 mL). The combined organic layers were then dried (Na_2SO_4), filtered, and concentrated and the resultant crude product was purified by flash chromatography (silica gel, EtOAc/hexanes, 1:60) to give a mixture of alkylated product **52** and starting material **56** (0.184 g, 3:2 ratio as judged by ^1H NMR, 51% yield counting pure product **52**) as a light yellow oil. To a solution of such mixture (0.166 g) in CH_2Cl_2 (6 mL) was added DIBAL-H (1.0 M in CH_2Cl_2, 2.20 mL, 2.20 mmol, 2.6 equiv per ester group) at -78 °C. The reaction mixture was slowly warmed to 23 °C over 3 h while stirring was continued. Upon completion, the reaction contents were quenched by the addition of 1 M Rochelle's salt (5 mL) and the resultant mixture was transferred to a separatory funnel, diluting with CH_2Cl_2 (15 mL). The layers were separated and the aqueous layer was extracted with CH_2Cl_2 (3 × 15 mL). The combined organic layers were then dried

(Na_2SO_4), filtered, and concentrated. The resultant crude product was purified by flash chromatography (silica gel, EtOAc/hexanes, 1:40→1:25) to give an alcohol (0.109 g, 98% yield) as a colorless oil with R_f = 0.38 (silica gel, EtOAc/hexanes, 1/4). To a solution of such alcohol (0.109 g, 0.50 mmol, 1.0 equiv) in CH_2Cl_2 (5 mL) was added Et_3N (0.10 mL, 0.75 mmol, 1.5 equiv), 4-DMAP (6.0 mg, 0.05 mmol, 0.1 equiv) and Ac_2O (0.06 mL, 0.60 mmol, 1.2 equiv) at 23 °C. The reaction mixture was stirred at 23 °C for 1 h. Upon completion, the reaction contents were quenched by the addition of saturated $NaHCO_3$ (5 mL) and the resultant mixture was transferred to a separatory funnel, diluting with CH_2Cl_2 (15 mL). The layers were separated and the aqueous layer was extracted with CH_2Cl_2 (3 × 15 mL). The combined organic layers were then dried (Na_2SO_4), filtered, and concentrated. The resultant crude product was purified by flash chromatography (silica gel, EtOAc/hexanes, 1:40) to give acetate **57** (0.107 g, 82% yield) as a colorless oil. **57**: R_f = 0.47 (silica gel, EtOAc/hexanes, 1/10); ^{1}H NMR (500 MHz, $CDCl_3$) δ 5.79 (t, *J* = 7.3 Hz, 1 H), 4.83 (t, *J* = 1.5 Hz, 1 H), 4.74 (d, *J* = 0.8 Hz, 1H), 3.87 (d, *J* = 11.1 Hz, 1 H), 3.79 (d, *J* = 11.1 Hz, 1 H), 3.09 (s, 1 H), 2.58 (dd, *J* = 14.4, 7.4 Hz, 1 H), 2.39 (dd, *J* = 14.4, 7.9 Hz, 1 H), 2.33 (dd, *J* = 9.2, 7.2 Hz, 1 H), 2.02 (s, 3 H), 1.89 (d, *J* = 1.1 Hz, 3 H), 1.83–1.80 (m, 1 H), 1.79 (s, 3 H), 1.76–1.63 (m, 3 H), 1.57–1.51 (m, 2 H).

Cyclobutene 58 and triene 59: To a microwave tube containing ^{t}BuXPhosAuCl (1.7 mg, 0.003 mmol, 0.05 equiv) was added DCE (0.8 mL) and $AgNTf_2$·MeCN (1.3 mg, 0.003 mg, 0.05 equiv) at 23 °C. The resultant suspension was

stirred for 15 min before a solution of **57** (16.0 mg, 0.082 mmol, 1.0 equiv) in DCE (0.2 mL) was added at 23 °C. The reaction mixture was then stirred at 50 °C for 2 h and quenched with Et_3N (0.01 mL). The resultant crude product was purified by flash chromatography (silica gel, EtOAc/hexanes, 1:60) to give the product (7.0 mg, 44% yield, mixture of **58** and **59**) as a colorless oil. **58** and **59**: R_f = 0.49 (silica gel, EtOAc/hexanes, 1/10); ^{1}H NMR (500 MHz, $CDCl_3$, only showing the region above 3.0) δ 6.55 (dd, *J* = 17.5, 11.0 Hz, 0.4 H, **59**), 5.88–5.85 (m, 0.4 H, **59**), 5.80 (s, 1 H, **58**), 5.35 (d, *J* = 7.0 Hz, 2 H, **58**), 5.15 (dd, *J* = 10.9, 1.4 Hz, 0.4 H, **59**), 4.96 (dd, *J* = 17.6, 1.4 Hz, 0.4 H, **59**), 4.18 (d, *J* = 10.5 Hz, 1 H, **58**), 3.88 (d, *J* = 9.6 Hz, 1.4 H, **58** and **59**), 3.70 (d, *J* = 10.5 Hz, 0.4 H, **59**).

Ester 63: To a flask containing Na (2.3 g, 100 mmol, 1.0 equiv) was added anhydrous MeOH (30 mL) at 0 °C. The suspension was stirred at 23 °C until all the sodium chuck had dissolved. To such solution was added mesityl oxide (**65**, 10.0 g, 100 mmol, 1.0 equiv) and methyl malonate (**66**, 13.2 g, 100 mmol, 1.0 equiv) successively at 23 °C and the reaction mixture was heated to 60 °C and stirred at such temperature for 8 h. The reaction contents were then cooled back to 23 °C and TMSCl (13.3 mL, 105 mmol, 1.05 equiv) and toluene (30 mL) was added. The white precipitates from cooling down was rapidly dissolved upon addition of TMSCl. The reaction mixture was then heated to 60 °C and stirred at such temperature for 4 h. Upon completion, the reaction contents were quenched by the addition of saturated $NaHCO_3$ (100 mL) and the resultant mixture was transferred to a separatory funnel, diluting with CH_2Cl_2 (200

mL). The layers were separated and the aqueous layer was extracted with CH_2Cl_2 (3 × 100 mL). The combined organic layers were then dried (Na_2SO_4), filtered, and concentrated. The resultant crude product was purified by flash chromatography (silica gel, EtOAc/hexanes, 1:20→1:10→1:6) to give alcohol **63** (10.7 g, 50% yield) as a colorless oil. **63**: R_f = 0.17 (silica gel, EtOAc/hexanes, 1/4); all spectroscopic data matched that reported in Ref. 32.

Enyne 64: To a solution of ketoester **63** (1.30 g, 6.13 mmol, 1.03 equiv) in THF (30 mL) was added NaH (60% dispersion in mineral oil, 260 mg, 6.5 mmol, 1.09 equiv) at 0 °C. The reaction contents were then stirred at 0 °C for 30 min before a solution of freshly made (*Z*)-5-trimethylsilyl-3-methyl-1-bromo-2-penten-4-yne[10] (**54**, 1.37 g, 5.94 mmol, 1.0 equiv) in THF (30 mL) was added dropwise. The reaction mixture was slowly warmed to 23 °C over 8 h while stirring was continued. Upon completion, the most of solvent was removed under reduced pressure and MeOH (50 mL) was added into the flask, followed by K_2CO_3 (2.46 g, 17.8mmol, 3.0 equiv). The reaction mixture was stirred at 23 °C for additional 1 h. Upon completion, the reaction contents were quenched by the addition of water (15 mL) and saturated aqueous NaCl (15 mL) and the contents were transferred to a separatory funnel, diluting with CH_2Cl_2 (100 mL). The layers were separated and the aqueous layer was extracted with CH_2Cl_2 (3 × 50 mL). The combined organic layers were then dried (Na_2SO_4), filtered, and concentrated and the resultant crude product was purified by flash chromatography (silica gel, EtOAc/hexanes, 1:50→1:40) to give alkylated enyne **64** (1.20 g, 70% yield)

as a light yellow solid. **64**: R_f = 0.22 (silica gel, EtOAc/hexanes, 1/4); ^{1}H NMR (500 MHz, $CDCl_3$) δ 5.85 (t, *J* = 7.2 Hz, 1 H), 5.38 (s, 1 H), 3.70 (s, 3 H), 3.69 (s, 3 H), 3.08 (s, 1 H), 2.93 (dd, *J* = 15.4, 7.3 Hz, 2 H), 2.83 (dd, *J* = 14.6, 7.1 Hz, 2 H), 2.46 (d, *J* = 17.4 Hz, 1 H), 2.35 (d, *J* = 16.8 Hz, 1 H), 1.82 (s, 3 H), 1.21 (s, 3 H), 1.08 (s, 3 H).

Enone 62: To a solution of **64** (1.09 g, 3.76 mmol, 1.0 equiv) in THF (18 mL) was added DIBAL-H (1.0 M in CH_2Cl_2, 11.3 mL, 11.3 mmol, 3.0 equiv) at -78 °C. The reaction mixture was stirred at -78 °C for 30 min and warmed to 23 °C over 15 min. The reaction mixture was then cooled down to -78 °C and carefully quenched with dropwise addition of MsOH (0.73 mL, 11.3 mmol, 3.0 equiv). The reaction mixture was then warmed to 23 °C and concentrated HCl (ca. 11 M, 2 mL) was added. The reaction contents were stirred at 23 °C for additional 30 min before it was poured into a separatory funnel, diluting with CH_2Cl_2 (100 mL) and water (50 mL). The layers were separated and the aqueous layer was extracted with CH_2Cl_2 (3 × 50 mL). The combined organic layers were then dried (Na_2SO_4), filtered, and concentrated and the resultant crude product was purified by flash chromatography (silica gel, EtOAc/hexanes, 1:40→1:25→1:20) to give enone **62** (0.562 g, 57% yield) as a light yellow solid. **62**: R_f = 0.41 (silica gel, EtOAc/hexanes, 1/4); ^{1}H NMR (500 MHz, $CDCl_3$) δ 6.91 (d, *J* = 10.4 Hz, 1 H), 6.06 (d, *J* = 10.4 Hz, 1 H), 5.64–5.62 (m, 1 H), 3.76 (s, 3 H), 3.10 (s, 1 H), 2.95 (dd, *J* = 13.7, 4.8 Hz, 1 H), 2.80 (dd, *J* = 13.7, 9.4 Hz, 1 H), 2.54 (d, *J* = 16.6 Hz, 1 H), 2.24 (d, *J* = 16.6 Hz, 1 H), 1.86 (s, 3 H), 1.20 (s, 3 H), 0.96 (s, 3 H).

Ketone 61: A flask of CuBr·DMS (0.210 g, 1.02 mmol, 1.2 equiv) was evacuated and refilled with argon for three times. To such flask was added THF (2 mL) and the suspension was cooled down to -78 °C before a solution of isopropenyl magnesium bromide (0.5 M in THF, 4.25 mL, 2.12 mmol, 2.5 equiv) was added slowly. The thus obtained orange solution was stirred at -78 °C for 30 min before a solution of substrate **62** (0.220 g, 0.85 mmol, 1.0 equiv) in THF (4 mL) was added at -78 °C. The reaction mixture was then transferred into a -40 °C cold bath and stirred at such temperature for 1 h. Upon completion, the reaction contents were quenched by the addition of saturated NH_4Cl (15 mL) and the contents were transferred to a separatory funnel, diluting with CH_2Cl_2 (20 mL). The layers were separated and the aqueous layer was extracted with CH_2Cl_2 (3 × 20 mL). The combined organic layers were then dried (Na_2SO_4), filtered, and concentrate. The resultant crude product was purified by flash chromatography (silica gel, EtOAc/hexanes, 1:25→1:20) to give ketone **61** (0.149 g, 58% yield) as a light yellow solid. **61**: R_f = 0.46 (silica gel, EtOAc/hexanes, 1/4); ^{1}H NMR (500 MHz, $CDCl_3$) δ 6.09 (dd, *J* = 7.7, 5.7 Hz, 1 H), 4.86 (s, 1 H), 4.80 (s, 1 H), 3.77 (s, 3 H), 3.20 (dd, *J* = 14.1, 6.0 Hz, 2 H), 3.14 (s, 1 H), 2.79–2.71 (m, 2 H), 2.56 (dd, *J* = 15.8, 9.2 Hz, 1 H), 2.15 (ddd, *J* = 14.3, 4.4, 2.1 Hz, 1 H), 1.89 (dd, *J* = 14.2, 2.0 Hz, 1 H), 1.85 (s, 3 H), 1.62 (s, 3 H), 1.05 (s, 3 H), 0.96 (s, 3 H).

Cyclobutene 60: To a test tube containing ^{t}BuXPhosAuCl (17.3 mg, 0.026 mmol, 0.04 equiv) and $AgNTf_2$·MeCN (11.3 mg, 0.026 mg, 0.04 equiv) was added CH_2Cl_2 (2 mL) at 23 °C. The resultant suspension was stirred for 15 min and then

transferred into a solution of ketone **61** (0.200 g, 0.66 mmol, 1.0 equiv) in CH_2Cl_2 (8 mL). The reaction mixture was then stirred at 23 °C for 1 h before it was quenched by the addition of Et_3N (5 drops, ca. 0.05 mL). The solvent was removed under reduced pressure and the resultant crude product was purified by flash chromatography (silica gel, EtOAc/hexanes, 1:25→1:20) to give alcohol **60** (0.170 g, 85% yield) as a colorless oil. **60**: R_f = 0.47 (silica gel, EtOAc/hexanes, 1/4); ^{1}H NMR (500 MHz, $CDCl_3$) δ 5.78 (s, 1 H), 5.71–5.69 (m, 1H), 3.70 (s, 3 H), 3.22 (t, *J* = 13.9 Hz, 1 H), 3.01 (d, *J* = 13.7 Hz, 1 H), 2.49 (dd, *J* = 14.2, 8.9 Hz, 1 H), 2.29 (dd, *J* = 13.8, 4.2 Hz, 1 H), 2.19 (d, *J* = 13.6 Hz, 1 H), 2.16–2.14 (m, 1 H), 2.07 (d, *J* = 13.4 Hz, 1 H), 1.93–1.88 (m, 2 H), 1.77 (s, 3 H), 0.98 (s, 3 H), 0.96 (s, 3 H), 0.90 (s, 3 H).

Rearranged product 65: A flask containing **60** (24.0 mg, 0.079 mmol, 1.0 equiv) and PIDA (30.6 mg, 0.095 mmol, 1.2 equiv) was degassed with argon (three times) and to this flash was added a solution of KOH (0.133 g, 2.37 mmol, 30.0 equiv) in MeOH (3 mL) at 23 °C. The resultant suspension was stirred for 1 h. Upon completion, the reaction contents were quenched by the addition of saturated NH_4Cl (15 mL) and the contents were transferred to a separatory funnel, diluting with CH_2Cl_2 (20 mL). The layers were separated and the aqueous layer was extracted with CH_2Cl_2 (3 × 20 mL). The combined organic layers were then dried (Na_2SO_4), filtered, and concentrate. The resultant crude product was purified by flash chromatography (silica gel, EtOAc/hexanes, 1:20→1:15) to give **65** (17.0 mg, 64% yield) as a colorless oil. **xx**: R_f = 0.64 (silica gel, EtOAc/hexanes, 1/4); ^{1}H NMR (500 MHz, $CDCl_3$) δ 5.73 (s, 1 H),

5.63 (d, *J* = 8.2 Hz, 1H), 3.67 (s, 3 H), 3.61 (s, 3 H), 2.77 (d, *J* = 11.4 Hz, 1 H), 2.34 (dd, *J* = 14.4, 8.6 Hz, 1 H), 2.17 (t, *J* = 12.5 Hz, 1 H), 2.09 (d, *J* = 13.4 Hz, 1 H), 1.97 (d, *J* = 13.4 Hz, 1 H), 1.91 (d, *J* = 14.3 Hz, 1 H), 1.74 (t, *J* = 1.8 Hz, 3 H), 1.71 (dd, *J* = 13.4, 4.7 Hz, 1 H), 1.43 (d, *J* = 15.4 Hz, 1 H), 1.37 (dd, *J* = 15.7, 7.2 Hz, 1 H), 1.09 (s, 3 H), 1.06 (s, 3 H), 0.82 (s, 3 H).

Benzoate 66: To a solution of **60** (22.6 mg, 0.075 mmol, 1.0 equiv) in THF (1 mL) was added LiHMDS (1.3 M in THF, 0.086 mL, 0.112 mmol, 1.5 equiv) at -78 °C. The reaction mixture was warmed to 23 °C and stirred at such temperature of 1 h before cooling down to -78 °C. To the solution was added a solution of benzoyl peroxide [$(BzO)_2$, 27.0 mg, 0.112 mmol, 1.5 equiv] in THF (0.2 mL) at -78 °C. The reaction mixture was then slowly warmed to 23 °C over 1 h. Upon completion, the reaction contents were quenched by the addition of saturated $NaHCO_3$ (15 mL) and the contents were transferred to a separatory funnel, diluting with CH_2Cl_2 (20 mL). The layers were separated and the aqueous layer was extracted with CH_2Cl_2 (3 × 20 mL). The combined organic layers were then dried (Na_2SO_4), filtered, and concentrate. The resultant crude product was purified by flash chromatography (silica gel, EtOAc/hexanes, 1:20→1:15) to give recovered **60** (14.1mg, 62% recovered) and alcohol **66** (11.4 mg, 36% yield) as a colorless oil. **66**: R_f = 0.22 (silica gel, EtOAc/hexanes, 1/4); ^{1}H NMR (500 MHz, $CDCl_3$) δ 8.12 (d, *J* = 7.2 Hz, 2 H), 7.58 (t, *J* = 7.5 Hz, 1 H), 7.47 (t, *J* = 7.7 Hz, 2 H), 6.55 (d, *J* = 12.5 Hz, 1 H), 5.81 (s, 1 H), 5.71 (d, *J* = 6.1 Hz, 1 H), 3.77 (s, 3 H), 3.13 (d, *J* = 13.3 Hz, 1 H), 2.75 (dd, *J* = 23.1, 13.0 Hz, 1 H), 2.50 (dd, *J* = 14.3, 8.6 Hz, 1 H),

2.10 (dd, *J* = 13.6, 2.3 Hz, 1 H), 2.00 (d, *J* = 12.1 Hz, 1 H), 1.77 (s, 3 H), 1.07 (s, 3 H), 1.03 (s, 3 H), 0.97 (s, 3 H).

TMS enol ether 69: A flask of CuBr·DMS (0.154 g, 0.75 mmol, 1.1 equiv) was evacuated and refilled with argon for three times. To such flask was added THF (1 mL) and the suspension was cooled down to -78 °C before a solution of isopropenyl magnesium bromide (0.5 M in THF, 3.12 mL, 1.56 mmol, 2.3 equiv) was added slowly. The thus obtained orange solution was stirred at -78 °C for 30 min before TMSCl (0.104 mL, 0.82 mmol, 1.2 equiv) and a solution of substrate **62** (0.177 g, 0.68 mmol, 1.0 equiv) in THF (2 mL) was added at -78 °C. The reaction mixture was then transferred into a -40 °C cold bath and stirred at such temperature for 1 h, before it was further warmed to 23 °C and stirred for additional 1 h. Upon completion, the reaction contents were quenched by the addition of ammonium hydroxide (15 mL) and the contents were transferred to a separatory funnel, diluting with hexane (20 mL). The layers were separated and the aqueous layer was extracted with hexane (3 × 20 mL). The combined organic layers were then dried (Na_2SO_4), filtered through a short pad of silica and washed with hexane (10 mL), and concentrated to give TMS enol ether **69** (0.190 g, 75% yield) as a light yellow solid. **69**: R_f = 0.69 (silica gel, EtOAc/hexanes, 1/4); ^{1}H NMR (500 MHz, $CDCl_3$) δ 6.01 (dd, *J* = 8.6, 3.8 Hz, 1 H), 4.90 (s, 1 H), 4.84 (s, 1 H), 4.57 (s, 1 H), 3.63 (s, 3 H), 3.13 (s, 1 H), 3.05 (s, 1 H), 2.94 (d, *J* = 15.6 Hz, 1 H), 2.70–2.62 (m, 2 H), 1.83 (s, 3 H), 1.78 (d, *J* = 13.4 Hz, 1 H), 1.56 (s, 3 H), 1.10 (s, 3 H), 0.91 (s, 3 H), 0.21 (s, 9 H).

Diol 71: To a solution of **69** (98.1 mg, 0.26 mmol, 1.0 equiv) in CH_2Cl_2 (3 mL) was added *m*-CPBA (<77%, 72.0 mg, 0.32 mmol, 1.2 equiv) at 0 °C. The reaction mixture was stirred at 0 °C for 1 h before Et_3N (0.09 mL, 0.655 mmol, 2.5 equiv) and TBAF (1.0 M in THF, 0.27 mL, 0.27 mmol, 1.03 equiv) was added at 23 °C successively. The reaction mixture was then stirred at 23 °C for 8 h. Upon completion, the reaction contents were quenched by the addition of saturated $NaHCO_3$ (10 mL) and the resultant mixture was transferred to a separatory funnel, diluting with CH_2Cl_2 (20 mL). The layers were separated and the aqueous layer was extracted with CH_2Cl_2 (3 × 10 mL). The combined organic layers were then dried (Na_2SO_4), filtered, and concentrated. The resultant crude product **70** was obtained as a yellow oil and used directly without further purification. **70**: R_f = 0.17 (silica gel, EtOAc/hexanes, 1/4). Pressing forward, to a flask containing anhydrous $CeCl_3$ (64.6 mg, 0.262 mmol, 1.0 equiv) was added THF (1 mL) and methylmagnesium bromide (3.0 M in ether, 0.26 mL, 0.79 mmol, 3.0 equiv) at 0 °C. The white suspension was stirred at 0 °C for 10 min before a solution of crude **70** in THF (2 mL) was added. The reaction mixture was warmed to 23 °C and stirred for 10 min before a second portion of methylmagnesium bromide (3.0 M in ether, 0.09 mL, 0.26 mmol, 1.0 equiv) was added and the reaction was further stirred for 10 min. Upon completion, the reaction contents were quenched by the addition of saturated Rochelle's salt (5 mL) and saturated NH_4Cl (5 mL) and the mixture was further stirred for 1h. It was then was transferred to a separatory funnel, diluting with CH_2Cl_2 (20 mL). The layers were separated and the aqueous layer was

extracted with CH_2Cl_2 (3 × 10 mL). The combined organic layers were then dried (Na_2SO_4), filtered, and concentrated. The resultant crude product was purified by flash chromatography (silica gel, EtOAc/hexanes, 1:15→1:10→1:6) to give alcohol **71** (44.0 mg, 50% yield) as a colorless oil. **71**: R_f = 0.10 (silica gel, EtOAc/hexanes, 1/4); ^{1}H NMR (500 MHz, $CDCl_3$, overlap with trace EtOAc) δ 6.11 (dd, *J* = 6.7, 6.3 Hz, 1 H), 5.05 (s, 1 H), 4.93 (s, 1 H), 4.12 (d, *J* = 11.7 Hz, 1 H), 3.69 (s, 3 H), 3.14 (s, 1 H), 2.61–2.54 (m, 3 H), 2.29 (br, s, 1 H), 2.07 (d, *J* = 15.3 Hz, 1 H), 1.83 (s, 3 H), 1.56 (s, 3 H), 1.44 (d, *J* = 15.0 Hz, 1 H), 1.29 (s, 3 H), 1.23 (s, 3 H), 0.79 (s, 3 H).

Cyclobutene 67: To a solution of diol **71** (22.0 mg, 0.066 mmol, 1.0 equiv) in CH_2Cl_2 (0.5 mL) was added trimethyl boroxine (2.8 mg, 0.022 mmol, 0.34 equiv) at 23 °C. The solution was stirred for 5 min and TLC analysis indicated full conversion of **71** into **72**. At the same time, to a test tube containing ^{t}BuXPhosAuCl (1.7 mg, 0.0026 mmol, 0.04 equiv) and $AgNTf_2$·MeCN (1.1 mg, 0.0026 mg, 0.04 equiv) was added CH_2Cl_2 (0.5 mL) at 23 °C. The resultant suspension was stirred for 15 min and then transferred into the solution of **72**. The reaction mixture was then stirred at 23 °C for 30 min before it was quenched by the addition of Et_3N (1 drop, ca. 0.01 mL). The solvent was removed under reduced pressure and the residual **73** was re-dissolved in MeOH (2 mL) and a solution of aqueous KF (1.0 M, 1 mL, 1 mmol, 15.2 equiv) was added. The homogenous mixture was stirred at 23 °C for 1 h and quenched by the addition of CH_2Cl_2 (10 mL) and saturated aqueous $NaHCO_3$ (10 mL). The reaction contents were transferred to a separatory funnel, the layers were separated and the

aqueous layer was extracted with CH_2Cl_2 (3 × 10 mL). The combined organic layers were then dried (Na_2SO_4), filtered, and concentrated. The resultant crude product was purified by flash chromatography (silica gel, EtOAc/hexanes, 1:15→1:10→1:6) to give alcohol **67** (19.1 mg, 87% yield) as a colorless oil. **67**: R_f = 0.11 (silica gel, EtOAc/hexanes, 1/4); ^{1}H NMR (500 MHz, $CDCl_3$, identical to the product obtained from **66**) δ 5.78 (s, 1 H), 5.65 (d, *J* = 6.6 Hz, 1 H), 4.54 (dd, *J* = 11.1, 7.4 Hz, 1 H), 3.61 (s, 3 H), 2.63 (d, *J* = 13.7 Hz, 1 H), 2.33 (dd, *J* = 14.6, 9.6 Hz, 1 H), 2.24 (d, *J* = 13.7 Hz, 1 H), 1.95 (dd, *J* = 13.9, 1.4 Hz, 1 H), 1.89–1.85 (m, 2 H)., 1.75 (s, 3 H), 1.67 (d, *J* = 7.3 Hz, 1 H), 1.56 (s, 3 H), 1.44 (d, *J* = 14.8 Hz, 1 H), 1.27 (s, 3 H), 1.16 (s, 3 H), 1.09 (s, 3 H).

Ketoaldehyde 68: To a solution of **67** (19.1 mg, 0.058 mmol, 1.0 equiv) in CH_2Cl_2 (1 mL) was added PIDA (22.4 mg, 0.070 mmol, 1.2 equiv) at 23 °C. The reaction mixture was stirred at 23 °C for 1 h and ethylene glycol (1 drop, ca. 0.01 mL) was added to quench excessive PIDA. The reaction mixture was further stirred for 15 min and the solvent and other volatiles were removed under reduced pressure. The resultant crude product was purified by flash chromatography (silica gel, EtOAc/hexanes, 1:20→1:15) to give ketoaldehyde **68** (9.6 mg, 51% yield) as a colorless oil. **68**: R_f = 0.34 (silica gel, EtOAc/hexanes, 1/4); ^{1}H NMR (500 MHz, $CDCl_3$) δ 9.74 (d, *J* = 3.8 Hz, 1 H), 5.79 (s, 1 H), 5.41–5.39 (m, 1 H), 3.70 (s, 3 H), 3.20 (d, *J* = 16.5 Hz, 1 H), 2.85 (d, *J* = 3.7 Hz, 1 H), 2.60 (s, 2 H), 2.45–2.39 (m, 2 H), 2.26 (d, *J* = 14.3 Hz, 1 H), 2.13 (s, 3 H), 1.69 (s, 3 H), 1.55 (s, 3 H), 1.15 (s, 3 H), 1.13 (s, 3 H).

Ketone 80: To a flask of **60** (4.6 mg, 0.015 mmol, 1.0 equiv) was added toluene (0.2 mL) and $RhCl(PPh_3)_3$ (0.7 mg, 0.00075 mmol, 0.05 equiv) at 23 °C under hydrogen atmosphere. The reaction mixture was stirred at 23 °C for 30 min before MeOH (0.2 mL) was added. The reaction was further stirred 23 °C for 8 h under hydrogen atmosphere. Upon completion, the reaction mixture was concentrated and the residue was purified by flash chromatography (silica gel, EtOAc/hexanes, 1:25→1:20) to give ketone **80** (4.0 mg, 86% yield). **80**: R_f = 0.47 (silica gel, EtOAc/hexanes, 1/4); ^{1}H NMR (500 MHz, $CDCl_3$) δ 5.55 (s, 1 H), 3.67 (s, 3 H), 3.16 (t, *J* = 14.1 Hz, 1 H), 2.96 (t, *J* = 9.5 Hz, 1 H), 2.88 (d, *J* = 14.2 Hz, 1 H), 2.47 (dd, *J* = 13.9, 8.2 Hz, 1 H), 2.23 (dd, *J* = 14.4, 4.2 Hz, 1 H), 2.03–1.98 (m, 3 H), 1.91 (dd, *J* = 14.2, 1.8 Hz, 1 H), 1.81 (dd, *J* = 17.9, 8.1 Hz, 1 H), 1.65 (s, 3 H), 1.61 (d, *J* = 8.2 Hz, 1 H), 1.54 (d, *J* = 8.1 Hz, 1 H), 1.00 (s, 3 H), 0.88 (s, 3 H), 0.75 (s, 3 H).

Alcohol 83: To a two-neck flask containing liquid NH_3 (ca. 5 mL) was added lithium metal (64.5 mg, 9.29 mmol, 52 equiv) at -78 °C. The resultant suspension was stirred at -78 °C until it turned deep blue and most lithium had dissolved. To such solution was added a solution of sub **60** (54.4 mg, 0.18 mmol, 1.0 equiv) in THF (2 mL) and ^{t}BuOH (0.2 mL) at -78 °C. The reaction mixture was then stirred at -78 °C for 1 h and the cold bath was removed. The reaction mixture was then quenched by the addition of saturated NH_4Cl (15 mL) and the contents were transferred to a separatory funnel, diluting with CH_2Cl_2 (20 mL). The layers were separated and the aqueous layer was

extracted with CH_2Cl_2 (3 × 20 mL). The combined organic layers were then dried (Na_2SO_4), filtered, and concentrate. The resultant crude product was purified by flash chromatography (silica gel, EtOAc/hexanes, 1:20→1:10) to give saturated alcohol **83** (28.6 mg, 52% yield) as a light yellow solid. **83**: R_f = 0.10 (silica gel, EtOAc/hexanes, 1/4); ^{1}H NMR (500 MHz, $CDCl_3$, overlap with trace EtOAc) δ 5.32 (t, *J* = 6.6 Hz, 1 H), 3.79–3.73 (m, 1 H), 3.64 (s, 3 H), 2.57 (d, *J* = 9.5 Hz, 1 H), 2.37 (dd, *J* = 14.9, 6.9 Hz, 1 H), 2.13–2.09 (m, 2 H), 2.01 (t, *J* = 11.1 Hz, 1 H), 1.92 (dd, *J* = 13.5, 2.8 Hz, 1 H), 1.88–1.83 (m, 2 H), 1.77 (d, *J* = 1.4 Hz, 3 H), 1.56–1.54 (m, 2 H), 1.45 (dd, *J* = 12.7, 3.4 Hz, 1 H), 1.14 (d, *J* = 13.6 Hz, 1 H), 1.01 (s, 3 H), 0.97 (s, 3 H), 0.76 (s, 3 H).

4.9 References

[1] (a) Ghisalberti, E. L.; Hockless, D. C. R.; Rowland, C.; White, A. H. *J. Nat. Prod.* **1992**, *55*, 1690; (b) Mannina, L.; Segre, A. L. *Tetrahedron* **1997**, *53*, 3135; (c) Miao, F.-P.; Liang, X.-R.; Yin, X.-L.; Wang, G.; Ji, N.-Y. *Org. Lett.* **2012,** *14*, 3815; (d) Xie, Z.-L.; Li, H.-J.; Wang, L.-Y.; Liang, W.-L.; Liu, W.; Lan, W.-J. *Nat. Prod. Commun.* **2013**, *8*, 67; (e) Adelin, E.; Servy, C.; Martin, M. T.; Arcile, G.; Iorga, B. I.; Retailleau, P.; Bonfill, M.; Ouazzani, J. *Phytochemistry* **2014**, *97*, 55; (f) Zhang, M.; Liu, J.-M.; Zhao, J.-L.; Li, N.; Chen, R.-D.; Xie, K.-B.; Zhang, W.-J.; Feng, K.-P.; Yan, Z.; Wang, N.; Dai, J.-G. *Chin. Chem. Lett.* **2016**, *27*, 957; (g) Zhang, M.; Liu, J.; Chen, R.; Zhao, J.; Xie, K.; Chen, D.; Feng, K.; Dai, J. *Org. Lett.* **2017,** *19*, 1168; (h) Zhang, M.; Liu, J.; Chen, R.; Zhao, J.; Xie, K.; Chen, D.; Feng, K.; Dai, J. *Tetrahedron*, **2017**, *73*, 7195; (i) Song, Y.-P.; Fang, S.-T.; Miao, F.-P.; Yin, X.-L.; Ji. N.-Y. *J. Nat. Prod.* **2018,** *81*, 2553; (j) Song, Y.-P.; Miao, F.-P.; Liang, X.-R.; Yin, X.-L.; Ji. N.-Y. *Phytochem. Lett*. **2019**, *32*, 38; (k) Zhao, D.-L.; Yang, L.-J.; Shi, T.; Wang, C.-Y.; Shao, C.-L.; Wang, C.-Y. *Sci, Rep.* **2019**, *9*, 13345. doi: 10.1038/s41598-019-49778-7; (l) Chen, S.; Li, H.; Chen, Y.; Li, S.; Xu, J.; Guo, H.; Liu, Z.; Zhu, S.; Liu, H.; Zhang, W. *Bioorg. Chem*. **2019**, *86*, 368; (m) Zou, J.-X.; Song, Y.-P.; Ji, N.-Y. *Nat. Prod. Res.* **2019**, doi: 10.1080/14786419.2019.1622110; (n) Li, W.-Y.; Liu, Y.; Lin, Y.-T.; Liu, Y.-C.; Guo, K.; Li, X.-N.; Luo, S.-H.; Li, S.-H. *Phytochemistry* **2020**, *170*, 112198. doi: 10.1016/j.phytochem.2019.112198.

[2] Barra, L.; Dickschat, J. S. *ChemBioChem*, **2017**, *18*, 2358.

[3] Hönig, M.; Carreira, E. M. *Angew. Chem., Int. Ed.* **2020**, *59*, 1192.

[4] Zheng, H.; Felix, R. J.; Gagné, M. R. *Org. Lett.* **2014**, *16*, 2272.

[5] (a) Snider, B. B.; Hui, R. A.; Kulkarni, Y. S. J. Am. Chem. Soc. 1985, 107, 2194; (b) Brady, W. T.; Giang, Y. F. J. Org. Chem. 1985, 50, 5177; (c) Oppolzer, W.; Nakao, A. *Tetrahedron Lett.* **1986**, *27*, 5471; (d) Ozawa, T.; Kanematsu, M.; Yokoe, H.; Yoshida, M.; Shishido, K. *J. Org. Chem.* **2012**, *77*, 9240; (e) Araki, T.; Ozawa, T.; Yokoe, H.; Kanematsu, M.; Yoshida, M.; Shishido, K. *Org. Lett.* 2013, *15*, 200.

[6] Trost, B. M.; Tanoury, G. J. *J. Am. Chem. Soc.* **1988**, *110*, 1636.

[7] Nieto-Oberhuber, C.; López, S.; E. Jiménez-Núñez, E. Echavarren, A. M. *Chem. Eur. J.* **2006**, *12*, 5916.

[8] Odabachian, Y.; Gagosz, F. *Adv. Synth. Catal.* **2009**, *351*, 379.

[9] Sun, J.; Conley, M. P.; Zhang, L.; Kozmin, S. A. *J. Am. Chem. Soc.* **2006**, *128*, 9705.

[10] (a) Odedra, A.; Wu, C. J.; Madhushaw, R. J.; Wang, S. L.; Liu, R. S. *J. Am. Chem. Soc.* **2003**, *125*, 9610; (b) Kulyk, S.; Dougherty Jr, W. G.; Kassel, W. S.; Zdilla, M. J.; Sieburth, S. M. *Org. Lett.* **2011**, *13*, 2180.

[11] López-Carrillo, V.; Echavarren, A. M. *J. Am. Chem. Soc.* **2010**, *132*, 9292.

[12] Homs, A., Obradors, C., Lebœuf, D. and Echavarren, A.M., *Adv. Synth. Catal.* **2014**, *356*, 221.

[13] Nelson, P. H.; Carr, S. F.; Devens, B. H.; Eugui, E. M.; Franco, F.; Gonzalez, C.; Hawley, R. C.; Loughhead, D. G.; Milan, D. J.; Papp, E.; Patterson, J. W.; Rouhafza, S.; Sjogren, E. B.; Smith, D. B.; Stephenson, R. A.; Talamas, F. X.; Waltos, A.-M.; Weikert, R. J.; Wu, J. C. *J. Med. Chem.* **1996,** *39*, 4181.

[14] (a) Moriarty, R. M.; Prakash, I.; Musallam, H. A. **1984**, *25*, 5867; (b) Iglesias-Arteaga, M. A.; Velázquez-Huerta, G. A. *Tetrahedron Lett.* **2005**, *46*, 6897; (c) Fraga, B. M.; Bressa, C.; González-Vallejo, V.; Suárez, S.; Guillermo, R. *Tetrahedron Lett.* **2011**, *52*, 7138; (d) Sánchez-Flores, J.; Pelayo-González, V. G.; Romero-Ávila, M.; Flores-Pérez, B.; Flores-Álamo, M.; Iglesias-Arteaga, M. A. *Steroids* **2013**, *78*, 234; (e) Viviano-Posadas, A. O.; Flores-Álamo, M.; Iglesias-Arteaga, M. A. *Steroids* **2016**, *113*, 22; (f) Jiang, X.-L.; Shi, Y.; Tian, W.-S. *J. Org. Chem.* **2017**, *82*, 4402.
[15] (a) Greene, A. E.; Muller, J.-C.; Ourisson, G. J. Org. Chem. **1974**, *39*, 186; (b) Bernet, B.; Bishop, P. M.; Caron, M.; Kawamata, T.; Roy, B. L.; Ruest, L.; Sauvé, G.; Soucy, P.; Deslongchamps, P. *Can. J. Chem.* 1985, *63*, 2810.
[16] (a) Davis, F. A.; Mancinelli, P. A.; Balasubraminian, K.; Nadir, U. K. *J. Am. Chem. Soc.* **1979**, *101*, 1044; (b) Boschelli, D., Smith, A. B., Ill; Stringer, O. D.; Jenkins, R. H., Jr.; Davis, F. A. *Tetrahedron Lett.* **1981**, *22*, 4385. For a review, see: Williamson, K. S.; Michaelis, D. J.; Yoon, T. P. *Chem. Rev.* **2014**, *114*, 8016.
[17] Ramachary, D. B.; Barbas, III, C. F. *Org. Lett.* **2005**, *7*, 1577 and references therein.
[18] Nicolaou, K. C.; Adsool, V. A.; Hale, C. R. H. *Org. Lett.* **2010**, *12*, 1552.
[19] (a) Lipshutz, B. H.; Dimock, S. H.; James, B. *J. Am. Chem. Soc.* **1993**, *115*, 9283; (b) Bertz, S. H.; Miao, G.; Rossiter, B. E.; Snyder, J. P. *J. Am. Chem. Soc.* **1995**, *117*, 11023.
[20] Imamoto, T.; Takiyama, N.; Nakamura, K.; Hatajima, T.; Kamiya, Y. *J. Am. Chem. Soc.* **1989**, *111*, 4392
[21] Kusama, H.; Hara, R.; Kawahara, S.; Nishimori, T.; Kashima, H.; Nakamura, N.; Morihira, K.; Kuwajima, I. *J. Am. Chem. Soc.* **2000,** *122*, 3811.
[22] Muthukumarasamy, K. M.; Handore, K. L.; Kakade, D. N.; Shinde, M. V.; Ranjan, S.; Kumar, N.; Sehrawat, S.; Sachidanandan, C.; Reddy, D.S. *Org. Biomol. Chem.* **2016**, *14*, 1569.
[23] Turner, R. B.; Goebel, P.; Mallon, B. J.; Doering, W. V. E.; Coburn Jr, J. F.; Pomerantz, M. *J. Am. Chem. Soc.* **1968**, *90*, 4315.
[24] Turner, R. B.; Meador, W. R. *J. Am. Chem. Soc.* **1957**, *79*, 4133.
[25] Graham, T. J.; Gray, E. E.; Burgess, J. M.; Goess, B. C. *J. Org. Chem.* **2010**, *75*, 226.
[26] (a) Chung, S.-K. *J. Org. Chem.* **1979**, *44*, 1014; (b) Ho, T.-L.; Chein, R.-J. *Helv. Chim. Acta* **2006**, *89*, 231; (c) Renata, H.; Zhou, Q.; Dünstl, G.; Felding, J.; Merchant, R. R.; Yeh, C.-H.; Baran, P. S. *J. Am. Chem. Soc.* **2015**, *137*, 1330.
[27] For Rh-catalyzed hydroboration of cyclopropanes, see: Rubina, M.; Rubin, M.; Gevorgyan, V. *J. Am. Chem. Soc.* **2003**, 125, 7198.
[28] Oshima, M.; Hiroyuki Yamazaki; H.; Shimizu, I.; Nisar, M.; Tsuji, J. *J. Am. Chem. Soc.* **1989**, *111*, 6280.
[29] (a) Yadav, J. S.; Shekharam, T.; Srinivas, D. *Tetrahedron Lett.* **1992**, *33*, 7973; (b) Cuerva, J. M.; Campaña, A. G.; Justicia, J.; Rosales, A.; Oller-López, J. L.; Robles, R.; Cárdenas, D. J.; Buñuel, E.; Oltra, J. E. *Angew. Chem., Int. Ed.* 2006, **45**, 5522.
[30] Aurrecoechea, J. M.; Iztueta, E. *Tetrahedron Lett.* **1995**, *36*, 7129.
[31] Zhou, Q.; Chen, X.; Ma, D. *Angew. Chem., Int. Ed.* **2010**, *49*, 3513.
[32] Nelson, P. H.; Nelson, J. T. *Synthesis* **1992**, 1287.

4.10 NMR Spectra of Selected Intermediates

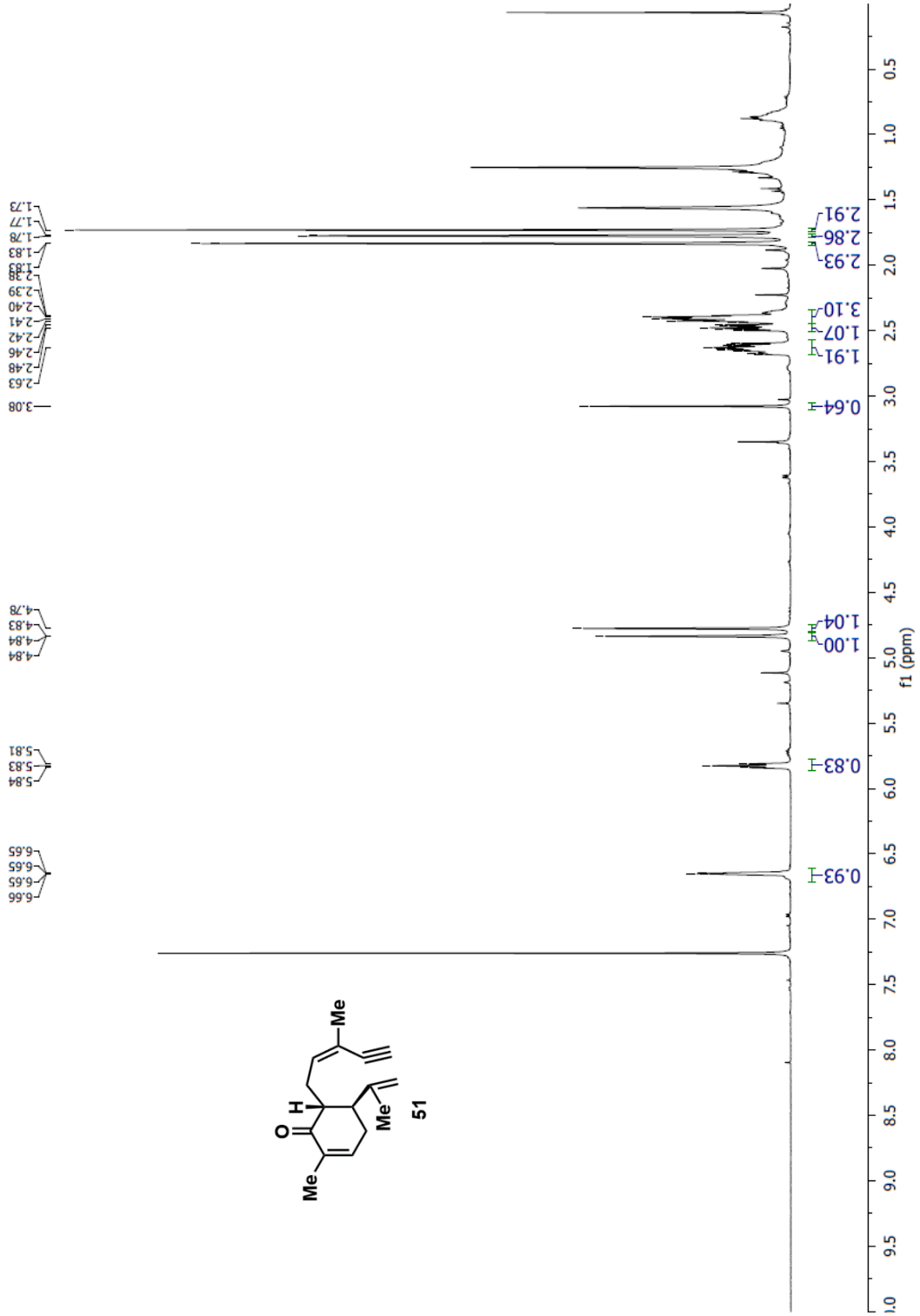

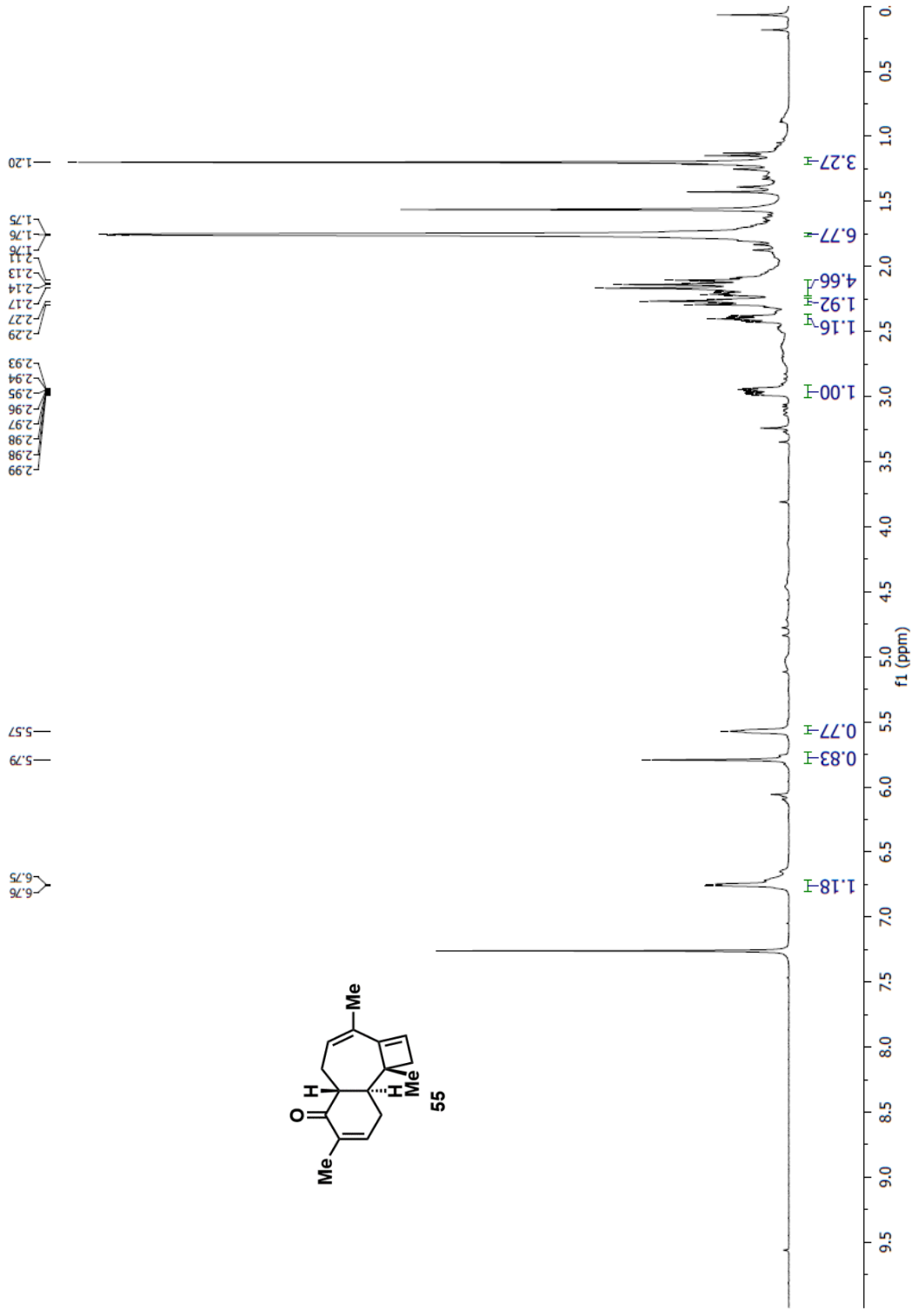
Me
H
O
H
Me
Me
55
f1 (ppm)

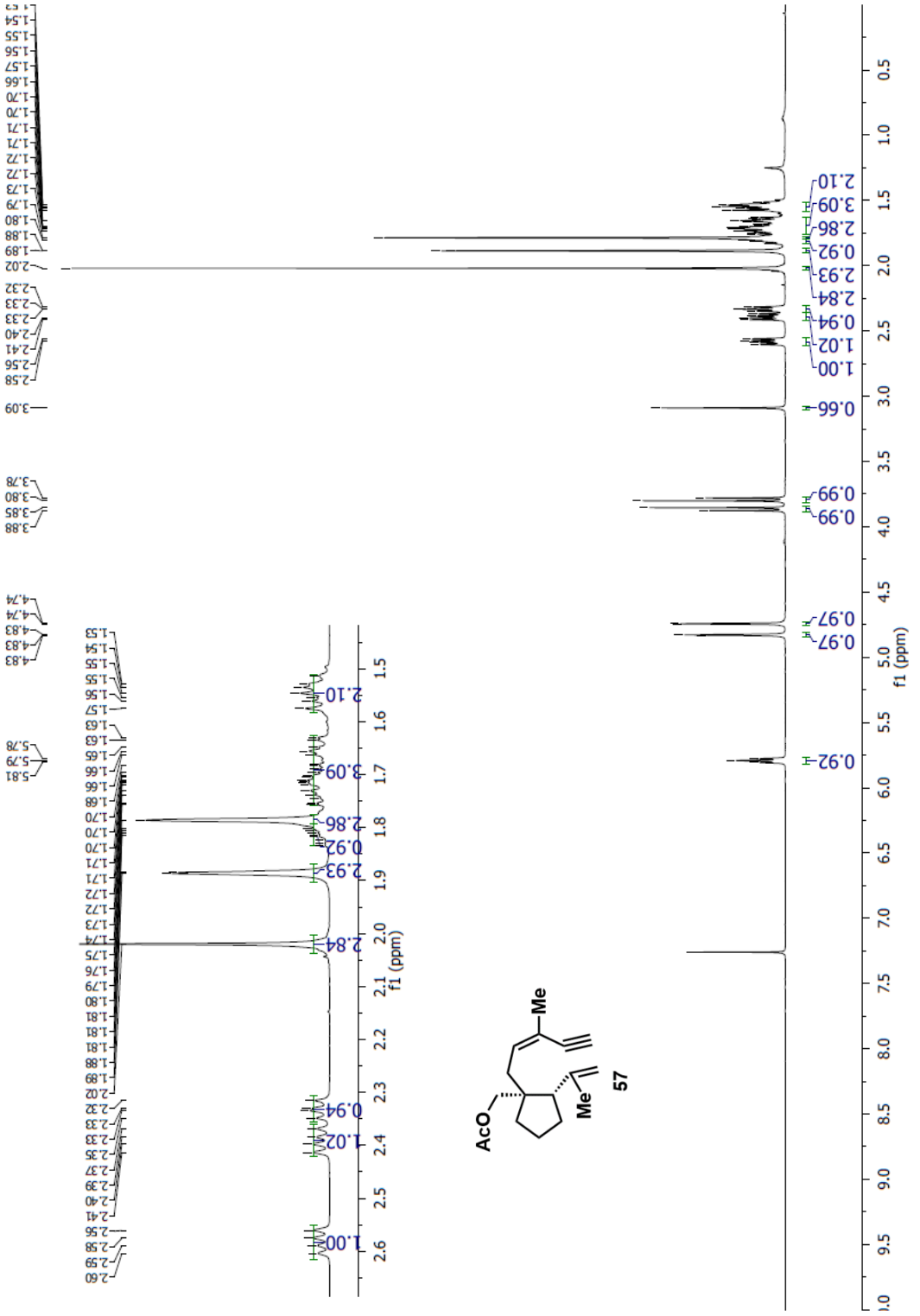
AcO
Me
Me
57
f1 (ppm)

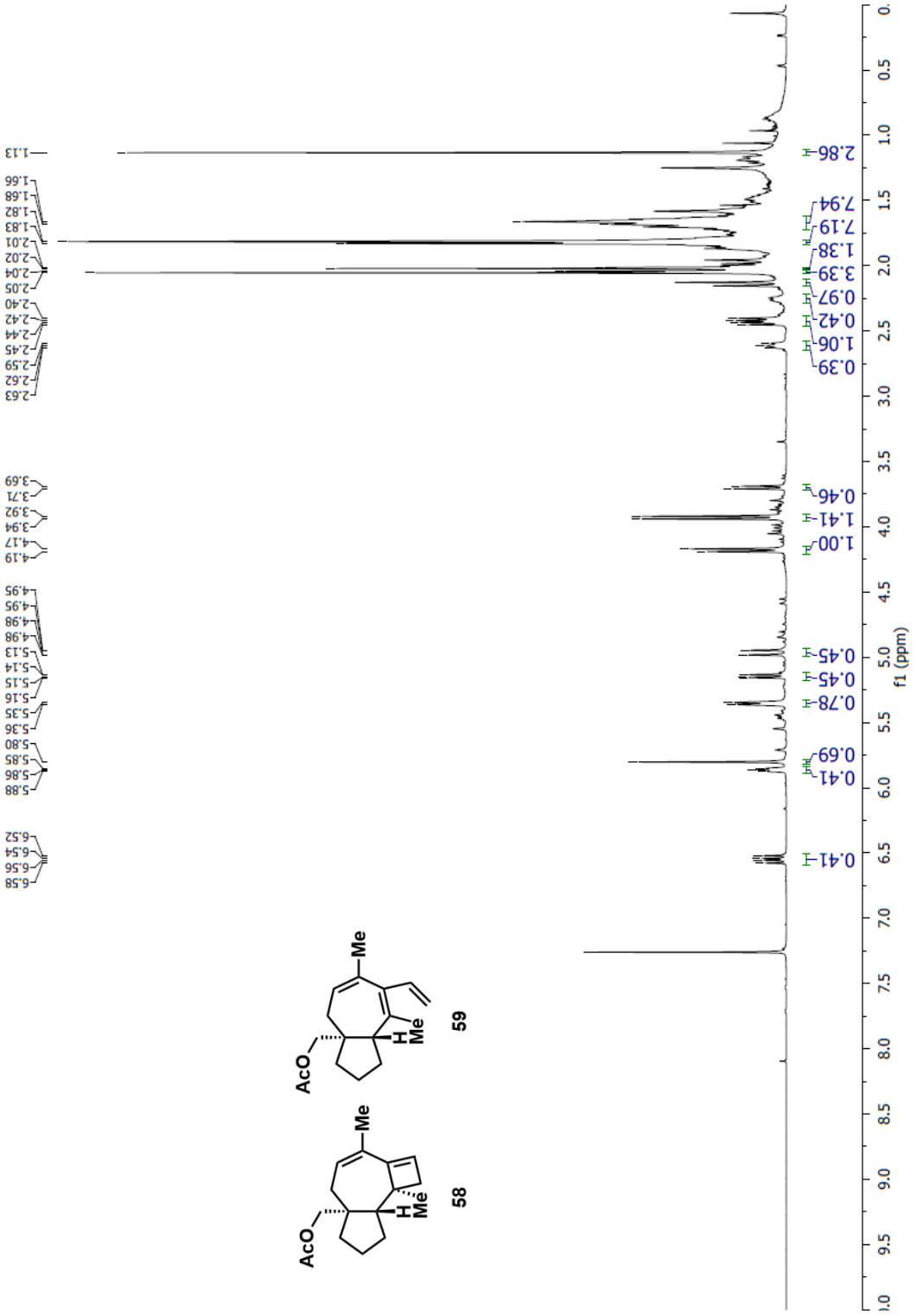
Me
AcO
H
Me
59
Me
AcO
H
Me
58
f1 (ppm)

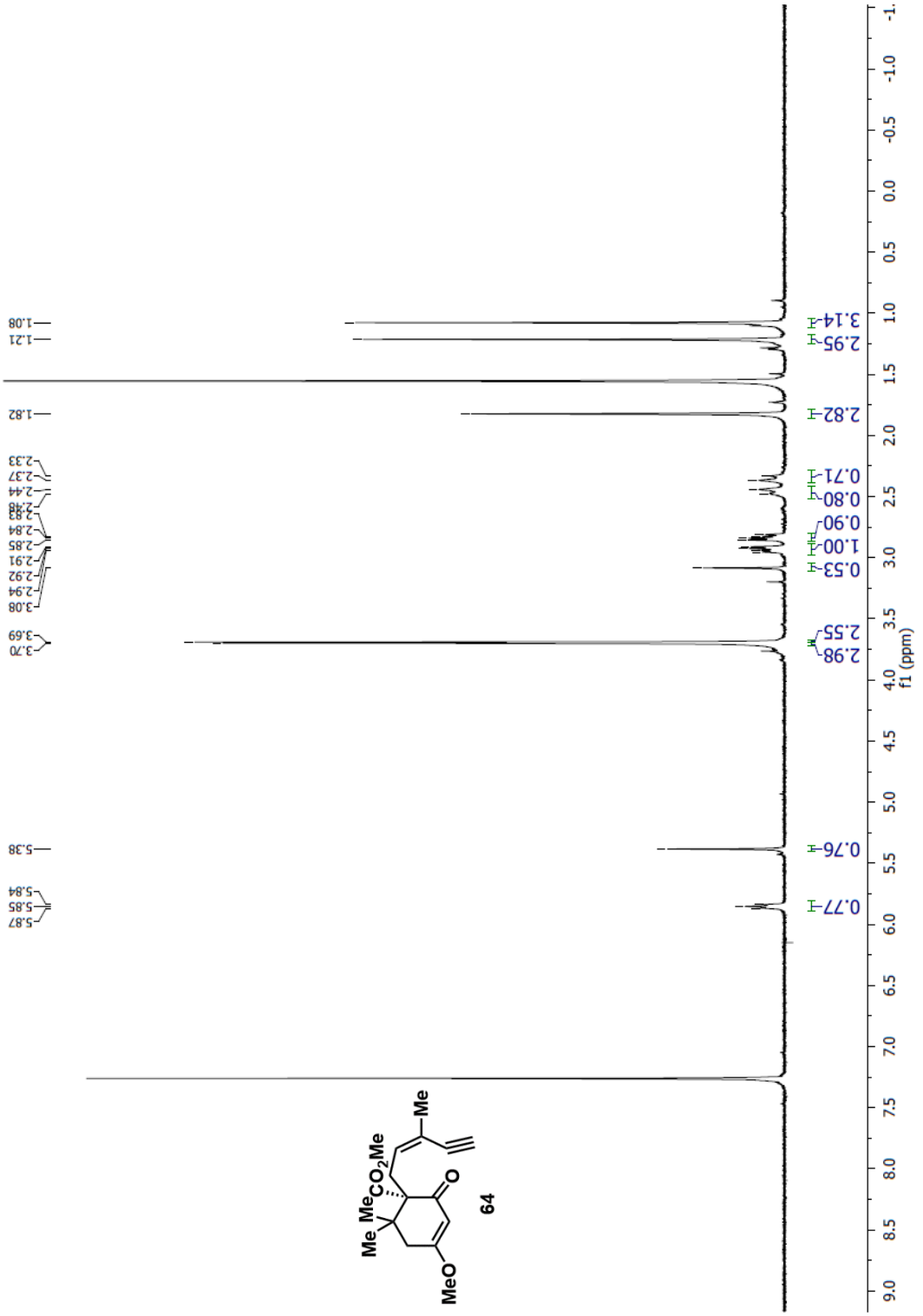
Me
Me
CO2Me
Me
O
MeO
64
f1 (ppm)

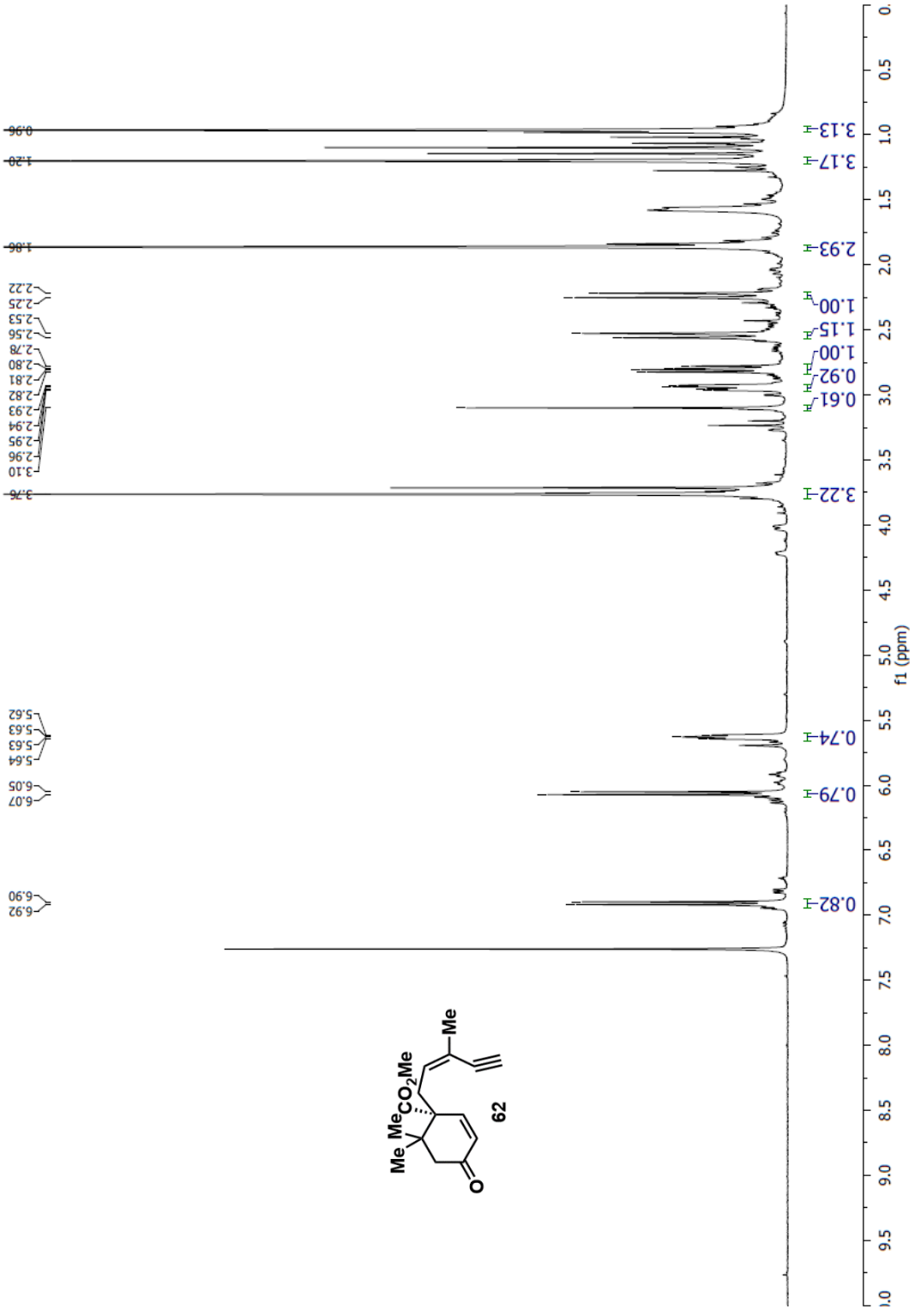
0.96
1.20
1.86
2.22
2.25
2.53
2.56
2.78
2.80
2.81
2.82
2.93
2.94
2.95
2.96
3.10
3.76
5.62
5.63
5.64
6.05
6.07
6.90
6.92
3.13
3.17
2.93
1.00
1.15
1.00
0.92
0.61
3.22
0.74
0.79
0.82
Me
CO2Me
Me
Me
O
62
f1 (ppm)

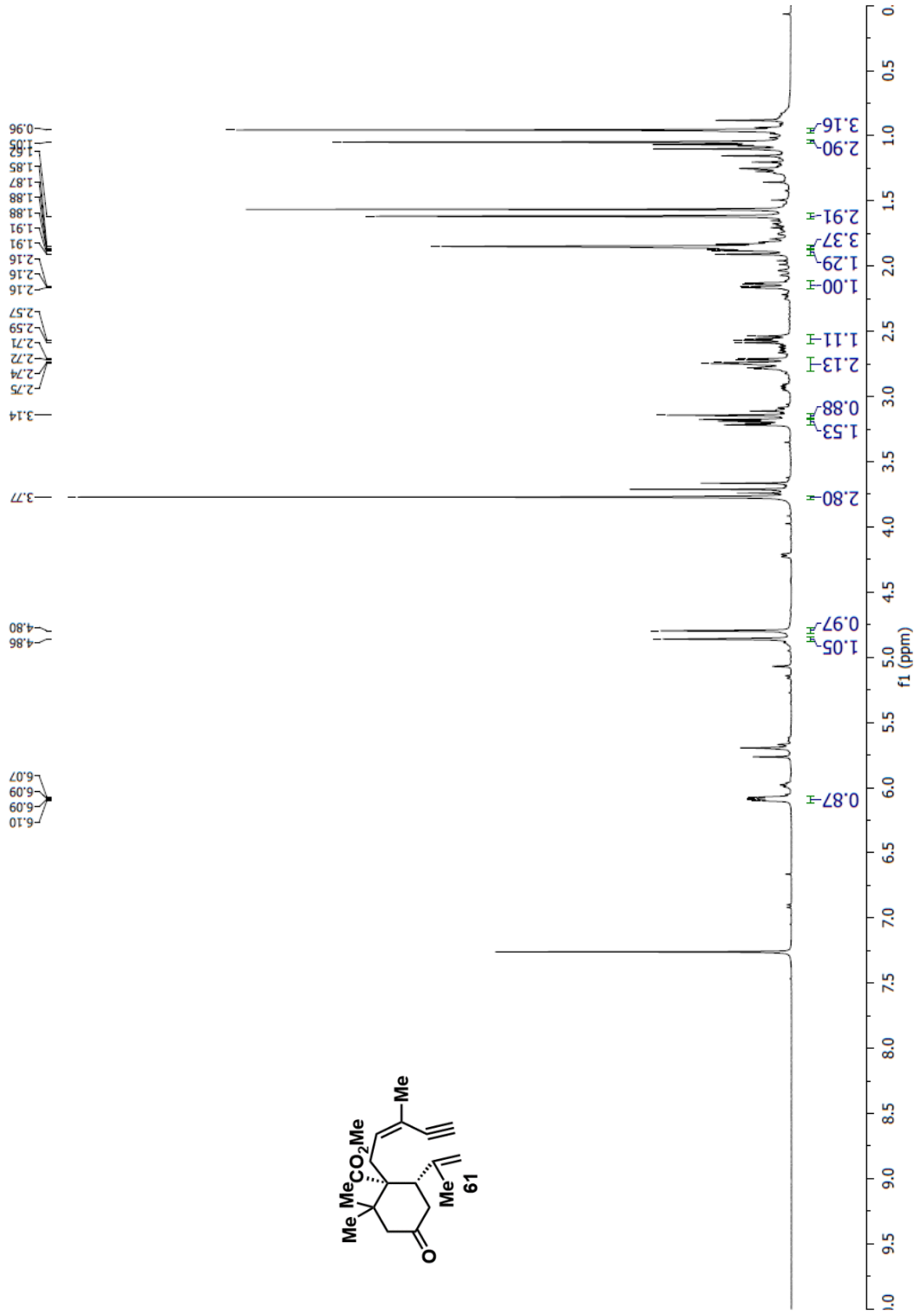
Me
Me
CO2Me
Me
Me
O
61
f1 (ppm)

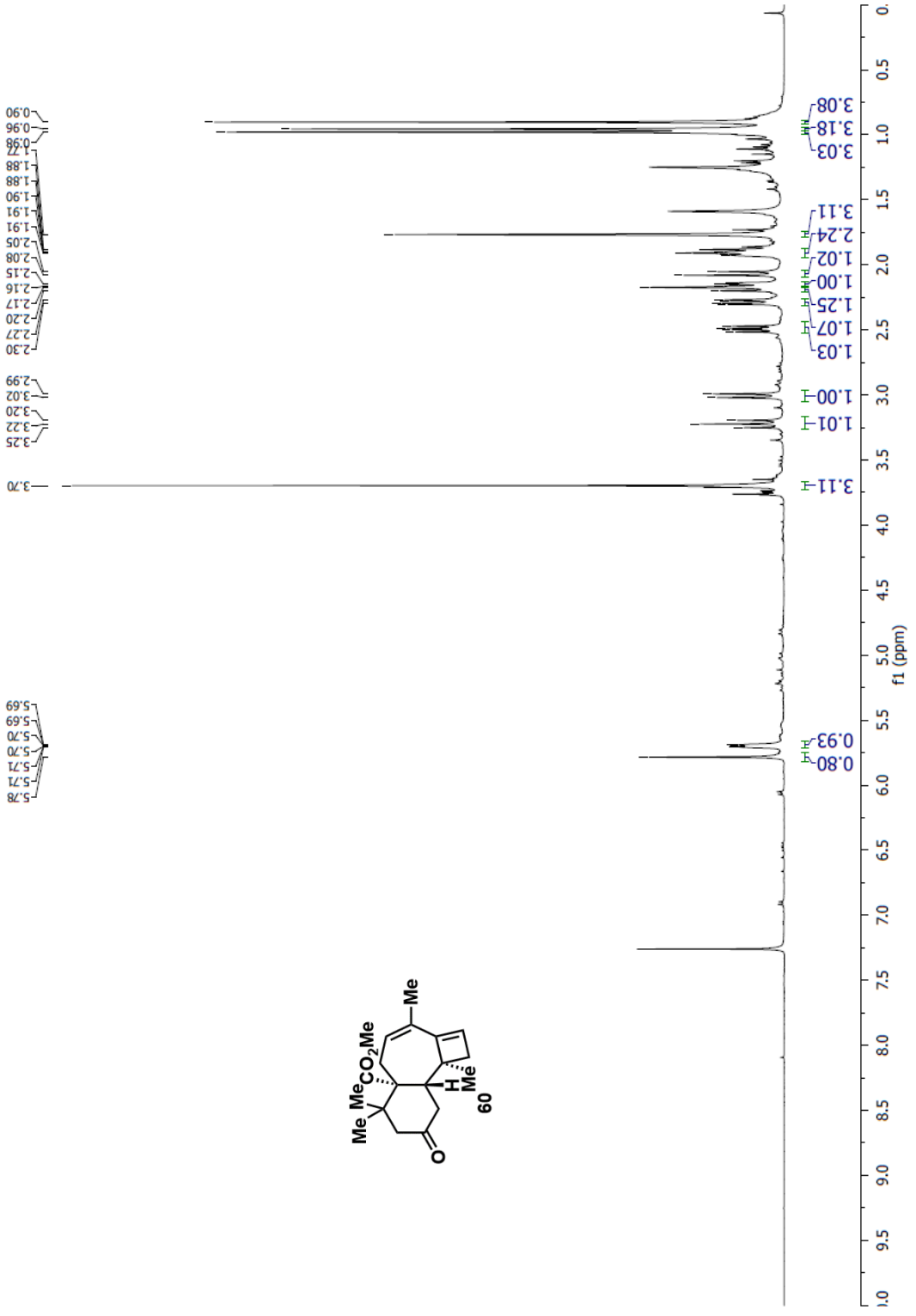
Me
Me
CO2Me
H
Me
Me
O
60
f1 (ppm)

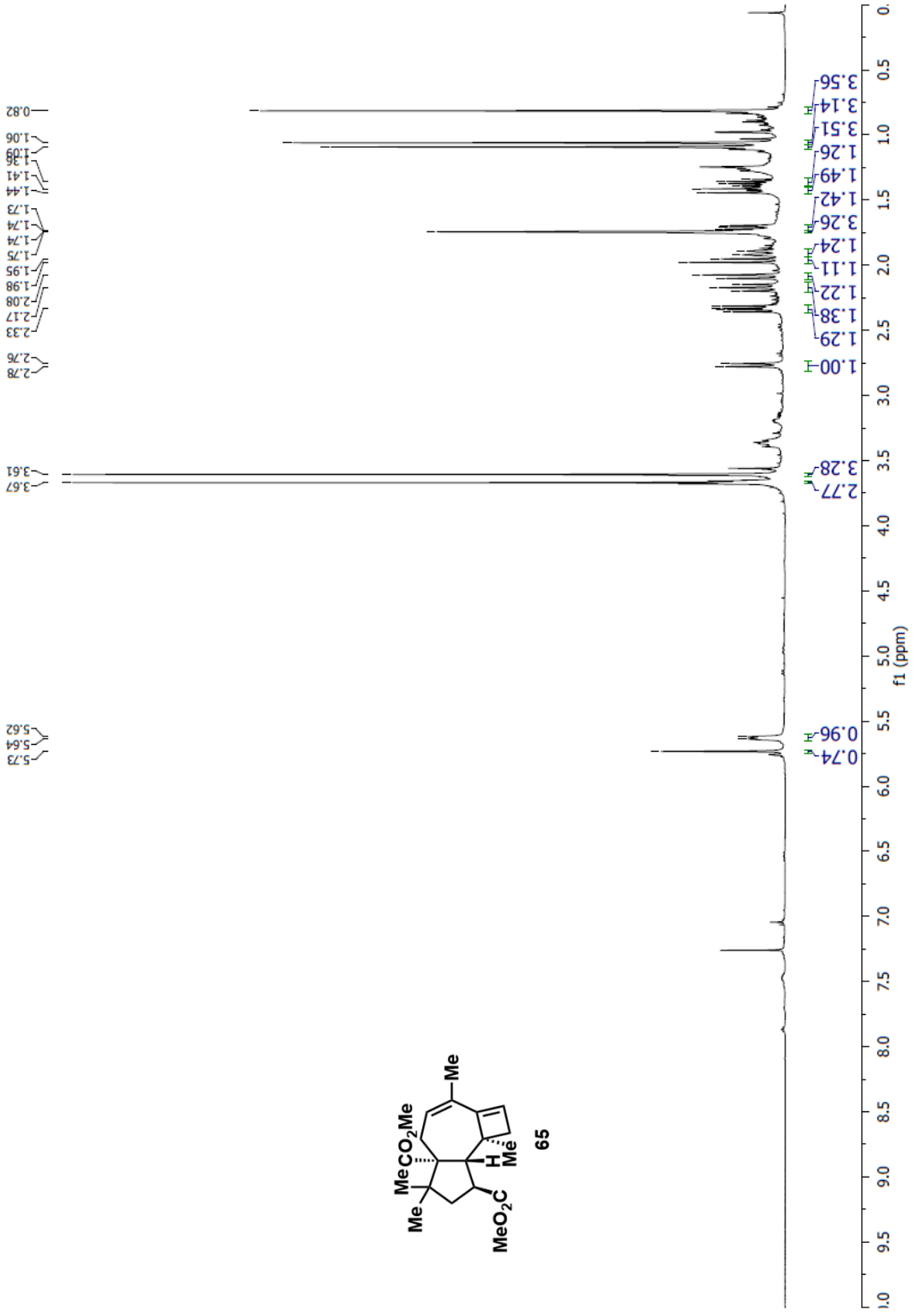
Me
MeCO2Me
Me
H
Me
Me
MeO2C
65
f1 (ppm)

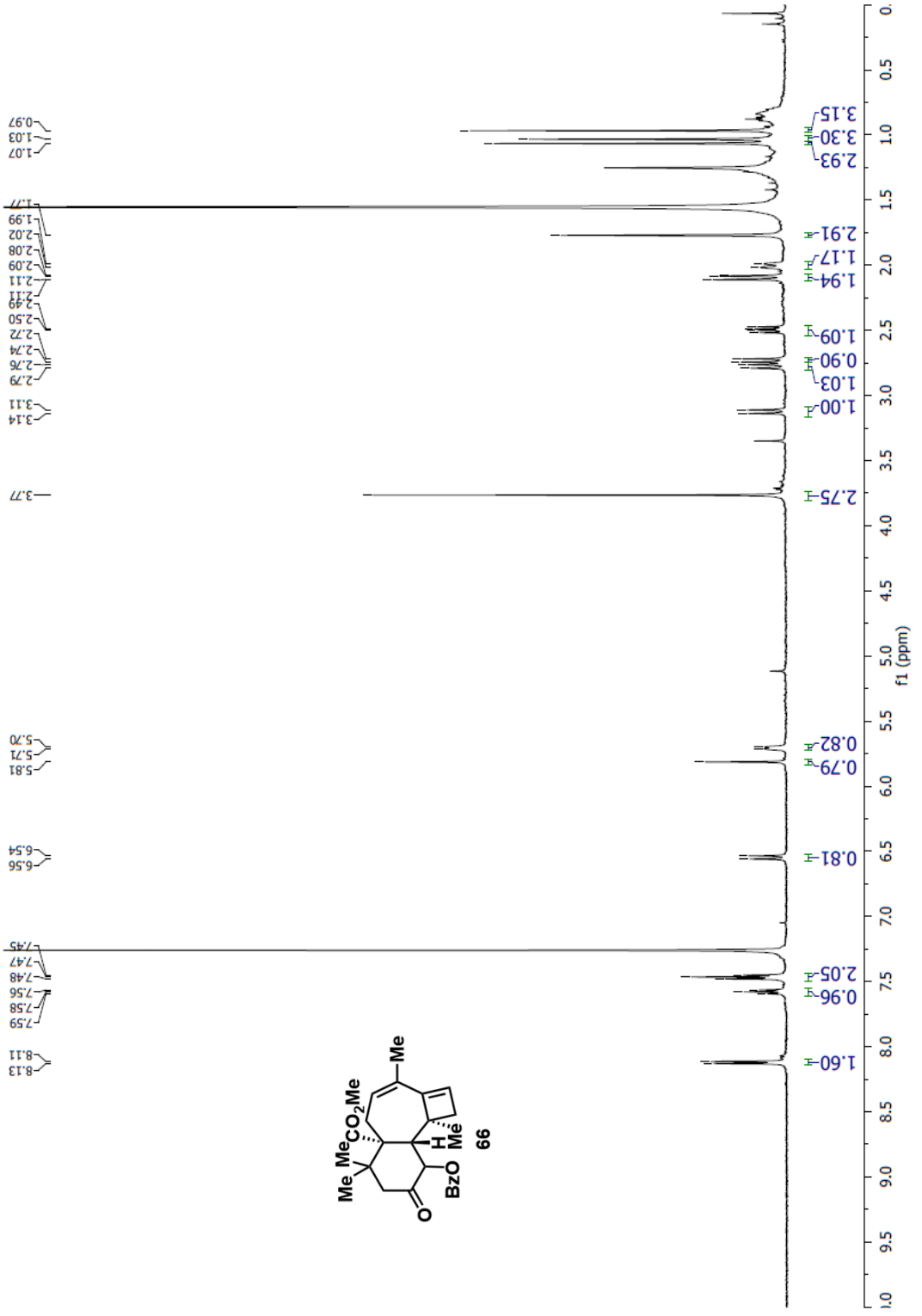
Me
Me
CO2Me
Me
H
Me
BzO
O
66
f1 (ppm)

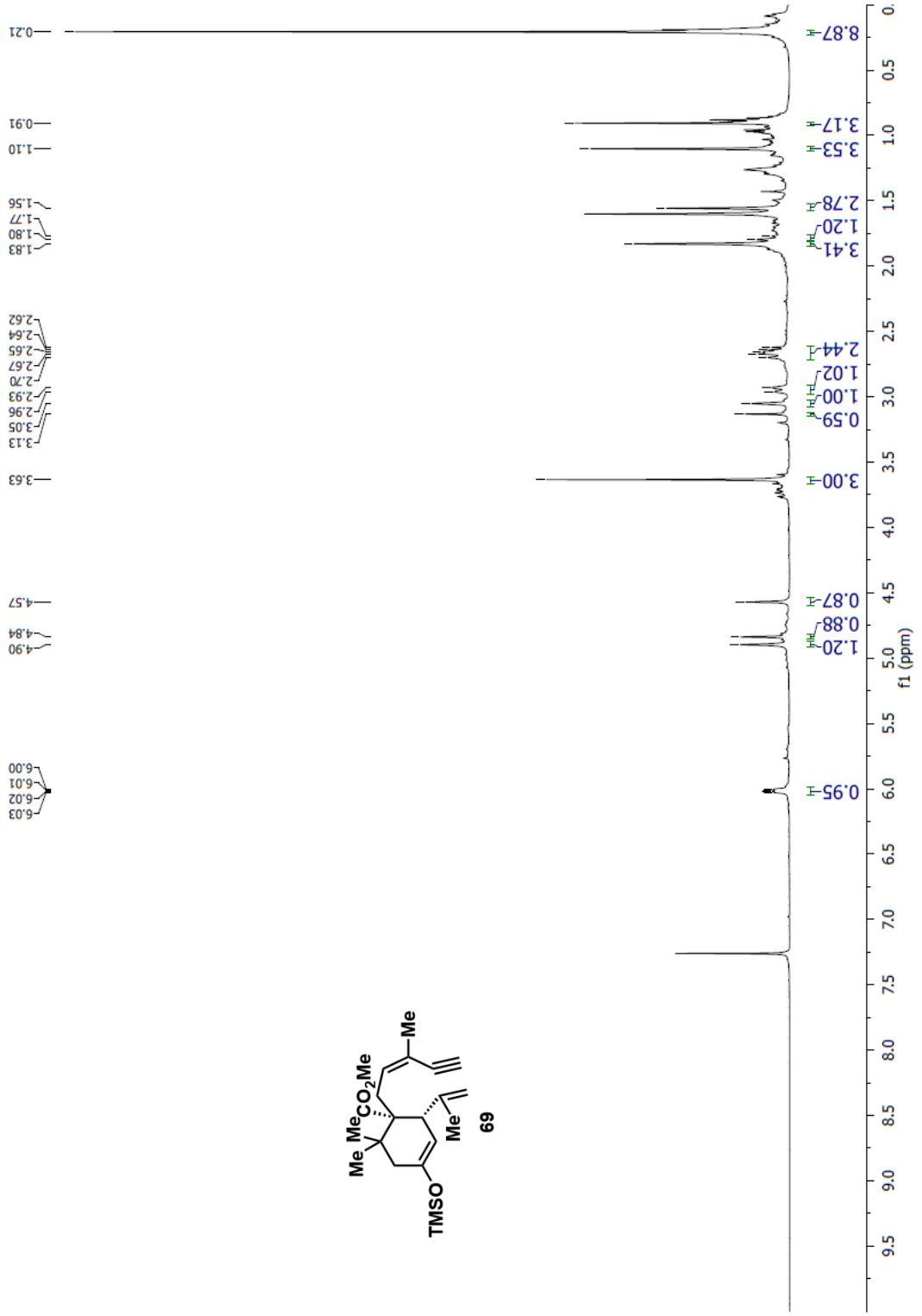
f1 (ppm)
69
Me
Me
CO2Me
Me
Me
TMSO

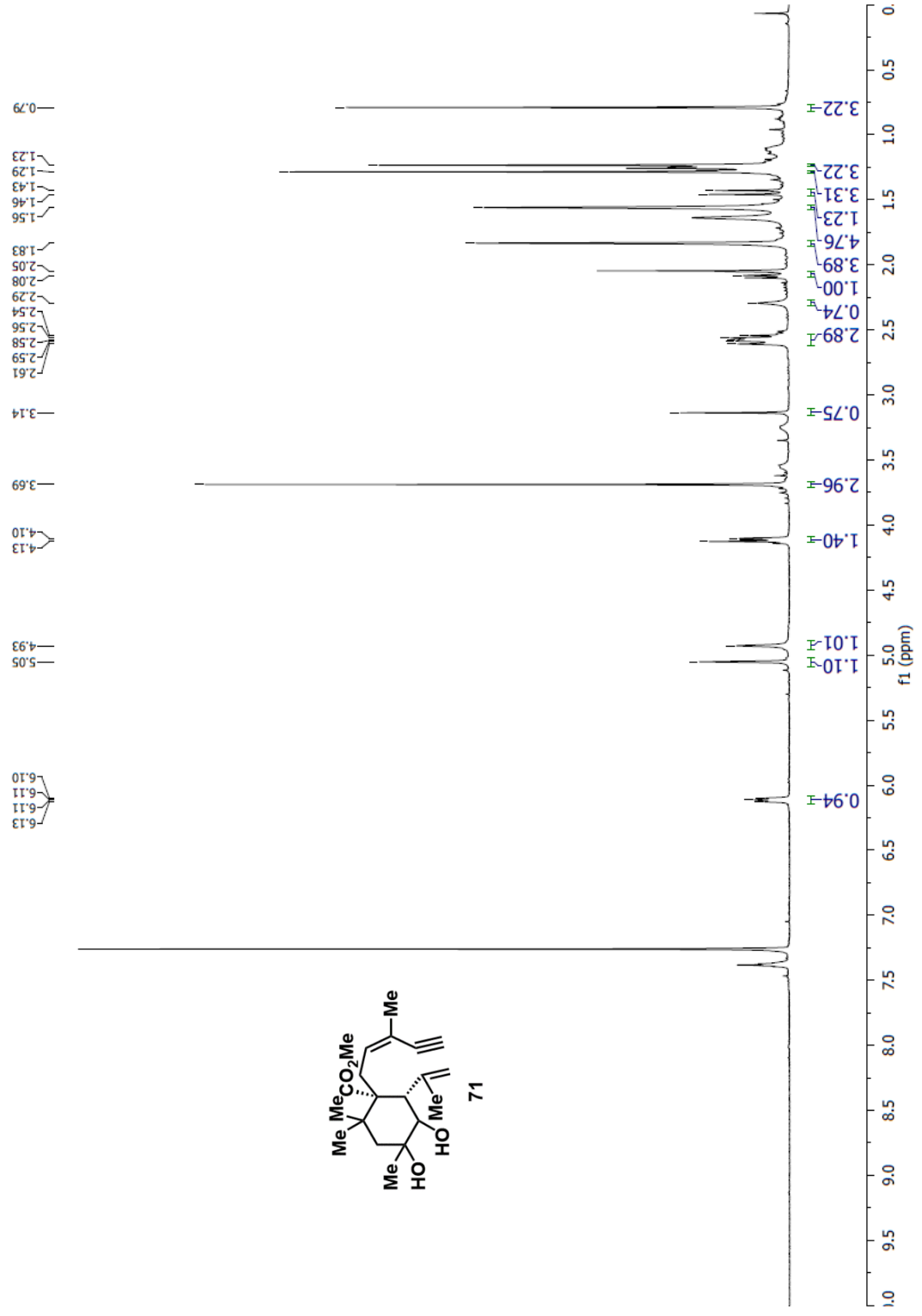
Me
Me
CO2Me
Me
HO
Me
Me
HO
71
f1 (ppm)

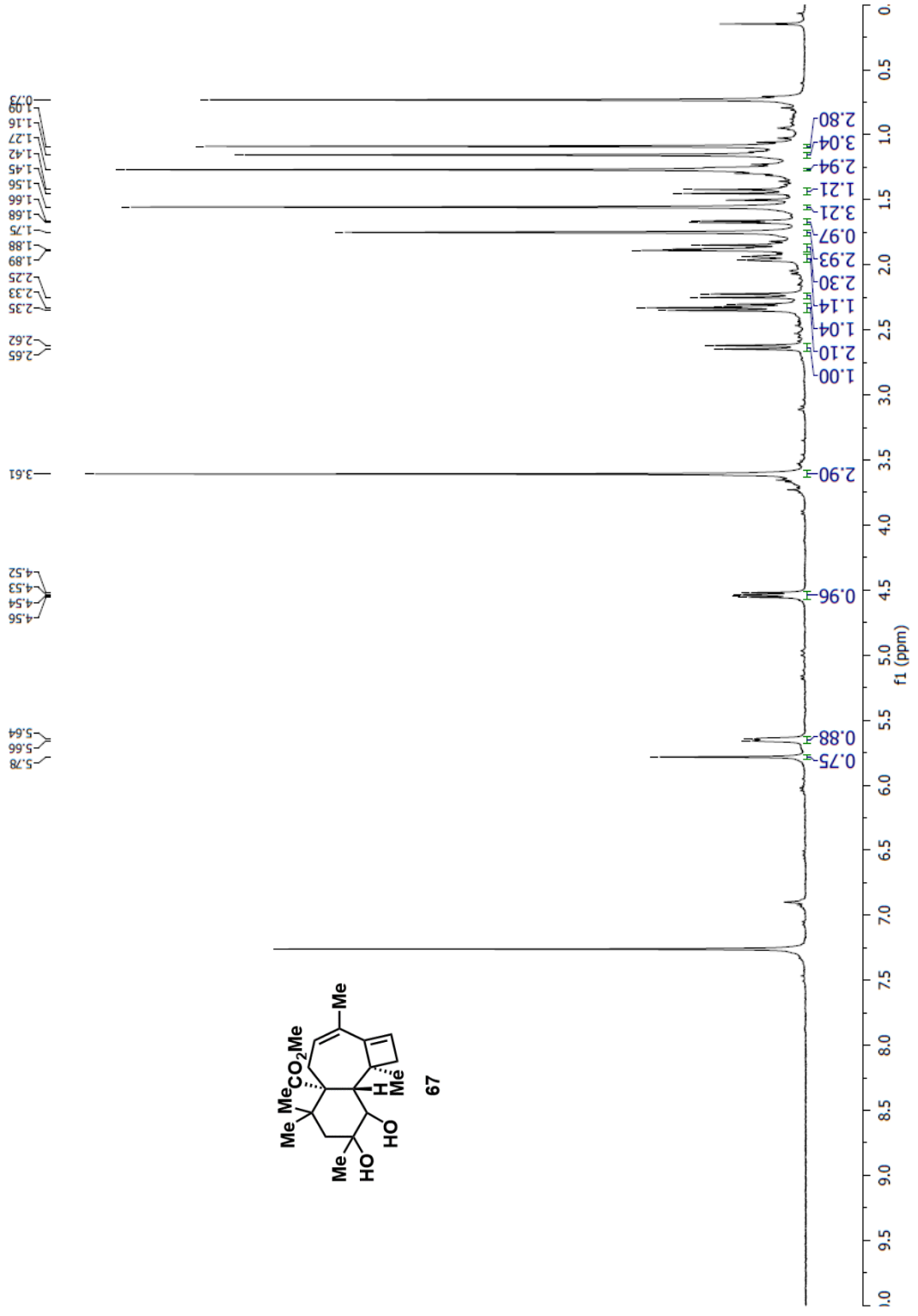
0.73
1.09
1.16
1.27
1.42
1.45
1.56
1.66
1.68
1.75
1.88
1.89
2.25
2.33
2.35
2.62
2.65
3.61
4.52
4.53
4.54
4.56
5.64
5.66
5.78
2.80
3.04
2.94
1.21
3.21
0.97
2.93
2.30
1.14
1.04
2.10
1.00
2.90
0.96
0.88
0.75
f1 (ppm)
Me
CO2Me
Me
Me
H
Me
HO
Me
HO
67

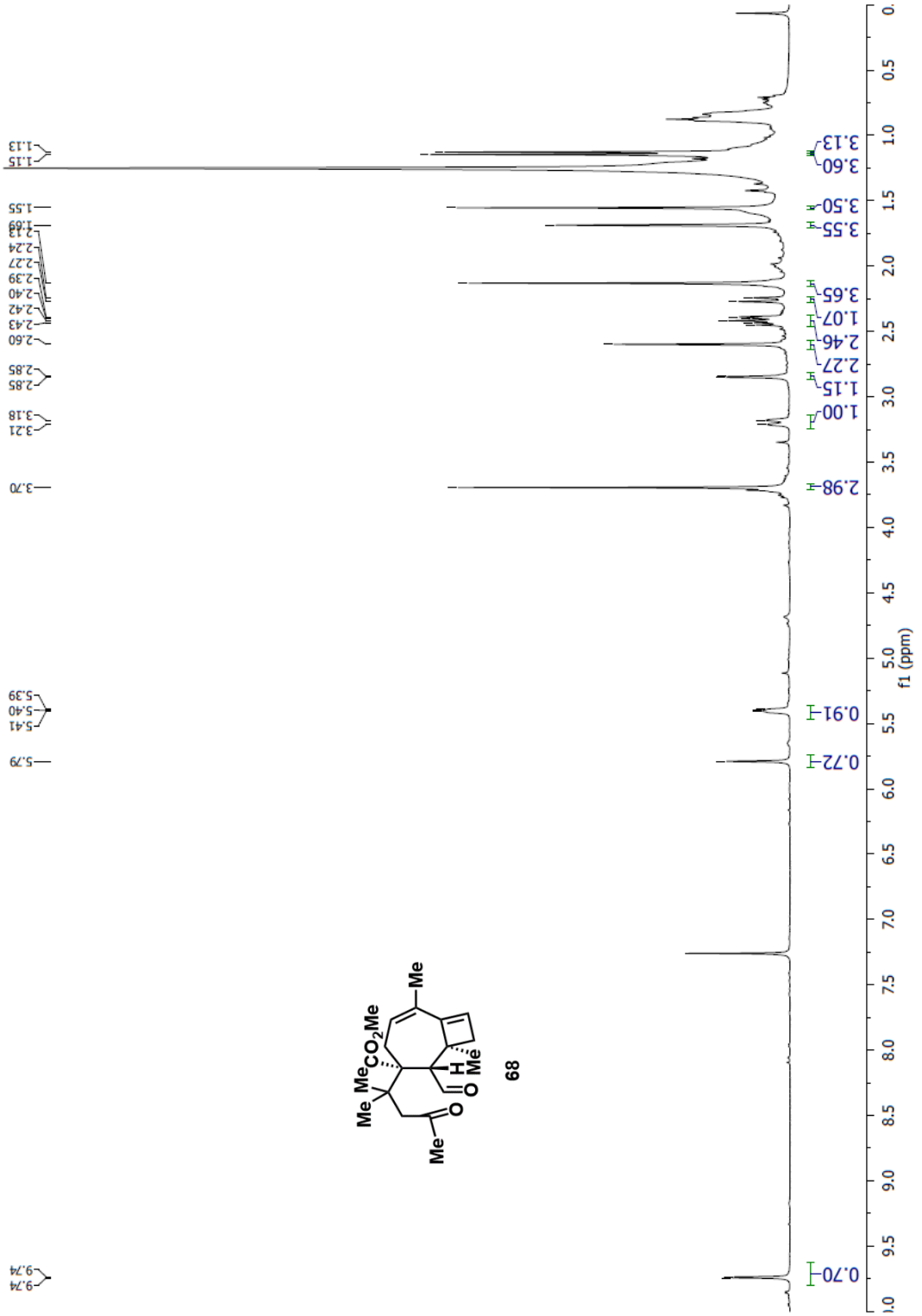
9.74
5.79
5.41
5.40
5.39
3.70
3.21
3.18
2.85
2.85
2.60
2.43
2.42
2.40
2.39
2.27
2.24
1.69
1.55
1.15
1.13
0.70
0.72
0.91
2.98
1.00
1.15
2.27
2.46
1.07
3.65
3.55
3.50
3.60
3.13
f1 (ppm)
Me
CO2Me
Me
Me
H
O
Me
O
Me

68

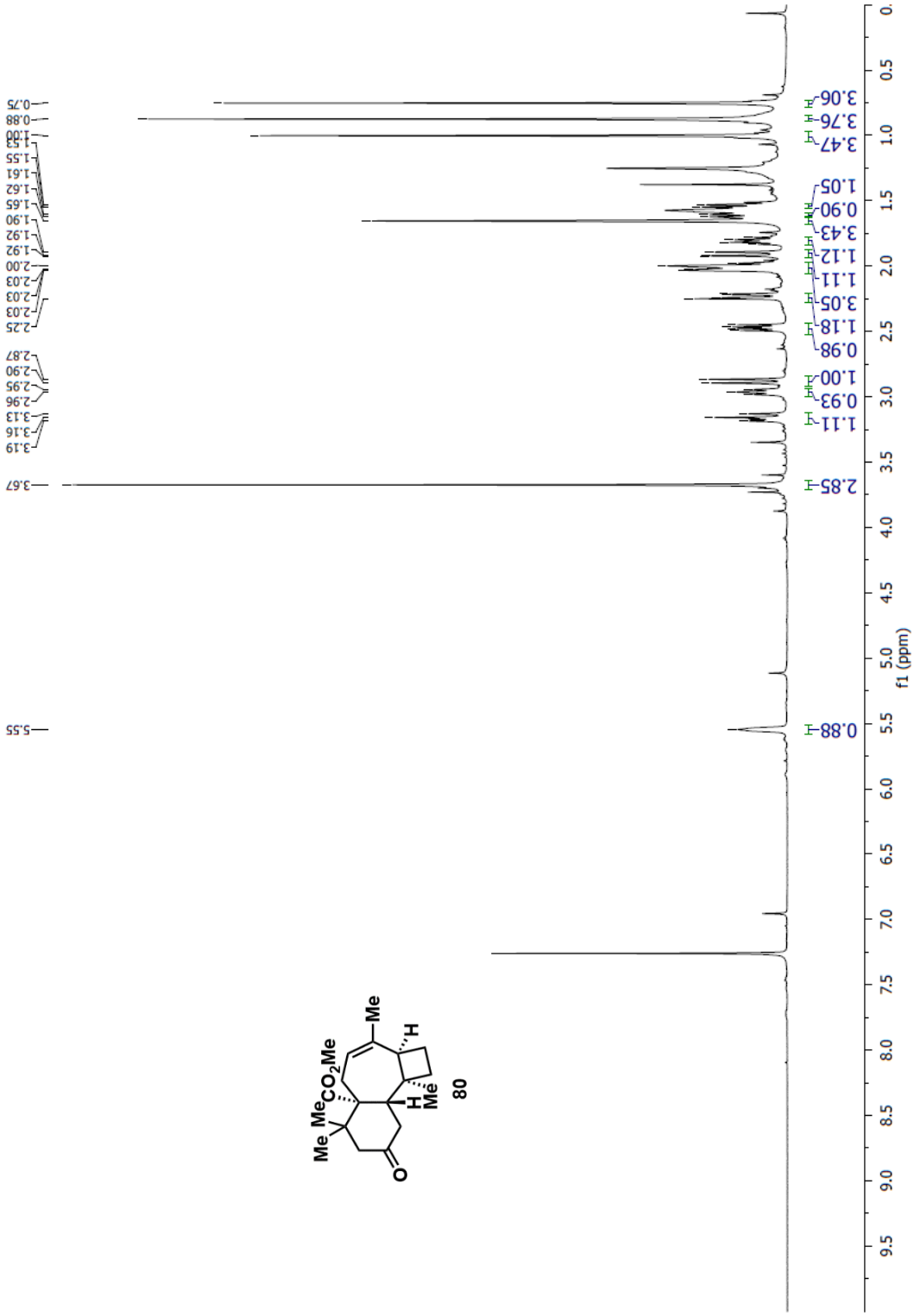
Me
H
Me
CO2Me
Me
Me
H
O
80
f1 (ppm)

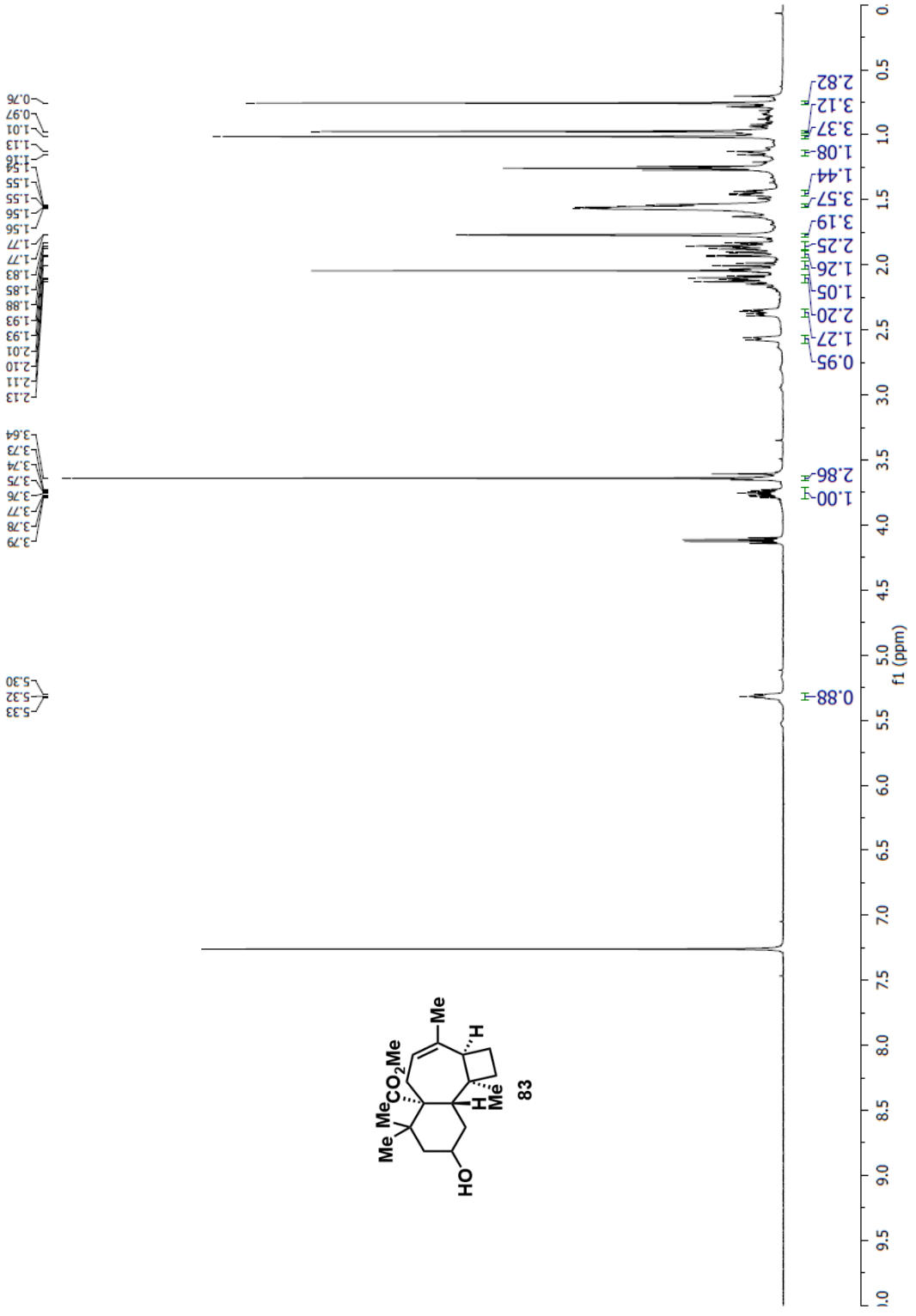
Me
H
Me
CO2Me
Me
Me
H
HO
83
f1 (ppm)